



INSTITUTO POLITECNICO NACIONAL
CENTRO INTERDISCIPLINARIO DE CIENCIAS MARINAS



**FEEDING ECOLOGY AND SEASONAL
MOVEMENT PATTERNS OF THE BLUE WHALE
IN THE EASTERN PACIFIC OCEAN**

TESIS

**QUE PARA OBTENER EL GRADO DE
DOCTORADO EN CIENCIAS MARINAS**

PRESENTA

GERALDINE ROSALIE BUSQUETS VASS

LA PAZ, B.C.S., JULIO DE 2017



INSTITUTO POLITÉCNICO NACIONAL
SECRETARIA DE INVESTIGACIÓN Y POSGRADO
ACTA DE REVISIÓN DE TESIS

En la Ciudad de La Paz, B.C.S., siendo las 12 horas del día 01 del mes de Junio del 2017 se reunieron los miembros de la Comisión Revisora de Tesis designada por el Colegio de Profesores de Estudios de Posgrado e Investigación de CICIMAR para examinar la tesis titulada:

**"FEEDING ECOLOGY AND SEASONAL MOVEMENT PATTERNS OF THE BLUE WHALE
IN THE EASTERN PACIFIC OCEAN"**

Presentada por el alumno:

BUSQUETS

Apellido paterno

VASS

materno

GERALDINE ROSALIE

nombre(s)

Con registro:

B	1	3	0	7	8	0
---	---	---	---	---	---	---

Aspirante de:

DOCTORADO EN CIENCIAS MARINAS

Después de intercambiar opiniones los miembros de la Comisión manifestaron **APROBAR LA DEFENSA DE LA TESIS**, en virtud de que satisface los requisitos señalados por las disposiciones reglamentarias vigentes.

LA COMISION REVISORA

Director(a) de Tesis

DRA. DIANE ENDRON LANIEL

DR. SERGIO AGUIRIGA GARCÍA

DR. HÉCTOR VILLALOBOS ORTIZ

DR. JAIME GÓMEZ GUTIERREZ

DR. SETH D. NEWSOME

PRESIDENTE DEL COLEGIO DE PROFESORES

DRA. MARÍA MARGARITA CASAS VALDEZ



**I.P.N.
CICIMAR
DIRECCIÓN**



**INSTITUTO POLITÉCNICO NACIONAL
SECRETARÍA DE INVESTIGACIÓN Y POSGRADO**

CARTA CESIÓN DE DERECHOS

En la Ciudad de La Paz, B.C.S., el día 14 del mes de Junio del año 2017

El (la) que suscribe M en C. GERALDINE ROSALIE BUSQUETS VASS Alumno (a) del Programa

DOCTORADO EN CIENCIAS MARINAS

con número de registro B130780 adscrito al CENTRO INTERDISCIPLINARIO DE CIENCIAS MARINAS

manifiesta que es autor(a) intelectual del presente trabajo de tesis, bajo la dirección de:

DRA. DIANE GENDRON LANIEL

y cede los derechos del trabajo titulado:

"FEEDING ECOLOGY AND SEASONAL MOVEMENT PATTERNS OF THE BLUE WHALE

IN THE EASTERN PACIFIC OCEAN"

al Instituto Politécnico Nacional, para su difusión con fines académicos y de investigación.

Los usuarios de la información no deben reproducir el contenido textual, gráficas o datos del trabajo sin el permiso expreso del autor y/o director del trabajo. Éste, puede ser obtenido escribiendo a la siguiente dirección: geraldine.busquets@gmail.com - dgendron@ipn.mx

Si el permiso se otorga, el usuario deberá dar el agradecimiento correspondiente y citar la fuente del mismo.

M en C. GERALDINE ROSALIE BUSQUETS VASS

Nombre y firma del alumno

INDEX

INDEX	I
DEDICATION	IV
ACKNOWLEDGEMENTS	V
THESIS ACHIEVEMENTS	VIII
LIST OF FIGURES	X
LIST OF TABLES	XIV
GLOSSARY	XVII
ABSTRACT	XXI
RESUMEN	XXIII
1. INTRODUCTION	1
2. BACKGROUND	10
3. JUSTIFICATION	21
4. HYPOTHESIS	22
5. OBJECTIVES	22
5.1. Specific objectives.....	22
6. MATERIALS AND METHODS	23
6.1. Study area	23
6.1.1. Northeast Pacific Ocean (NEP)	26
6.1.2. Southeast Pacific Ocean (SEP)	31
6.2. Sample collection and selection	32
6.3. Skin biopsy separation into skin strata	35
6.4. Standardizing blue whale skin sample preparation	37
6.5. Stable isotope analysis	38

6.6. Statistical analysis	39
6.6.1. Assessing the effect of different processing methods in the isotope values of blue whale skin samples	39
6.6.2. Comparing the variability of blue whale skin isotope values by strata	39
6.6.3. Estimating blue whale skin strata isotopic incorporation rate	40
6.6.4. Determining the isotopic niche width and trophic overlap of blue whales in the eastern Pacific, by region (SEP and NEP) and sex (females and males)	42
6.6.5. Quantifying the relative contribution of different foraging zones to the blue whale diet in the NEP	44
6.6.6. Estimating blue whale baleen growth rates and isotopic niche width to infer the movement patterns of individual blue whales in the NEP	45
7. RESULTS.....	46
7.1. Assessing the effect of different processing methods in the isotope values of blue whale skin samples	46
7.2. Comparing the variability of blue whale skin isotope values by strata	46
7.3. Estimating blue whale skin strata isotopic incorporation rate	49
7.4. Isotopic niche width and trophic overlap of blue whales in the eastern Pacific Ocean by region and sex	56
7.4.1. Blue whales in the NEP and SEP	56
7.4.2. Female and male blue whales in the eastern Pacific Ocean	59
7.5. Quantifying the relative contribution of different foraging zones to the blue whale diet in the NEP	61
7.6. Estimating blue whale baleen growth rates and isotopic niche width to infer the seasonal movement patterns of individual blue whales in the NEP	63
7.7. $\delta^{13}\text{C}$ values of skin and baleen plates	69
8. DISCUSSION	73

8.1. Influence of lipid-extraction and DMSO preservation on skin $\delta^{13}\text{C}$ and $\delta^{15}\text{N}$ values	73
8.2. Skin $\delta^{15}\text{N}$ isotopic incorporation rates	73
8.3. Isotopic niche width and overlap of blue whales in the SEP and NEP	75
8.4. Relative contribution of different foraging zones to the blue whale diet in the NEP	77
8.5. Blue whale baleen growth rates and isotopic niche width to infer seasonal movement patterns of individual blue whales	78
8.6. $\delta^{15}\text{N}$ trophic discrimination factors	81
8.7. Temporal consistency of baseline $\delta^{15}\text{N}$ values among foraging zones	81
8.8. $\delta^{13}\text{C}$ values in blue whale skin and baleen plates	83
8.9. $\delta^{13}\text{C}$ and $\delta^{15}\text{N}$ values along the baleen plate of a blue whale calf.....	83
8.10. Summary	85
9. CONCLUSIONS	86
10. RECOMENDATIONS	87
11. REFERENCES	88
12. APPENDIX	120

DEDICATION

I would like to dedicate this work to my amazing and passionate family:

Salvador Busquets, alias piap: Dad, you gave me the tools in life to become a stronger person in every sense by giving me all your love, patience, guidance and support. Today I feel more confident than ever in my own skin because of your teachings.

Chally Soto, alias miam: Mom, you have taught me how to always stand for my ideals, but also to be a critic of them. Thanks to you, I am ready to fight every day to achieve my biggest dreams, I have become a dreamer with a purpose.

Valerie Busquets (valpal), my sister: My best friend in life, whom has shown me to have passion for my work. We have shared so many adventures together, you are my other half. I adore you!

Dante Busquets (hermaniosos), and his son Bruno: My big brother, I admire you deeply. I carry in my heart all those amazing moments we have shared.

Mario A. Pardo, my husband! The owner of my most extreme emotions. The love of my life, my friend, my professor, my colleague, my everything. I have grown into the person I am today because of our free love, that has bonded us forever. I admire you and love you deeply. You are one of my favorite persons in life and I could have never imagined finding someone like YOU. YOU ARE EMBEDDED IN MY SOUL. I LOVE YOU MARIO.

My grandmother: We never know how fragile we are until we lose those we love. I carry within all the love and unforgettable moments that we shared in life, love you for the eternity.

My friends and family.

My furry creatures (Tika and Kaia; Rest in Peace: Orca, Tsunami, Benito): My little treasures (dead and live) and family. Because there is nothing more rewarding and heart comforting than cuddling with my critters.

To the blue whale: One of the biggest creations of evolution and the muse of all my projects. There is nothing more life-fulfilling for me than scanning the sea surface in search for cetaceans.

Big things have small beginnings....

This project started as a simple proposal while volunteering in a blue whale ship survey off Santa Barbara, California in 2012. Ever since, it evolved slowly through a series of incredible events that truly convinced me that we are the owners of our destiny while we are alive. Small steps and perseverance can take you anywhere you want, as long as you are ready to push yourself. Get out of your comfort zone and the magic will happen. Today I know that in the end time is ticking, we must live every day with passion even when we are tired and sad, even when things are not as we expected. Sooner or later we will all become dust....be true to yourself and others every single day, work hard, dream big and above all enjoy yourself.

ACKNOWLEDGEMENTS

This PhD thesis is the result of the collaboration of several institutions, colleagues and professors. I am deeply beholden of the intensive support that I have received during the development of this project. I would like to acknowledge the Centro Interdisciplinario de Ciencias marinas – Instituto Politécnico Nacional (CICIMAR-IPN) that allowed me to participate in the PhD program, and all the institutions that funded this project: the CONACYT (Consejo Nacional de Ciencia y Tecnología), BEIFI (Beca de Estímulo Institucional de Formación de Investigadores), Beca mixta CONACYT, COFA (Comisión de Operación y Fomento de Actividades Académicas del Instituto Politécnico Nacional), SAI-CICIMAR (Subdirección Académica y de Investigación del CICIMAR-IPN), Center for Stable Isotopes (CSI) at the University of New Mexico, Cascadia Research Collective (CRC), American Cetacean Society-Monterey Bay Chapter and Cetacean Society International.

First, I would like to thank my thesis director, **Dr. Diane Gendron**, whom I thank for introducing me to the world of cetaceans, being my unconditional mentor and my inspiration to work harder every day. All the opportunities that she has given me, working in diverse projects and guiding bachelor students, have contributed to my development as researcher. I feel privileged to have been her student since the Master Degree, and cannot wait to develop more projects with her counseling.

Dr. Seth D. Newsome gave me an opportunity without even knowing me. He opened the doors of his house and of his laboratory to me without restriction. After that I have never stopped learning from him. I thank him for all his patience, dedication, edits, guiding, and support. The energy that he transmits in every meeting is contagious, and he was the wings of this project, he gave me wings to pursue the first publication. There are no words to express how grateful I am to Seth Newsome and also his amazing family (Anne, Tessa & Mizou!).

My thesis committee guided me constantly throughout 4 years of my life to finish this project, and I would like to thank each one of them. **Dr. Sergio Aguiñiga-García**, since the very beginning he strongly supported and trusted my ideas, even when the goals seemed far away. I thank him for always trusting my judgment and for helping me achieve my goals. **Dr. Jaime Gómez-Gutiérrez**, one of my role model scientist, he was very critical of my work, pushing me to go further, to question everything. I truly admire him and his work. It has been an incredible journey learning about the biology of krill with Dr. Gómez-Gutiérrez, and also working with him during cetacean surveys (and krill surveys!). I also want to thank him for thoroughly reviewing my thesis, his comments helped greatly improve this work. **Dr. Hector Villalobos**, my R mentor and Guru! I thank him for all the time and patience invested in this project, he has been incredibly supportive, and was always available to help me, especially during the last steps of the publication. I feel extremely privileged to have had such an incredible and professional thesis committee.

My co-author **Jeff K. Jacobsen**, has been a key element in the development of this project. His advice, help and guidance were constant. I would like to thank him for all his support and contributions. He also gave me a space in his house and allowed me to make an unconventional laboratory in one of the rooms, thanks JEFF!

John Calambokidis gave me an amazing opportunity to work with one of the largest blue whale skin tissue bank in the world and I really appreciate that he trusted me to develop this project. I thank his constant critic, key observations and support.

To my colleagues **Gabriela Serra-Valente** and **Kelly Robertson**, from the National Oceanic and Atmospheric Administration-Southwest Fisheries Science Center (NOAA-SWFSC), both invested so much time helping me, I think I will be forever in debt. Their constant support via e-mail was a trigger to the logistics of this project. Their kindness and friendship during this process was very motivating for me.

Angel H. Ruvalcaba Díaz, from the stable isotope laboratory at CICIMAR-IPN, helped me intensively during the processing of samples, and really appreciate him sharing with me his knowledge on stable isotope analysis.

It took a great amount of effort getting all the paperwork needed to start and end each of the eight semesters of this PhD project. This work would have never been possible without the support of **Lic. Humberto Heleodoro Ceseña Amador** (Thank you Dr. for all you support, patience and help!), **Cesar Servando Casas Nuñez** (Thank you for letting me invade the office and bombard you with questions), **Lic. Maria Magdalena Mendoza Talpa** (For all the patience and support during my grant applications), **Lic. Jesús Adriana Toledo Acosta**, **Lic. Luz De La Paz Pinales Soria**, **M.A. Alondra Virginia Fernández**, **Lic. Jasmin Noyola Mendoza**, **Alma Sulema Arista Castro**, **Deyanira Rangel Meza**, **Lic. Ma de Jesús Aguilar Luna** and **Filiberto**. I would also like to thank the support and friendship of **Margarita Vargas Velázquez**, **Isadora Josefina Retes Arrambidez**, **Ma. De Lourdes Pineda Álvarez**, **Juan García Rangel**, **Martina Verdugo Ojeda**, and **Doña Martha Palma**. Also I want to thank all the personal at CICIMAR-IPN, NOAA-SWFSC and the University of New Mexico that helped me during the process of developing this project.

Mario A. Pardo-Rueda, my Bayesian professor. He has helped me throughout the process of learning the proper statistical methods, and has taught me to be extremely critical of my own work. He also encouraged me to trust myself, be pro-active in science, and to never let my background stop me from achieving my goals. I want to thank him for the time he has invested in helping me learn how to write code in R. It has changed the way I think and I am eager to learn to loop everything! I LOVE you, Dr. Pardous.....!!

I don't know what would I have done without all my amazing friends and lab mates in Mexico, La Paz, in La Jolla, in Arcata, and in New Mexico. I want to thank **Milena Mercuri**, **Christian Salvadeo**, **Louisa Renero**, **Yadira Trejo**, **Fabiola Guerrero de la Rosa**, **Jenny Noble**, **Max Noble**, **Cath Arnold**, **Azucena Ugalde de la Cruz**,

Susana Cárdenas, Roberto Aguilera Angulo, Emily Evans, Marion Cruz, Gabriela Garcia, Hiram Rosales Nanduca, Anidia Blanco Jarvio, Tim Means, Carlos Means, Mark Lowry and Marylin Lowry for their friendship, all our adventures and endless discussions about life. This part of my life is really important to keep me going. I would also like to thank my friends at the lab in La Paz and from CSI, **Leticia Carrillo, Ana Sofia Merina, Carlos Dominguez, Cristina Casillas, Vianney Jimenez, Aurora Paniagua, Emma Elliot-Smith, Sara Foster, Viorel Atudorei, Laura Burkemper, Laura Pages and Dave Vanhorn, Allyson Richins, Mauriel Rodriguez Curras, Mirsha (Ricardo) Mata, John Whiteman, Debora Boro** and all the amazing people that I have met during the road of this PhD life. I would never change the course that I took and you all where there for me, thank you for sharing a part of your life with me.

I would also like to acknowledge the institutions that facilitated the use of tissues samples and issued the permits to collect and process these samples: NOAA-SWFSC, CRC, CICIMAR-IPN, Humboldt State University-Vertebrate Museum, Museo de la Ballena y Ciencias del Mar (La Paz, BCS), the California Department of Parks and Recreation-Prairie Creek Redwoods State Park, NOAA/NMFS and SEMARNAT. I am also very grateful to all the personnel from the former institutions, the Stranding Network of California, and the CSI of the University of New Mexico who participated in the collection and processing of the tissue samples. I would also like to thank the John H. Prescott Marine Mammal Rescue Assistance Grant Program that has provided grants to the stranding networks. Jim Rice, Jerry Loomis, Thorvald Holmes, and Francisco J. Gómez-Díaz collaborated during the process of locating potential baleen plates for this study and I am very beholden for their support. We would also like to give special recognition to Kelly Robertson who helped with the logistics of sample selection and the sex identification of an important baleen sample at the genetics lab in SWFSC.

All whale tissues used in this study were collected and processed under special permits issued by the Secretaría de Medio Ambiente y Recursos Naturales (SEMARNAT) in México (codes: 180796-213-03, 071197- 213-03, DOO 750-00444/99, DOO.0-0095, DOO 02.-8318, SGPA/DGVS-7000, 00624, 01641, 00560, 12057, 08021, 00506, 08796, 09760, 10646, 00251, 00807, 05036, 01110, 00987; CITES export permit: MX 71395), and the National Oceanic and Atmospheric Administration–National Marine Fisheries Service (NOAA/NMFS) (NMFS MMPA/Research permits codes: NMFS-873; 1026; 774-1427; 774-1714; 14097; 16111; CITES import permit: 14US774223/9) in the United States of America.

THESIS ACHIEVEMENTS

PEER-REVIEWED PUBLICATION:

Busquets-Vass G., S. D. Newsome, J. Calambokidis, G. Serra-Valente, J. K. Jacobsen, S. Aguíñiga-García & D. Gendron. 2017. **Estimating blue whale skin isotopic incorporation rates and baleen growth rates: Implications for assessing diet and movement patterns in mysticetes.** PLoS ONE 12(5): e0177880. <https://doi.org/10.1371/journal.pone.0177880>

MANUSCRIPT IN PREPARATION:

Busquets-Vass G., S. D. Newsome, J. Calambokidis, G. Serra-Valente, J. K. Jacobsen, S. Aguíñiga-García & D. Gendron. 2017. **Isotopic niche width of the blue whale in the eastern Pacific Ocean.**

Busquets-Vass G., S. D. Newsome, J. Calambokidis, G. Serra-Valente, J. K. Jacobsen, S. Aguíñiga-García & D. Gendron. 2017. **Feeding ecology of the blue whale in the northeast Pacific Ocean inferred by stable isotopes of nitrogen.**

PRESENTATIONS:

Busquets-Vass, G. R., S. D. Newsome, J. Calambokidis, S. Aguíñiga-García, G. Serra-Valente, J. K. Jacobsen & D. Gendron. 2016. **Trophic overlap between blue whale foraging zones in the eastern Pacific Ocean.** XXXV Reunión Internacional para el estudio de los mamíferos marinos. La Paz, Baja California Sur, Mexico, May 1-5, 2016. Oral presentation.

Busquets-Vass, G. R., S. D. Newsome, J. Calambokidis, S. Aguíñiga-García, G. Serra-Valente, J. K. Jacobsen & D. Gendron. 2015. **Foraging ecology and movement patterns of blue whales in the eastern Pacific Ocean inferred by stable isotopes.** Abstract (Proceedings) 21st Biennial Conference on the Biology of Marine Mammals, San Francisco, California, December 14-18, 2015. Poster presentation.

Busquets-Vass, G. R., S. D. Newsome, J. Calambokidis, S. Aguíñiga-García, G. Serra-Valente, J. K. Jacobsen & D. Gendron. **Feeding ecology of the blue whale in the northeast Pacific.** TV Interview: Tiempo de Ciencia, CONACYT-CIB. Available online: <https://www.youtube.com/watch?v=sfoAGn7Wa54>

SUBVENTIONS:

American cetacean society - Monterey Bay chapter request for grant proposals. May 2014. This subvention was used specifically for stable isotope analysis of blue whale skin samples. **\$1500 U.S. dollars.**

Cetacean Society International. September 2014. This subvention was used specifically for stable isotope analysis of blue whale baleen plates. **\$1000 U.S. dollars.**

AWARDS:

2015-2016- Outstanding Academic Achievement of the year 2015-2016. Award granted for having the highest GPA (10/10).

2016- Best PhD oral presentation: Busquets-Vass, G. R., S. D. Newsome, J. Calambokidis, S. Aguiñiga-García, G. Serra-Valente, J. K. Jacobsen & D. Gendron. 2016. Trophic overlap between blue whale foraging regions in the eastern Pacific **Ocean**. XXXV Reunion Internacional para el estudio de los mamíferos marinos. La Paz, Baja California Sur, Mexico. May 1-5, 2016.

(SEE APPENDIX X)

LIST OF FIGURES

Figure 1. Blue whale. The mottled bluish-grey skin color pattern is unique to each individual whale. **A.** Blue whale photographed in 1996. **B.** The same blue whale photographed in 2005. Red circles show a section of the mottled pattern to demonstrate that it does not change over time.....1

Figure 2. Distribution of blue whale song (or call type) worldwide, classified into nine regional types (1 to 9). (Image modified and reprinted from McDonald *et al.*, 2006).....2

Figure 3. Eastern Pacific Ocean. A) Eastern Pacific Ocean limits (image modified and reprinted from OET & NOAA-OER workshop). B) Eastern Pacific Ocean major surface currents (image modified and reprinted from Tomczak & Godfrey, 2003).....25

Figure 4. Eastern Pacific Ocean sampling zones. Dots represent blue whale skin samples collected in the California Current System (CCS), Gulf of California (GC), Costa Rica Dome (CRD), and Galapagos/Peru (GALPE). Dots with a cross represent blue whale baleen plates collected from six dead stranded whales (stranding data for one whale was not available).....33

Figure 5. Krill and lanternfish samples collected in the Gulf of California and Galapagos. Dots represent krill (red) and lanternfish (black) samples collected in: A) Gulf of California (GC) and B) Galapagos (GAL).....34

Figure 6. Methods for blue whale skin and baleen plate preparation. (A) Skin biopsy separation into strata: Stratum Basale (SB), Stratum Spinosum (SS) Stratum Externum (SE). The dermal papillae (DP) can be observed embedded in the skin. Dashed lines show where the cuts were made to separate the skin into strata. (B) Blue whale baleen plate sampling: baleen powder was sub-sampled in 1 cm intervals along the outer edge of the plate starting from the proximal section of the plate nearest the gum.....36

Figure 7. GLM analysis relating skin $\delta^{15}\text{N}$ values to time (Julian Date, presented in years). Points represent the actual $\delta^{15}\text{N}$ values of blue whale skin collected in different zones of the northeast Pacific. Lines represent the fit of the GLM model and the fringe around the lines show the 95% confidence intervals. The gray shaded area represents the mean \pm SD of the trophic-corrected blue whale skin values for each foraging zone; Gulf of California (GC), California Current System (CCS), and Costa Rica Dome (CRD).....53

Figure 8. GAM analysis of the seasonal trend of skin strata $\delta^{15}\text{N}$ values in two foraging zones. The points represent the actual $\delta^{15}\text{N}$ values of skin collected from whales within the Gulf of California (open circles) and the California Current System (open triangles). The colored lines represent the GAM model fit (predictions) and the fringe around the lines show the 95% confidence intervals. The gray shaded area represents the mean \pm SD of the trophic-corrected blue whale skin values for each foraging zone: Gulf of California (GC), the California Current System (CCS) and the Costa Rica Dome (CRS).....54

Figure 9. Isotopic niche width (SEA_c) of the blue whale in the eastern Pacific Ocean. The ellipses represent the isotopic niche width area of the Gulf of California (blue), California Current System (green), Costa Rica Dome (red) and Galapagos/Peru (orange).....58

Figure 10. Isotopic niche width (SEAc) of female and male blue whales in the eastern Pacific Ocean. The ellipses represent the isotopic niche width area of the females (red) and males (black) in the: A. NEP (northeast Pacific) and B. SEP (southeast Pacific).....60

Figure 11. Bayesian dietary isotopic mixing model results: Scaled posterior densities of the probability of the proportional contributions of different sources (zones) to consumer's diet (blue whale). A. Bayesian Mixing Model using a $\Delta^{15}\text{N}:1.6\pm0.5\text{‰}$; B. Bayesian Mixing Model using a $\Delta^{15}\text{N}:1.9\pm0.3\text{‰}$. CCS, California Current System; CRD, Costa Rica Dome; GC, Gulf of California.....62

Figure 12. $\delta^{15}\text{N}$ values along the baleen plates from six whales, identified as A–F. Points represent actual values. The continuous line (blue: males; red: females) represents the GAM model fit and the narrow fringe around the lines represent the 95% confidence intervals. The gray shaded area represents the mean \pm SD of the trophic-corrected blue whale skin values for each foraging zone: Gulf of California (GC), the California Current System (CCS) and the Costa Rica Dome (CRS).....66

Figure 13. $\delta^{15}\text{N}$ and $\delta^{13}\text{C}$ values along the baleen plates from the female calf, baleen code G. Points represent actual values. The continuous line represents the GAM model fit and the narrow fringe around the lines represent the 95% confidence intervals. The gray shaded area represents the mean \pm SD of the $\delta^{15}\text{N}$ trophic-corrected blue whale skin values for each foraging zone: Gulf of California (GC), the California Current System (CCS) and the Costa Rica Dome (CRS).....67

Figure 14. Isotopic niche width (SEAc) of the seven blue whale baleen plates (A to G). The ellipses represent the isotopic niche width area of the baleen plate of each whale.....68

Figure 15. GAM analysis relating skin $\delta^{13}\text{C}$ values to Julian day (presented in months). The points represent the actual $\delta^{13}\text{C}$ values of skin collected from whales within the Gulf of California (open circles) and the California Current System (open triangles). Lines represent the fit (projections) of the GAM model and the fringe around the lines show the 95% confidence intervals.....71

Figure 16. $\delta^{13}\text{C}$ values along the baleen plates from six whales, identified as A-F. Points represent actual values, the continuous line (blue: males; red: females) represents the GAM model fit and the fringe around the lines show the narrow 95% confidence intervals.....72

LIST OF TABLES

Table 1. Skin samples (Skin biopsies and sloughed skin) collected in the eastern Pacific Ocean, selected from three tissue banks (NOAA-SWFSC, CRC, and CICIMAR-IPN). CCS, California Current System; GC, Gulf of California; CRD, Costa Rica Dome; GALPE, Galapagos/Peru.....32

Table 2. Max-*t* test results comparing the effect of different treatments on skin $\delta^{15}\text{N}$, $\delta^{13}\text{C}$ and weight percent C/N ratios. LE, lipid-extracted skin; Diff, estimated differences between group means; CI, confidence intervals; SE, Standard error; *t*, test value; *P*, adjusted p values reported, values in bold were considered statistically significant (<0.05).....47

Table 3. Max-*t* test results for the comparison of $\delta^{13}\text{C}$ and $\delta^{15}\text{N}$ values among different skin strata in the Gulf of California (GC) and California Current System (CCS). δ , isotope; Diff, estimated differences between group means; CI, confidence intervals; SE, Standard error; *t*, test value; *P*, adjusted p values reported, values in bold were considered statistically significant (<0.05).....48

Table 4. GLM results relating blue whale skin $\delta^{15}\text{N}$ values to time (Julian date) in the Gulf of California (GC), California Current System (CCS) and Costa Rica Dome (CRD). α , intercept parameter; β , slope parameter; SME, standard error of the mean; CL, confident intervals of the mean; *t*, test values; *P*, p values reported, values in bold were considered statistically significant (<0.05); ^a time, in the model represents number of days.....51

Table 5. Trophic-corrected blue whale skin $\delta^{15}\text{N}$ values for each foraging zone. Values were estimated by using the prey zone mean \pm SD (Table 6) and assuming $\Delta^{15}\text{N}$ of 1.6‰.....51

Table 6. Mean (\pm SD) $\delta^{13}\text{C}$, $\delta^{15}\text{N}$, and weight percent C/N ratios of potential blue whale prey in the eastern Pacific Ocean. *N.s.*, *Nyctiphanes simplex*; Lf, Lanterfish; *T.s.*, *Thysanoesa spinifera*; *E.p.*, *Euphausia pacifica*.....52

Table 7. GAM results for the seasonal trends of $\delta^{15}\text{N}$ and $\delta^{13}\text{C}$ values in different skin strata sampled in the Gulf of California (GC) and California Current System (CCS). *E.df.*, Estimated degrees of freedom; F, test of whether the smoothed function significantly reduces model deviance; *P*, p-values in bold were considered statistically significant (<0.05).....55

Table 8. $\delta^{15}\text{N}$ isotopic incorporation rates of blue whale skin strata in the Gulf of California and California Current System. The number of days were estimated by extrapolating from the GAM predictions (model fit and the upper and lower 95% confidence limits) for skin $\delta^{15}\text{N}$ values to change by 1.6‰ to isotopically equilibrate with local prey in each zone.....56

Table 9. $\delta^{15}\text{N}$ and $\delta^{13}\text{C}$ (Mean \pm SD) in the eastern Pacific Ocean. NEP, Northeastern Pacific; SEP, Southeastern Pacific; GC, Gulf of California; CCS, California Current System; CRD, Costa Rica Dome; GALPE, Galapagos/Peru.....57

Table 10. Isotopic niche width (SEA_B and SEA_C) of blue whale skin in the eastern Pacific Ocean. NEP, Northeastern Pacific; SEP, Southeastern Pacific; GC, Gulf of California; CCS, California Current System; CRD, Costa Rica Dome; GALPE, Galapagos/Peru; CI, credibility intervals.....57

Table 11. Trophic overlap between different zones in the eastern Pacific Ocean. GC, Gulf of California; CCS, California Current System; CRD, Costa Rica Dome; GALPE, Galapagos/Peru.....58

Table 12. Isotopic niche width (SEA_B and SEA_C) of female and male blue whales skin in the eastern Pacific Ocean. NEP, Northeastern Pacific; SEP, Southeastern Pacific; CI, credibility intervals.....59

Table 13. Trophic overlap between female and male blue whales in the eastern Pacific Ocean. NEP, northeast Pacific; SEP, southeast Pacific.....59

Table 14. Probability of the proportional contributions (%) of different sources (zones) to consumer’s diet (blue whales in the NEP). GC, Gulf of California; CCS, California Current System; CRD, Costa Rica Dome; CI, credibility intervals.....61

Table 15. Information of baleen plates collected from seven blue whales (A–G). ND, no data.....64

Table 16. GAM results to assess the fluctuations of $\delta^{15}N$ and $\delta^{13}C$ in baleen plates. *E.df.*, Estimated degrees of freedom; *F*, test of whether the smoothed function significantly reduces model deviance; *P*, p-values in bold were considered statistically significant (<0.05).....65

Table 17. Blue whale baleen growth rate: estimated by using the distance between sequential $\delta^{15}N$ minimums along the baleen plates from whales A to C......65

Table 18. Mean (\pm SD) $\delta^{13}C$, $\delta^{15}N$ and weight percent C/N ratios of blue whale baleen plates collected from stranded whales......67

Table 19. Isotopic niche width (SEA_B and SEA_C) of blue whale skin in the eastern Pacific Ocean. CI, credibility intervals.....68

Table 20. Trophic overlap between different baleen of blue whales identified as A to G......69

GLOSSARY

Anabolism: Metabolic pathways that require inputs of energy. It includes all the reactions that require energy –such as the synthesis of glucose, fats, or DNA– they are called anabolic reactions or anabolism (constructive metabolism). The useful forms of energy that are produced in catabolism are employed in anabolism to generate complex structures from simple ones, or energy-rich states from energy-poor ones (Berg *et al.*, 2002).

Baleen growth rate: Rate of deposition and formation of the transverse ridges of keratin that constitute the baleen plates from mysticetes. Baleen grow from the gums down, but also abrade at the terminal end, therefore the tissue has a growth rate and a wear rate. Ridges inrorqual baleen are believed to form annually (Lockyer, 1981; Schell *et al.*, 1989b).

Baleen plates: Baleen consists of transversely oriented keratin plates (inert tissue) that are attached to the lateral parts of the upper jaw of mysticetes, leaving open a portion off the palate along its midline. Thus, baleen forms two masses hanging from the upper jaw in the form of a comb, one on each side of the oral cavity. Typically, mysticetes can have approximately 300 plates in each side of the upper jaw (Perrin *et al.*, 2002; Berta *et al.*, 2006). Baleen plates are largest in the middle part of the jaw and decrease in size towards both the anterior and posterior part of the mouth. Baleen are enclosed by a grey-white substance, known as *Bartenzwischensubstanz*, and it also fills the space between the base of each neighboring plate (Fudge *et al.*, 2009).

Catabolism: Metabolic pathways that convert energy into biologically useful forms. It includes the reactions that transform fuels into cellular energy, or catabolic reactions, more generally called catabolism (destructive metabolism). During these reactions, complex molecules are broken into smaller parts, and therefore are oxidized to

release energy, or allocate it to other metabolic processes (*i.e.* anabolism) (Berg *et al.*, 2002).

Delta (δ): Stable isotope ratios (*e.g.* $^{13}\text{C}/^{12}\text{C}$; $^{15}\text{N}/^{14}\text{N}$) are usually expressed as delta (δ) values, the normalized ratio of an unknown sample to an internationally accepted standard (Newsome *et al.*, 2010). It is calculated from the ratio-of-ratios: $\delta^{13}\text{C}$ or $\delta^{15}\text{N} = 1000 [(R_{\text{sample}} / R_{\text{standard}}) - 1]$, where $R = ^{13}\text{C}/^{12}\text{C}$ or $^{15}\text{N}/^{14}\text{N}$ ratio of sample and standard. Values are in units of parts per thousand or per mil (‰) and the internationally accepted standards are atmospheric N_2 for $\delta^{15}\text{N}$ and Vienna-Pee Dee Belemnite limestone (V-PDB) for $\delta^{13}\text{C}$ (Fry, 2006).

Metabolic energy: Energy is generally defined in terms of potential capacity to perform work, is an abstraction that can be measured only in its transformation from one form to another (Kleiber, 1975). To perform work, cells require a constant supply of metabolic energy. The energy-rich molecule adenosin triphospate (ATP) usually provides this energy. All cells can generate ATP by breaking down organic nutrients (carbohydrates, lipids, and proteins) (Nelson & Michael, 2005; Miller & Harley, 2009).

Feeding ecology: The processes that determine the general diet of organisms. These processes include physiological, morphological, behavioral and environmental factors that influence diet selection (Carss, 1995).

Isotope: Atoms of the same element that have the same number of protons (z) and electrons (e^-), but have a different atomic mass (A), or number of neutrons (N). In nature, there are heavy and light isotopes. Heavy isotopes are atoms that have more neutrons (N) compared to the light isotopes, and are less abundant than light isotopes. The difference in mass between the heavy and the light isotopes of the same element confers them different fractionation properties, and thus its distribution in the ecosystems and biological systems is distinct (Unkovich *et al.*, 2001; Fry, 2006).

Isotopic incorporation rate: The rate of elemental incorporation into animal tissues. Tissues assimilate dietary nutrients at different temporal scales. The isotopic incorporation rate, is the time that takes for a tissue to incorporate the specific stable isotope ratios of any food source (Newsome *et al.*, 2010). This rate is approximately proportional to body mass (m_b) to the $3/4$ power (Martínez del Río & Wolf, 2005; Martínez Del Río *et al.*, 2009).

Isotopic niche: Isotopic niche is an area (in δ -space) with isotopic values (δ -values) as coordinates. The isotopic niche of organisms can be estimated by using Standard Isotopic Bayesian Ellipses Areas, measured in ‰^2 units (Jackson *et al.*, 2011). A common tool to estimate these ellipses is the package SIBER in R language (Stable Isotope Bayesian Ellipses in R). The areas of the ellipses represent the isotopic niche width (or isotopic niche space), and are produced by estimating the co-variance matrix of $\delta^{13}\text{C}$ and $\delta^{15}\text{N}$, which is the equivalent to the standard deviation for univariate data (Jackson *et al.*, 2011).

Radioactive isotope: Unstable isotopes that decompose by emission of nuclear electrons or helium nucleus and radiation, thus becoming a stable nuclear composition. During decay alpha particles, beta particles, and gamma particles may be emitted (Poulsen, 2010).

Skin: The integument of an animal. This tissue is the external limiting layer that protects the body of animals from the environment. It is formed by the dermis and epidermis. The dermis provides structural support to the epidermis. The epidermis serves as the physical and chemical barrier between the interior body and the external environment, the epidermis is constituted by different layers of cells or stratum (basale, spinosum and externum). The outermost layers of skin (stratum externum) is continuously sloughed to environment as sloughed skin (Geraci *et al.*, 1986; Brodell & Rosenthal, 2008).

Stable isotope: Isotopes that are relatively stable and do not decompose or decay through time (Fry, 2006; Poulsen, 2010).

Stable isotope mixing models: Models that are designed to estimate the relative contribution of a set of isotopically distinct dietary resources to a consumer's diet, based on their respective isotope values. There are several statistical packages that can be used to apply these models. MixSIAR GUI is a graphical user interface in R that allows to develop and run Bayesian stable isotope mixing models (Semmens *et al.*, 2009; Parnell *et al.*, 2010). This package incorporates several years of advances in Bayesian mixing models. The Bayesian framework improve upon simple linear models by taking into account the uncertainty in source values and prior information Semmens *et al.*, 2009; Parnell *et al.*, 2010).

Trophic discrimination: In trophic studies, trophic discrimination denotes the difference between the isotopic composition of a consumer and its diet. These differences are product of metabolic fractionation of the heavy and the light isotopes. Trophic discrimination is estimate by using the formula: $\Delta {}^hX_{A-B} = \delta {}^hX_A - \delta {}^hX_B$, where A is the consumer's tissue, B is the diet and hX is the isotope system of interest (Martínez Del Rio *et al.*, 2009; Newsome *et al.*, 2010).

Trophic level: A trophic level refers to a level or a position in a food web. Each level is occupied by organisms that have similar dietary requirements. The relative trophic position of an organism is determined by the distance between the organism and the direct use of solar energy. Trophic level 1 in any given food web is occupied by primary producers (Odum & Barrett, 2004).

Vagrant: (zoology) a migratory animal that is off course (Collins English Dictionary, 2014).

Zone: An area characterized by a particular set of organisms whose presence is determined by environmental conditions (Collins English Dictionary, 2014).

ABSTRACT

Blue whales in the eastern Pacific Ocean migrate between ecosystems that exhibit contrasting baseline nitrogen ($\delta^{15}\text{N}$) and carbon ($\delta^{13}\text{C}$) isotope values and these differences are reflected in their prey. I hypothesized that blue whale tissues also record these isotopic differences, and thus provide insights into the feeding ecology and seasonal movement patterns of this species. To test this, I analyzed the $\delta^{15}\text{N}$ and $\delta^{13}\text{C}$ values of blue whale skin ($n = 444$) and baleen plates ($n = 7$) collected in the northeast Pacific (California Current System, Gulf of California and Costa Rica Dome), and skin ($n = 25$) collected in the southeast Pacific (Galapagos/Peru), from 1996 to 2015. Skin $\delta^{15}\text{N}$ exhibited regional gradients: Gulf of California ($14.8 \pm 0.9\text{‰}$), California Current System ($13.3 \pm 0.9\text{‰}$), Costa Rica Dome ($12.1 \pm 1\text{‰}$) and Galapagos-Peru ($7.4 \pm 0.9\text{‰}$). These gradients were in accordance with those of their potential prey within each foraging zone, demonstrating that blue whale skin $\delta^{15}\text{N}$ values can be used to make inferences of this species' diet. Isotopic niche metrics (Standard Bayesian Ellipse Areas- ‰^2) showed a trophic overlap (0.1-0.2%) among the first three zones (Gulf of California, California Current System, and Costa Rica Dome). This trophic overlap could be attributed to the isotopic turnover of the skin (163 ± 91 days), which I indirectly estimated by using a generalized additive model of the seasonal trends in $\delta^{15}\text{N}$ skin strata (stratum basale, externum and sloughed skin) collected in the Gulf of California and California Current System. $\delta^{15}\text{N}$ range (5-9‰) and isotopic niche width of whale skin in Galapagos/Peru did not overlap (0%) with the other zones, indicating that these whales generally did not feed further north. In the northeast Pacific, two Bayesian dietary mixing models (MixSIAR) revealed that the relative contribution of the California Current System and Gulf of California to the blue whale's diet was 30–35 % and 47–54 %, respectively, suggesting that blue whales forage intensively in both zones. The contribution from the Costa Rica Dome (16–18 %) was lower, indicating that feeding is less intense in this zone. A mean ($\pm\text{SD}$) baleen growth rate of $15.5 \pm 2.2 \text{ cm y}^{-1}$ was estimated by using seasonal oscillations in $\delta^{15}\text{N}$ values along baleen from three whales (two females and one male). These oscillations also showed some individual whales have a high fidelity to

specific foraging zones in the northeast Pacific across years. The absence of oscillations in $\delta^{15}\text{N}$ values along the baleen from three male whales suggests these individuals remained within a specific zone for several years prior to death. $\delta^{13}\text{C}$ values of both whale tissues (skin and baleen) and prey were not distinct among foraging zones. An exception to the latter patterns were the $\delta^{13}\text{C}$ values of the baleen plate from a calf, that were $\sim 2\text{‰}$ lower than adult whales. This pattern is probably driven by the nutrient transfer during lactation, given that maternal milk has a high lipid content, and lipids have lower $\delta^{13}\text{C}$ values. This pattern has also been described in different marine mammal tissues (e.g. bone collagen and teeth). The $\delta^{15}\text{N}$ oscillation in the baleen of this calf could be reflecting the weaning period, when the calf switches diet, from milk to zooplankton. The results of this study provide new insights into the feeding ecology in terms of the use of different feeding zones, individual seasonal movement strategies that are potentially sex-specific, and tissue physiology (isotopic incorporation rate of skin, baleen growth rate, and mother-to-offspring transfer of nutrients during lactation) of blue whales in the eastern Pacific Ocean.

RESUMEN

Las ballenas azules en el Océano Pacífico oriental migran entre ecosistemas que exhiben valores isotópicos de nitrógeno ($\delta^{15}\text{N}$) y carbono ($\delta^{13}\text{C}$) contrastantes a nivel de la base de la red trófica y estas diferencias se reflejan en sus presas. Se hipotetizó que los tejidos de ballena azul registran estas diferencias isotópicas y por lo tanto proporcionar información de la ecología alimentaria y los patrones de movimiento estacionales de esta especie. Para probar esta hipótesis, se analizaron los valores de $\delta^{15}\text{N}$ y $\delta^{13}\text{C}$ en piel de ballena azul ($n = 444$) y barbas ($n = 7$) colectadas en el Pacífico nororiental (Sistema de la Corriente de California, Golfo de California y Domo de Costa Rica), y piel ($n = 25$) colectada en el Pacífico suroriental (Galápagos/Perú) de 1996 a 2015. El $\delta^{15}\text{N}$ en piel exhibió gradientes regionales: Golfo de California ($14.8 \pm 0.9\text{‰}$), Sistema de la Corriente de California ($13.3 \pm 0.9\text{‰}$), Domo de Costa Rica ($12.1 \pm 1\text{‰}$) y Galápagos-Perú ($7.4 \pm 0.9\text{‰}$). Estos gradientes fueron consistentes con los de sus presas potenciales en cada zona de alimentación, demostrando que los valores de $\delta^{15}\text{N}$ en piel de ballena azul son útiles para realizar inferencias sobre la dieta de esta especie. Las medidas de nicho isotópico (Áreas Estándar de Elipses Bayesianas- ‰^2) mostraron una superposición trófica (0.1-0.2%) entre las tres primeras regiones (Golfo de California, Sistema de la Corriente de California y Domo de Costa Rica). Esta superposición trófica se asoció a la tasa de incorporación isotópica de la piel (163 ± 91 días), que se estimó utilizando un modelo aditivo generalizado de las tendencias estacionales en el $\delta^{15}\text{N}$ de las capas de la piel (capa basal, externa y piel descamada) colectada en el Golfo de California y el Sistema de la Corriente de California. El rango de $\delta^{15}\text{N}$ (5-9‰) y la amplitud del nicho isotópico de la piel de ballena en Galápagos/Perú no se solaparon (0%) con las otras regiones, indicando que estas ballenas azules generalmente no se alimentan en zonas norteñas. En el Pacífico nororiental, dos modelos de dieta Bayesianos (MixSIAR) mostraron que la contribución relativa del Sistema Corriente de California y del Golfo de California a la dieta de la ballena azul fue de 30–35 % y 47–54 %, respectivamente, lo que sugiere que estas ballenas se alimentan intensamente en ambas zonas. La contribución relativa del Domo de Costa Rica

(16–18 %) fue menor, lo que indica que las ballenas se alimentan en menor intensidad en esta zona. La tasa de crecimiento de las barbas de ballena azul fue 15.5 ± 2.2 cm año⁻¹. Esta tasa de crecimiento se estimó mediante el uso de las oscilaciones estacionales de $\delta^{15}\text{N}$ a lo largo de las barbas de tres ballenas (dos hembras y un macho). Estas oscilaciones indican que algunos individuos de ballena azul tienen una alta fidelidad a zonas específicas en el Pacífico nororiental a través de los años. La ausencia de oscilaciones en $\delta^{15}\text{N}$ a lo largo de las barbas de tres machos sugiere que estos individuos permanecieron dentro de una zona específica durante varios años antes de su muerte. El $\delta^{13}\text{C}$ en tejidos de las ballenas (piel y barbas) y presas no fueron contrastantes entre las diferentes zonas de alimentación. Una excepción a este patrón fueron los valores de $\delta^{13}\text{C}$ de la barba de una cría, que fueron ~2‰ menores que en los adultos. Este patrón probablemente está asociado a la transferencia de nutrientes durante la lactancia, dado que la leche tiene un alto contenido de lípidos y estos lípidos tienen valores bajos de $\delta^{13}\text{C}$. Este mismo patrón se ha descrito en otros tejidos (e.g. colágeno de huesos y dientes) de mamíferos marinos. La oscilación del $\delta^{15}\text{N}$ de la barba de la cría podría estar reflejando el periodo de destete, durante el cual la cría cambia de dieta, de leche a zooplancton. Los resultados de este estudio proporcionan nuevas perspectivas sobre la ecología alimentaria en términos de uso de diferentes zonas de alimentación, las estrategias de movimiento estacional individuales que potencialmente son sexo-específicas y la fisiología de los tejidos (tasa de incorporación isotópica de la piel, tasa de crecimiento de las barbas y transferencia de nutrientes durante la lactancia) de las ballenas azules en el Océano Pacífico oriental.

1. INTRODUCTION

The blue whale (*Balaenoptera musculus*) is an endangered migratory marine mammal (Reilly *et al.*, 2008a) that is classified in the Infraorder Cetacea, Parvorder Mysticeti (Baleen whales), Family Balaenopteridae (Rorquals) (Berta & Sumich, 2006). This species can measure up to 30 meters in total length (Berta & Sumich, 2006) and weigh ~57 tons (Barlow *et al.*, 2008), hence is also referred to as the largest mammal on Earth (Berta & Sumich, 2006). One of the main characteristics of the species is its mottled bluish-grey skin color, which is unique to each whale, allowing to identify them individually by using photographic-identification (Fig. 1) (Sears, 1987). Blue whales are distributed worldwide. McDonald *et al.* (2006) suggested that blue whale song, or call types, can be used to identify populations, and described nine call types worldwide (Fig. 2).

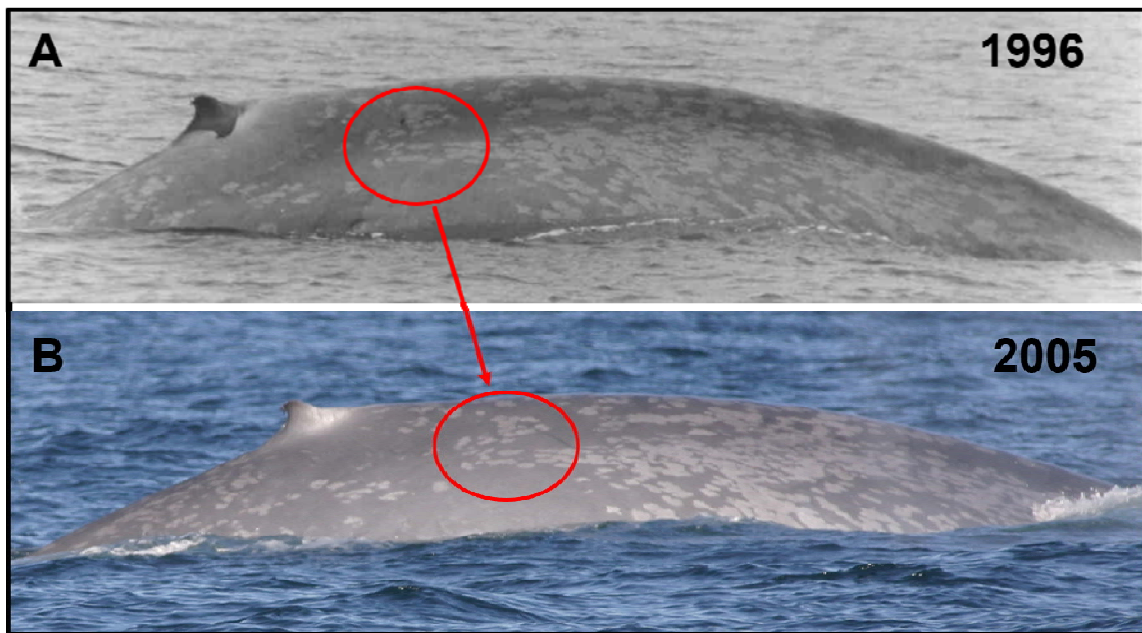


Figure 1. Blue whale. The mottled bluish-grey skin color pattern is unique to each individual whale. **A.** Blue whale photographed in 1996. **B.** The same blue whale photographed in 2005. Red circles show a section of the mottled pattern to demonstrate that it does not change over time.

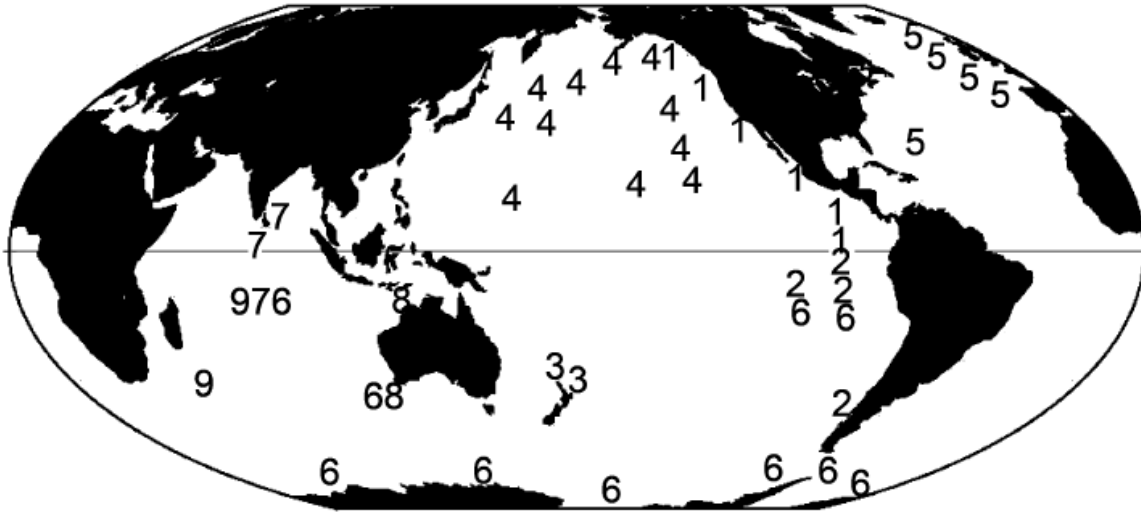


Figure 2. Distribution of blue whale song (or call type) worldwide, classified into nine regional types (1 to 9). (Image modified and reprinted from McDonald *et al.*, 2006).

In the eastern Pacific Ocean, there are still many gaps in our understanding of the feeding ecology and seasonal movement patterns of the blue whale. In the northeast Pacific (NEP) the sampling effort (*i.e.* cetacean surveys, tagging individual whales, and tissue collection) has been greater compared to the southeast Pacific (SEP). Acoustic recordings on call type (Stafford *et al.*, 2001), photographic-identification (Calambokidis *et al.*, 2009a), and satellite track (Bailey *et al.*, 2009) data suggest that the blue whales observed within the NEP are a separated population from the blue whales in the northwest Pacific. Thus, they can be divided into the putative northeast (*i.e.* California feeding population) and northwest populations.

In the NEP, during summer and fall, blue whales are distributed as far north as the Gulf of Alaska (Rice, 1974; Calambokidis *et al.*, 2009a; Bailey *et al.*, 2009), but the highest aggregations have been observed off southern California (Calambokidis & Barlow, 2004). By mid-fall (~October), blue whales usually migrate south to the west coast of the Baja California Peninsula (Reilly & Thayer, 1990; Mate *et al.*, 1999; Calambokidis & Barlow, 2004; Etnoyer *et al.*, 2004, 2006; Bailey *et al.*, 2009) and then continue migrating to one of two regions that are recognized as overwintering

zones: a calving ground in the Gulf of California (Tershy *et al.*, 1990; Gendron, 2002; Sears *et al.*, 2013; Pardo *et al.*, 2013), or the Costa Rica Dome, in the eastern tropical Pacific (Reilly & Thayer, 1990; Mate *et al.*, 1999; Bailey *et al.*, 2009). Blue whales are present year round in the Costa Rica Dome (Reilly & Thayer, 1990), and calves have been occasionally observed, but little is known about the population dynamics in this zone (Hoyt, 2009). The general migratory patterns of blue whales in the NEP were initially described by Rice (1974) and subsequently complemented with satellite tracks from individual blue whales (Mate *et al.*, 1999; Etnoyer *et al.*, 2004, 2006; Bailey *et al.*, 2009; Hazen *et al.*, 2016), cetacean surveys, and photographic-identifications (Reilly & Thayer, 1990; Carretta *et al.*, 2000; Gendron, 2002; Calambokidis, 2009; Calambokidis *et al.*, 2009a; Ugalde de la Cruz, 2015). However, there are still many gaps in our understanding of individual movement patterns across multi-year timescales.

Blue whales in the NEP forage throughout their annual migratory cycle mainly on aggregations of krill (Order: Euphausiacea) (Nemoto & Kawamura, 1977; Gendron, 1990, 2002; Schoenherr, 1991; Del Angel-Rodríguez, 1997; Fiedler *et al.*, 1998; Croll *et al.*, 2005; Matteson, 2009; Jiménez-Pinedo, 2010) and occasionally on other crustaceans (*i.e.* copepods, *Calanus* spp.; pelagic red crab *Pleurocondes planipes*) (Nemoto & Kawamura, 1977; Calambokidis & Steiger, 1997) or small fish (*i.e.* lanternfish: Family Myctophidae) (Jiménez-Pinedo, 2010). The observation that blue whales forage year-round suggests that this species has high energetic demands relative to other migratory mysticetes like the humpback whale (*Megaptera novaeangliae*) (Baraff *et al.*, 1991) and the gray whale (*Eschrichtius robustus*) (Oliver *et al.*, 1983), that typically fast for months during their breeding season in low latitudes. Even though there is evidence that blue whales forage year-round in the NEP, the relative contribution of different foraging zones to the species diet has never been estimated.

In the southeast Pacific Ocean (SEP) there are potentially two breeding population units or subspecies, the Antarctic and the Chilean populations

(Torres-Florez *et al.*, 2014). The presence of Antarctic blue whales in SEP and in the eastern tropical Pacific have only been described by acoustic records (Stafford *et al.*, 2004; Torres-Florez *et al.*, 2014), therefore it has been suggested that the whales that produce these vocalizations are vagrants or admixed individuals (Torres-Florez *et al.*, 2014). In the case of the Chilean population, the evidence obtained via blue whale surveys (aerial and boat-based), genetic analysis, photo-identification techniques, and satellite-tracking suggests that these whales visit Chilean waters to feed and nurse their calves during the austral summer-fall months (December to May) and then migrate to the eastern tropical Pacific to feed (and possibly also reproduce) in the austral winter-spring months (June to November), particularly to the zones near Peru and Galapagos (Hucke-Gaete *et al.*, 2004; Torres-Florez *et al.*, 2014, 2015). Recently, photo-identification techniques revealed that one blue whale photographed and identified in Galapagos migrated to the Costa Rica Dome (Douglas *et al.*, 2015). However, it's still unclear if a large proportion of Chilean whales from the SEP migrate as far as the Costa Rica Dome to feed. If the former assumption was true, these blue whales would exhibit a trophic overlap with the blue whales that visit the Costa Rica Dome. However, whether there is a trophic overlap or the magnitude of this overlap is not known.

Understanding the feeding ecology and seasonal movement patterns of the blue whale can provide insights into the predator-prey interactions, energy transfer in marine food webs, resource partitioning, habitat selection, and population dynamics and structure. This information is critical for the management and conservation of this species. However, obtaining information on these ecological aspects is a challenging task because of the complexity of the life history of the blue whale. Some of the limiting factors are: 1). its wide-range distribution, which difficult the location of the individuals; 2). its migratory patterns, that involve the movement between diverse ecosystems; and 3). its diving behavior, whales spend 75 to 95 % of the time submerged and therefore most of their activities occur underwater (Lagerquist *et al.*, 2000). To overcome some of these limiting factors and obtain information to assess the feeding ecology and seasonal movement patterns of migratory mysticetes at

different spatial and temporal scales, a useful approach has been the use of endogenous markers like stable isotope ratios in mysticetes tissues (Schell *et al.*, 1989a, 1989b; Caraveo-Patiño & Soto, 2005; Caraveo-Patiño *et al.*, 2007; Lysiak, 2009; Newsome *et al.*, 2010; Witteveen *et al.*, 2011, 2012).

Stable isotope ratios (*e.g.* $^{15}\text{N}/^{14}\text{N}$, $^{13}\text{C}/^{12}\text{C}$, $\text{S}^{34}/\text{S}^{32}$, H^2/H^1 , $\text{O}^{18}/\text{O}^{16}$), hereafter referred as isotope values, within animal tissues are intrinsic biogeochemical tracers that can provide information of the diet, relative trophic position, isotopic niche width, trophic overlap, movement patterns, animal physiology, and from the different ecosystems that organisms use (DeNiro & Epstein, 1978, 1981; Gannes *et al.*, 1998; Kelly, 2000; Newsome *et al.*, 2010; Jackson *et al.*, 2011). The isotopic values of the abiotic and biotic components of ecosystems are products of different physical, chemical and metabolic fractionations of the heavy and light isotopes (DeNiro & Epstein, 1978, 1981; Unkovich *et al.*, 2001; Michener & Lajtha, 2007). Primary producers incorporate the baseline isotope values into the food webs of ecosystems (Rau & Anderson, 1981; Rau *et al.*, 1982, 1983; Kline, 1999; Perry *et al.*, 1999; Graham *et al.*, 2010). Physiological processes produce predictable offsets in isotope values between consumers and their diet, which is often called trophic discrimination. In general, consumer tissues have carbon ($\delta^{13}\text{C}$) and nitrogen ($\delta^{15}\text{N}$) isotope values that are 0.5–3.0‰ and 2–5‰ higher than that of their prey respectively, depending on the species, diet quality, and type of tissue analyzed (Schoeller, 1999; Martínez Del Río *et al.*, 2009; Newsome *et al.*, 2010).

Tissues assimilate dietary inputs at different temporal scales. Most metabolically active tissues (*e.g.* blood cells, liver, skin, muscle) reflect recent dietary inputs, consumed within days to months (DeNiro & Epstein, 1978, 1981; Rau *et al.*, 1983; Schoeller, 1999; Vander Zanden & Rasmussen, 2001), depending on their isotopic incorporation rates that typically scale with body mass such that larger animals have slower incorporation rates (Thomas & Crowther, 2015). In contrast, metabolically inert tissues (*e.g.* whiskers, nails, baleen) deposit at distinct intervals, and each deposition of tissue retains the isotopic composition of dietary sources

incorporated when anabolized, thus reflecting dietary input over several years depending on tissue growth rate (Martínez Del Río *et al.*, 2009; Newsome *et al.*, 2010). Consequently, to make accurate inferences on ecological aspects (e.g. feeding ecology and movement patterns) of free ranging animals by using SIA it is essential to have information on the isotopic incorporation rate of metabolically active tissues and the growth rates of metabolically inert tissues; otherwise, the interpretation of the data can be highly misleading.

Skin samples collected via dart biopsy sampling from free-ranging whales (Barrett-Lennard *et al.*, 1996), and baleen plates from stranded mysticetes are typically the type of tissues that can be obtained for stable isotope analysis, and these tissues have been useful to infer diet and seasonal movements of this difficult to study group of cetaceans (Schell *et al.*, 1989a, 1989b; Rowntree *et al.*, 2008; Witteveen *et al.*, 2011, 2012; Matthews & Ferguson, 2013, 2015).

Cetacean skin is divided in a dermis and epidermis. The dermis consists a series of dermal papillae or dermal ridges that are embedder in the epidermis. Dermal ridges are evenly-spaced and aligned parallel, obliquely to the long axis of the body and fins (Harrison & Thurley, 1974). The epidermis is a metabolically active tissue, located above the dermis, and is subdivided into cellular strata: the stratum basale, the stratum spinosum, and the stratum externum (Harrison & Thurley, 1974; Geraci *et al.*, 1986). Skin growth begins in the stratum basale a single row of cells that continuously divide via mitotic divisions. Newly formed cells constantly displace the older cells upward, first to the stratum spinosum, and subsequently to the stratum externum, the outermost layer of skin. Finally, the stratum externum is shed off to the environment, and this skin stratum is called sloughed skin (Harrison & Thurley, 1974; Geraci *et al.*, 1986; Gendron & Mesnick, 2001). The variation in the isotopic composition among these strata has never been described for any cetacean species. The isotopic incorporation rates of cetacean skin have only been measured in controlled “diet switch” feeding experiments on captive odontocetes (Browning *et al.*, 2014; Giménez *et al.*, 2016). These studies used exponential fit models because

theoretically, after diet switch, changes in the isotopic composition of tissues will follow an exponential curve over time (Tieszen *et al.*, 1983; Voigt, 2003; Evans-Ogden *et al.*, 2004; Podlesak *et al.*, 2005). Estimates of the isotopic incorporation for carbon ($\delta^{13}\text{C}$) and nitrogen ($\delta^{15}\text{N}$) in odontocete skin slightly differ; incorporation for $\delta^{13}\text{C}$ is 2 to 3 months, while that for $\delta^{15}\text{N}$ is longer and more variable at 2 to 6 months (Browning *et al.*, 2014; Giménez *et al.*, 2016). The increasing use of stable isotope analysis in mysticetes tissues to characterize diet and movement patterns requires the development of a method to estimate skin isotopic incorporation rates for free-ranging populations.

The integration of different isotopic metrics has allowed to use the isotope values in cetacean skin to model their diet, characterize isotopic niche width and estimate trophic overlap between different groups or species (Semmens *et al.*, 2009; Parnell *et al.*, 2010; Jackson *et al.*, 2011; Witteveen *et al.*, 2012; Foote *et al.*, 2013). Dietary isotopic mixing models currently can be analyzed in a Bayesian framework (e.g. using the packages “SIAR” and “MixSIAR” in R) (Semmens *et al.*, 2009; Parnell *et al.*, 2010). These models use the isotopic data from consumers (cetacean) and their potential dietary sources (prey) to estimate the probability of the contribution of each source to the consumers’ diet (Semmens *et al.*, 2009; Parnell *et al.*, 2010). The isotopic niche of organisms (including cetacean) can be estimated by using Standard Isotopic Bayesian Ellipses Areas (e.g. using the package “SIBER” in R), measured in ‰² units (Jackson *et al.*, 2011). The areas of the ellipses represent the isotopic niche width (or isotopic niche space) of organisms, and are produced by estimating the covariance matrix of $\delta^{13}\text{C}$ and $\delta^{15}\text{N}$, which is the equivalent to the standard deviation for univariate data (Jackson *et al.*, 2011). The trophic overlap between groups or species can then be calculated by estimating the area of the isotopic niche space that intersects between different groups or species (Jackson *et al.*, 2011). Quantifying the isotopic niche of organisms provides information on resource use, geographic diversity and the degree of trophic overlap among other groups or communities (Newsome *et al.*, 2007). So far, these models have never been used to make inferences on the feeding ecology of blue whales.

Baleen consists of a series of keratin plates inserted in the upper gum of mysticetes that functions as a filter-feeding apparatus (Berta *et al.*, 2006). In contrast to skin, baleen is a metabolically inert tissue that grows continuously from the gums and abrades at the terminal end (Fudge *et al.*, 2009). The oscillations in isotope values along the length of baleen plates can be used to estimate growth rates and generate multi-year records of individual movement strategies, habitat use, and diet (Schell *et al.*, 1989a, 1989b; Best & Schell, 1996; Lee *et al.*, 2005; Mitani *et al.*, 2006; Bentaleb *et al.*, 2011; Matthews & Ferguson, 2015). Baleen growth rates have been estimated in several species of mysticetes (Schell *et al.*, 1989a, 1989b; Best & Schell, 1996; Mitani *et al.*, 2006; Bentaleb *et al.*, 2011; Aguilar *et al.*, 2014), but currently there are no published estimates for blue whale baleen.

Potential prey of blue whales in the NEP (California Current System: west coast of U.S. and Baja California peninsula, Gulf of California, and Costa Rica Dome) and SEP (Galapagos/Peru) have contrasting isotope values (Sydeman *et al.*, 1997; Miller, 2006; Becker *et al.*, 2007; Aurióles-Gamboa *et al.*, 2009, 2013; Hipfner *et al.*, 2010; Williams, 2013; Carle, 2014; Busquets-Vass *et al.*, 2017) due to differences in oceanographic and biogeochemical processes that influence baseline isotope values in these zones (Popp *et al.*, 2007; Aurióles-Gamboa *et al.*, 2009, 2013; Williams, 2013; Williams *et al.*, 2014). Specifically, $\delta^{15}\text{N}$ values of prey (e.g. krill) are higher in the Gulf of California, intermediate in the California Current System, lower in the Costa Rica Dome, and lowest in Galapagos/Peru (Sydeman *et al.*, 1997; Miller, 2006; Becker *et al.*, 2007; Hipfner *et al.*, 2010; Aurióles-Gamboa *et al.*, 2013; Williams, 2013; Carle, 2014). In the present research, I hypothesized that blue whale skin strata (stratum basale, stratum externum, and sloughed skin) and baleen plates record these isotopic differences, and by using the seasonal patterns in isotope values of these tissues I indirectly estimated the isotopic incorporation rate of blue whale skin and baleen growth rates. Then, I characterized the feeding ecology and movement patterns of the eastern Pacific Ocean blue whales at different levels: 1). I determined the isotopic niche width and trophic overlap among blue whales in the NEP and SEP;

2). Estimated the relative contribution of different foraging zones to the blue whale's diet in the NEP; 3). Inferred the movement patterns of blue whales in the NEP by using the oscillations along baleen plates; and 4). I also assessed if carbon isotopes ($\delta^{13}\text{C}$) were useful for examining blue whale diet and movement patterns in the eastern Pacific Ocean, however, I expected little variation in $\delta^{13}\text{C}$ values of prey among foraging zones based on previous studies of zooplankton in these zones (Sydemann *et al.*, 1997; Miller, 2006; Becker *et al.*, 2007; Aurióles-Gamboa *et al.*, 2009, 2013; Hipfner *et al.*, 2010; Williams, 2013; Carle, 2014). Overall, the results of this study provide new insights into the tissue physiology, feeding ecology, and individual foraging strategies of the blue whales in the eastern Pacific Ocean.

2. BACKGROUND

The blue whale is classified as “endangered” in the red list of the International Union for Conservation of Nature (IUCN) (Reilly *et al.*, 2008af). To dimension the importance of the remaining blue whale populations today, it is important to mention the past interactions of humans with this species during the whaling era. This species, like many other cetacean species, was almost hunted to extinction during the whaling era because of the great value of whale oil. In the second half of the nineteenth century and throughout the first half of the twentieth century, the development of modern whaling techniques made it possible to hunt the large whales or “Great Whales”, and eventually the blue whale became one of the main targets because it yielded a much larger amount of whale oil, meat, and baleen. Blue whale populations were protected at different years, but by the 1966 blue whale hunting was banned worldwide by the International Whaling Commission (IWC), although illegal whaling continued until the 1970s (Calambokidis *et al.*, 2009b; Mikhalev, 1997; Reilly *et al.*, 2008a). Approximately 370,000 blue whales were killed worldwide. A rough estimate of the present blue whale global abundance worldwide is 10,000 to 25,000 individuals (Reilly *et al.*, 2008a).

After 50 years of protected status the recovery of the blue whale populations has been slow in comparison to other mysticete species (e.g. humpback whale) (Reilly *et al.*, 2008b). Interspecific competition and changes in prey abundance, which in turn would result in nutritional stress and low reproductive rates, are a possible explanation for the slow recovery. Hence, studies that assess the feeding ecology and movement patterns of blue whales are essential to obtain information about potential trophic overlap (between different groups of blue whales and/or other mysticetes species), their energetic requirements, vulnerability to changes in prey abundance, and population dynamics.

The NEP blue whale population, generally referred to as the California feeding population, is considered one of the healthiest worldwide (Calambokidis *et al.*, 2009a;

Torres-Florez *et al.*, 2014). Numerous studies have focused on describing the acoustic behavior (Stafford *et al.*, 2001; Oleson *et al.*, 2007a, 2007b, 2007c; Paniagua-Mendoza *et al.*, 2017), abundance (Carretta *et al.*, 2000; Calambokidis & Barlow, 2004; Barlow & Forney, 2007; Ugalde de la Cruz, 2008; Barlow, 2010; Becker *et al.*, 2012), distribution (Calambokidis *et al.*, 1990; Gendron, 2002; Reilly & Thayer, 1990; Mate *et al.*, 1999; Carretta *et al.*, 2000; Etnoyer *et al.*, 2004, 2006; Croll *et al.*, 2005; Calambokidis *et al.*, 2009a; Bailey *et al.*, 2009; Pardo *et al.*, 2013, 2015; Ugalde de la Cruz, 2015), genetic aspects (Costa-Urrutia *et al.*, 2013; Moreno-Santillán *et al.*, 2016; Leduc *et al.*, 2017), health (Acevedo-Whitehouse *et al.*, 2010; Flores-Cascante, 2012), reproduction (Gendron, 2002; Sears *et al.*, 2013), physiology (Acevedo-Gutiérrez *et al.*, 2002; Flores-Lozano, 2006; Rueda-Flores, 2007; Espino-Pérez, 2009; Martinez-Levasseur *et al.*, 2013; Morales-Guerrero *et al.*, 2016; Busquets-Vass *et al.*, 2017) and diet (Schoenherr, 1991; Del Angel-Rodríguez, 1997; Fiedler *et al.*, 1998; Croll *et al.*, 2005; Matteson, 2009) of this population. However, there are still gaps in our understanding about their feeding ecology and individual movement strategies across years.

The results of satellite telemetry tags deployed on NEP whales (Acevedo-Gutiérrez *et al.*, 2002; Croll *et al.*, 2005; Bailey *et al.*, 2009), and *in situ* feeding observations (Gendron, 1990, 2002; Schoenherr, 1991; Fiedler *et al.*, 1998; Acevedo-Gutiérrez *et al.*, 2002; Croll *et al.*, 2005; Bailey *et al.*, 2009) indicate that blue whales mainly feed in localized zones where the high primary production and topographic characteristics of the bottom enhance the formation of dense aggregations of krill, thus it has been hypothesized that the species movement patterns are closely linked to the oscillations in prey abundance in different ecosystems. These studies also proposed that blue whales are highly vulnerable to changes in prey abundance given that their feeding strategy, commonly known as lunge-feeding, has an elevated energetic cost, and thus limits the diving time of individual whales (Acevedo-Gutiérrez *et al.*, 2002; Goldbogen *et al.*, 2011, 2013; Potvin *et al.*, 2012).

Blue whales are classified as a stenophagous-planktivore species, foraging almost exclusively on krill aggregations (Nemoto, 1959; Nemoto & Kawamura, 1977; Gendron, 1990; Schoenherr, 1991; Del Angel-Rodríguez, 1997; Fiedler *et al.*, 1998; Croll *et al.*, 2005; Matteson, 2009; Jiménez-Pinedo, 2010). Off California blue whales feed on dense aggregations of the krill species *Thysanoessa spinifera* and *Euphausia pacifica* (Schoenherr, 1991; Fiedler *et al.*, 1998; Croll *et al.*, 2005). Nevertheless, blue whales have also been observed feeding on pelagic red crab (*Pleuroncodes planipes*) off the Baja California peninsula (Calambokidis & Steiger, 1997), though these events are considered opportunistic. Furthermore, in the Gulf of California, although blue whales prey extensively on dense aggregations of mainly the krill species *Nyctiphanes simplex* (Gendron, 1990; Del Angel-Rodríguez, 1997), molecular scatology revealed that lanternfish from the family Myctophidae was also present in 98 % of the fecal samples (Jiménez-Pinedo, 2010). In the Costa Rica Dome, blue whales have been observed feeding mainly on krill aggregations (Matteson, 2009). The former information suggests that blue whales are mainly stenophagous on krill, however their lunge feeding strategy facilitates the opportunistic consumption of other prey resources in different ecosystems. Currently, although there is evidence that feeding occurs along in the summer-fall zones (California Current System) and the winter-spring zones (Gulf of California and Costa Rica Dome), the relative contribution of these feeding zones to the blue whales' diet has never been estimated; and the information on individual movement strategies across several years is still uncommon, since satellite telemetry tags (at best) collect a single year of movement information from each whale.

In the SEP, the information on the feeding ecology, seasonal movement patterns and population structure of this species is scarce. The feeding ecology of the Chilean population has been briefly described. In the austral summer months (Dec–May) blue whales have been observed feeding intensively off Chile. It has been proposed that these blue whales feed on krill in this zone, however this information has not been confirmed by fecal sample analysis. Photo-identification and satellite tracking (Torres-Florez *et al.*, 2014) confirmed that these whales migrate to lower

latitudes (eastern tropical Pacific) in the austral winter months (Jun–Nov), including Galapagos and zones near Peru. In Galapagos blue whales have been observed foraging on large aggregations of krill (Palacios, 1999). Interestingly, the former information suggests that like the NEP blue whales, SEP whales forage year-round throughout their annual migratory cycle, thus exhibit similar energetic requirements. Recently, the results from genetic analysis (microsatellite and mtDNA sequence analyses) indicated that the eastern tropical Pacific is differentially used by blue whales from the SEP and NEP. These results also revealed that the whales from the SEP showed a stronger affinity to the zones of Peru and Ecuador, whereas the whales from the NEP were more inclined to use Costa Rica Dome (Leduc *et al.*, 2017). However, one blue whale migrated from the zone of Galapagos to the Costa Rica Dome, indicating that some of the SEP whales can also use the Costa Rica Dome. If blue whales from the Chilean population visit the Costa Rica Dome, these individuals would be using the same food resources than the blue whales in the NEP, and a trophic overlap would be expected between blue whales in the SEP and NEP.

Several methods have been used to study the feeding ecology of migratory marine mammals. These methods include: 1). Direct observations of feeding behavior (Würsig & Clark, 1993), 2). Stomach content analysis (Nemoto & Kawamura, 1977), 3). Feces analysis, via visual identification of prey structures (Del Angel-Rodríguez, 1997; Fiedler *et al.*, 1998) or molecular scatology (Deagle *et al.*, 2005), 4). energy reserve estimations inferred by blubber thickness (Vikingsson, 1990) or body condition (using aerial photographs) (Christiansen *et al.*, 2014), 5). Fatty acids profiles of blubber (Walton *et al.*, 2008), and 6). Stable isotope ratios analysis of tissues (Newsome *et al.*, 2010). The first three methods can only be used to obtain information of feeding strategies and of the recently consumed prey at a given location. Energy reserve estimation and measurements of body condition are useful to infer seasonal feeding and energetic requirements, but yield little information on the amount of feeding. Fatty acid analysis of marine mammal blubber has been used to study stock structure, dietary changes over time, and dietary differences between sex

and age classes (reviewed in Walton *et al.*, 2008). Nevertheless, to make accurate interpretation of fatty acid profiles it is preferable to have access to samples of the whole blubber layer from the species of interest, which can only be obtained from species that can be captured, like pinnipeds (*e.g.* seals, sea lions, fur seals, walruses), or whale species that are legally hunted. The analysis of stable isotope ratios in animal tissues is a method that has been increasingly used over the last two decades because it can provide quantitative information to infer diet, nutrient transfer, trophic relationships, habitat use, movement patterns, population connectivity, and tissue physiology of animals (Post, 2002; Newsome *et al.*, 2007; Graham *et al.*, 2010; Newsome *et al.*, 2010).

To use stable isotope analysis as a tool to study ecological aspects and the physiology of animals it is necessary to understand some fundamentals of the method. Isotopes are atoms from the same element that have the same number of protons and electrons but different number of neutrons (Unkovich *et al.*, 2001). The number of protons in an atom is called atomic number, and the number of nucleons (both number of protons and neutrons) determines the mass number. Therefore, heavy isotopes are atoms that have more neutrons in their nucleus compared to the lighter isotopes. Stable isotopes are atoms that are relatively stable over time, and do not undergo radioactive decay. Most compounds on Earth are composed of an overwhelmingly abundant lighter isotope and one or two heavy isotopes of relatively minor abundance (Unkovich *et al.*, 2001). For example, in terrestrial environments the percent abundance of the lighter isotope of carbon (^{12}C) is 98.98 %, whereas the heavy isotope (^{13}C) is 1.11 % (Unkovich *et al.*, 2001; Fry, 2006). These fundamental isotope abundances on Earth were determined at the start of the universe, during the Big Bang, in interstellar space and in stars where new atoms are produced during nuclear reactions of fission and fusion (Penzias, 1979; reviewed in Fry, 2006). Stable isotope ratios, of the heavy-to-light isotopes (*e.g.* $^{13}\text{C}/^{12}\text{C}$), are generally expressed as delta (δ) values, or the normalized ratio of an unknown sample to an arbitrary (but internationally accepted) standard. These relative values of deviation from an internationally accepted standard are expressed in per mil (‰) units (or part per

thousand) (Unkovich *et al.*, 2001; Fry, 2006) (see Materials and Methods, section 6.5 for details on δ calculation).

The mass differences between the isotopic forms of an element cause isotopes to react differently in physical processes and chemical reactions. Molecules with heavier isotopes have chemical bonds that are more stable, and so take more energy to break. During isotopic exchange reactions (also known as equilibrium reactions or thermodynamic fractionation), which are dependent on isotopic bond strength differences, the heavier isotope usually accumulates in the compound or phase which is the densest (and/or with the highest oxidation state), or where bonds are strongest. Thus, the dense compound becomes enriched in the heavier isotopes, whereas the less dense compound becomes depleted on the heavier isotopes, but enriched on the lighter isotopes (Gannes *et al.*, 1998; Unkovich *et al.*, 2001; Fry, 2006). In contrast, lighter isotopes tend to form weaker bonds and react faster to form products, compared to the heavier isotopes. In kinetic reactions, which are determined by reaction rates of molecules, light isotopes usually react faster. As a consequence of this physicochemical differences between isotopes of different mass, the abundance of stable isotopes of an element will vary between chemical species. The change in the abundance of isotopes, due to physical or chemical processes is termed fractionation. In enzyme-mediated reactions, the enzyme can “discriminate” against one isotopic species over another, which then results in isotope fractionation or a differential distribution of the heavy and the light isotopes (Gannes *et al.*, 1998; Unkovich *et al.*, 2001; Fry, 2006).

In ecological studies, the principle of stable isotope analysis is that the isotopic composition (*i.e.* the stable isotope ratios of the heavy-to-light isotope) of animal tissues generally resemble its diet (DeNiro & Epstein, 1978, 1981; Gannes *et al.*, 1998; Vander Zanden *et al.*, 2001, 2015). However, the isotopic composition of consumers' tissues is not identical to its diet, because there are fractionation processes during metabolism which selectively result in the excretion of the lighter isotopes (DeNiro & Epstein, 1978, 1981; Gannes *et al.*, 1998; Newsome *et al.*, 2010;

Vander Zanden *et al.*, 2015). Therefore, usually consumers tissues are enriched on the heavy isotopes and have higher isotope values, compared to those of their diet.

Another factor that determines the isotopic composition of animal tissues is the isotopic composition at the base of the food webs, or baseline isotope values (Rau & Anderson, 1981; Rau, 1982; Rau *et al.*, 1983; Kline, 1999; Perry *et al.*, 1999), which are the primary sources of inorganic N or C (or other elements) that are used by primary producers from the environment and then incorporated to the food web. A primary source can be either natural (e.g. upwelled new nitrate: NO_3^- , and ammonium: NH_4^+ ; bicarbonate: HCO_3^- ; dissolved carbon dioxide $\text{CO}_{2(aq)}$), recycled inorganic N or C (from animal activity, ammonification, etc.), or of anthropogenic origin (e.g. NH_4^+ or NO_3^- pollutants from river runoff or sewage) (Unkovich *et al.*, 2001). Thus, isotope values not only provide information of the food sources consumed, but also of the ecosystems where these sources have been consumed (Hobson, 1999; Hobson *et al.*, 1996). However, an important factor that has to be considered when using stable isotopes in animal tissues to make inferences on different ecological aspects is that tissues are anabolized at different rates, depending on their biochemical composition, thus reflect information on the food sources consumed at different temporal scales (from days to several years), depending on their specific isotopic incorporation rates in metabolically active tissue or growth rates for metabolically inert tissue (DeNiro & Epstein, 1978, 1981; Tieszen *et al.*, 1983; Schoeller, 1999; Vander Zanden & Rasmussen, 2001; Post, 2002).

Nitrogen ($\delta^{15}\text{N}$: $^{15}\text{N}/^{14}\text{N}$) and carbon ($\delta^{13}\text{C}$: $^{13}\text{C}/^{12}\text{C}$) isotope values are the most common isotope systems used to assess ecological aspects of marine organism because both systems are mainly determined by the food that has been assimilated (McConnaughey & McRoy, 1979; Martínez Del Río *et al.*, 2009; Hobson *et al.*, 2010; Newsome *et al.*, 2010). Nitrogen in animal tissues is mainly sourced from the proteins of animal's diet, (Gannes *et al.*, 1998; Newsome *et al.*, 2010). Consumer's tissues have $\delta^{15}\text{N}$ values that are +2‰ to +5‰ higher than their diet. This difference, appears

to be related with trophic discrimination (or fractionation) during deamination and transamination. Deamination enzymes preferably remove ^{14}N , thus excreted nitrogen (*i.e.* ammonia, uric acid, or urea) is ^{14}N -enriched. Transamination favors ^{14}N -containing amine groups, as a result, the nitrogen of glutamate, which is usually source for transamination to other amino acids and deamination in the urea cycle, is ^{15}N -enriched compared to nitrogen in dietary glutamate and other amino acids (reviewed in Gannes *et al.*, 1998). In any given ecosystem, $\delta^{15}\text{N}$ values of consumers will increase (typically +2‰ to +5‰ with each trophic level) in a stepwise manner in relation to its baseline isotope values, therefore the relative trophic position of consumers within a food web can also be estimated via stable isotope analysis of animal tissues (DeNiro & Epstein, 1978, 1981; Martínez Del Río *et al.*, 2009; Newsome *et al.*, 2010). Animals that feed on primary producers will have lower isotope values and trophic level compared to those that feed on secondary or tertiary consumers, which will exhibit higher isotope values (and trophic level). In general, $\delta^{15}\text{N}$ values in marine organisms have been used to make inferences on diet, tissue physiology, trophic level, and movement between ecosystems that exhibit contrasting baseline isotope values (DeNiro & Epstein, 1978, 1981; Rau *et al.*, 1983; Newsome *et al.*, 2010; McMahon *et al.*, 2013, 2015).

Carbon in animal tissues is sourced from dietary proteins, lipids and carbohydrates, which may have different isotope composition (see Materials and Methods, section 6.4) (Nelson & Michael, 2005; Newsome *et al.*, 2010). In marine ecosystems, generally consumer's tissues have $\delta^{13}\text{C}$ values that are +0.5‰ to 3‰ higher compared to those of their diet. $\delta^{13}\text{C}$ values have been used in the same manner as $\delta^{15}\text{N}$ values to study marine organisms, however, this isotope system also provides information of the movement of animals between coastal/oceanic and benthic/pelagic ecosystems (Rau & Anderson, 1981; Kline, 1999; Perry *et al.*, 1999; Martínez Del Río *et al.*, 2009; Newsome *et al.*, 2010; Carle, 2014). In general, in coastal or nearshore ecosystems nutrient inputs via upwelling events result in higher phytoplankton growth rates. During photosynthesis, primary producers preferentially uptake ^{12}C , thus in coastal zones the $\delta^{13}\text{C}$ values of aqueous CO_2 increase by a few

per mil (‰) (Goericke & Fry, 1994; Popp, 1998). When nutrients are depleted, the low concentrations of CO₂ lead to lower isotopic fractionation and thus the δ¹³C values of phytoplankton remains higher in the coastal (Goericke & Fry, 1994; Popp, 1998; Newsome *et al.*, 2010). In contrast, in oceanic or offshore ecosystems, low nutrient inputs lead to low growth rates, resulting in lower δ¹³C compared to coastal ecosystems (Goericke & Fry, 1994; Popp, 1998). Phytoplankton size and taxa-specific isotopic fractionation are two factors that can also affect the δ¹³C gradient between coast and oceanic ecosystems (Pancost *et al.*, 1997; Rau *et al.*, 2001). In the case of benthic and pelagic ecosystems, the former generally has higher δ¹³C values than the latter (Hobson & Ambrose, 1995).

Only three studies that have used stable isotope analysis in blue whale tissues (feces, muscle and skin). Rau (1982) reported the isotope values (δ¹⁵N and δ¹³C) for blue whale muscle collected from a whale that was struck and killed by a ship in the waters off San Diego, California, USA. The isotopic data of this whale and other marine organisms was used to describe the relationship between trophic level and stable isotopes values. Subsequently, Gendron *et al.* (2001) compared the isotope values of the tissues (feces and skin) of three rorqual species (blue whale; fin whale, *Balaenoptera physalus*; and Bryde's whale, *Balaenoptera edeni*), and those of their potential prey (krill and sardines) sampled within the Gulf of California. The results of this study showed that tissue δ¹⁵N values were higher in Bryde's whales (skin: 15.8 ± 0.6‰), lower in fin whales (skin: 15.4 ± 1.1‰; feces: 11.1 ± 1.0‰), and lowest in blue whale tissues (skin: 12.9 ± 0.3‰; feces: 8.6‰). The isotopic gradient among species was associated to the stenophagous feeding habits of blue whales (mainly feeding on krill), the generalist feeding habits of fin whales (feeding on both krill and fish), and the ictyophagous feeding habits of Bryde's whale (usually feeding on fish and rarely on krill). Therefore, the Bryde's whale had the highest trophic level, the fin whale intermediate trophic level, and the blue whale had the lowest trophic level. The relationship between trophic level and δ¹³C values in skin of the three rorquals was not clear, because the blue whales (-18.2 ± 0.6‰) and the Bryde's whales (-18.1 ± 1.5‰) exhibited similar values, whereas the fin whale (-16.0 ± 0.6‰)

had higher values. A possible explanation to this is that $\delta^{13}\text{C}$ values were reflecting the movement between coastal ecosystems with higher values (fin whales), and oceanic ecosystems with lower values (blue whale and Bryde's whale). The limitation of the former studies was sample size, given that some of their conclusions were drawn from $n < 5$.

Busquets-Vass (2008), analyzed the isotope values variability in blue whale tissues collected within the Gulf of California by using a larger database (feces, $n = 11$; skin, $n = 104$), and included prey samples (Krill species *Nyctiphanes simplex*, $n = 16$). This study was the first to briefly describe the isotopic variability among blue whale skin strata (stratum basale, externum and sloughed skin) in the Gulf of California. The range of blue whale skin $\delta^{15}\text{N}$ (11 to 17‰) and $\delta^{13}\text{C}$ (-18 to 15‰) values was much broader than the previously described by Rau (1982) and Gendron *et al.* (2001). Blue whale skin $\delta^{15}\text{N}$ values showed a marked seasonal increase (January-April), which was associated to the seasonal diet switch of this species, from prey in the California Current System with lower values to the prey of the Gulf of California with higher values. Thus, it was concluded that blue whale skin isotopic incorporation rate was approximately 3 months. Blue whale skin $\delta^{13}\text{C}$ did not exhibit any seasonal trends, and this result was linked to the movement of blue whales between coastal and oceanic ecosystems, which would result in intermediate $\delta^{13}\text{C}$ values between both ecosystems. In this study trophic discrimination factors ($\Delta^{15}\text{N}$ and $\Delta^{13}\text{C}$), or the per mil difference between blue whale skin and prey, were estimated to be between 1.4‰ to 1.6‰ for $\delta^{15}\text{N}$ and 1.2‰ for $\delta^{13}\text{C}$. One of the confines of this study was the lack biological samples such as blue whale skin and prey samples collected in different feeding zone, which would provide conclusive results on whether the seasonal variability observed in blue whale skin isotope values was effectively reflecting diet switch. In addition, the estimation of skin isotopic incorporation rate was made for the overall skin, integrating all skin strata, instead of separating each skin strata.

A study that combines the use of niche metrics (Dietary isotopic mixing models and stable isotope Bayesian ellipses) with a large dataset of isotope values in blue whale tissues (e.g. skin and baleen) and potential prey tissues obtained in different regions of the eastern Pacific Ocean would provide a wider scope of the feeding ecology and seasonal movement patterns of this species. This information cannot be obtained otherwise, given that observational data (marine mammal surveys) and tagging techniques have logistic and economical limitations. From a conservation perspective, this information is essential to understand how this species uses different ecosystems, and could eventually help define critical habitats.

3. JUSTIFICATION

Numerous studies have asserted that the high energetic demands of the blue whales in conjunction with the elevated cost of their feeding strategy (lunge-feeding) make this species particularly vulnerable to changes in prey abundance (Acevedo-Gutiérrez *et al.*, 2002; Croll *et al.*, 2005). This assertion is further supported by the fact that after 50 years of protection from commercial whaling, the recuperation of this species has been slow in comparison to other mysticetes (Reilly *et al.*, 2008a; Calambokidis *et al.*, 2009b). A crucial factor in determining the reproductive success and survival of individuals is the ecosystems they occupy (Gunnarson *et al.*, 2005). Blue whales migrate between different ecosystems in search of potential prey sources. Studies that address the feeding ecology and movement patterns of blue whales can contribute to understand the importance of different ecosystems to the species life cycle. A limitation is that blue whales have a wide geographic distribution, thus feeding observations are limited to boat-based surveys in specific regions. Currently, although the general migratory patterns and feeding ecology of this species has been described in the eastern Pacific Ocean, specific information on their diet, trophic width and individual movement patterns is still lacking in both the NEP and SEP.

Stable isotope analysis of blue whale tissues (skin and baleen) and potential prey can provide information on their feeding ecology and seasonal movement patterns among different ecosystems. In this context, the present study would be the first to characterize the isotopic niche width of the blue whales in the eastern Pacific Ocean, quantify the relative contribution of the different foraging zones of the NEP to the blue whale's diet, and describe individual seasonal movement patterns across several years. The blue whale skin database used for this research potentially represents the largest worldwide, and offered a unique opportunity to study this species. Furthermore, these types of collaborative studies enhance the proper design of management plans to assure the protection of this species throughout its migratory cycle.

4. HYPOTHESIS

Blue whale tissues (skin and baleen plates) record biogeochemical changes, at an isotopic level, which occur at the base of different food webs in the eastern Pacific Ocean. Hence, stable isotope analysis of blue whale tissues would provide information of the feeding ecology and seasonal movement patterns of this species.

5. OBJECTIVE

Characterize some aspects of the feeding ecology and seasonal movement patterns of blue whales in the eastern Pacific Ocean by using stable isotopes of nitrogen and carbon in different tissues (skin and baleen) of this species.

5.1. Specific objectives

- a) Assess the effect of different processing methods in the isotope values of blue whale skin samples
- b) Compare the variability of blue whale skin isotope values by strata
- c) Estimate blue whale skin strata isotopic incorporation rate
- d) Determine the isotopic niche width and trophic overlap of blue whales in the eastern Pacific, by region (SEP and NEP) and sex (females and males)
- e) Quantify the relative contribution of different foraging zones to the blue whale diet in the NEP
- f) Estimate blue whale baleen growth rates and isotopic niche width to infer the movement patterns of individual blue whales in the NEP

6. MATERIALS AND METHODS

6.1. Study area

The present research focused its sampling effort on the eastern Pacific Ocean (Fig. 3). There is no strict consensus on how to divide the eastern Pacific from the western Pacific, but the Ocean Exploration Trust (OET) and the National Oceanic and Atmospheric Administration Office of Ocean Exploration and Research (NOAA-OER) held a workshop on 2014 and suggested the limits shown in Figure 3A. Given the geographic extension, there are numerous processes that influence the dynamics of this region at different levels. In general, the prevailing winds (the northern hemisphere westerlies, the northern trade winds, the southeast trade winds and the “roaring forties” or southern hemisphere westerlies) sweep across the ocean surface and drive the ocean surface circulation (Tomczak & Godfrey, 2003). The major ocean surface currents, which are product of the patterns of the prevailing winds, are shown in Figure 3B. The surface currents in the Pacific Ocean link up to form gyres, which are large areas that are defined by the currents flowing in a circular pattern (Fig. 3B) (Tomczak & Godfrey, 2003). Due to the geographic extension of the eastern Pacific, I will limit this section to describe some of the general biogeochemical and oceanographic processes that affect the distribution of stable isotopes of nitrogen and carbon in the ocean; specifically, the processes that can alter the baseline isotope values of food webs.

As mentioned in the Background section (2. Background, 14–17 p.), the “primary sources” of inorganic N or C, are directly used by primary producers from the surroundings. This process incorporates the baseline stable isotope rations into the food webs or the trophic structure (Unkovich *et al.*, 2001). In marine ecosystems, dissolved inorganic forms of nitrogen (nitrate NO_3^- , ammonium NH_4^+ , and dissolved gaseous nitrogen N_2) represent the most important form of primary sources that sustains planktonic and benthic primary production (Dugdale, 1967). The ^{15}N abundance of dissolved inorganic N can vary spatially and temporally due to

physicochemical processes and this influences the baseline isotope values of food webs. Additionally, N_2 fixation and assimilation (Hoering & Ford, 1960; Macko *et al.*, 1982), and biological oxidation-reduction processes (nitrification and denitrification) (Cline & Kaplan, 1975) have shown to modify the isotope ratios of primary N sources; and catabolic biochemical processes (excretion of organic or inorganic N sources, decomposition and remineralization) can also result in production of regenerated N pools with $\delta^{15}N$ values distinctly different from those of primary sources (Miyake & Wada, 1971). Thus, baseline nitrogen isotope values in marine ecosystems are mainly influenced by variations in the natural abundance of ^{15}N of dissolved inorganic nitrogen, and the metabolism of primary producers.

Dissolved inorganic C is the largest pool of carbon in marine ecosystems. This C pool is product of the equilibrium exchange reactions of the atmospheric carbon dioxide (CO_2) with the ocean carbonate system. Bicarbonate (HCO_3^-) is the most abundant pool of dissolved inorganic carbon and comprises virtually all (~99 %) of the total pool (Benson & Krause, 1984). The second abundant pool of dissolved inorganic carbon is CO_2 . Variations in the stoichiometry of carbonate- CO_2 can significantly alter the $\delta^{13}C$ signatures of source dissolved inorganic carbon used by primary producers. Other factors that influence the ^{13}C natural abundance, and thus the baseline carbon isotope values, are localized patterns of photosynthesis, respiration and decomposition, upwelling of deep-ocean water (which due to decomposition of isotopically light material, contain ^{13}C -depleted inorganic C) (Anderson & Arthur, 1983), species composition of phytoplankton communities (Pancost *et al.*, 1997), photon flux density, temperature, latitude and nutrient availability (Goericke & Fry, 1994; Uncovich *et al.*, 2001). It is important to note that carbon is initially fractionated during photosynthesis by primary producers. In general, carbon fractionation is mainly due to enzymatic reactions which catalyze initial carboxylation. Carboxylation is regulated by the enzyme ribulose-1,5-biphospate carboxylase (RUBISCO) for C_3 plants and phytoplankton (although there is evidence that some diatoms also use a form of the C_4 pathway) (Fontugne & Dupplesey, 1981; Roberts *et al.*, 2007). RUBISCO has a higher affinity for $^{12}CO_2$ than $^{13}CO_2$, thus discriminates against ^{13}C .

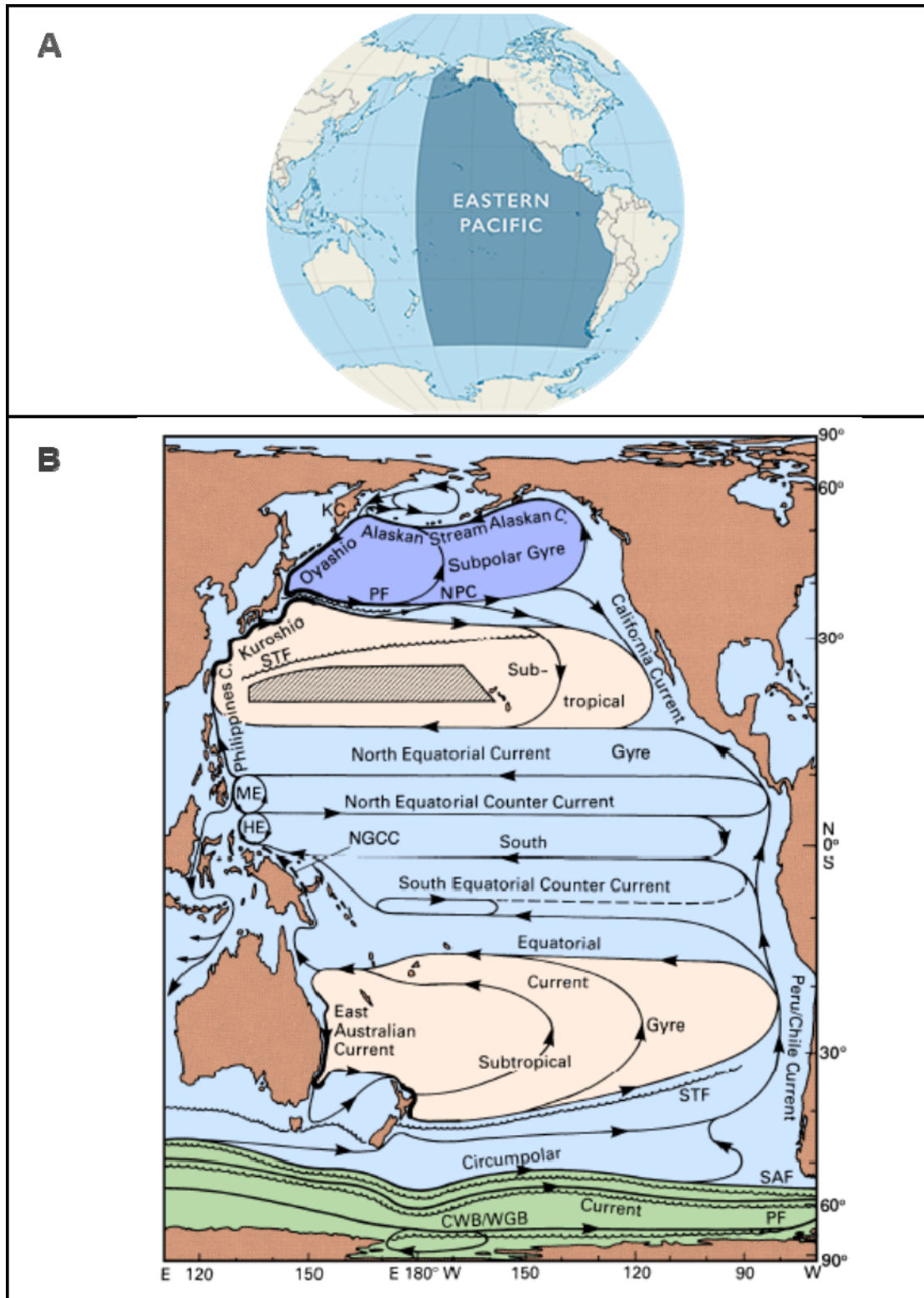


Figure 3. Eastern Pacific Ocean. A) Eastern Pacific Ocean limits (image modified and reprinted from OET & NOAA-OER workshop). B) Eastern Pacific Ocean major surface currents (image modified and reprinted from Tomczak & Godfrey, 2003).

The range of carbon fractionation between tissues of marine phytoplankton and CO_2 or HCO_3^- dissolved in seawater can be between 27‰ to over 30‰ (Sackett *et al.*, 1965).

In the present study, the sampling effort comprehends several zones from the NEP (California Current System, Gulf of California and the Costa Rica Dome) and the SEP (Galapagos and Peru) in the eastern Pacific Ocean. These zones have contrasting baseline isotope values of nitrogen, whereas carbon isotope values are less variable between zones. In the following subsections, I will mention briefly some of the main oceanographic characteristics of these zones and the potential processes that influence the baseline isotope values:

6.1.1. Northeast Pacific Ocean (NEP)

The California Current System, is formed by the California Current, which is the eastern limb of the north Pacific gyre. The California Current flows in direction to the equator (equatorward) throughout the year, along the west coast of U.S. and the Baja California Peninsula, to the North Equatorial current (Fig. 3B). Except near the coast, the California Current is a surface current (0–300 m). Off Central California the California Current subarctic subsurface waters (0–500 m). Near the coast (within 150 Km) the California Current there is a seasonal (during fall and winter) change in direction of the surface flow. The flow is often poleward, flows along Southern California and Baja California, and it is referred to as the Inshore Countercurrent (or Davidson Current). In addition to the seasonal Inshore Countercurrent, the California Undercurrent, which is considered to originate in the eastern equatorial Pacific, also flows poleward along the North America Coast. This current is characterized low temperature, low salinity and high dissolved oxygen, except on its western side (850 to 900 km off the California Coast), in the California frontal zone, where physicochemical characteristics change abruptly (Lynn & Simpson, 1987; Collins *et al.*, 2003).

The California Current is a highly productive zone and represents a key ecosystem for numerous species of marine megafauna including cetaceans (Barlow *et al.*, 2008; Pardo *et al.*, 2015). Enhanced productivity in the California Current System is the result of seasonal upwelling, which is caused mainly by seasonal northwesterly winds and the coastal topography. Although the California Current is an open ocean system, the effect of upwelling and its biological response confers complex physicochemical characteristics to this zone with time/scales of variability smaller compared to the open ocean. This zone also exhibits dissolved nitrate with relatively high $\delta^{15}\text{N}$ values, compared to the central and western Pacific, which exhibit $\delta^{15}\text{N}$ values similar to the deep ocean. It has been suggested that the unusual $\delta^{15}\text{N}$ values of the California Current System are product of the entrance of waters from the eastern tropical Pacific via the California Undercurrent. The eastern tropical Pacific has a marked oxygen minimum zone (Liu & Kaplan, 1989). Oxygen minimum zones, or shadow zones, are regions of the ocean where dissolved oxygen in the water column is reduced or absent (Below 2 mg/l), due to poor ventilation, low water circulation, and a high demand of microbial aerobic respiration (Ulloa *et al.*, 2013). These regions are considered “hotspots” for oxygen-sensitive nitrogen transformations, where nitrate is the main terminal electron acceptor for the oxidation of organic matter. Thus, denitrification and anaerobic ammonium oxidation (anammox) contribute to the removal of fixed nitrogen as N_2 (reviewed in Ulloa *et al.*, 2013). Denitrification preferentially consumes $^{14}\text{NO}_3^-$ which results in an increase in nitrate $\delta^{15}\text{N}$ values in oceanic zones that have marked oxygen minimum zones (Liu & Kaplan, 1989; Voss *et al.*, 2001; Popp *et al.*, 2007; Aurióles-Gamboa *et al.*, 2013). As described in the Background section (2. Background, 14–17 p.), $\delta^{13}\text{C}$ also tend to be higher in coastal ecosystems vs. offshore ecosystems in this zone; although sporadic inputs of nutrients via upwelling events can also influence baseline $\delta^{13}\text{C}$. The difference in coastal (nearshore) vs. oceanic (offshore ecosystems) $\delta^{13}\text{C}$ in the norther part of the California Current have been used to infer the longitudinal movements of pinnipeds (reviewed in Newsome *et al.*, 2010).

El Niño – La Niña, Southern Oscillations (ENSO), are inter-annual variation in the wind intensity and surface temperatures, which affect the eastern tropical Pacific. El Niño, is a warm phase oscillation, and La Niña is a cold phase. These oscillations change the intensity of the major currents, and affect the mean depth of the thermocline (Durazo *et al.*, 2005), which in turn could modify the baseline isotope values of $\delta^{13}\text{C}$ and $\delta^{15}\text{N}$ of the California Current System. Altabet *et al.* (1999) studied the nitrogen isotope biogeochemistry of the sinking particles, and linked the reduction of NO_3^- concentrations and particle flux to an El Niño phase. The modifications in baseline isotope values would be mainly attributed to the reduction or suppression of upwelling during El Niño phase. Although the effects of ENSO in the baseline isotope values can be measured, it is difficult to determine if these variations extend to the complete trophic food web in the California Current System, as well as in the eastern tropical Pacific.

The Gulf of California is in the northwestern portion of Mexico (Fig. 4). This zone is highly productive; thus, it is one of the most important fishing region of Mexico, and refuge to a wide variety of marine organisms (Lluch-Cota *et al.*, 2007). It is 1130 km long and 80–209 km wide. This inland sea separates the semiarid Baja California Peninsula from arid States of Sonora, Sinaloa and Nayarit. The southern part of the Gulf of California is in direct contact with the Pacific. The mountain range (1–3 km of elevation) of the Baja California Peninsula reduces the effect of the Pacific in the Gulf of California's climate, which results in higher evaporation rates and a wide range of annual temperatures in the atmosphere and the surface seawater. In the northern region of the Gulf of California the mean depth is 200 m. The Gulf increases in depth towards the entrance (or mouth), with depth basins reaching over 3000 km (Álvarez-Borrego & Lara-Lara, 1991; Lluch-Cota *et al.*, 2007). Atmospheric forcing is a strongly seasonal; weak southeasterly winds blow through the summer and stronger northwesterly during winter (Marinone *et al.*, 2004). In winter mean sea surface temperatures are between 15°C and 17°C, and in summertime 30°C and 32°C (Thunell, 1998).

The circulation of the Gulf of California is influenced by semiannual seasonal changes and the diurnal, semidiurnal and fortnightly tidal cycles. Tides co-oscillate with those of the Pacific Ocean and the semidiurnal component, with amplitudes at the north four times greater than those in the mouth. It has been proposed that the Pacific Ocean forces the Gulf of California through an internal baroclinic Kelvin wave of annual period, which enters on the eastern coast of the Gulf and traverses cyclonically around the entire coastline (Ripa, 1997). This hypothesis would explain the seasonal circulation and the balances of temperature and salinity. Other important features of the Gulf of California circulation are the large-scale gyres in the northern Gulf and meso-scale seasonal gyres along the center of the Gulf (Lavín *et al.*, 1997).

In the Gulf of California there are several water masses. Above 200 m, there are three water masses: the California Current water mass, of low temperature ($12 < T^{\circ}\text{C} < 18$) and low salinity ($S_{\text{‰}} < 34.5$); the Eastern Tropical Pacific superficial water mass with intermediate temperature ($T > 18^{\circ}\text{C}$) and salinity ($S_{\text{‰}} < 35$), and the Gulf of California water mass which has higher temperature ($12 > T^{\circ}\text{C} < 22$) and salinity ($S_{\text{‰}} > 35$), thus is located above the other two water masses (Torres-Orozco, 1993). There also three water masses at depth: Sub-superficial Subtropical water mass ($34.5 < S_{\text{‰}} < 35$; $9 < T^{\circ}\text{C} < 18$), Pacific Intermediate water mass ($34.5 < S_{\text{‰}} < 34.8$; $4 < T^{\circ}\text{C} < 9$), and Deep water from the Pacific ($S_{\text{‰}} < 34.5$; $T < 4^{\circ}\text{C}$; Torres-Orozco, 1993).

Nutrient input in the Gulf of California is mostly attributed to year-round, strong tidal mixing around the islands, and the wind-driven coastal upwelling during winter along the eastern coast. Lower sea surface temperature on the west coast of the Gulf, during summer, has been interpreted as coastal upwelling, but several lines of evidence indicate that this pattern is related to the differences in temperature between the mainland side of the Gulf and the peninsular side (Mitchell *et al.*, 2002).

The Gulf of California has unusually high $\delta^{15}\text{N}$ at the base of the food web, and by extension all marine organisms within this zone tend to exhibit relatively higher

$\delta^{15}\text{N}$ values compared to those of other zones in the NEP (Altabet *et al.*, 1999; Aurióles-Gamboa *et al.*, 2013), including the California Current System. This pattern is possibly attributed to a combination of factors: the NO_3^- concentrations in the Gulf of California, the presence of the oxygen minimum zone, the year-round tidal mixing around the islands, and coastal upwelling. In summer, NO_3^- concentrations can reach 25 μM at depth; hence, tidal mixing and upwelling enhances the injection of nutrients including NO_3^- that are at depth. In addition to the presence of NO_3^- at depth, the Gulf has a strong oxygen minimum zone between 300 and 900 m, and largely corresponds to the intrusion of Pacific Intermediate Water into the Gulf from the eastern tropical north Pacific. As mentioned earlier, in the absence of O_2 bacteria turn to nitrate to respire organic matter via denitrification, which preferentially removes ^{14}N -enriched nitrate and leaves the residual nitrate strongly ^{15}N -enriched (Altabe *et al.*, 1999; Voss *et al.*, 2001; Popp *et al.*, 2007; Newsome *et al.*, 2010; Aurióles-Gamboa *et al.*, 2013). This combination would potentially explain the high $\delta^{15}\text{N}$ in the Gulf of California food webs. As described earlier, $\delta^{13}\text{C}$ also tends to be higher in coastal ecosystems vs. offshore ecosystems in this zone, and this difference has been useful to differentiate offshore and nearshore bottlenose dolphin ecotypes (Díaz-Gamboa, 2003).

The Costa Rica Dome (Fig. 4) is an open-ocean upwelling zone with great biological importance. This dome is localized near 9°N, 90°W. It is caused by a seasonally changing combination of interconnected features (Fiedler & Lavin, 2006). It is similar to other tropical thermocline domes because it is part of an east-west thermocline ridge associated with equatorial circulation, surface currents flow cyclonically around it, and its seasonal cycle is affected by large-scale wind patterns (Fiedler & Lavin, 2006). Primary and secondary production are relatively high at the Dome, and it is common to observe cetacean aggregations in this zone (Reilly & Thayer, 1990; Pardo *et al.*, 2015). Relatively low $\delta^{15}\text{N}$ values in particulate organic matter (POM) have been described in this zone, particularly in the upper 50 m. A possible explanation to this observation is that there is incomplete nitrate utilization, attributed to the preferential selection of $^{14}\text{NO}_3^-$ (^{14}N -enriched nitrate) by

phytoplankton (Newsome *et al.*, 2010; Williams *et al.*, 2014). Zooplankton $\delta^{13}\text{C}$ values tend to be lower compared to other zones (López-Ibarra, 2008), however, changes in nutrient availability potentially affect phytoplankton growth rates, thus it exhibits a high variability.

6.1.2. Southeast Pacific Ocean (SEP)

The SEP comprehends a wide variety of ecosystems, however the samples used for this study comprehend mainly the zones from Galapagos and Peru (GALPE; Fig. 4). Galapagos is an offshore archipelago that is near extremely productive eastern boundary current systems, which include the Panama and Humboldt (also known as Peru current) Currents (Sachs & Ladd, 2010). The zone off Peru is considered one of the most important upwelling zone in the eastern tropical Pacific (Lavín *et al.*, 2006). This zone supports one of the largest fishery in the world, although it has an extremely high inter-annual variability (Lavín *et al.*, 2006). Blue whales have been frequently observed feeding in this zone (Donovan, 1984). $\delta^{15}\text{N}$ values of sea lion pup hair (Aurioles-Gamboa *et al.*, 2009) in these zones were unusually lower than those described for the Gulf of California (Aurioles-Gamboa, *et al.*, 2009). This pattern could be related to the fact that the oxygen minimum zone is generally thinner in Galapagos and Peru, hence, denitrification would not affect the upper layers of the water. In this scenario, baseline $\delta^{15}\text{N}$ values in Galapagos and Peru would resemble those of open ocean and deep ocean food webs (Farrell *et al.*, 1995; Aurioles-Gamboa *et al.*, 2009). This hypothesis would be in accordance with the results of bottom sediments $\delta^{15}\text{N}$ (5.5‰) from samples collected near Galapagos, which exhibited isotope values 5.3‰ lower than those of bottom sediments in the Gulf of California (10.8‰) (Farrell *et al.*, 1995; Aurioles-Gamboa *et al.*, 2009). In the case of $\delta^{13}\text{C}$, a regional variability could also reflect differences between coastal vs oceanic ecosystems in Galapagos and Peru. However, the $\delta^{13}\text{C}$ values of sea lion pups was not contrasting between pups sampled in Galapagos (Galapagos sea lion, *Zalophus wollebaeki*) vs Gulf of California (California sea lion, *Z. californianus*),

indicating that baseline $\delta^{13}\text{C}$ values in both hemispheres are mostly uniform (Goericke & Fry, 1994; Aurióles-Gamboa *et al.* 2009).

6.2. Sample collection and selection

Blue whale skin biopsies and sloughed skin (Table 1) were selected from tissue banks at NOAA Southwest Fisheries Science Center (NOAA-SWFSC), Cascadia Research Collective (CRC), and Centro Interdisciplinario de Ciencias Marinas-Instituto Politecnico Nacional (CICIMAR-IPN). These samples were collected from 1996–2015 in the NEP (Gulf of California-**GC**, California Current System-**CCS** and Costa Rica Dome-**CRD**; Table 1, Fig. 4) and SEP (Galapagos/Peru-**GALPE**; Table 1, Fig. 4). Skin samples were collected during marine mammal surveys conducted by NOAA-SWFSC, CRC, and CICIMAR-IPN. Skin biopsies were collected via dart sampling methods (Barrett-Lennard *et al.*, 1996), and sloughed skin was directly collected from the water with a net (Gendron & Mesnick, 2001) or from suction cups of satellite-tagged whales.

Table 1. Skin samples (Skin biopsies and sloughed skin) collected in the eastern Pacific Ocean, selected from three tissue banks (NOAA-SWFSC, CRC, and CICIMAR-IPN). CCS, California Current System; GC, Gulf of California; CRD, Costa Rica Dome; GALPE, Galapagos/Peru.

Eastern Pacific Ocean	Zone	Skin biopsy (<i>n</i>)	Sloughed skin (<i>n</i>)	Months
Northeastern Pacific (NEP)	CCS	129	93	June–December
	GC	115	81	January–April
	CRD	26	0	June–December
Southeastern Pacific (SEP)	GALPE	25	0	June–December

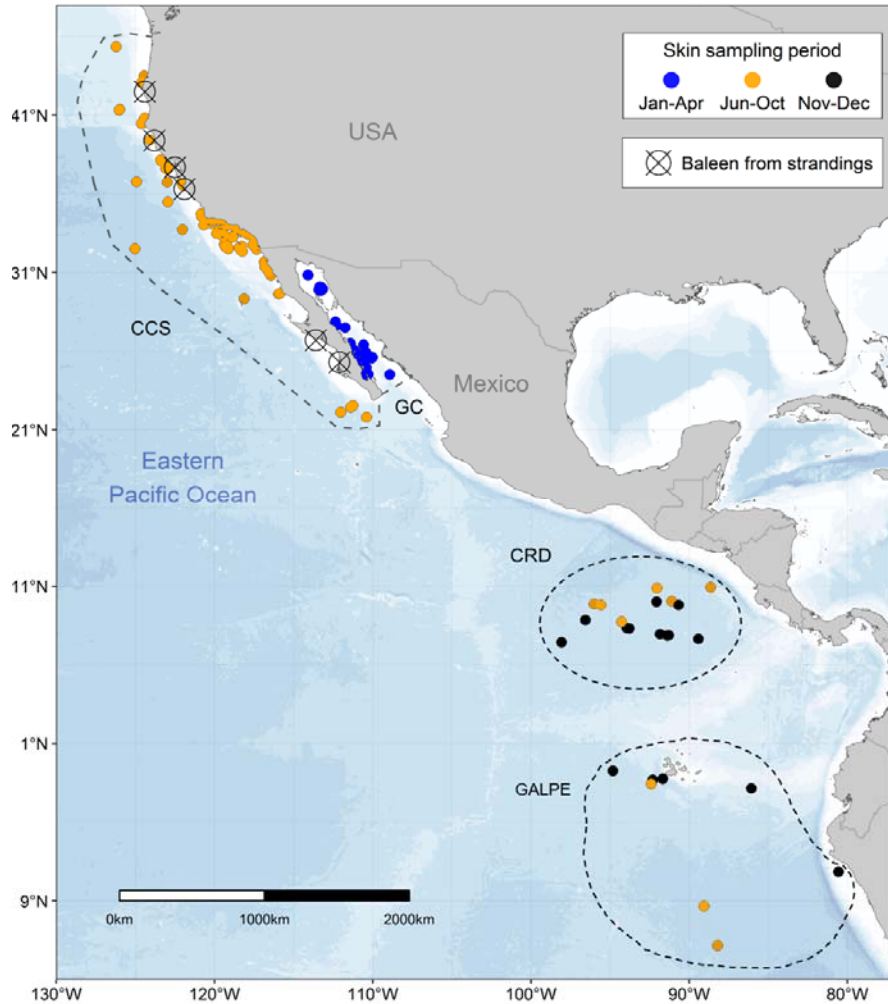


Figure 4. Eastern Pacific Ocean sampling zones. Dots represent blue whale skin samples collected in the California Current System (CCS), Gulf of California (GC), Costa Rica Dome (CRD), and Galapagos/Peru (GALPE). Dots with a cross represent blue whale baleen plates collected from six dead stranded whales (stranding data for one whale was not available).

Krill ($n = 34$; Fig. 5A) and lanternfish ($n = 7$; Fig. 5A) samples were opportunistically collected during marine mammal surveys conducted by CICIMAR-IPN within the GC (January–April; 2005–2015). Krill samples were collected by towing a conical net (diameter 50 cm., mesh size 200 μ m) when blue whales were observed feeding near the surface. Lanternfish samples were collected with a fishing net (mesh size 5 mm), when aggregations were found near the surface. Prey samples were

preserved frozen in liquid nitrogen (-195°C). The assignment of lanternfish to the Family Myctophidae (Wisner, 1974) and classification of krill species (Brinton *et al.*, 2000) was made using identification guides; *Nyctiphanes simplex* was the only krill species present in all samples. Additionally, the tissue bank at CICIMAR-IPN had samples ($n = 3$) from the krill collected in Galapagos (Fig. 5B), which were donated by an external researcher (PhD. Daniel Palacios), and we included these samples in our analysis.

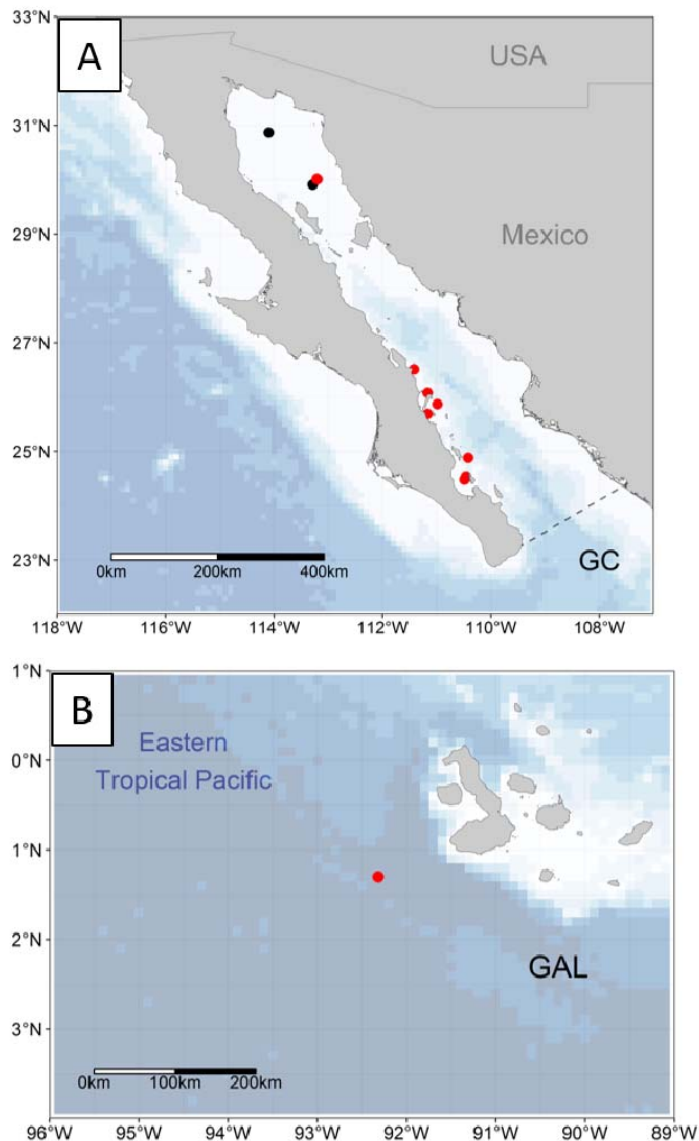


Figure 5. Krill and lanternfish samples collected in the Gulf of California and Galapagos. Dots represent krill (red) and lanternfish (black) samples collected in: A) Gulf of California (GC) and B) Galapagos (GAL).

Baleen plates collected from seven dead stranded blue whales were obtained from Humboldt State University Vertebrate Museum (HSU-VM), CICIMAR-IPN, the California Department of Parks and Recreation-Prairie Creek Redwoods State Park (CDPR-PCRSP), and the Oregon Marine Mammal Stranding Network (OMMSN). Stranding reports including sex identification were available for all but one individual. The sex of this whale was determined at NOAA-SWFSC using genetic methods (Morin *et al.*, 2005, 2006).

6.3. Skin biopsy separation into strata

To assess the isotope variability between blue whale skin strata it was necessary to identify tissue structure. Histological preparations of five skin biopsies were stained with hematoxylin & eosin following the protocol of Sheehan and Hrapchak (1980). Based on these preparations the skin biopsy was divided into two strata: (1) stratum basale, closest to the blubber, and (2) stratum externum, the outermost layer that easily separated from the stratum spinosum (Fig. 6A). We did not include stratum spinosum in our analysis because we assumed it would exhibit intermediate isotope values between the stratum basale and the stratum externum. Some skin biopsy samples were incomplete as they had been used for previous studies, and only one of the two strata were available. Sloughed skin samples were also included in the analysis, but were only available for some years.

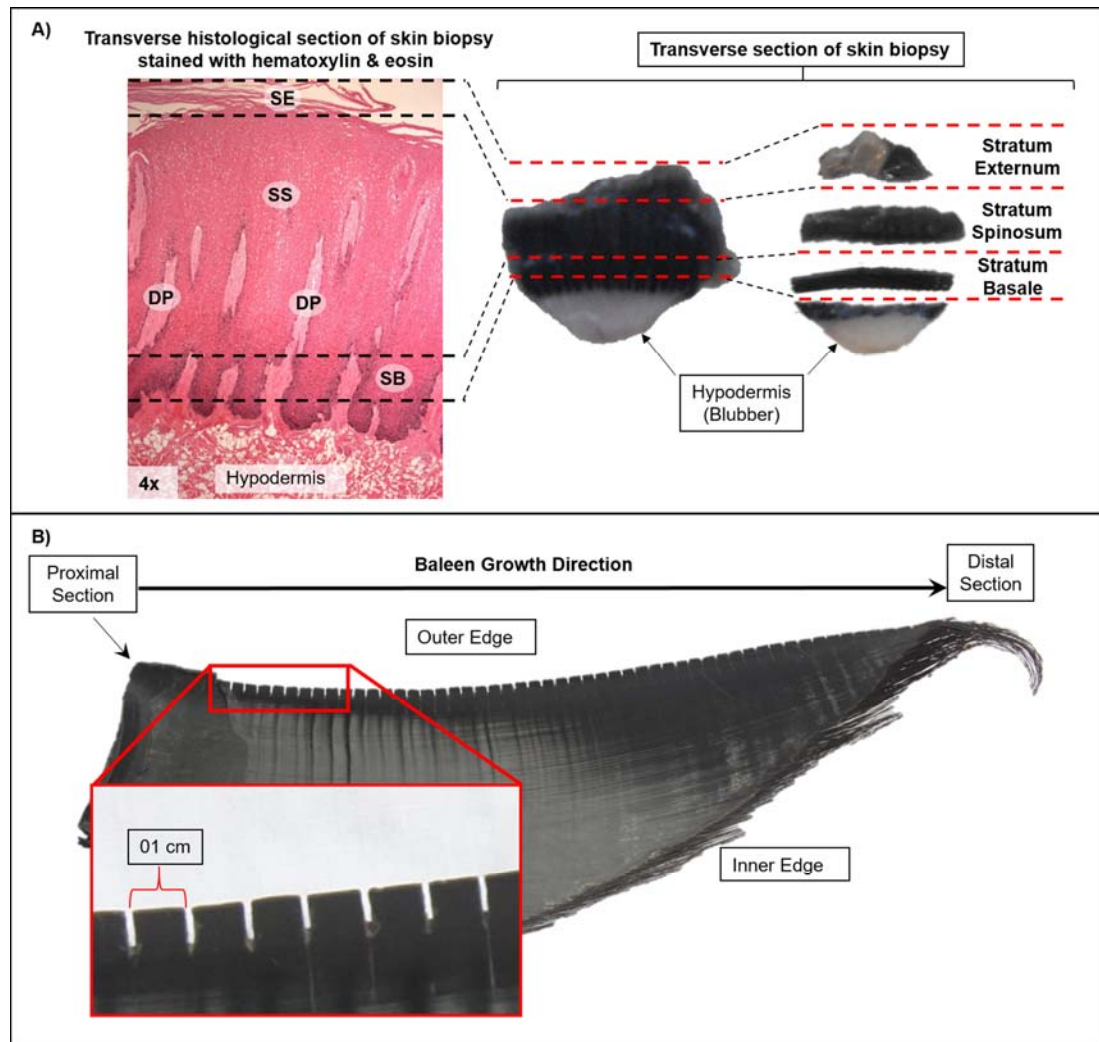


Figure 6. Methods for blue whale skin and baleen plate preparation. (A) Skin biopsy separation into strata: Stratum Basale (SB), Stratum Spinosum (SS) Stratum Externum (SE). The dermal papillae (DP) can be observed embedded in the skin. Dashed lines show where the cuts were made to separate the skin into strata. (B) Blue whale baleen plate sampling: baleen powder was sub-sampled in 1 cm intervals along the outer edge of the plate starting from the proximal section of the plate nearest the gum.

6.4. Standardizing blue whale skin sample preparation

Numerous studies show that two factors that are unrelated to ecology can alter isotope values of metabolically active tissues. The first factor is tissue lipid content. Lipids have lower $\delta^{13}\text{C}$ values than associated carbohydrates and proteins (DeNiro & Epstein, 1977; McConnaughey & McRoy, 1979; Newsome *et al.*, 2010). Thus, the potential influence of lipid content on bulk tissue $\delta^{13}\text{C}$ values must be considered when using stable isotope analysis of animal tissues to make ecological inferences (Newsome *et al.*, 2010; Lesage *et al.*, 2010; Ryan *et al.*, 2012). Chemical lipid-extraction removes the influence of lipids on bulk tissues, but a side effect of this procedure is that it may affect $\delta^{15}\text{N}$ values of tissues (Lesage *et al.*, 2010; Ryan *et al.*, 2012). To evaluate the effect of lipid-extraction on the isotope values of blue whale skin, five skin samples were divided into two subsamples, one subsample was lipid-extracted with three ~24 hour soaks in a 2:1 chloroform:methanol solvent solution, rinsed with ionized water and lyophilized. The second subsample was simply lyophilized, and analyzed as bulk tissue.

The second factor that can alter tissue isotopic composition is how samples are preserved prior to isotopic analysis. Ideally, all tissues would be stored frozen since freezing does not alter isotope values (Kaehler & Pakhomov, 2001; Sarakinos *et al.*, 2002; Barrow *et al.*, 2008; Newsome *et al.*, 2010). Most of the skin samples selected for this study were stored frozen prior to isotope analysis, but some ($n = 100$) were stored in a 20% salt saturated solution of dimethyl sulfoxide (DMSO). Previous studies have shown that the effect of DMSO on the isotope values of tissues can be removed via lipid-extraction (Todd *et al.*, 1997; Lesage *et al.*, 2010; Burrows *et al.*, 2014). To determine if this strategy would work for blue whale skin samples preserved in DMSO, we selected 25 sloughed skin samples from the GC (2005–2007). During field collection, each of these skin samples were divided into two sections and preserved one of two ways for one year before they were prepared for isotope analysis: the first set was preserved in DMSO and the second (control) set was frozen in liquid nitrogen (-195°C).

6.5. Stable isotope analysis

All skin and prey samples were lipid-extracted, lyophilized, and homogenized by grinding them into a fine powder; as noted above the small set of subsamples that were analyzed to test the effects of lipid-extraction were not lipid-extracted (bulk tissue). Baleen plates were cleaned with a solution of 2:1 chloroform:methanol to remove surface contaminants. Sub-samples of keratin powder were collected with a Dremel rotatory drill fitted to a flexible engraving shaft at 1 cm intervals along the outer edge of each baleen, starting at the proximal section inserted in the gum (which represents the newest tissue) (Fig. 6B). Baleen grows uniformly on the transverse perspective at a constant (but unknown) rate; thus our sampling strategy would yield equal time intervals between adjacent sub-samples (Schell *et al.*, 1989a, 1989b; Best & Schell, 1996; Caraveo-Patiño & Soto, 2005; Mitani *et al.*, 2006; Bentaleb *et al.*, 2011; Aguilar *et al.*, 2014). Previous studies have confirmed the consistency of isotope values along the length of two adjacent baleen plates of a gray whale (*Eschrichtius robustus*) (Caraveo-Patiño & Soto, 2005) and two plates from opposing sides of the mouth of a bowhead whale (*Balaena mysticetus*) (Schell *et al.*, 1989b). Consequently, we assumed that each baleen provides a consistent record of the past foraging history for each blue whale. Lastly, we compiled $\delta^{13}\text{C}$ and $\delta^{15}\text{N}$ data from the literature of potential blue whale prey zones in the eastern Pacific Ocean (see Results, section 7.3.).

Approximately 0.5-0.6 mg of each tissue sample (dried skin, baleen, and prey) was weighed into a tin capsule. Carbon ($\delta^{13}\text{C}$) and nitrogen ($\delta^{15}\text{N}$) isotope values were measured with a Costech 4010 elemental analyzer coupled to Thermo Scientific Delta V isotope ratio mass spectrometer at the Center for Stable Isotopes at the University of New Mexico (Albuquerque, NM). Isotope data are reported as delta δ values, $\delta^{13}\text{C}$ or $\delta^{15}\text{N} = 1000 [(R_{\text{sample}} / R_{\text{standard}}) - 1]$, where $R = {}^{13}\text{C}/{}^{12}\text{C}$ or ${}^{15}\text{N}/{}^{14}\text{N}$ ratio of sample and standard (Fry, 2006). Values are in units of parts per thousand or per mil (‰) and the internationally accepted standards are atmospheric N_2 for $\delta^{15}\text{N}$ and Vienna-Pee Dee Belemnite limestone (V-PDB) for $\delta^{13}\text{C}$ (Fry, 2006). Within-run

analytical precision was estimated via analysis of two proteinaceous internal reference materials, which was $\pm 0.2\text{‰}$ for both $\delta^{13}\text{C}$ and $\delta^{15}\text{N}$ values. We also measured the weight percent carbon and nitrogen concentration of each sample and used the C/N ratio as a proxy of lipid content (Logan *et al.*, 2008).

6.6. Statistical analysis

6.6.1. Assessing the effect of different processing methods in the isotope values of blue whale skin samples

All statistical analyses were performed using R language (R Development Core, 2017). The effects of preservation (DMSO-lipid extracted vs frozen-lipid extracted) and the different treatments (lipid removal vs bulk tissue) on skin $\delta^{13}\text{C}$, $\delta^{15}\text{N}$ and C/N ratios were evaluated with a max-*t test* for multiple comparisons of means. This procedure was chosen because it is designed to work in scenarios of unbalanced group sizes, non-normality and heteroscedasticity (Herberich *et al.*, 2010).

6.6.2. Comparing the variability of blue whale skin isotope values by strata

The isotope values variability between skin strata (basale, externum, sloughed skin) was also evaluated by using the max-*t test*, which has a higher power to detect differences between group means compared to other methods (Herberich *et al.*, 2010). These analyses were performed separately for each zone (GC and CCS) and isotope ($\delta^{13}\text{C}$ or $\delta^{15}\text{N}$). The CRD and GALPER skin isotope values were excluded from these analysis as sloughed skin samples were not available for these zones.

6.6.3. Estimating blue whale skin strata isotopic incorporation rate

The prey data were used to establish the reference mean (\pm SD) baseline isotope values within each zone, hereafter called the prey zone mean, which was estimated by pooling the means and variances of all the data. The pooled prey zone mean for the GC included lanternfish and the krill species *Nyctiphanes simplex*, because molecular analysis of fecal samples has shown that blue whales forage only on combined aggregations of both taxonomic groups in this zone (Del Angel-Rodríguez, 1997; Jiménez-Pinedo, 2010). Lanternfish was the only teleost fish present in blue whale fecal samples (Jiménez-Pinedo, 2010). In the CCS, we included isotope values of its main prey, the krill species *Thysanoessa spinifera* and *Euphausia pacifica* (Fiedler *et al.*, 1998; Croll *et al.*, 2005). In the CRD, diving behavior and the presence of whale fecal samples confirmed that blue whales forage on patches of krill (Matteson, 2009), however, the species of krill was not identified, so we used previously reported data for krill in this zone (Williams, 2013).

Our approach to estimate the blue whale skin isotopic incorporation rate was to mimic a diet switch in controlled feeding experiments, but at population level (sampling the same individual whale across its annual migratory cycle is logistically impossible). Blue whales in the northeast Pacific are ideal for this approach because they feed year-round and seasonally migrate between zones that have distinct baseline isotope values (Altabet *et al.*, 1999; Miller, 2006; Miller *et al.*, 2008; Williams, 2013; Aurióles-Gamboa *et al.*, 2013; Williams *et al.*, 2014). To achieve this, first we evaluated if blue whale skin $\delta^{13}\text{C}$ and $\delta^{15}\text{N}$ values exhibited seasonal trends in the GC (Jan-Apr) and the CCS (Jun-Dec). Sampling effort within each zone was not homogenous for all years, thus blue whale skin samples collected in different years were integrated into a single analysis. We assessed the seasonal trend by fitting a generalized additive model (GAM) of the skin $\delta^{15}\text{N}$ and $\delta^{13}\text{C}$ values as functions of time (Julian day, which ranges from 1 to 365). This was done separately for each skin stratum (basale, externum, and sloughed skin) in both foraging zones (GC and CCS). We used GAMs because they are especially useful when the functional form of the

relationship between the response (e.g. $\delta^{15}\text{N}$ and $\delta^{13}\text{C}$ values) and explanatory variables (e.g. time) is unknown (Yee & Mitchell, 1991). GAMs were fitted using the “mgcv” package in R (Wood, 2006; R Development Core, 2017). To model the main trend of the data, the smoothing parameters (degrees of freedom) were set to three. This conservative approach can be applied when sample size is low (Xiang, 2001). Blue whale skin strata $\delta^{13}\text{C}$ did not show seasonal trends (see Results, section 7.7.), therefore, the isotopic incorporation rate was only estimated for skin $\delta^{15}\text{N}$.

To compare the $\delta^{15}\text{N}$ values of the three skin strata to potential prey, we assumed a trophic discrimination factor ($\Delta^{15}\text{N}$) of 1.6‰, based on controlled feeding experiments on captive bottlenose dolphins (*Tursiops truncatus*) (Browning *et al.*, 2014; Giménez *et al.*, 2016), and calculated the trophic-corrected mean blue whale skin values for each zone by adding this trophic discrimination factor to the prey zone mean values. These trophic-corrected skin values would represent the expected mean $\delta^{15}\text{N}$ values if blue whale skin had fully equilibrated with that of local prey (or reached steady-state isotopic equilibrium), and we assumed that this method would allow us to assign any given blue whale skin isotope value to a specific foraging zone.

Based on the gradient in the prey mean isotope values for each foraging zone (GC > CCS > CRD; see Results), and the trophic-corrected blue whale skin values (see Results), our hypothesis was that blue whales would arrive to the GC with lower skin $\delta^{15}\text{N}$ values due to consumption of prey in the CCS and CRD. Skin isotope values would then increase throughout the winter season as they equilibrate with local prey (see Results). In contrast, most whales would arrive in the CCS with higher skin isotope values, except for individuals that migrated from the CRD. Thus, we predicted that skin isotope values would decrease throughout the summer season as skin isotopically equilibrated with the local prey in the CCS. Therefore, we used the GAMs seasonal predictions to estimate the isotopic incorporation rate for each skin stratum, as the days that it would take for the skin $\delta^{15}\text{N}$ to increase (GC) or decrease (CCS) by the assumed trophic discrimination factor ($\Delta^{15}\text{N}= 1.6\text{‰}$) to reach isotopic equilibrium with the local diet. This period was derived by extrapolating from the

distance between the predicted extremes in $\delta^{15}\text{N}$ for each stratum, from the lowest to the highest in the GC and vice versa for the CCS (see Results, Appendix I and II). In this case, we assumed that the equivalent to the diet switch stage would be the lowest initial $\delta^{15}\text{N}$ value within the GC and the highest initial $\delta^{15}\text{N}$ value in the CCS (see Results, Appendix I and II). We used the same method with the 95% upper and lower confidence intervals to assess uncertainty. Unfortunately, the uncertainty associated to individual variability in isotopic incorporation rates given the potential variation in individual arrival and departure times to/from the GC and CCS, could not be considered in the model.

Due to sample size limitations, we had to integrate all the skin data collected in different years into a single seasonal model to estimate blue whale $\delta^{15}\text{N}$ isotopic incorporation rate. This assumes that the relative difference in prey $\delta^{15}\text{N}$ values between foraging zones is consistent across years, which has been suggested in previous studies (Aurioles-Gamboa *et al.*, 2013; Fleming *et al.*, 2016). We evaluated this assumption by fitting a generalized linear model (GLM) of skin $\delta^{15}\text{N}$ values as a function of time (Julian Date, or date of sample collection). Julian Dates are a continuous count of days based on a standard starting point, which we chose as January 1, 1970 (Universal Time, Coordinated). This analysis was made separately for each foraging zone (GC, CCS and CRD) by using all skin strata, which allowed us to evaluate the trends in skin $\delta^{15}\text{N}$ across years in each zone. The GLMs were fitted by using the “glm” function in R (reviewed in Mangiafico, 2016).

6.6.4. Determining the isotopic niche width and trophic overlap of blue whales in the eastern Pacific, by region (SEP and NEP) and sex (females and males)

Isotopic niche width was estimated by using stable isotope Bayesian ellipses (SEAB), implemented with the R package “SIBER 2.1.0” (Jackson *et al.*, 2011). The shape and size of the ellipses is defined by the co-variance matrix of $\delta^{13}\text{C}$ and $\delta^{15}\text{N}$, while its position is specified by the means of both variables. Isotopic niche parameters are estimated in a Bayesian framework, which has the advantage of

using explicit probabilistic inference. To estimate parameters, this method uses vague normal priors for the means describing the likely range of $\delta^{13}\text{C}$ and $\delta^{15}\text{N}$, and a vague Inverse-Wishart prior for the covariance matrix (Jackson *et al.*, 2011; McCarthy 2007). Markov Chain Monte Carlo Simulations are used to construct the posterior estimates of the parameters. Parameters were finally constructed by using the priors and the likelihoods. This approach allows to incorporate uncertainties associated to parameter construction and small sample size into niche metrics. The isotopic niche width is expressed as the Bayesian standard ellipse area (SEA_B) in ‰^2 . SEA_B contains approximately 95 % of the data. To graphically represent the isotopic niche width of all groups we used the standard ellipse areas corrected for small sample size (SEA_C), which has the same properties than SEA_B , but is unbiased to sample size. The overlap between isotopic niches was estimated as a proportion of the non-overlapping area between two ellipses. This proportion ranged from 0 when the ellipses were distinct, to 1 when there was a total overlap in niche space. Isotopic niche width was estimated separately for each foraging zone in the NEP (CCS, GC and CRD), and SEP (GALPE). With the aim of increasing sample size and obtaining additional isotopic information, the skin biopsies of GALPE ($n=25$) were also divided into strata (stratum basale and externum).

A proportion of the blue whale skin samples selected from the different tissue banks (NOAA-SWFSC, CRC, and CICIMAR-IPN) were sexed by using genetic methods (Morin *et al.*, 2005, 2006). To further explore if blue whale females and males exhibited differences in their isotopic niche we compared these groups separately for the NEP and SEP, by using SEA_B and posteriorly calculating the degree of overlap between isotopic niches spaces, which as mentioned earlier it is expressed as the proportion of the non-overlapping area between to ellipses, and its scaled from 0 to 1.

6.6.5. Quantifying the relative contribution of different foraging zones to the blue whale diet in the NEP

The relative contribution of different foraging zones to the isotopic composition of the blue whale skin collected in the NEP was estimated by using a Bayesian dietary isotopic mixing model. The model was developed with the package “MixSIAR 3.1” for R (Stock and Semmens, 2016). These models are used to calculate the likely proportional contribution of different prey to a consumer’s diet based on their respective isotope values and the trophic discrimination factor (Acevedo-Gutiérrez *et al.*, 2002; Semmens *et al.*, 2009; Parnell *et al.*, 2010). Analyzing these models in a Bayesian framework allows to consider the uncertainty associated to the final estimations of the relative contribution of different prey sources to the consumer’s diet. I used vague priors for the Bayesian model, because of the lack of information on the proportional contribution of different prey to the diet of blue whales in the NEP.

The variables introduced to the model were the nitrogen isotope values ($\delta^{15}\text{N}$) of the consumers (blue whales), potential prey (see 7. Results, section 7.3., 49 p.) and I used the trophic discrimination factor derived from the longest controlled feeding experiment with captive bottlenose dolphins ($\Delta^{15}\text{N}$: $1.6 \pm 0.5\text{‰}$) (Giménez *et al.*, 2016), which is similar to the trophic discrimination factor estimated for the blue whale ($\Delta^{15}\text{N}$: 1.4–1.6‰) in the GC (Busquets, 2008). I only used one biotracer, $\delta^{15}\text{N}$ values, because $\delta^{13}\text{C}$ values did not show seasonal trends in blue whale skin which could indicate that this biotracer is not effectively reflecting diet (see Results, section 7.7.). I only used one biotracer, $\delta^{15}\text{N}$ values, because $\delta^{13}\text{C}$ values did not show seasonal trends in blue whale skin which could indicate that this biotracer is not effectively reflecting diet (see Results, section 7.7.).

Given that these models are highly sensitive to the trophic discrimination factor, I additionally ran a Bayesian dietary isotopic mixing model using a trophic discrimination factor of $\Delta^{15}\text{N}$: $1.9 \pm 0.5\text{‰}$, which was estimated in this study by using

isotopic data of blue whale baleen plates and prey (see 8. Discussion, section 8.6. $\delta^{15}\text{N}$ trophic discrimination factors, 82 p).

6.6.6. Estimating blue whale baleen growth rates and isotopic niche width to infer the movement patterns of individual blue whales in the NEP

Oscillations in $\delta^{13}\text{C}$ and $\delta^{15}\text{N}$ values of baleen plates were also evaluated with a GAM model and smoothing parameters were selected by standard data-driven methods for time series using Akaike Information Criteria (Peng *et al.*, 2006; Chuang *et al.*, 2011). Similar to skin, baleen $\delta^{13}\text{C}$ values were not distinct among foraging zones (see Results, section 7.7.), consequently growth rates were estimated using $\delta^{15}\text{N}$ values. Blue whale baleen growth rate was determined by assuming that the oscillation in $\delta^{15}\text{N}$ values along the total length of the outer edge of the baleen plates represent the annual movement between winter/spring and summer/fall foraging grounds. Thus, the distance between two sequential $\delta^{15}\text{N}$ minimums represents the growth of the baleen plate during a single year (Schell *et al.*, 1989a, 1989b; Best & Schell, 1996; Bentaleb *et al.*, 2011; Aguilar *et al.*, 2014). To characterize the movement of whales among isotopically distinct foraging zones, we compared baleen $\delta^{15}\text{N}$ values with the trophic-corrected $\delta^{15}\text{N}$ values for each foraging zone based on the same $\Delta^{15}\text{N}$ used in the skin analysis (Browning *et al.*, 2014; Giménez *et al.*, 2016). Additionally, I calculated the isotopic niche width and overlap of the seven blue whale baleen plates by using SEA_B (see Materials and Methods, section 6.6.4).

7. RESULTS

7.1. Assessing the effect of different processing methods in the isotope values of blue whale skin samples

The max-*t* test results comparing the effect of different treatments (bulk tissue vs lipid-extracted; frozen vs DMSO) on skin $\delta^{15}\text{N}$, $\delta^{13}\text{C}$ and C/N ratios are presented in Table 2 (Appendix III and IV). Lipid-extracted skin (-16.5 ± 0.1) had mean $\delta^{13}\text{C}$ values that were significantly higher (1.9‰) than the bulk skin samples (-18.4 ± 0.4 ; $t = -10.4$, $p = <0.001$), and the weight percent C/N ratios of bulk skin were significantly higher (4.2 ± 0.1) than lipid extracted samples (3.2 ± 0.0 ; $t = 12.9$, $p = <0.001$). In contrast, skin $\delta^{15}\text{N}$ values did not differ significantly between lipid-extracted (14.6 ± 0.3) and bulk skin (14.5 ± 0.3 ; $t = -0.4$, $p = 0.7$). Lastly, $\delta^{15}\text{N}$, $\delta^{13}\text{C}$, and C/N ratios of skin samples stored in DMSO ($\delta^{15}\text{N}$: 13.9 ± 0.9 ; $\delta^{13}\text{C}$: -16.9 ± 0.5 ; C/N: 3.0 ± 0.2) did not differ significantly from skin samples stored frozen ($\delta^{15}\text{N}$: 14.0 ± 0.9 ; $\delta^{13}\text{C}$: -16.9 ± 0.6 ; C/N: 3.0 ± 0.2); $\delta^{15}\text{N}$: $t = 0.2$, $p = 0.8$; $\delta^{13}\text{C}$: $t = 0.2$, $p = 0.8$; and C/N: $t = -0.4$, $p = 0.7$.

7.2. Comparing the variability of blue whale skin isotope values by strata

The max-*t* test results comparing the $\delta^{15}\text{N}$ and $\delta^{13}\text{C}$ values among skin strata (basale, externum and sloughed skin) in each zone (GC and CCS) are shown in Table 3 (Appendix V). Skin $\delta^{15}\text{N}$ and $\delta^{13}\text{C}$ did not differ significantly between different skin strata within the GC (Table 3). In the CCS, mean $\delta^{15}\text{N}$ values of sloughed skin ($13.6 \pm 0.7\text{‰}$) and stratum externum ($13.4 \pm 1.1\text{‰}$) did not differ significantly ($t = -0.4$, $p = 0.7$), and both of these strata had slightly but significantly higher $\delta^{15}\text{N}$ (stratum externum: $t = 2.6$, $p = <0.001$; sloughed skin: $t = -4.9$, $p = <0.001$) than the stratum basale ($13.0 \pm 0.8\text{‰}$). $\delta^{13}\text{C}$ values did not differ significantly among strata in the CCS (Table 3).

Table 2. Max-*t* test results comparing the effect of different treatments on skin $\delta^{15}\text{N}$, $\delta^{13}\text{C}$ and weight percent C/N ratios. LE, lipid-extracted skin; Diff, estimated differences between group means; CI, confidence intervals; SE, Standard error; *t*, test value; *P*, adjusted p values reported, values in bold were considered statistically significant (<0.05).

A. Comparison between bulk skin vs lipid-extracted skin

Mean \pm SD (<i>n</i>)								
Variable	Bulk skin	Lipid extracted	Treatment comparison	Diff	CI: 95%	SE	<i>t</i>	<i>P</i>
$\delta^{15}\text{N}$	14.5 \pm 0.3 (5)	14.6 \pm 0.3 (5)	Bulk skin - Lipid extracted	-0.1	-0.6 – 0.4	0.2	-0.4	0.7
$\delta^{13}\text{C}$	-18.4 \pm 0.3 (5)	-16.5 \pm 0.1 (5)	Bulk skin - Lipid extracted	-1.9	-2.3 – -1.5	0.2	-10.4	<0.001
C/N ratio	4.2 \pm 0.1 (5)	3.2 \pm 0.0 (5)	Bulk skin - Lipid extracted	1.0	0.8 – 1.2	0.1	12.9	<0.001

B. Comparison between skin preserved in DMSO vs preserved Frozen

Mean \pm SD (<i>n</i>)								
	Frozen/LE	DMSO/LE	Treatment comparison	Diff	CI: 95%	SE	<i>t</i>	<i>P</i>
$\delta^{15}\text{N}$	14.0 \pm 0.9 (25)	13.9 \pm 0.9 (25)	Frozen/LE - DMSO/LE	0.1	-0.5 – 0.6	0.2	0.2	0.8
$\delta^{13}\text{C}$	-16.9 \pm 0.6 (25)	-16.9 \pm 0.5 (25)	Frozen/LE - DMSO/LE	0.0	-0.3 – 0.4	0.2	0.2	0.8
C/N ratio	3.0 \pm 0.2 (25)	3.1 \pm 0.2 (25)	Frozen/LE - DMSO/LE	-0.0	-0.1 – 0.1	0.1	-0.4	0.7

Table 3. Max-*t* test results for the comparison of $\delta^{13}\text{C}$ and $\delta^{15}\text{N}$ values among different skin strata in the Gulf of California (GC) and California Current System (CCS). δ , isotope; Diff, estimated differences between group means; CI, confidence intervals; SE, Standard error; *t*, test value; *P*, adjusted p values reported, values in bold were considered statistically significant (<0.05).

Zone	δ	Mean \pm SD (<i>n</i>)			Strata comparison	Diff	CI: 95%	SE	<i>t</i>	<i>P</i>
		Stratum Basale	Stratum Externum	Sloughed Skin						
GC	$\delta^{15}\text{N}$	14.9 \pm 0.7 (101)	14.9 \pm 0.8 (85)	14.7 \pm 1.0 (81)	Basale - Sloughed	0.2	-0.2–0.5	0.1	1.1	0.5
					Externum - Sloughed	0.2	-0.2–0.5	0.2	1.1	0.5
					Externum - Basale	0.0	-0.2–0.3	0.1	0.1	1
	$\delta^{13}\text{C}$	-16.7 \pm 0.7 (101)	-16.7 \pm 0.5 (85)	-16.7 \pm 0.6 (81)	Basale - Sloughed	0.0	-0.2–0.3	0.1	0.4	0.9
					Externum - Sloughed	0.1	-0.2–0.3	0.1	0.5	0.9
					Externum - Basale	0.0	-0.2–0.2	0.1	0.1	1
CCS	$\delta^{15}\text{N}$	13 \pm 0.8 (120)	13.4 \pm 1.1 (63)	13.6 \pm 0.7 (93)	Basale - Sloughed	-0.5	-0.8 – -0.3	0.1	-4.9	<0.001
					Externum - Sloughed	-0.1	-0.5–0.2	0.2	-0.7	0.7
					Externum - Basale	0.4	0.0–0.8	0.2	2.6	<0.001
	$\delta^{13}\text{C}$	-16.8 \pm 0.7 (120)	-16.9 \pm 0.7 (63)	-17 \pm 0.9 (93)	Basale - Sloughed	0.2	-0.1–0.4	1.4	1.4	0.3
					Externum - Sloughed	0.0	-0.2–0.4	0.5	0.5	0.9
					Externum - Basale	-0.1	-0.3–0.1	-0.9	-0.9	0.6

7.3. Estimating blue whale skin strata isotopic incorporation rate

The GLM model of blue whale skin $\delta^{15}\text{N}$ values as a function of time (Julian Date) was not significant ($t = -1.4$; $p = 0.3$) in the CRD (1999–2003; Table 4, Fig. 7). Conversely, the relationship between these variables was significant and positive in the GC ($t = 3.1$; $p < 0.001$) and the CCS ($t = 7.3$; $p < 0.001$) (Table 4, Fig. 7). The GLM model predicts an overall increase of 1.2‰ over 15 years (1996–2011) in the CCS, and an increase of 0.8‰ over 13 years (2002–2015) in the GC (Table 4, Fig. 7); overall, these shifts results in a 0.1‰ increase per year in each zone. Thus, skin $\delta^{15}\text{N}$ values showed a slight and consistent trend in both zones, therefore the gradient in $\delta^{15}\text{N}$ values between zones would also remain constant. This result would validate the integration of blue whale skin $\delta^{15}\text{N}$ values in a single seasonal GAM model to infer skin $\delta^{15}\text{N}$ isotopic incorporation rate for each zone.

Prey from the three zones had distinct $\delta^{15}\text{N}$ values (Tables 5 and 6), with values decreasing from the GC to the CCS and CRD. The trophic-corrected blue whale skin $\delta^{15}\text{N}$ values for each foraging zone are presented in Table 5. The magnitude of differences in prey between these zones ranged from 1.9‰ to 6.1‰ (Table 6), which allowed us to assign the origin of measured $\delta^{15}\text{N}$ values of the different blue whale skin strata, independently of the zone where whales were sampled (Table 5, Fig. 8).

The GAM results of the relationship between blue whale skin $\delta^{15}\text{N}$ values and time (seasonal trend) are shown in Table 7. The GAM that used $\delta^{15}\text{N}$ values in blue whale skin stratum basale and externum in relation to time indicated a weak, but slightly significant positive relationship in the GC, and a weak, but slightly significant negative relationship for the CCS (Table 7, Fig. 8). These relationships were anticipated based on the observed pattern in prey $\delta^{15}\text{N}$ values among zones and the trophic-corrected blue whale skin values for each foraging zone (Tables 6 and 7). For samples collected in the GC, $\delta^{15}\text{N}$ values increased to ~ 17 ‰ by April (Fig. 8), which likely reflected isotopic equilibration with the $\delta^{15}\text{N}$ of local prey (Table 5). The

opposite pattern was observed in the CCS, where the $\delta^{15}\text{N}$ values decreased with time to a low of $\sim 13\text{‰}$ by December (Fig. 8), which also suggests gradual equilibration of the tissue to the local prey. In contrast, the relation between sloughed skin $\delta^{15}\text{N}$ values and time was not significant in the GC or CCS (Table 7). The GAM model for sloughed skin showed a parabolic relationship with time, with a slight tendency of the $\delta^{15}\text{N}$ values to increase and subsequently decrease with time in both zones (Fig. 8). Therefore, we used the same method than that for the stratum basale and externum within each zone to estimate the isotopic incorporation rate of sloughed skin (Appendix I).

The CRD skin $\delta^{15}\text{N}$ values were used as a reference to determine if the isotopic signal of this foraging zone was present in the skin sampled in the GC and the CCS. Some of the observed $\delta^{15}\text{N}$ values in the stratum basale and stratum externum from skin sampled in the CCS could represent transitional values between the CRD isotopic signal and the CCS signal. One of the values observed in the stratum externum sampled in August was assigned to the CRD (Fig. 5).

The deviance explained in the relationship between skin $\delta^{15}\text{N}$ values and time for all six GAM models was low (6.7 to 21.1%; Table 7) due to the high degree of dispersion observed in skin data. This degree of variation was expected since the duration of time individual whales had spent in the zone where skin was collected was unknown at the time of sampling. As such, this variation is likely driven by a combination of recently arrived whales that had isotope values reflective of other foraging zones, individuals in the equilibration period with intermediate isotope values that represent a mixture of prey consumed in two foraging zones, or individuals that had reached skin steady-state isotopic equilibrium with the isotopic composition of local prey (Fig. 8).

Table 4. GLM results relating blue whale skin $\delta^{15}\text{N}$ values to time (Julian date) in the Gulf of California (GC), California Current System (CCS) and Costa Rica Dome (CRD). α , intercept parameter; β , slope parameter; SME, standard error of the mean; CL, confident intervals of the mean; t , test values; P , p values reported, values in bold were considered statistically significant (<0.05); ^a time, in the model represents number of days.

Zone	<i>n</i>	Model	Coefficient \pm SME	CI (95%)	<i>t</i>	Residual deviance	<i>df</i>	AIC	<i>P</i>
GC	267	$\delta^{15}\text{N}_{\text{skin}} = 12.4 + 1.8e^{-4} \cdot \text{time}^a$	$\alpha = 12.4 \pm 0.6$ $\beta = 1.8e^{-4} \pm 4.7e^{-5}$	11.2 – 13.7 8.5e ⁻⁵ – 3.0e ⁻⁴	3.8	190.6	265	673.8	< 0.001
CCS	276	$\delta^{15}\text{N}_{\text{skin}} = 10.5 + 2.2e^{-4} \cdot \text{time}^a$	$\alpha = 10.5 \pm 0.4$ $\beta = 2.2e^{-4} \pm 3.0e^{-5}$	9.7 – 11.2 2.0e ⁻⁴ – 2.8e ⁻⁴	7.3	184.9	274	678.7	< 0.001
CRD	16	$\delta^{15}\text{N}_{\text{skin}} = 17 - 4.5e^{-4} \cdot \text{time}^a$	$\alpha = 17 \pm 4.7$ $\beta = 4.5e^{-4} \pm 4.2e^{-4}$	7.9 – 26.2 -1.3e ⁻³ – 3.8e ⁻⁴	-1.4	38.2	36	114.08	0.3

Table 5. Trophic-corrected blue whale skin $\delta^{15}\text{N}$ values for each foraging zone. Values were estimated by using the prey zone mean \pm SD (Table 6) and assuming $\Delta^{15}\text{N}$ of 1.6‰.

Zone	Prey zone mean (\pm SD) $\delta^{15}\text{N}$	$\Delta^{15}\text{N}$	Trophic-corrected blue whale skin $\delta^{15}\text{N}$
Gulf of California	14.6 \pm 1.0	1.6	16.2 \pm 1.0
California Current System	10.4 \pm 0.3	1.6	12.0 \pm 0.3
Costa Rica Dome	8.5 \pm 1.1	1.6	10.1 \pm 1.1

Table 6. Mean (\pm SD) $\delta^{13}\text{C}$, $\delta^{15}\text{N}$, and weight percent C/N ratios of potential blue whale prey in the eastern Pacific Ocean. *N.s.*, *Nyctiphanes simplex*; Lf, Lanterfish; *T.s.*, *Thysanoesa spinifera*; *E.p.*, *Euphausia pacifica*.

Zones	Years	Prey	n	Mean \pm SD			Source
				$\delta^{13}\text{C}$	$\delta^{15}\text{N}$	C/N	
Gulf of California	2000-2001	<i>N.s.</i>	5	-17.7 \pm 0.1	12.6 \pm 0.1	-	(Jaume-Schinkel, 2004)
	2004	<i>N.s.</i>	1	-17.8	15.0	2.9	This study
	2005	<i>N.s.</i>	7	-17.9 \pm 0.5	14.6 \pm 0.6	3.2 \pm 0.1	This study
	2006	<i>N.s.</i>	7	-17.8 \pm 1.4	13.5 \pm 1.6	3.0 \pm 0.0	This study
	2006-2007	<i>N.s.</i>	8	-18.1 \pm 0.5	14.7 \pm 0.8	-	(Sampson <i>et al.</i> , 2010)
	2013	<i>N.s.</i>	3	-18.2 \pm 1.8	13.8 \pm 1.2	3.4 \pm 0.0	This study
	2014	<i>N.s.</i>	5	-18.1 \pm 0.2	15.4 \pm 1.5	3.3 \pm 0.2	This study
	2015	<i>N.s.</i>	11	-18.3 \pm 0.9	14.1 \pm 0.8	3.3 \pm 0.1	This study
	2013	Lf	3	-17 \pm 0.3	18.1 \pm 0.5	3.2 \pm 0.1	This study
	2014	Lf	1	-16.7	18.1	3.3	This study
2015	Lf	3	-17.7 \pm 0.6	16.7 \pm 1.5	3.2 \pm 0.1	This study	
Mean \pm SD^a				-17.9 \pm 0.9	14.6 \pm 1		
California Current System	1994	<i>T.s./E.p.</i>	5	-20.2 \pm 0.3	11.2 \pm 0.5	-	(Sydeman <i>et al.</i> , 1997)
	2000	<i>E.p.</i>	24	-20.0 \pm 0.1	9.7 \pm 0.2	-	(Miller, 2006)
	2000	<i>T.s.</i>	58	-18.6 \pm 0.1	11.2 \pm 0.1	-	(Miller, 2006)
	2002	<i>E.p.</i>	11	-17.9 \pm 0.3	9.1 \pm 0.2	-	(Miller, 2006)
	2002	<i>T.s.</i>	21	-16.9 \pm 0.3	10.1 \pm 0.1	-	(Miller, 2006)
	2001-2002	<i>E.p.</i>	10	-19.7 \pm 0.8	9.9 \pm 0.4	-	(Becker <i>et al.</i> , 2007)
	2002	<i>T.s.</i>	5	-18.6 \pm 2	11.1 \pm 0.8	-	(Hipfner <i>et al.</i> , 2010)
	2013	<i>T.s.</i>	10	-17.3 \pm 0.4	9.6 \pm 0.6	-	(Carle, 2014)
Mean \pm SD^a				-18.6 \pm 0.4	10.4 \pm 0.3		
Costa Rica Dome	2007-2008	Krill	14-15	-20.8 \pm 2 ^b	8.5 \pm 1.1	5.8 \pm 0.2	(Williams, 2013)
Mean \pm SD				-20.8 \pm 2^b	8.5 \pm 1.1		
Galapagos		Krill	3	-21.7 \pm 0.1	4.5 \pm 0.1	3.4 \pm 0.1	This study
Mean \pm SD				-21.7 \pm 0.1	4.5 \pm 0.1		

^a The mean \pm SD isotope values of the prey from these zones were estimated by pooling the means and variances of the data from this study and from the literature.

^b Krill samples used in that study were not lipid-extracted. Williams *et al.* (2013) provided a mean weight percent C/N ratio of 5.8 for bulk krill samples. If krill $\delta^{13}\text{C}$ data from the Costa Rica Dome is lipid-normalized using this C/N ratio and equations in McConnaughey and McRoy (1979), the mean $\delta^{13}\text{C}$ value would be -19.4‰ and there would be greater overlap in $\delta^{13}\text{C}$ values among prey of different zones (Costa Rica Dome, California Current System and Gulf of California).

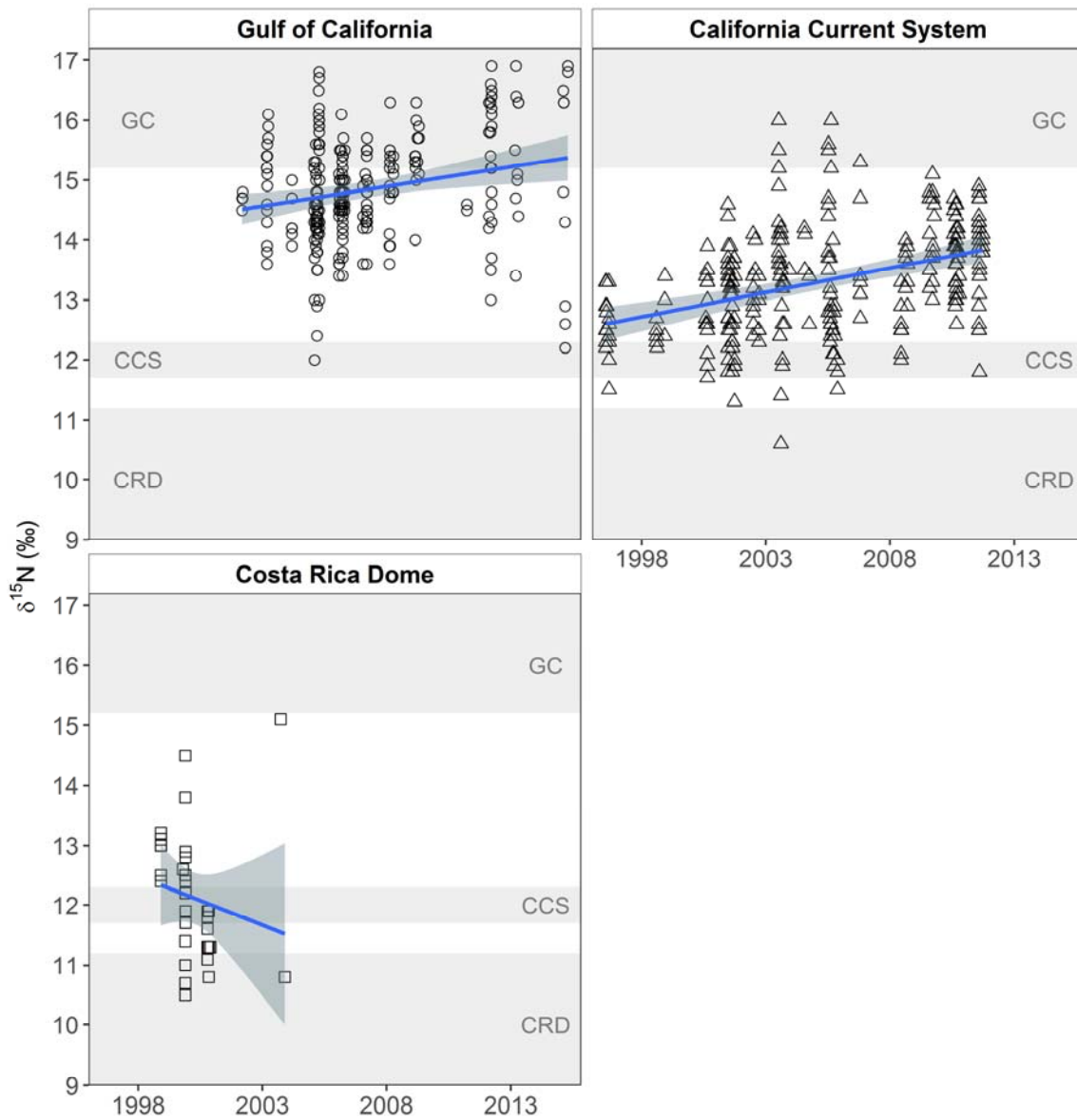


Figure 7. GLM analysis relating skin $\delta^{15}\text{N}$ values to time (Julian Date, presented in years). Points represent the actual $\delta^{15}\text{N}$ values of blue whale skin collected in different zones of the northeast Pacific. Lines represent the fit of the GLM model and the fringe around the lines show the 95% confidence intervals. The gray shaded area represents the mean \pm SD of the trophic-corrected blue whale skin values for each foraging zone; Gulf of California (GC), California Current System (CCS), and Costa Rica Dome (CRD).

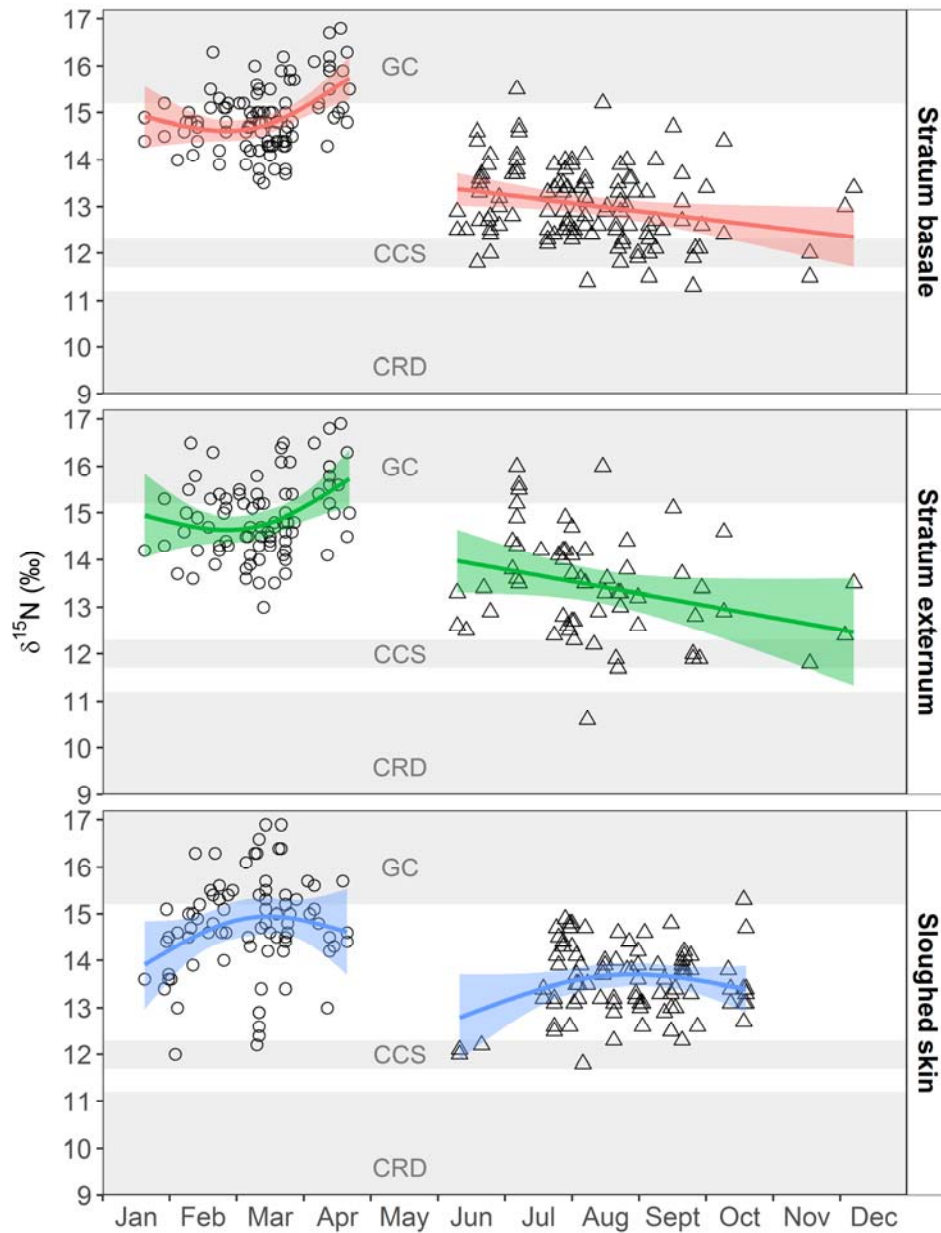


Figure 8. GAM analysis of the seasonal trend of skin strata $\delta^{15}\text{N}$ values in two foraging zones. The points represent the actual $\delta^{15}\text{N}$ values of skin collected from whales within the Gulf of California (open circles) and the California Current System (open triangles). The colored lines represent the GAM model fit (predictions) and the fringe around the lines show the 95% confidence intervals. The gray shaded area represents the mean \pm SD of the trophic-corrected blue whale skin values for each foraging zone: Gulf of California (GC), the California Current System (CCS) and the Costa Rica Dome (CRS).

Table 7. GAM results for the seasonal trends of $\delta^{15}\text{N}$ and $\delta^{13}\text{C}$ values in different skin strata sampled in the Gulf of California (GC) and California Current System (CCS). *E.df.*, Estimated degrees of freedom; *F*, test of whether the smoothed function significantly reduces model deviance; *P*, p-values in bold were considered statistically significant (<0.05).

Isotope	Skin stratum	Zone	<i>n</i>	<i>E.df.</i>	<i>F</i>	Adjusted R ²	<i>P</i>	Deviance explained (%)
$\delta^{15}\text{N}$	Basale	GC	101	1.9	13.4	0.2	< 0.001	21.1
	Basale	CCS	120	1.0	8.4	0.6	< 0.01	6.7
	Externum	GC	85	1.9	7.4	0.1	< 0.01	14.7
	Externum	CCS	63	1.0	5.5	0.1	< 0.05	8.3
	Sloughed skin	GC	81	1.8	3.3	0.1	0.7	7.7
	Sloughed skin	CCS	93	1.8	2.6	0.0	0.7	6.7
$\delta^{13}\text{C}$	Basale	GC	101	1.0	0.2	-0.0	0.7	0.2
	Basale	CCS	120	1.9	3.6	0.1	< 0.05	6.2
	Externum	GC	85	1.5	1.3	0.1	0.4	2.8
	Externum	CCS	63	1.5	0.6	0.0	0.6	2.8
	Sloughed skin	GC	81	1.0	1.3	0.0	0.3	1.6
	Sloughed skin	CCS	93	1.0	0.1	-0.0	0.8	0.1

Estimates of $\delta^{15}\text{N}$ isotopic incorporation rate of blue whale skin strata in each foraging zone are shown in Table 8 and Appendix II. In the GC, the stratum basale (81 d), stratum externum (81 d), and sloughed skin (90 d) had similar incorporation rates (Table 8). In the CCS, the stratum basale had longer incorporation rates (262 d) than the stratum externum (192 d). Sloughed skin (272 d) had the lowest isotopic incorporation rate in CCS, although the later estimate had a high degree of uncertainty (Table 8). The average skin strata isotopic incorporation rate in the CCS (242 d) was 158 days lower than the GC (84 d) (Table 8). The overall mean of the $\delta^{15}\text{N}$ isotopic incorporation rate of blue whale skin was estimated, integrating all strata in both zones (163 d, Table 8).

Table 8. $\delta^{15}\text{N}$ isotopic incorporation rates of blue whale skin strata in the Gulf of California and California Current System. The number of days were estimated by extrapolating from the GAM predictions (model fit and the upper and lower 95% confidence limits) for skin $\delta^{15}\text{N}$ values to change by 1.6‰ to isotopically equilibrate with local prey in each zone.

Zone	Skin Stratum	$\delta^{15}\text{N}$ isotopic incorporation rate of blue whale skin		
		Model fit	Lower limit	Upper limit
Gulf of California	Basale	81	90	69
	Externum	81	112	69
	Sloughed Skin	90	60	149
Mean \pm SD		84 \pm 5		
California Current System	Basale	262	222	360
	Externum	192	160	240
	Sloughed Skin	272	163	816
Mean \pm SD		242 \pm 44		
Overall Mean \pm SD		163 \pm 91		

7.4. Isotopic niche width and trophic overlap of blue whales in the eastern Pacific Ocean by region and sex

7.4.1. Blue whales in the NEP and SEP

The R code of SIBER used to estimate the isotopic niche width and overlap in this study is available in Appendix VII. The mean \pm SD values of $\delta^{15}\text{N}$ exhibited a marked gradient among prey (Table 6) and blue whale skin (Table 9; Appendix VI) of different zones in the eastern Pacific Ocean. In the case of $\delta^{13}\text{C}$ values the gradient was not as marked as for $\delta^{15}\text{N}$ values (Tables 6 and 9). The gradients of both isotopes were further explored by calculating the trophic width (isotopic niche width) and overlap between zones using Bayesian Standard Ellipse Areas (SEA_B) and SEA corrected for small sample size (SEA_c).

Table 9. $\delta^{15}\text{N}$ and $\delta^{13}\text{C}$ (Mean \pm SD) in the eastern Pacific Ocean. NEP, Northeastern Pacific; SEP, Southeastern Pacific; GC, Gulf of California; CCS, California Current System; CRD, Costa Rica Dome; GALPE, Galapagos/Peru.

Eastern Pacific Ocean	Zone	$\delta^{15}\text{N}$	$\delta^{13}\text{C}$
NEP	GC	14.8 \pm 0.9	-16.6 \pm 0.9
	CCS	13.3 \pm 0.9	-16.9 \pm 0.8
	CRD	12.1 \pm 1	-17.2 \pm 0.5
SEP	GALPE	7.4 \pm 0.9	-18.0 \pm 1.1

The estimated isotopic niche width and trophic overlap are shown in Figure 9, Tables 10 and 11. The isotopic niche width of all zones was similar, ranging from 1.7 to 2.7‰² (Table 10). However, the posterior estimations of the probability of the isotopic niche width for each zone showed a clear separation among all the ellipses (Fig. 9). This separation or gradient was mainly driven by $\delta^{15}\text{N}$ (Fig. 9); whereas all zones exhibited similar range in $\delta^{13}\text{C}$ values of all zones (Fig. 9). The trophic overlap among zones was estimated as a proportion (%) of the non-overlapping area between the comparison of two ellipses (Table 11). The CCS showed a trophic overlap between the GC (0.1%; Table 11) and the CRD (0.2%; Table 11), which as observed earlier further suggests this zone has intermediate values. In contrast, GALPE did not overlap between any of the zones from the NEP (0%; Table 11).

Table 10. Isotopic niche width (SEA_B and SEA_C) of blue whale skin in the eastern Pacific Ocean. NEP, Northeastern Pacific; SEP, Southeastern Pacific; GC, Gulf of California; CCS, California Current System; CRD, Costa Rica Dome; GALPE, Galapagos/Peru; CI, credibility intervals.

Eastern Pacific Ocean	Zone	Mean SEA_C ‰ ²	Mean SEA_B ‰ ²	CI (95%)
NEP	GC	2.5	2.4	2.1 – 2.8
	CCS	2.2	2.2	1.9 – 2.4
	CRD	1.8	1.7	1.2 – 2.3
SEP	GALPER	2.7	2.7	2.0 – 3.6

Table 11. Trophic overlap between different zones in the eastern Pacific Ocean.

GC, Gulf of California; CCS, California Current System; CRD, Costa Rica Dome; GALPE, Galapagos/Peru.

Zone comparison	Proportion (%) of the non-overlapping area of the two ellipses
GC – CCS	0.1
GC – CRD	0
GC – GALPE	0
CCS – CRD	0.2
CCS – GALPE	0
CRD – GALPE	0

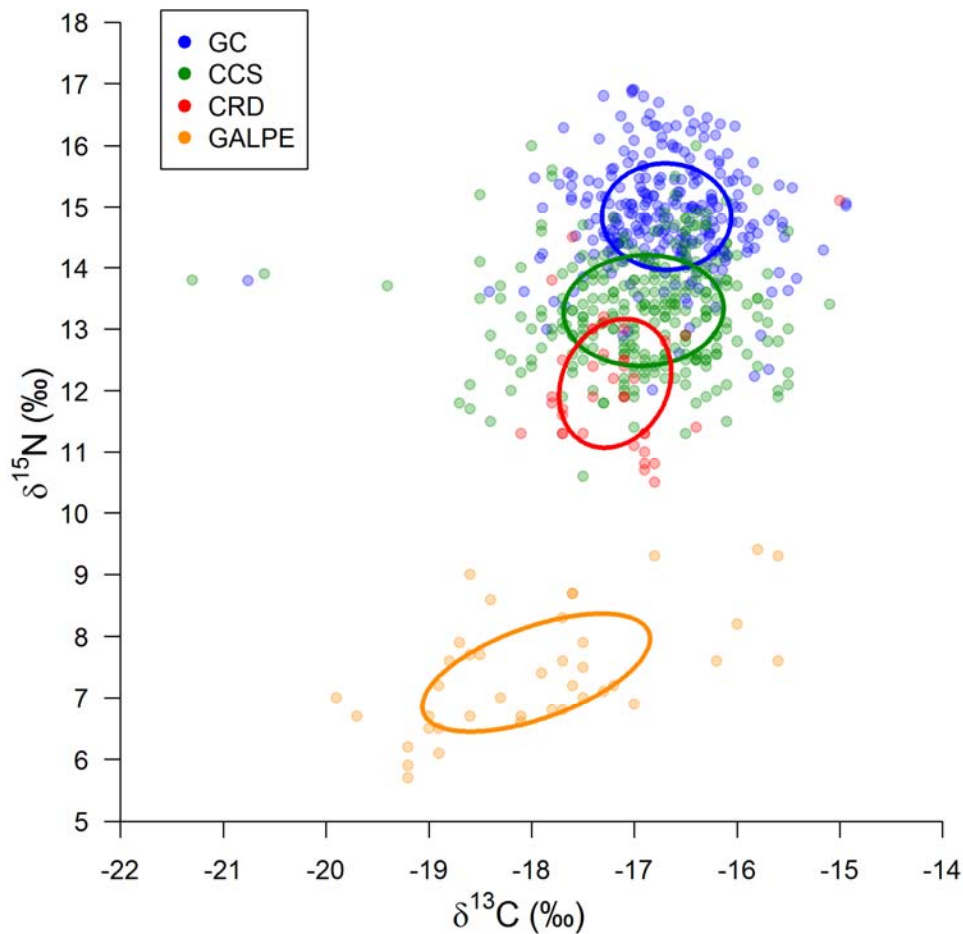


Figure 9. Isotopic niche width (SEAc) of the blue whale in the eastern Pacific Ocean. The ellipses represent the isotopic niche width area of the Gulf of California (GC), California Current System (CCS), Costa Rica Dome (CRD) and Galapagos/Peru (GALPE).

7.4.2. Female and male blue whales in the eastern Pacific Ocean

The results of the SEA_B , in Table 13 and Figure 10, showed that blue whale skin strata of females in the NEP ($\delta^{15}N$: 14.0 ± 1.2 , $\delta^{13}C$: -16.9 ± 0.8 , $n = 214$) and SEP ($\delta^{15}N$: 7.4 ± 0.9 , $\delta^{13}C$: -18.0 ± 1.2 , $n = 18$) had a slightly wider isotopic niche than males (NEP, $\delta^{15}N$: 14.0 ± 1.2 , $\delta^{13}C$: -16.6 ± 0.6 , $n = 134$; and SEP, $\delta^{15}N$: 7.5 ± 1.0 , $\delta^{13}C$: -17.7 ± 0.8 , $n = 7$). The probability that blue whale females have a wider isotopic niche than males is 100% in the NEP, and 60% in the SEP. The trophic overlap (Table 13) between females and males was high in both the NEP (0.5%) and SEP (0.6%).

Table 12. Isotopic niche width (SEA_B and SEA_C) of female and male blue whales skin in the eastern Pacific Ocean. NEP, Northeastern Pacific; SEP, Southeastern Pacific; CI, credibility intervals.

Eastern Pacific Ocean	Sex	Mean SEA_C ‰ ²	Mean SEA_B ‰ ²	CI (95%)
NEP	Female	3.0	3.0	2.6 – 3.3
	Male	2.2	2.1	1.8 – 2.3
SEP	Female	2.8	2.9	1.9 – 4.0
	Male	2.1	2.4	1.1 – 4.1

Table 13. Trophic overlap between female and male blue whales in the eastern Pacific Ocean. NEP, northeast Pacific; SEP, southeast Pacific.

Eastern Pacific Ocean	Sex comparison	Proportion (%) of the non-overlapping area of the two ellipses
NEP	Females – Males	0.5
SEP	Females – Males	0.6

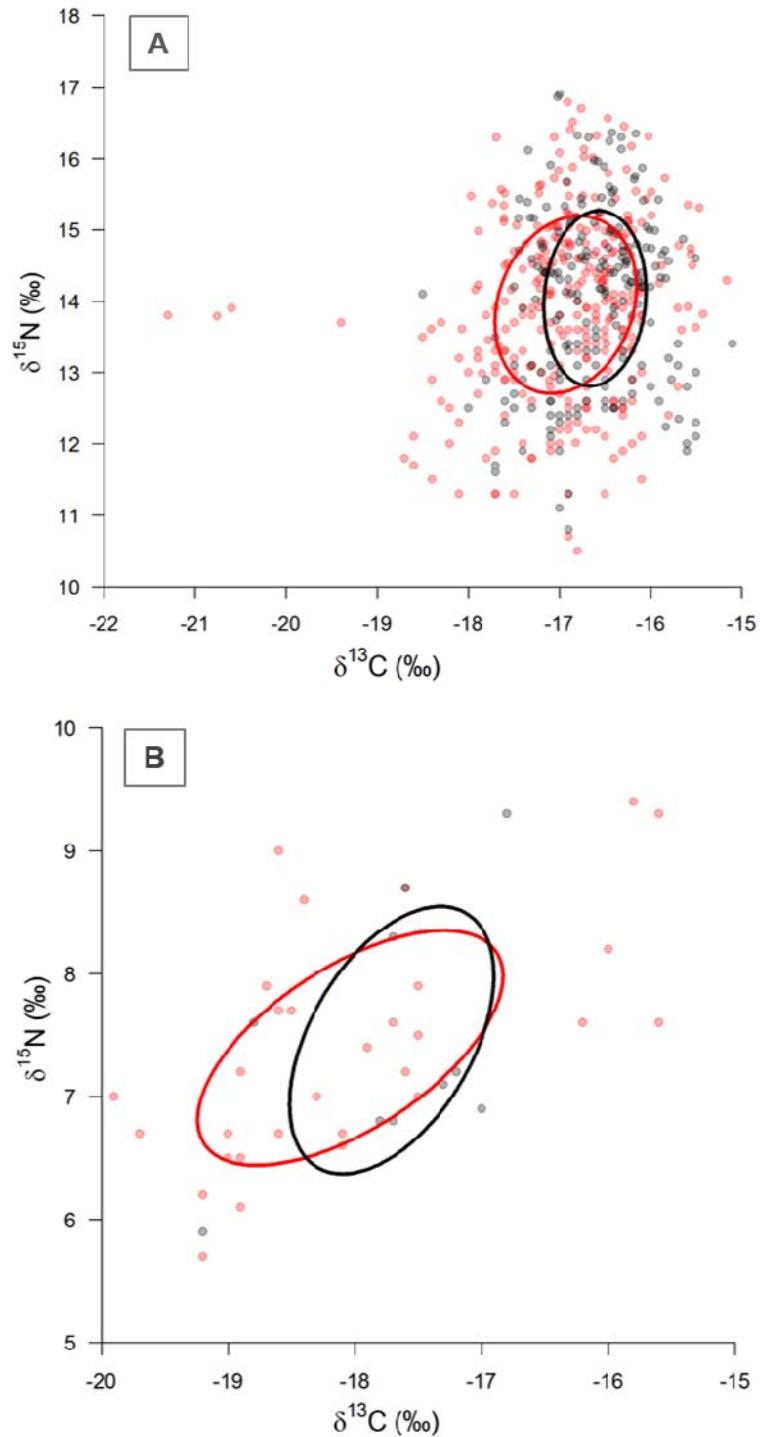


Figure 10. Isotopic niche width (SEAc) of female and male blue whales in the eastern Pacific Ocean. The ellipses represent the isotopic niche width area of the females (red) and males (black) in the: A. NEP (northeast Pacific) and B. SEP (southeast Pacific).

7.5. Quantifying the relative contribution of different foraging zones to the blue whale diet in the NEP

The results from the Bayesian dietary mixing model using a trophic discrimination factor of $\Delta^{15}\text{N}: 1.6 \pm 0.5\text{‰}$ show that the mean \pm SD posterior probability contribution of the CCS ($0.30 \pm 15\%$) and the GC ($0.54 \pm 05\%$) to the blue whale's diet in the NEP was high (Table 14, Fig. 11A). Although the estimated probability for GC was $\sim 24\%$ higher than the CCS. In contrast, the estimation for the CRD was lower at $0.16 \pm 10\%$. The code of the Bayesian dietary mixing model, deviance information criteria, summary statistics, and model diagnosis of this model are available in Appendix VIII.

In the case of the Bayesian dietary mixing model using a trophic discrimination factor of $\Delta^{15}\text{N}: 1.9 \pm 0.5\text{‰}$, the mean \pm SD posterior probability contribution of all zones were similar to the model using $\Delta^{15}\text{N}: 1.6 \pm 0.5\text{‰}$ (Table 14, Fig. 11B). Deviance information criteria, summary statistics, and model diagnosis of this model are available in Appendix IX.

Table 14. Probability of the proportional contributions (%) of different sources (zones) to consumer's diet (blue whales in the NEP). GC, Gulf of California; CCS, California Current System; CRD, Costa Rica Dome; CI, credibility intervals.

A. Bayesian Mixing Model using a $\Delta^{15}\text{N}: 1.6 \pm 0.5\text{‰}$						
Zone	Mean \pm SD (%)	Probability of proportion (CI)				
		25%	50%	75%	95%	
GC	0.54 ± 05	0.54	0.53	0.57	0.62	
CCS	0.30 ± 15	0.18	0.31	0.43	0.51	
CRD	0.16 ± 10	0.07	0.15	0.24	0.34	

B. Bayesian Mixing Model using a $\Delta^{15}\text{N}: 1.9 \pm 0.5\text{‰}$						
Zone	Mean \pm SD (%)	Probability of proportion (CI)				
		25%	50%	75%	95%	
GC	0.47 ± 06	0.42	0.47	0.51	0.57	
CCS	0.35 ± 17	0.20	0.36	0.50	0.60	
CRD	0.18 ± 12	0.08	0.17	0.28	0.39	

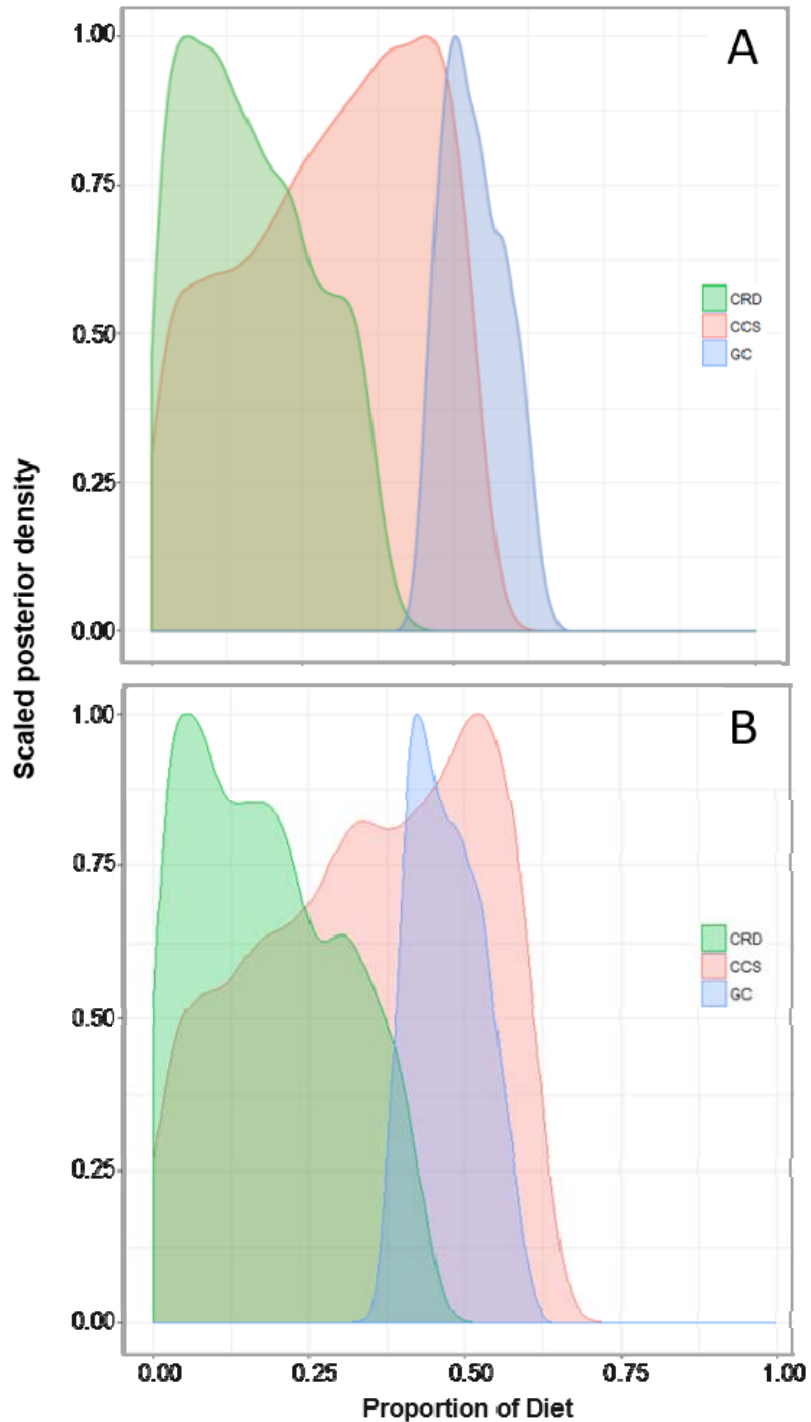


Figure 11. Bayesian dietary isotopic mixing model results: Scaled posterior densities of the probability of the proportional contributions of different sources (zones) to consumer's diet (blue whale). A. Bayesian Mixing Model using a $\Delta^{15}\text{N}$: $1.6 \pm 0.5\text{‰}$; B. Bayesian Mixing Model using a $\Delta^{15}\text{N}$: $1.9 \pm 0.3\text{‰}$. CCS, California Current System; CRD, Costa Rica Dome; GC, Gulf of California.

7.6. Estimating blue whale baleen growth rates and isotopic niche width to infer the seasonal movement patterns of individual blue whales in the NEP

Stranding information of baleen plates collected from seven blue whales (A to F), is presented in Table 15 and Figure 4. The cause of death of whales A, B, C, E and F was ship strike. Whale G, a calf, potentially died due to malnutrition. In the case of whale D, the cause of death is unknown since the stranding information for this whale was not available.

The results of the GAM models to assess the fluctuations in $\delta^{15}\text{N}$ values along baleen plates, and of baleen growth rates estimations are shown in Tables 16 and 17, respectively. The GAM fit showed that the amplitude of the oscillations differed among individuals (Tables 16 and 17, Figs. 12 and 13). Three baleen plates (A–C, one male and two females; Tables 15 and 17) exhibited the expected fluctuations in $\delta^{15}\text{N}$ ranging from 10.6‰ to 14.9‰ (Fig. 12A–12C), and the length of baleen between these fluctuations ranged between 13 and 19 cm (Table 17). The other three baleen plates (D–F, all males; Tables 15 and 17) maintained relatively constant $\delta^{15}\text{N}$ values, ranging between 11.7‰ and 13.1‰ along the plate (Fig. 12D–12F).

By using the trophic-corrected skin $\delta^{15}\text{N}$ values based on that of prey (Table 5), it was possible to associate these oscillations with the potential foraging zone that each individual whale visited. From these data, it could be inferred that whale B moved between all three zones, showing relatively regular cycles (Fig. 12B), whereas whale C did not enter the GC, but moved constantly between the CCS and the CRD, in less regular cycles (Fig. 12C). Whale A remained mainly within the CCS, potentially only migrating twice to the CRD (Fig. 12A). In the case of whales D, E and F, the data suggests that these individuals remained within the CCS, throughout several years (Fig. 12D–12F). Only whales A, B, and C were used to estimate the baleen growth rates (Fig. 12A–12C). The mean (\pm SD) growth per year of baleen plates was estimated for each whale (A= 13.5 ± 2.2 ; B= 14.8 ± 1.7 ; C= 17.5 ± 1.5 cm y^{-1} ; Table 17), and also integrated in an overall mean (\pm SD) (15.5 ± 2.2 cm y^{-1} ; Table 17). The

mean(\pm SD) of $\delta^{15}\text{N}$ values are presented in Table 18, and the GAM fit for the blue whale calf (Sample code G) is presented in Figure 13. This whale exhibited a single wide oscillation in $\delta^{15}\text{N}$ along the baleen plate (Fig. 13).

Table 15. Information of baleen plates collected from seven blue whales (A–G).

ND, no data.

Sample Code	Whale Length (m)	Sex	Age Category	Stranding Date	Latitude	Longitude
A	21.3	M	Adult	01/11/2015	42.5	-124.4
B	25.9	F	Adult	28/03/2007	25.3	-112.1
C	22.3	F	Adult	19/10/2009	39.4	-123.8
D*	ND	M*	ND	ND	ND	ND
E	26.5	M	Adult	03/09/1988	37.7	-122.5
F	20.7	M	Adult	23/06/1986	36.3	-121.9
G	16.0	F	Calf	04/04/2013	26.7	-113.6

*The stranding data for this baleen plate was unavailable, the sex identity was determined at NOAA-SWFSC by using the genetic methods in Morin *et al.* (2005; 2006)

The results of the isotopic niche width and trophic overlap among the seven blue whale baleen plates are shown in Figure 14, Tables 19 and 20. Baleen plates of adult female blue whales (B and C; Table 19) exhibited a wider isotopic niche than males (Table 19, Fig. 14). The blue whale female calf has the narrowest isotopic niche (G; Table 19). All baleen from adult whales overlapped (Table 20, Fig. 14). Conversely, the female calf, code G, did not exhibit a trophic overlap with the rest of the baleen. The separation of the ellipse (or the isotopic niche space) of the calf, from the rest of the whales, was driven by the carbon isotopes, $\delta^{13}\text{C}$ (Fig. 14).

Table 16. GAM results to assess the fluctuations of $\delta^{15}\text{N}$ and $\delta^{13}\text{C}$ in baleen plates. *E.df.*, Estimated degrees of freedom; *F*, test of whether the smoothed function significantly reduces model deviance; *P*, p-values in bold were considered statistically significant (<0.05).

Isotope	Baleen code	<i>n</i>	<i>E.df.</i>	<i>F</i>	Adjusted R ²	<i>P</i>	Deviance explained (%)
$\delta^{15}\text{N}$	A	41	23.8	61.4	1	< 0.001	99.0
	B	68	27.2	108.0	1	< 0.001	98.7
	C	67	27.3	95.9	1	< 0.001	98.6
	D	55	23.3	25.2	0.9	< 0.001	95.7
	E	71	26.5	27.2	0.9	< 0.001	94.8
	F	58	23.8	31.3	0.9	< 0.001	96.3
	G	49	20.9	244.4	0.9	< 0.001	99.6
$\delta^{13}\text{C}$	A	41	21.9	55.8	1	< 0.001	98.8
	B	68	20.3	15.6	0.9	< 0.001	89.3
	C	67	27.7	64.9	1	< 0.001	98.0
	D	55	24.9	68.4	1	< 0.001	98.5
	E	71	27.5	65.1	1	< 0.001	97.8
	F	58	25.0	25.1	0.9	< 0.001	95.7
	G	49	19.7	21.3	0.9	< 0.001	94.9

Table 17. Blue whale baleen growth rate: estimated by using the distance between sequential $\delta^{15}\text{N}$ minimums along the baleen plates from whales A to C.

Baleen code	Sex	Intervals between $\delta^{15}\text{N}$ minimums (cm)	Growth rate (cm y ⁻¹)
A	Male	10-24	14.0
		24-37	13.0
Mean ± SD			13.5 ± 0.7
B	Female	4-17	13.0
		17-31	14.0
		31-48	17.0
		48-63	15.0
Mean ± SD			14.8 ± 1.7
C	Female	9-27	18.0
		27-46	19.0
		46-62	16.0
Mean ± SD			17.5 ± 1.5
Overall Mean ± SD			15.5 ± 2.2

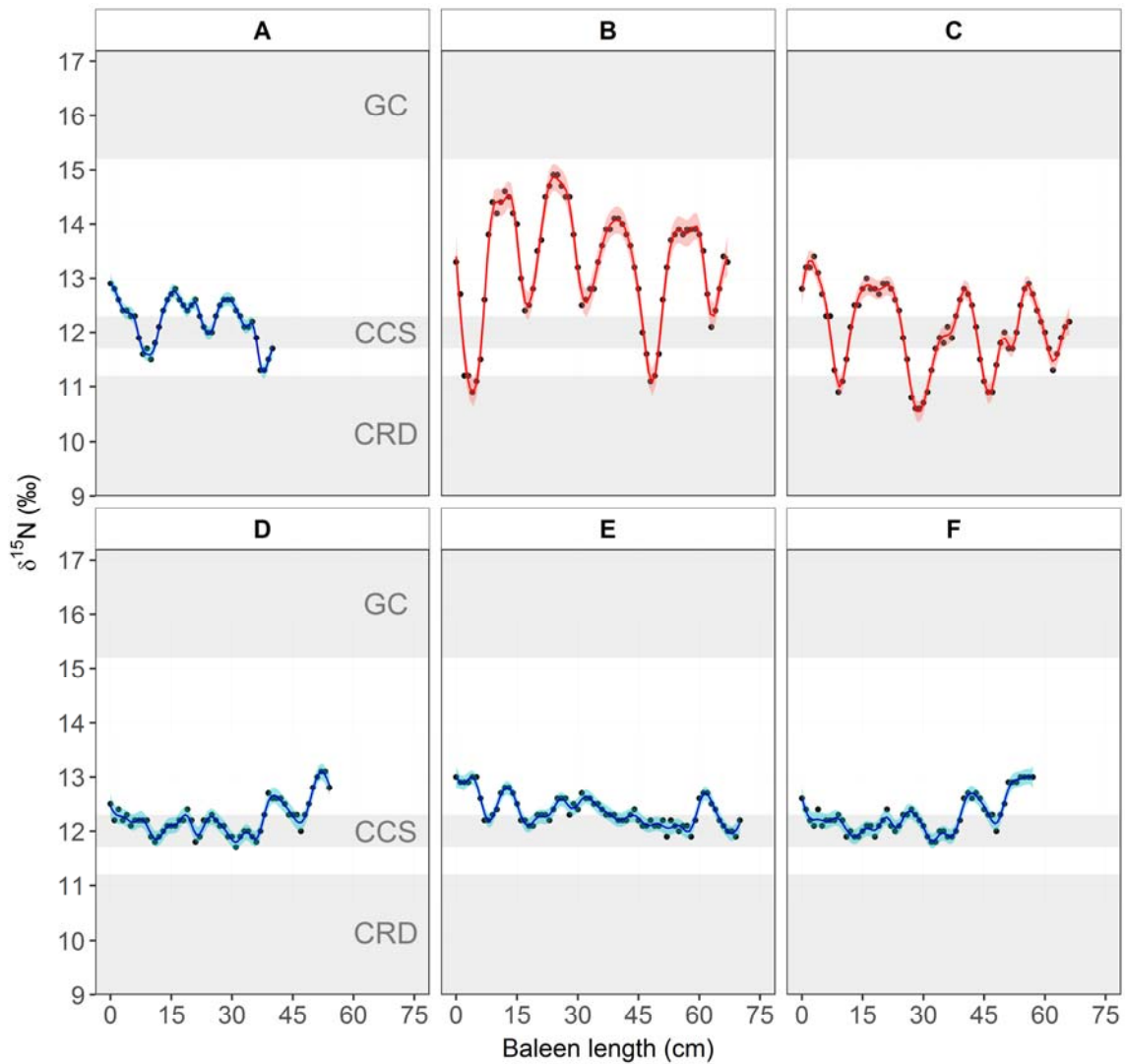


Figure 12. $\delta^{15}\text{N}$ values along the baleen plates from six whales, identified as A–F. Points represent actual values. The continuous line (blue: males; red: females) represents the GAM model fit and the narrow fringe around the lines represent the 95% confidence intervals. The gray shaded area represents the mean \pm SD of the trophic-corrected blue whale skin values for each foraging zone: Gulf of California (GC), the California Current System (CCS) and the Costa Rica Dome (CRS).

Table 18. Mean (\pm SD) $\delta^{13}\text{C}$, $\delta^{15}\text{N}$ and weight percent C/N ratios of blue whale baleen plates collected from stranded whales.

Baleen code	Sex	<i>n</i>	Mean \pm SD		
			$\delta^{13}\text{C}$	$\delta^{15}\text{N}$	C/N
A	M	40	-16.8 ± 0.4	12.2 ± 0.4	3.4 ± 0.1
B	F	67	-17.0 ± 0.5	13.3 ± 1.1	3.6 ± 0.1
C	F	66	-17.3 ± 0.3	12.1 ± 0.7	3.5 ± 0.0
D	M	54	-17.4 ± 0.3	12.2 ± 0.3	3.5 ± 0.1
E	M	70	-17.2 ± 0.4	12.4 ± 0.3	3.5 ± 0.0
F	M	57	-17.4 ± 0.4	12.3 ± 0.4	3.5 ± 0.1
G	F	49	-19.3 ± 0.1	12.0 ± 0.5	3.5 ± 0.0

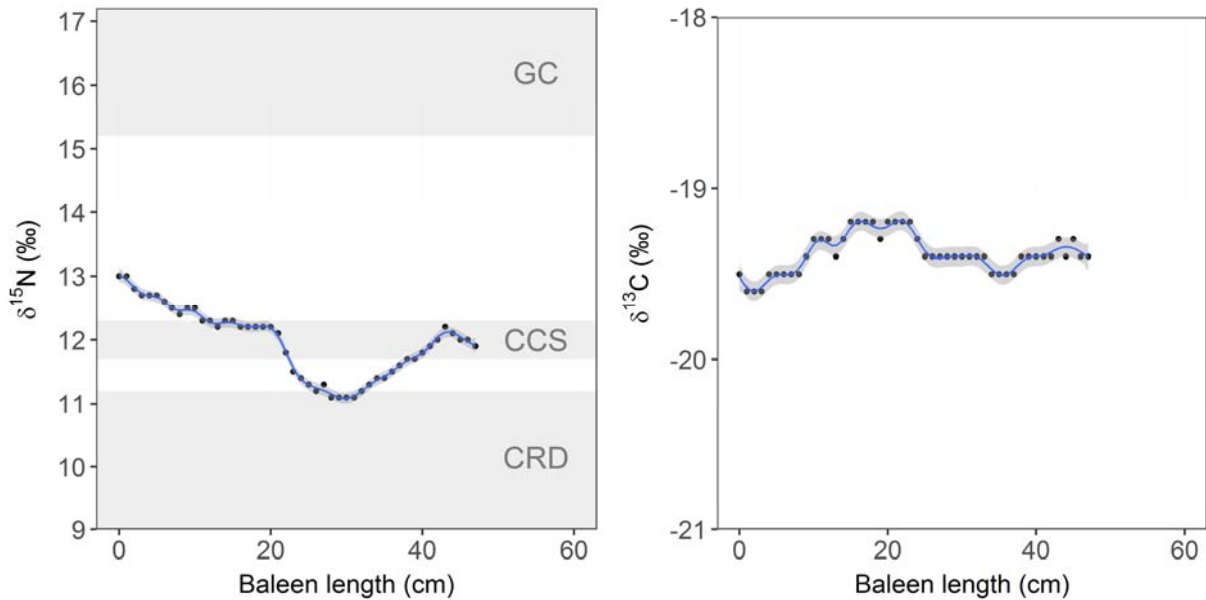


Figure 13. $\delta^{15}\text{N}$ and $\delta^{13}\text{C}$ values along the baleen plates from the female calf, baleen code G. Points represent actual values. The continuous line represents the GAM model fit and the narrow fringe around the lines represent the 95% confidence intervals. The gray shaded area represents the mean \pm SD of the $\delta^{15}\text{N}$ trophic-corrected blue whale skin values for each foraging zone: Gulf of California (GC), the California Current System (CCS) and the Costa Rica Dome (CRS).

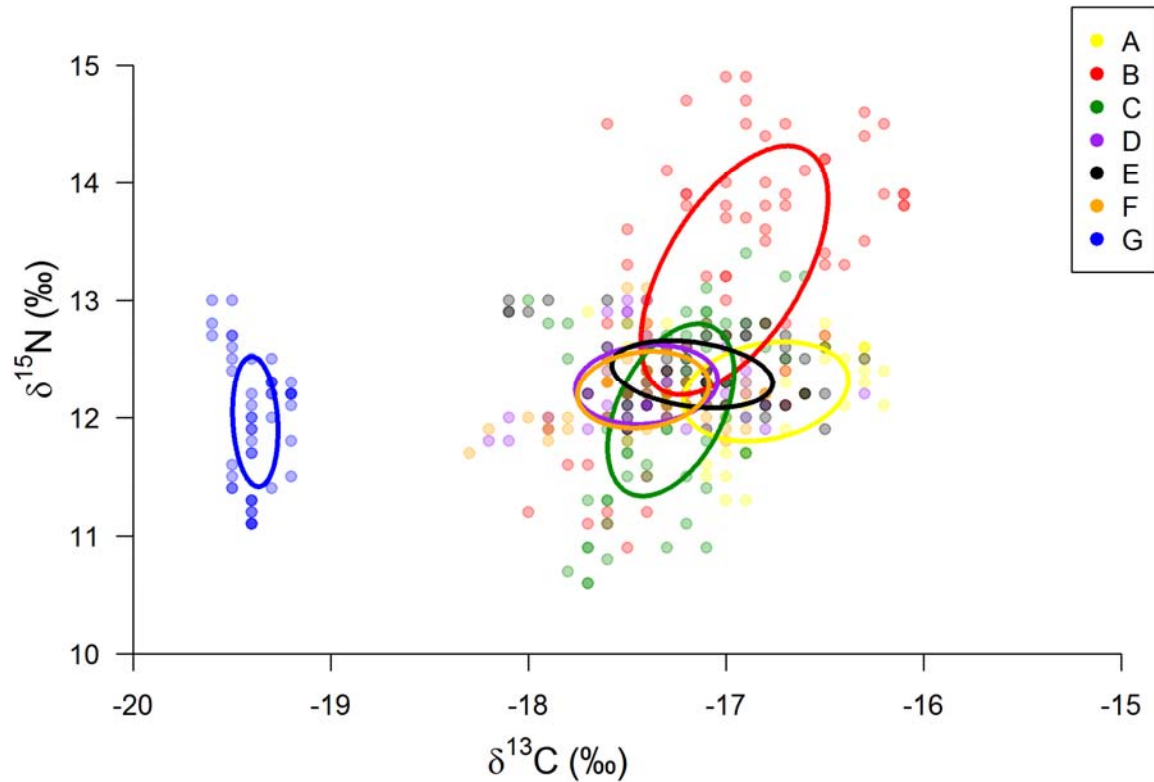


Figure 14. Isotopic niche width (SEA_C) of the seven blue whale baleen plates (A to G). The ellipses represent the isotopic niche width area of the baleen plate of each whale.

Table 19. Isotopic niche width (SEA_B and SEA_C) of blue whale skin in the eastern Pacific Ocean. CI, credibility intervals.

Baleen code	Mean SEA_C ‰ ²	Mean SEA_B ‰ ²	CI (95%)
A	0.5	0.5	0.4 – 0.7
B	1.3	1.3	1.0 – 1.6
C	0.6	0.5	0.5 – 0.8
D	0.4	0.4	0.3 – 0.5
E	0.3	0.4	0.3 – 0.4
F	0.3	0.3	0.3 – 0.4
G	0.2	0.2	0.1 – 0.3

Table 20. Trophic overlap between different baleen of blue whales identified as A to G.

Baleen comparison	Proportion (%) of the non-overlapping area of the two ellipses
A – B	0.1
A – C	0.1
A – D	0.1
A – E	0.2
A – F	0.1
A – G	0
B – C	0.1
B – D	0.1
B – E	0.1
B – F	0.1
B – G	0
C – D	0.3
C – E	0.3
C – F	0.3
C – G	0
D – E	0.4
D – F	0.8
D – G	0
E – F	0.3
E – G	0
F – G	0

7.7. $\delta^{13}\text{C}$ values of skin and baleen plates

The mean $\delta^{13}\text{C}$ value of the prey in the GC was 0.7‰, 2.9‰ and 3.8‰ higher than the other zones (CCS, CRD and GALPE; Table 6). However, the standard deviation of the CRD overlapped with all the zones and it was not possible to accurately assign the origin of measured $\delta^{13}\text{C}$ from skin nor baleen plates. As mentioned in earlier, the isotopic niche width results also showed that the range of $\delta^{13}\text{C}$ were similar for all zones (see Results, section 7.4).

The GAM model revealed a very weak though significant positive relationship between the $\delta^{13}\text{C}$ and time for the stratum basale sampled within the CCS (Table 7, Fig. 15). The GAMs applied to the other skin strata, from the other two foraging

zones, did not show any relationship between the $\delta^{13}\text{C}$ values and time (Table 7, Fig. 15), and thus the isotopic incorporation rate of $\delta^{13}\text{C}$ in blue whale skin could not be estimated.

Mean (\pm SD) $\delta^{13}\text{C}$ values of the seven baleen plates (A–G) are presented in Table 18. The GAM fits (Table 16, Fig. 16) showed that all individuals presented small oscillations in the $\delta^{13}\text{C}$ values along the baleen that ranged between -18.3 to -16.1. These oscillations could not be linked to the foraging zones because of the overlap in prey $\delta^{13}\text{C}$ among zones (Table 6). Therefore, baleen growth rates were inferred only using baleen $\delta^{15}\text{N}$ values. The only exception to this pattern were the $\delta^{13}\text{C}$ values along the baleen plate of the calf whale G (Fig. 13), which exhibited $\sim 2\text{‰}$ lower values than the adult blue whales (Table 13, Fig. 13), and this was also observed via the estimation of isotopic niche width and trophic overlap of baleen plates (Tables 19 and 20, Fig. 13).

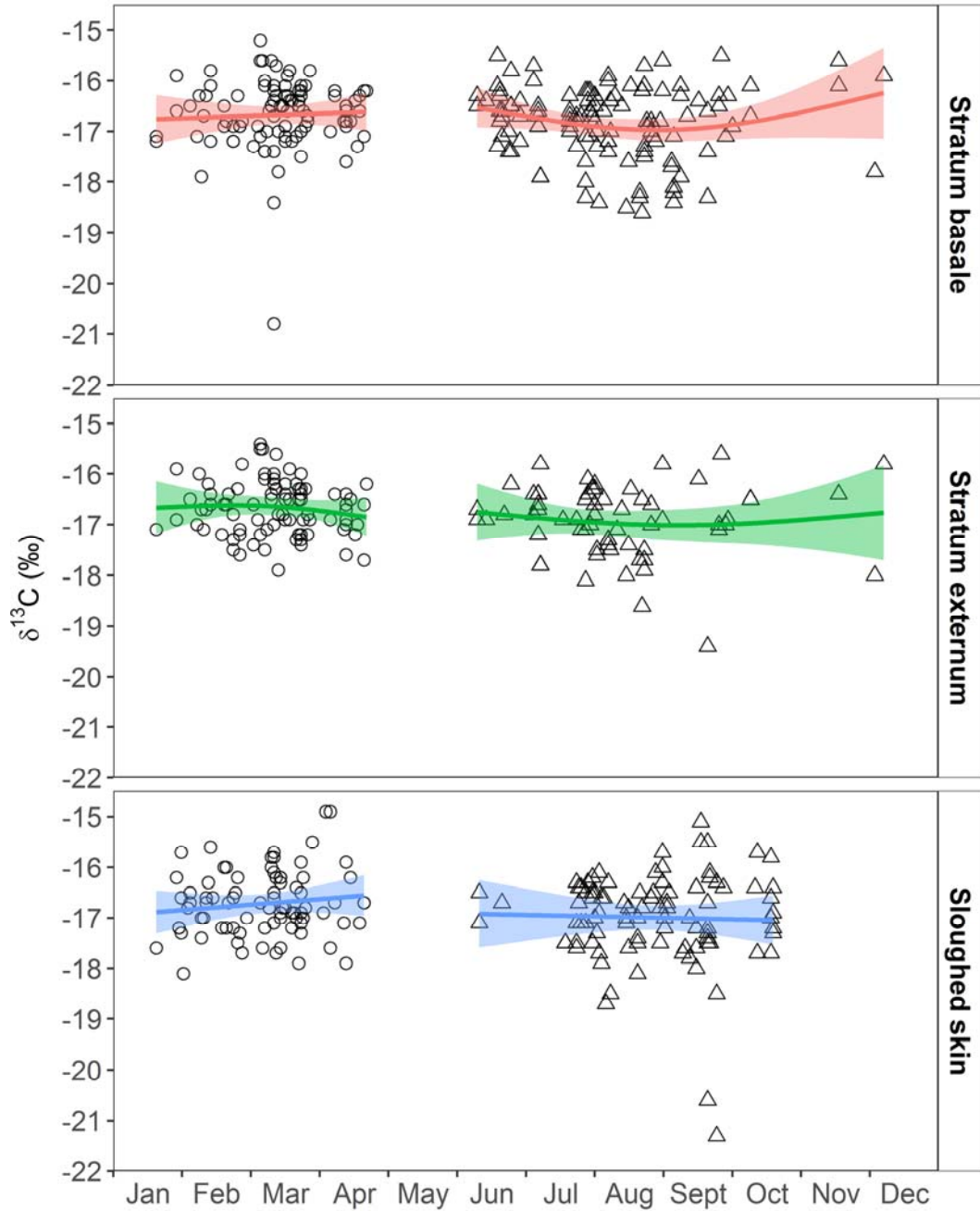


Figure 15. GAM analysis relating skin $\delta^{13}\text{C}$ values to Julian day (presented in months). The points represent the actual $\delta^{13}\text{C}$ values of skin collected from whales within the Gulf of California (open circles) and the California Current System (open triangles). Lines represent the fit (projections) of the GAM model and the fringe around the lines show the 95% confidence intervals.

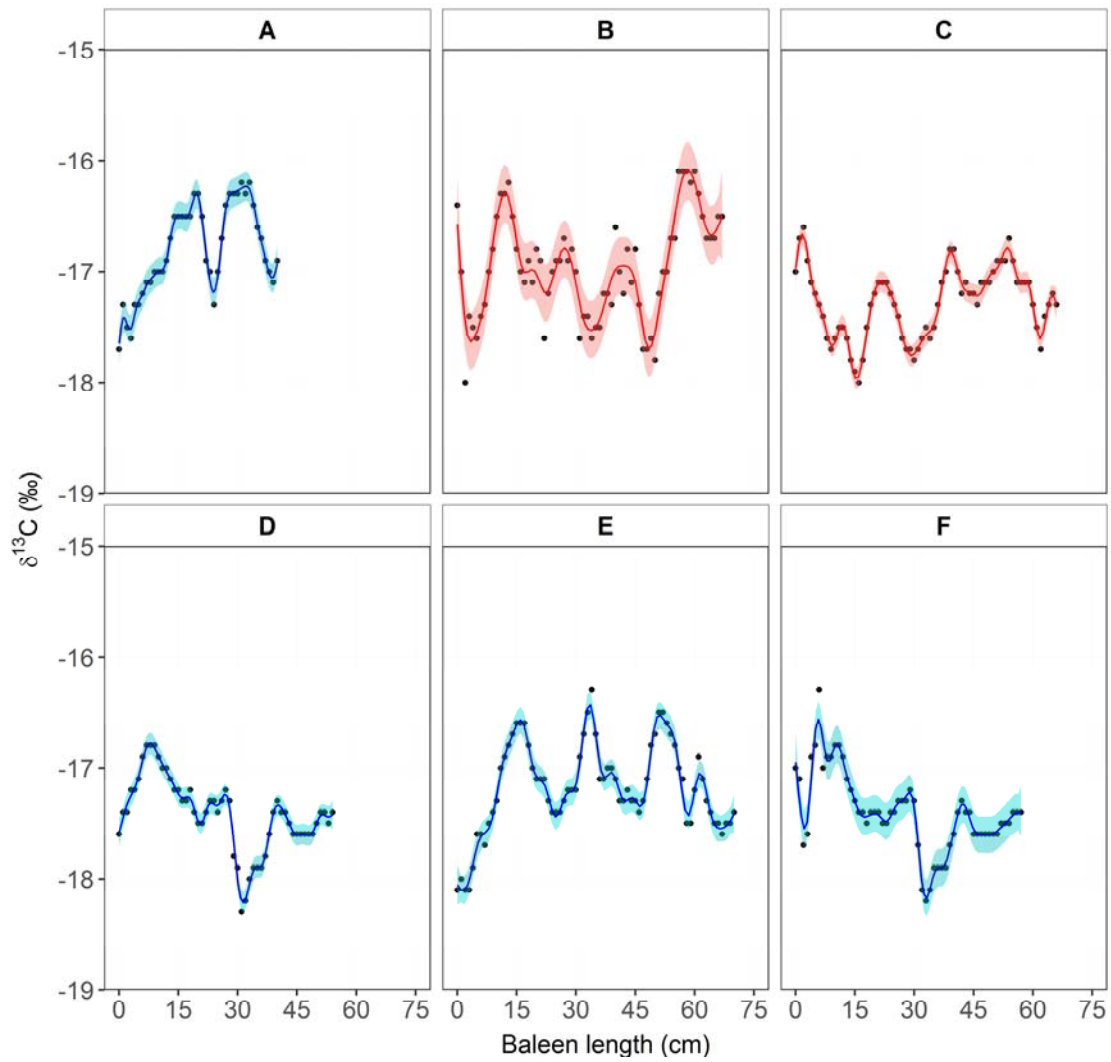


Figure 16. $\delta^{13}\text{C}$ values along the baleen plates from six whales, identified as A-F. Points represent actual values, the continuous line (blue: males; red: females) represents the GAM model fit and the fringe around the lines show the narrow 95% confidence intervals.

8. Discussion

8.1. Influence of lipid-extraction and DMSO preservation on skin $\delta^{13}\text{C}$ and $\delta^{15}\text{N}$ values

Our results suggest that lipid-extraction is necessary to remove biases in skin $\delta^{13}\text{C}$ values associated with lipid content (Table 2), which agrees with previous studies on mysticetes (Lesage *et al.*, 2010; Ryan *et al.*, 2012). In regard to the effects of lipid-extraction on $\delta^{15}\text{N}$ values of cetacean skin, some authors (Lesage *et al.*, 2010; Ryan *et al.*, 2012; Giménez *et al.*, 2016) recommend analyzing bulk tissues because lipid-extraction can influence $\delta^{15}\text{N}$ values, although this effect varied between species (Lesage *et al.*, 2010; Ryan *et al.*, 2012) and tissues (Ryan *et al.*, 2012). In our study, we only compared the $\delta^{15}\text{N}$ of five biopsy samples from which we analyzed paired bulk and lipid-extracted subsamples; however, $\delta^{15}\text{N}$ values between these treatments did not differ significantly, which would be in accordance with the results reported for other marine organisms (Ingram *et al.*, 2007). With regard to preservation in DMSO (Table 2), after lipid-extraction, blue whale skin $\delta^{13}\text{C}$, $\delta^{15}\text{N}$ and C/N ratios of samples preserved in DMSO were similar to those of samples preserved frozen. Our results concur with previous studies that show lipid-extraction via a 2:1 chloroform:methanol solvent solution was a sound method for removing the combined effect that DMSO and tissue lipid content have on skin $\delta^{13}\text{C}$ values (Lesage *et al.*, 2010; Burrows *et al.*, 2014).

8.2. Skin $\delta^{15}\text{N}$ isotopic incorporation rates

Only two studies have estimated isotopic incorporation rates of cetacean skin, and both utilized controlled feeding experiments on captive bottlenose dolphins (Browning *et al.*, 2014; Giménez *et al.*, 2016). Our approach was to use gradients in baseline $\delta^{15}\text{N}$ values between the GC and CCS as a natural diet switch experiment (Fig. 8, Appendix I and II). Our mean estimate of $\delta^{15}\text{N}$ isotopic incorporation rates (163 ± 91 d; Table 8) for blue whale skin is similar to that observed in the longest

experiment on captive bottlenose dolphins (180 ± 71 d) (Giménez *et al.*, 2016). The similarity in incorporation rate estimates for these two distantly related cetacean species that differ in weight by over two orders of magnitude is striking, but suggests that these estimates can be applied to other odontocetes and mysticetes.

We found that isotopic incorporation rates varied among skin strata and foraging zones (Table 8); however, all of these estimates fell within the range of those observed for bottlenose dolphins in previous studies (106-275 d and ~60-90 d) (Browning *et al.*, 2014; Giménez *et al.*, 2016). It is possible that the observed variation in skin incorporation rates among zones could be influenced by water temperature (Schneider *et al.*, 2005; Chelton *et al.*, 2007; Lluch-Cota *et al.*, 2007; McClatchie *et al.*, 2009; Escalante *et al.*, 2013; Pardo *et al.*, 2013), with higher rates in the warmer waters of GC in comparison to the CCS (Table 8). In cold waters, marine mammals reduce peripheral blood flow to maintain a constant internal body temperature, which results in a decrease of epidermal metabolism (Irving & Hart, 1957; Boily, 1995; Silva, 2004). In contrast, incursion into warmer waters accelerates the turnover of superficial skin cells and increase the proliferation rate of cells by intensifying blood flow to the skin stratum basale (St Aubin *et al.*, 1990). Observations suggest that odontocetes, such as belugas (*Delphinapterus leucas*) (St Aubin *et al.*, 1990) and killer whales (*Orcinus orca*) (Durban & Pitman, 2012), move from colder to warmer waters to molt or promote skin regeneration. A study on blue whales in the GC and CCS found that at sites with lower water temperatures, sloughed skin was observed less often in comparison to warmer sites (Gendron & Mesnick, 2001).

A novel approach in this study was to analyze different skin strata: basale, externum, and sloughed skin (Figs. 5A and 5; Appendix IV). We hypothesised that the different skin strata could provide information about temporal shifts in diet. The stratum basale, where cells are constantly produced, would most likely reflect the most recent dietary information, while the isotopic composition of stratum externum and sloughed skin would record information of the diet consumed in the past, perhaps when individuals were in a different foraging zone than the one where skin samples

were collected. The isotopic comparison of strata in the CCS supports this hypothesis since the stratum basale had significantly lower $\delta^{15}\text{N}$ values than the stratum externum and sloughed skin (Table 3), suggesting that the stratum basale was equilibrating with local prey, characterized by lower $\delta^{15}\text{N}$ values than those which occur in the GC (Tables 5 and 6). In the GC, skin strata did not have significantly different $\delta^{15}\text{N}$ values; however, some sloughed skin samples collected in February and March had $\delta^{15}\text{N}$ values that were similar to those expected if the skin was grown in the CCS (Table 5, Fig. 8), suggesting that sloughed skin samples have a higher probability of providing information about past diets. Thus, skin samples collected from migratory mysticetes can reflect information about past diets independent of where sampling occurs, demonstrating that skin is a valuable tissue to estimate relative contributions of food consumed in different foraging zones utilized during the annual life cycle. Since collecting skin from free ranging cetaceans is cost- and time-intensive, we recommend dividing skin biopsies into strata and collecting sloughed skin when available to increase the amount of information that can be gleaned from isotope analysis of this tissue.

8.3. Isotopic niche width and overlap of blue whales in the SEP and NEP

The isotopic niche width (or trophic width) of the blue whales in the NEP and SEP were similar in area $\%_0^2$ (Table 10), indicating that in all zones the species has a similar isotopic niche. This analysis showed the marked gradient among zones in the NEP (Tables 9 to 11, Fig. 9), and between hemispheres (NEP vs SEP). The main separation of the ellipses was driven by $\delta^{15}\text{N}$ values, whereas $\delta^{13}\text{C}$ values had a similar range in all four zones (Fig. 9). The gradients in $\delta^{15}\text{N}$ values were in accordance with the gradients of their main prey in each foraging zone (Table 6), indicating that blue whale skin is recording the biogeochemical changes at the base of the food webs. Hence, blue whale skin is a useful tissue to make inferences of the feeding ecology of this species in the eastern Pacific Ocean. As mentioned in the Materials and Methods section (see 6. Materials and Methods, 6.1. Study area; 23–31 p.), the baseline gradients between these zones are mainly driven by the presence of

an oxygen minimum zone in the eastern tropical Pacific, which influences both the CCS and the GC, via superficial and sub-superficial currents. The unusually high $\delta^{15}\text{N}$ values of the GC could also be attributed to high NO_3^- concentrations (25 μM) at depth, which are incorporated to the upper layers during upwelling events. In the CRD incomplete nitrate utilization could be an explanation to its lower baseline $\delta^{15}\text{N}$ values, however, there could be other processes that are not well understood (Williams *et al.*, 2014). The factors that determines the unusually low $\delta^{15}\text{N}$ values in GALPE are still not well understood. It is possible that this system is less influenced by the presence of the oxygen minimum zone, given that this layer is not as thick (in vertical extension) as in the upper eastern tropical Pacific. Hence, this zone would exhibit baseline $\delta^{15}\text{N}$ values that are similar to open-ocean systems.

In the NEP, the CCS was the only zone that overlapped with the other two zones (GC and CRD), confirming that this zone exhibits intermediate values (Table 11, Fig. 9). The dispersion of the skin data was high among the different zones in the NEP (Fig. 9), this can be attributed to the skin isotopic incorporation rate (~ 163 days), given that skin samples have a high probability of reflecting feeding events that occurred in the past, independently of the zone where the individual whale was sampled.

The zone of the SEP (GALPE) exhibited mean \pm SD that were 4.7 to 7.4‰ lower than the NEP (Table 9), and the trophic overlap analysis showed that the blue whale skin nitrogen isotope values from this zone did not overlap with the zones in the NEP (Table 11, Fig. 9). This was also consistent when comparing the isotope values of prey from the GALPE to those of the other zones (Table 6). Remarkably, the difference observed between the mean blue whale skin $\delta^{15}\text{N}$ values of the GC and Galapagos (7.4‰) fall within the same range (7.9‰) observed in a previous study that compared the $\delta^{15}\text{N}$ values in hair of sea lion pups sampled in the GC and Galapagos (Aurióles-Gamboá *et al.*, 2009); a species that has a higher trophic level than the blue whale.

Blue whale skin $\delta^{15}\text{N}$ data, obtained in this study, is supporting the hypothesis that blue whales from zones of GALPE usually do not migrate and feed further north, in the CRD. Interestingly, this result is in accordance with those found by using genetic analysis, which indicated that the blue whales in the SEP showed a higher affinity to the waters of Peru and Ecuador, whereas the blue whales in the NEP favored the CRD (Leduc *et al.*, 2017). Even though one blue whale was reported to migrate from Galapagos to the CRD (Douglas *et al.*, 2015), the former evidence suggests that these events are uncommon.

The similar range in $\delta^{13}\text{C}$ values in all four zones (Fig. 9) is also in accordance with the range observed in prey within each zone (Table 6). This result indicates that the baseline $\delta^{13}\text{C}$ values in both hemispheres are mostly uniform, which has been proposed in other studies (Auriolos-Gamboa *et al.* 2009). However, within each specific zone the local variability in $\delta^{13}\text{C}$ values in different ecosystems (coast/oceanic or benthic/pelagic), could be useful to study resident marine mammals.

8.4. Relative contribution of different foraging zones to the blue whale diet in the NEP

This study represents the first effort to estimate the relative contribution of different feeding zones to the blue whale's diet. Typically, it had been suggested that all mysticetes species go through fasting periods in their overwintering grounds, to invest energy only in reproduction (*i.e.* courtship, mating) and nursing their calves. The blue whale is a notable exception to this long-believed assumption. The predicted contribution from the CCS and GC was of 30–35 % and 47–54 % (Table 14 and Fig. 11), respectively, indicating that whales forage on both zones. The estimation for the GC is a novel result, since it would be the first for the GC and would support the assertion that this zone is an important feeding zone for this species. Previous studies have suggested that the CCS is an important blue whale feeding ground (Barlow *et al.*, 2004), however it has never been estimated the global proportion of the contribution of this zone to the blue whale's diet. The two models estimated a

contribution of 30–35 % to the diet of this species. A physiological factor that could affect this estimation would be the specific $\delta^{15}\text{N}$ isotopic incorporation rate of skin in this zone (~242 days), which is lower than the GC (~84 days). If skin has a lower isotopic incorporation rate the isotopic signal of the GC would remain within the tissue for a longer period, even when the whales are feeding in CCS. Thus, the GC relative contribution would be overestimated, and the CCS underestimated.

The prediction of the relative contribution from the CRD to the blue whale's diet was 16–18 %. This result could reflect that blue whale sampled in the CCS and GC, generally don't migrate to the CRD or do not feed intensively, given that skin is not frequently reflecting the isotopic signal of this zone. This assumption would also be supported by the fact the photo-recaptures between the CRD and the two other zones, GC and CCS, are relatively low (Ugalde de la Cruz, 2015). In this photo-identification study, the author compared 101 photos of blue whales photographed in the CRD to the blue whale photographic catalog from the GC. In the GC catalog, there are ~800 different blue whales. Only seven blue whales photo-identified in the Gulf were photo-recaptured in the CRD.

The results of the Bayesian dietary isotopic mixing model would support that blue whale have higher energetic requirements compared to other mysticetes, and the species is highly vulnerable to changes in the abundance of their prey. This would also support the hypothesis that blue whale distribution is strongly linked to that of their prey, as it has been previously proposed (Acevedo-Gutiérrez *et al.*, 2002; Gendron, 2002; Croll *et al.*, 2005).

8.5. Blue whale baleen growth rates and isotopic niche width to infer seasonal movement patterns of individual blue whales

The estimate of baleen growth rates for blue whales ($\sim 15.5 \pm 2.2 \text{ cm y}^{-1}$; Table 17), from this study, are consistent with previous estimates for other balaenopterids, such as the fin whale ($20 \pm 2.6 \text{ cm y}^{-1}$) (Bentaleb *et al.*, 2011; Aguilar *et al.*, 2014),

and minke whale (*Balenoptera acutorostrata*, 12.9 cm y⁻¹) (Mitani *et al.*, 2006), as well as for other mysticetes such as bowhead whales (16–25 cm y⁻¹ in adults) (Schell *et al.*, 1989a, 1989b). In contrast, baleen growth rate estimates were lower than those for southern right whales (*Eubalaena australis*, ~27 cm y⁻¹) (Best & Schell, 1996). Variation in baleen growth rates among blue whales sampled in this study (Table 17) could be influenced by differences in individual movement strategies (Fig. 12A–12C), a hypothesis proposed in previous studies of other mysticete species (Schell *et al.*, 1989b; Bentaleb *et al.*, 2011; Aguilar *et al.*, 2014; Matthews & Ferguson, 2015). For example, variation in the period of time spent within a specific foraging zone or in migration between zones would produce wider or narrower oscillations in baleen $\delta^{15}\text{N}$, which would influence growth rate estimates (Table 19, Fig. 12).

Three of the six baleen plates we analyzed did not show marked oscillations in the $\delta^{15}\text{N}$ values (Fig. 12D–12F). These individuals were males: two adults, and one of unknown age class (Tables 15 and 17). A potential explanation for a lack of inter-annual variation in $\delta^{15}\text{N}$ is that these whales remained close or within the CCS foraging zone for several years prior to their death. By applying the mean annual growth rate of ~15.5 cm y⁻¹ to the baleen records of these three males, they remained within the CCS ecosystems for ~3.5 (Fig. 12D), ~4.5 (Fig. 12E) and ~3.7 (Fig. 12F) years. In contrast, the other three baleen plates, collected from one male and two females, exhibited oscillations in the $\delta^{15}\text{N}$ values along their outer edge that indicate cyclical migrations between foraging zones during ~2.5 (Fig. 12A), ~4.3 (Fig. 12B) and ~4.2 (Fig. 12C) years.

The observed differences in movement strategies of blue whale individuals may be influenced by a combination of the following factors. One general explanation is related to changes in the availability of prey in different foraging zones because it is known that blue whale distribution is influenced by variations in the abundance of their primary prey (Bailey *et al.*, 2009; Calambokidis *et al.*, 2009a). A more specific explanation is that females are more likely to migrate to warmer waters in winter/spring to nurse their calves, a hypothesis that has been proposed for other

mysticetes, although other mysticetes generally do not feed while on their winter/spring breeding grounds (Corkeron & Connor, 1999). Moreover, the patterns in the baleen of whale C and B (Fig. 12C–12B) suggest a high fidelity of females to returning to specific winter/spring foraging grounds year after year. This result is supported by photo-identification and genetic analysis (Gendron, 2002; Sears *et al.*, 2013; Costa-Urrutia *et al.*, 2013) of females that winter in the GC. Moreover, the results of the skin isotopic niche width analysis between whales of different sex (see Results, sections 7.4.2) indicated that in both regions (NEP and SEP) females had a slightly wider niche (Table 12, Fig. 9), which would also suggest that generally females move more frequently between zones, compared to male (Fig. 9).

In the case of males, our data indicate that only one male, out of four, migrated twice to the CRD (Fig. 12A). The female:male sex ratio (1.4:1) in the GC is biased towards females (Gendron, 2002; Costa-Urrutia *et al.*, 2013), suggesting that only a portion of the males in the NEP are using this zone in winter/spring. Photo-identification data has also shown that some males have a high site fidelity to the GC (Gendron, 2002). Baleen isotope data from male A in our study also indicates that it had a high fidelity to the CRD, since it migrated only to this zone (Fig. 12A). Conversely, baleen data from the other three males D, E, F (Fig. 12D–12F) indicated that these whales remained within the CCS several years before their death. Blue whales are not frequently sighted in the CCS during winter and spring (Forney & Barlow, 1998; Carretta *et al.*, 2000), although this could be attributed to low search effort during this season. However, vocalizations specific to male blue whales have been recorded year-round in the CCS (Stafford *et al.*, 2001; Oleson *et al.*, 2007a, 2007b, 2007c). Therefore, we hypothesize that there are two migratory strategies for blue whale males in the NEP. Some individuals migrate to winter/breeding grounds in the GC or CRD, while others remain within the CCS. How these two migratory strategies influence mating success for males is not known.

8.6. $\delta^{15}\text{N}$ trophic discrimination factors

$\delta^{15}\text{N}$ trophic discrimination factors have not been estimated for blue whale tissues, therefore our approach was to assume a 1.6‰ (Table 5) discrimination factor between whales and their prey based on the controlled feeding experiments on bottlenose dolphins (Browning *et al.*, 2014; Giménez *et al.*, 2016). Borrell *et al.* (Borrell *et al.*, 2012) suggested using a trophic discrimination factor of 2.8‰ for balaenopterid skin and baleen plates. However, the mean (\pm SD) baleen $\delta^{15}\text{N}$ value of the three male blue whales (D: 12.2 ± 0.3 ; E: 12.4 ± 0.3 ; F: 12.3 ± 0.4 ; Table 18, Fig. 12D–12F) that presumably remained within the CCS for ~2–3 years prior to death, and by extension were isotopically equilibrated with local food sources, were enriched by only 1.7–1.9‰ relative to local prey sources (10.5 ± 0.2 ; Table 6). This is similar to both: the estimates for skin of captive bottlenose dolphins ($\Delta^{15}\text{N}$: 1.6 ± 0.5 ‰) (Browning *et al.*, 2014; Giménez *et al.*, 2016), and to the estimates of the trophic discrimination factor for blue whales in the GC inferred by comparing the isotope values of blue whale prey, skin and blue whale fecal samples ($\Delta^{15}\text{N}$: 1.4 to 1.6‰) (Busquets-Vass, 2008).

8.7. Temporal consistency of baseline $\delta^{15}\text{N}$ values among foraging zones

The observed seasonal trend in skin $\delta^{15}\text{N}$ values within each zone and the oscillations along baleen plates support our hypothesis that these tissues record baseline shifts in nitrogen isotope values across the NEP. Our approach assumes that such baseline gradients are temporarily consistent at a decadal scale. To test this assumption, it would be ideal to have prey $\delta^{15}\text{N}$ data from each foraging zone for each year blue whales were sampled; however, such sampling resolution is logistically impossible. Our approach was to use a GLM to evaluate inter-annual trends in skin $\delta^{15}\text{N}$ values, which showed that they slightly increased in the GC and CCS (see Results); no evident trend was observed in the CRD (Table 4, Fig. 7).

Published datasets show that isotope values of blue whale prey and zooplankton collected from the CCS were consistent over decadal timescales (1994, 2000-2001, 2013) and between sites (Monterey Bay and British Columbia) (Sydeman *et al.*, 1997; Rau *et al.*, 2003; Miller, 2006; Hipfner *et al.*, 2010; Carle, 2014). Moreover, the $\delta^{15}\text{N}$ values in blue whale baleen plates that were assigned to the CCS show a remarkably consistent pattern regardless of when the baleen was collected (1980s vs. 2000s; Table 15, Fig. 12). These patterns suggest that a relatively stable $\delta^{15}\text{N}$ baseline existed in the CCS for nearly three decades. Furthermore, these data suggest that the slight inter-annual increase in skin $\delta^{15}\text{N}$ values of blue whales in the CCS is likely the result of uneven seasonal sampling rather than a shift in the baseline.

$\delta^{15}\text{N}$ values of the dominant krill species (*Nyctiphanes simplex*) in the GC are variable, likely due to their omnivorous feeding behavior (Mauchline, 1980), but are consistently higher than krill in the CCS and the CRD (Table 6) (Jaume-Schinkel, 2004; Miller, 2006; Becker *et al.*, 2007; Hipfner *et al.*, 2010; Sampson *et al.*, 2010; Williams, 2013; Aurióles-Gamboa *et al.*, 2013; Carle, 2014). Isotope data for potential blue whale prey from the CRD were only available from one study (Table 6) (Williams, 2013), but zooplankton data also suggest that this zone has lower $\delta^{15}\text{N}$ values in comparison to the CCS and GC (Popp *et al.*, 2007). Additionally, baleen $\delta^{15}\text{N}$ patterns from whales that likely visited the CRD (Fig. 12A–12C) indicate that baseline $\delta^{15}\text{N}$ values may be consistently lower than those of the other zones. Another factor that may contribute to the observed differences in $\delta^{15}\text{N}$ values among foraging zones is that blue whales in the GC forage on combined aggregations of krill and higher trophic level lanternfish (Jiménez-Pinedo, 2010). Thus, blue whale tissues synthesized in the GC will have higher $\delta^{15}\text{N}$ values that result from a combination of baseline and diet factors relative to tissues grown in other foraging zones in the NEP (Table 5, Appendix II, Figs. 7 and 11).

In the case of the SEP, the low sampling effort limits our inferences on whether there is a consistency in the baseline values in this region across years. However,

other studies using zooplankton and marine mammals, may indicate that there is a relatively stable baseline in this zones, given that the values reported are consistently lower than other zones (Aurioles-Gamboa *et al.*, 2009; Páez-Rosas *et al.*, 2012; Drago *et al.*, 2016), and in similar magnitude than the observed in the present study (Aurioles-Gamboa *et al.*, 2009).

8.8. $\delta^{13}\text{C}$ values in blue whale skin and baleen plates

$\delta^{13}\text{C}$ incorporation rates for skin could not be estimated because of the similarity in $\delta^{13}\text{C}$ values among prey from different foraging zones (Table VI), and by extension $\delta^{13}\text{C}$ values were not useful to estimate baleen growth rates. The lack of marked gradients in $\delta^{13}\text{C}$ values also extended to the zones of GALPE. Another variable that could contribute to the lack of spatial signal in $\delta^{13}\text{C}$ is movement of blue whales between coastal ^{13}C -enriched and ^{13}C -depleted oceanic ecosystems (Newsome *et al.*, 2010) within a specific foraging zone (Bailey *et al.*, 2009). Thus, any latitudinal variation in blue whale skin and baleen $\delta^{13}\text{C}$ values between the CCS, GC, and CRD may be obscured by longitudinal movement between coastal and offshore areas within foraging zones.

8.9. $\delta^{13}\text{C}$ and $\delta^{15}\text{N}$ values along the baleen plate of a blue whale calf

The $\delta^{13}\text{C}$ and $\delta^{15}\text{N}$ values of the blue whale calf were distinct (Figs. 13 and 14). Baleen $\delta^{15}\text{N}$ only exhibited one marked oscillation (Fig. 13). Similar $\delta^{15}\text{N}$ patterns have been observed in juvenile right whales (Lysiak, 2009), and have been associated to the weaning period. The decrease in $\delta^{15}\text{N}$ may be reflecting the diet switch from a higher trophic level diet of milk to a lower trophic level diet of zooplankton. Lactating females catabolize their own tissues to produce milk, therefore milk generally has similar $\delta^{15}\text{N}$ values to maternal tissues. In fin whale, milk proteins exhibited similar $\delta^{15}\text{N}$ values ($9.8 \pm 0.4\text{‰}$) compared to those of skin ($10 \pm 0.3\text{‰}$) and muscle ($9.9 \pm 0.6\text{‰}$) from adult fin whales (Borrell *et al.*, 2012, 2015). Therefore, nursing calves should have a relatively higher trophic level than their mothers,

because they are literally feeding on the mother's tissues. However, the mother-to-offspring trophic discrimination varies between marine mammal species. Generally, in species that feed on protein rich diets (e.g. fish), like pinniped (e.g. fur seal, *Callorhinus ursinus*, and California sea lion), the nursing offspring is one trophic level higher ($\sim 3\text{‰}$) than their mothers (Newsome *et al.*, 2010); these results were obtained by analyzing bone collagen, and tooth annuli in sea lions. However, in some species of marine mammals, milk is isotopically lighter than other maternal tissues, and the mother-to-offspring trophic discrimination is much lower ($\Delta^{15}\text{N} = 0.5\text{‰}$) (Jenkins *et al.*, 2001). Busquets-Vass (2008) determined that the mother-to-offspring trophic discrimination between skin of blue whale nursing females and skin of their calves was $\Delta^{15}\text{N} = 1\text{‰}$.

The former information can be used to make inferences on the $\delta^{15}\text{N}$ oscillation and patterns in the blue whale calf baleen (Fig. 13). A possible scenario is that this blue whale calf was potentially born in the CRD, were the mother would have lower $\delta^{15}\text{N}$ ($\sim 11\text{‰}$), but the calf would exhibit $\delta^{15}\text{N}$ values that resemble those of the CCS ($\sim 12\text{‰}$), due to the trophic discrimination during milk consumption. In Figure 13, this period would be the interval between the 49 to 43 cm of the baleen (the oldest section of the baleen). The period of diet switch, from milk to zooplankton, would be the flat long phase when the $\delta^{15}\text{N}$ values drop between the 42 to 20 cm of the baleen. The posterior increase in $\delta^{15}\text{N}$ values would reflect another diet switch, but this time from krill with lower $\delta^{15}\text{N}$ values in the CRD to krill with higher values in the CCS. This calf finally stranded on the west coast of the Baja California Peninsula (Table 15, Fig. 4). The possible cause of death was malnutrition, due to its poor body condition. Malnutrition could be related with the weaning period, when calves have to start searching for food to feeding on their own (when they are 7 to 8 months old), and sometimes are not successful.

$\delta^{13}\text{C}$ values were relatively constant and $\sim 2\text{‰}$ lower than those observed in adults (Table 18, Figs. 13–14, and 16), thus the isotopic niche of the calf did not overlap with the adults exhibiting a marked separation driven by $\delta^{13}\text{C}$ values (Table

20, Fig. 14). $\delta^{13}\text{C}$ transfer from mother-to-offspring during nursing is variable between different species of marine mammals. Generally, $\delta^{13}\text{C}$ are lower in the offspring tissues compared to the mothers; although in some cases they are higher or equal to the mother tissues (Newsome *et al.*, 2006; Cherel *et al.*, 2015). One of the main factors that affects $\delta^{13}\text{C}$ transfer from mother-to-offspring is the lipid content of milk. Lipids are ^{13}C -depleted, thus have lower $\delta^{13}\text{C}$ values than associated carbohydrates and protein (see Material and Methods, section 6.4) (DeNiro & Epstein, 1977; McConnaughey & McRoy, 1979). Animals with lipid-rich milk nurse their young with a diet that has lower $\delta^{13}\text{C}$. Bulk milk samples from mammary glands of hunted fin whales, in western Spain, had $\delta^{13}\text{C}$ values that were $\sim 6\text{‰}$ lower compared to lipid-free milk (Borrell *et al.*, 2016). Given that blue whale milk also has a high concentration of fat (35 to 50 %), the low $\delta^{13}\text{C}$ in the baleen of the calf would be expected, due to nutrient transfer. Therefore, the lower $\delta^{13}\text{C}$ values along the baleen plate of the calf (Fig. 13) potentially indicate that although this calf had gone through the weaning period, his lipid reserves were still reflecting the nutrient transfer during the lactation period. Interestingly, this information would allow to categorize stranded blue whales as calves, if the information on length is unavailable.

8.10. Summary

Overall the results of the present study show that blue whale tissues (skin and baleen) are effectively recording baseline differences of the ecosystems different where whales feed. Therefore, this technique is extremely useful to make inferences on tissue physiology, feeding ecology and movement patterns of this species in the eastern Pacific Ocean. Specifically, the results support the hypothesis that blue whale feed year-round, which would also indicate that this species has high energetic demands, and are highly vulnerable to changes in the abundance of prey. In a conservation perspective, this information is essential to develop adequate management plans for the species.

9. CONCLUSIONS

- Blue whale tissues are effectively recording baseline isotopic gradients among the ecosystems where they migrate and feed.
- Skin $\delta^{15}\text{N}$ exhibited marked gradients in the eastern Pacific Ocean, which decrease from GC, CCS, CRD to GALPE. These gradients were consistent with those of prey within each zone, demonstrating that blue whale skin can be used to make inferences of the feeding ecology of this species.
- Blue whale skin isotopic incorporation rate, is similar to odontocetes, and skin strata (basale, externum, sloughed skin) can record different feeding periods. Baleen growth rate for blue whales is similar to other mysticetes.
- Blue whales from SEP, generally do not migrate to feed to the CRD. Whereas, in the NEP, blue whales feed in similar intensity in the CCS and GC, and in lesser intensity in the CRD.
- Individual blue whales exhibited distinct movement patterns that may be sex-specific strategies. Females generally tend to migrate seasonally among the different feeding zones, whereas males can either migrate or restrict their movements and remain within specific zones for several years.
- $\delta^{13}\text{C}$ values of both whale tissues (skin and baleen) and prey were not distinct among foraging zones. Thus, were not useful to infer about the physiology, diet or movement patterns of adult blue whales.
- $\delta^{13}\text{C}$ and $\delta^{15}\text{N}$ along baleen of a blue whale calf reflected nutrient transfer during lactation and the weaning period.

10. RECOMENDATIONS

We recommend collecting skin samples (biopsies and sloughed skin) throughout the seasonal residency of migratory mysticetes within specific foraging zones, and dividing skin biopsies into strata. This approach allows to make accurate interpretations of skin isotopic data by increasing the probability of obtaining information about diet at the place of collection in addition to data about past diet from other foraging zones. Moreover, analyzing both skin and baleen can provide information on the inter-annual variability of baseline isotope values within and among isotopically distinct feeding zones, as well as provide information about the migratory strategies of individual whales over several years of life. Information about individual migratory strategies over several years cannot currently be obtained from satellite-tagging technologies, which at best can collect a single year of movement information (Bailey *et al.*, 2009).

This study used some of the skin samples available from the SEP, and the results contributed with important information on the feeding ecology of the species in this zone. However, we recommend collecting baleen plates and increasing the skin sample tissue banks for this zone. The combination of both tissues would provide additional information that would expand our understanding on the individual movement strategies of this population.

11. REFERENCES

- Acevedo-Gutiérrez, A., D. A. Croll & B. R. Tershy. 2002. High feeding costs limit dive time in the largest whales. *J. Exp. Biol.*, 205: 1747–1753.
- Acevedo-Whitehouse, K., A. Rocha-Gosselin & D. Gendron. 2010. A novel non-invasive tool for disease surveillance of free-ranging whales and its relevance to conservation programs. *Anim. Conserv.*, 13: 217–225.
- Aguilar, A., J. Giménez, E. Gómez-Campos, L. Cardona & A. Borrell. 2014. $\delta^{15}\text{N}$ value does not reflect fasting in mysticetes. *PLoS One*, 9: e92288.
- Altabet, M. A., C. Pilskaln, R. Thunell, C. Pride, D. Sigman, F. Chavez & R. Francois. 1999. The nitrogen isotope biogeochemistry of sinking particles from the margin of the Eastern North Pacific. *Deep Sea Res. Part I Oceanogr. Res. Pap.*, 46: 655–679.
- Álvarez-Borrego, S. & J. L. Lara-Lara. 1991. *The physical environment and primary productivity of the Gulf of California*. 555-567, In: B. R. T. & J. P. Dauphin (eds). *The Gulf and peninsular province of the Californias*. American Association of Petroleum Geologists. Memoirs No. 47. Oklahoma.
- Anderson, T. F. & M. A. Arthur. 1983. *Stable isotopes of oxygen and carbon and their application to sedimentologic and paleoenvironmental problems*. 1.1–1.151, In: M. A. Arthur, T. F. Anderson, J. Veizer & L. S. Land. *Society of Economic Paleontologists and Mineralogists*, Tulsa, Oklahoma.
- Aurioles-Gamboa, D., S. D. Newsome, S. Salazar-Pico & P. L. Koch. 2009. Stable isotope differences between sea lions (*Zalophus*) from the Gulf of California and Galapagos Islands. *J. Mammal.*, 90: 1410–1420.

- Aurioles-Gamboa, D., M. Rodríguez-Pérez, L. Sánchez-Velasco & M. Lavín. 2013. Habitat, trophic level, and residence of marine mammals in the Gulf of California assessed by stable isotope analysis. *Mar. Ecol. Prog. Ser.*, 488: 275–290.
- Bailey, H., B. R. Mate, D. M. Palacios, L. Irvine, S. J. Bograd & D. P. Costa. 2009. Behavioural estimation of blue whale movements in the northeast Pacific from state-space model analysis of satellite tracks. *Endanger Species Res.*, 10: 93–106.
- Baraff, L. S., P. J. Clapham & D. K. Mattila. 1991. Feeding behavior of a humpback whale in low-latitude waters. *Mar. Mammal Sci.*, 7: 197–202.
- Barlow, J. 2010. Cetacean abundance in the California Current estimated from a 2008 ship-based line-transect survey. U.S. Department of Commerce, NOAA Technical Memorandum, NMFS-SWFSC-456. 19 p.
- Barlow, J. & K. A. Forney. 2007. Abundance and population density of cetaceans in the California Current ecosystem. *Fish Bull.*, 105: 509–526.
- Barlow, J., M. Kahru & B. J. Mitchell. Cetacean biomass, prey consumption, and primary production requirements in the California Current Ecosystem. *Mar. Ecol. Prog. Ser.*, 371: 509–526.
- Barrett-Lennard, L. G., T. G. Smith & G. M. Ellis. 1996. A cetacean biopsy system using lightweight pneumatic darts, and its effect on the behavior of killer whales. *Mar. Mammal Sci.*, 12: 14–27.
- Barrow, L. M., K. A. Bjorndal & K. J. Reich. 2008. Effects of preservation method on stable carbon and nitrogen isotope values. *Physiol. Biochem. Zool.*, 81: 688–693.

- Becker, E. A., K. A. Forney, M. C. Ferguson & J. Barlow. 2012. Predictive modeling of cetacean densities in the California Current ecosystem based on summer/fall ship surveys in 1991- 2008. NOAA Technical Memorandum NMFS-SWFSC-499, U.S. Department of Commerce, National Marine Fisheries Service, Southwest Fisheries Science Center, La Jolla, CA. 45 p.
- Becker, B. H., M. Z. Peery & S. R. Beissinger. 2007. Ocean climate and prey availability affect the trophic Level and reproductive success of the marbled murrelet, an endangered seabird. *Mar. Ecol. Prog. Ser.*, 329: 267–279.
- Benson, B. B. & D. Jr. Krause. 1984. The concentrations and isotopic fractionation of oxygen dissolved in freshwater and seawater in equilibrium with the atmosphere. *Limnol. Ocenogr.*, 29: 620–632.
- Bentaleb, I., C. Martin, M. Vrac, B. Mate, P. Mayzaud, D. Siret, R. de Stephanis & C. Guinet. 2011. Foraging ecology of mediterranean fin whales in a changing environment elucidated by satellite-tracking and baleen plate stable isotopes. *Mar. Ecol. Prog. Ser.*, 438: 285–302.
- Berg, J., J. Tymoczko & L. Stryer. 2002. *Biochemistry*. W.H. Freeman, Ed. Nueva York, 1515 p.
- Berta, A., J. Sumich & K. Kovacs. 2006. Marine mammals: Evolutionary biology. Third edit. Academic Press, Ed. San Diego, CA. 547 p.
- Best, P. B. & D. M. Schell. 1996. Stable isotopes in southern right whale (*Eubalaena australis*) baleen as indicators of seasonal movements, feeding and growth. *Mar. Biol.*, 124: 483–494.

- Boily, P. 1995. Theoretical heat flux in water and habitat selection of phocid seals and beluga whales during the annual molt. *J. Theor. Biol.*, 172: 235–244.
- Borrell, A., J. Giménez & A. Aguilar. 2012. Discrimination of stable isotopes in fin whale tissues and application to diet assessment in cetaceans. *Rapid Commun. Mass Spectrom.*, 26: 1596–1602.
- Borrell, A., E. Gómez-Campos & A. Aguilar. 2016. Influence of reproduction on stable-isotope ratios: nitrogen and carbon isotope discrimination between mothers, fetuses, and milk in the fin whale, a capital breeder. *Physiol. Biochem. Zool.*, 89: 41–50.
- Brinton, E., M. D. Ohman, A. W. Townsend, M. D. Knight & A. L. Bridgeman. 2000. *Euphausiids of the World Ocean (cd-room Expert System)*. Springer-Verlag, Heildeberg.
- Browning, N. E., C. Dold, J. I-Fan & G. A. J. Worthy. 2014. Isotope turnover rates and diet-tissue discrimination in skin of ex situ bottlenose dolphins (*Tursiops truncatus*). *Clin. Cancer Res.*, 217: 214–221.
- Burrows, D. G, W. L Reichert & M. B. Hanson. 2014. Effects of decomposition and storage conditions on the $\delta^{13}\text{C}$ and $\delta^{15}\text{N}$ isotope values of killer whale (*Orcinus orca*) skin and blubber tissues. *Mar. Mammal Sci.*, 30: 747–762.
- Busquets-Vass, G. 2008. Variabilidad de isotopos estables nitrógeno y carbono en piel de ballena azul (*Balaenoptera musculus*). M.Sc. Thesis, Centro Interdisciplinario de Ciencias Marinas-Instituto Politécnico Nacional. 84 p.
- Busquets-Vass G., S. D. Newsome, J. Calambokidis, G. Serra-Valente, J. K. Jacobsen, S. Aguíñiga-García & D. Gendron. 2017. Estimating blue whale skin

isotopic incorporation rates and baleen growth rates: Implications for assessing diet and movement patterns in mysticetes. *PLoS ONE*, 12(5): e0177880.

Calambokidis, J. 2009. Abundance estimates of humpback and blue whales off the US West Coast based on mark-recapture of photo-identified individuals through 2008. Report # PSRG-2009-07 to Pacific Scientific Review Group, San Diego, CA 3-5 November 2009.

Calambokidis, J. & J. Barlow. 2004. Abundance of blue and humpback whales in the eastern North Pacific estimated by capture-recapture and line-transect methods. *Mar. Mammal Sci.*, 20: 63–85.

Calambokidis, J., J. Barlow, J. K. B. Ford, T. E. Chandler & A. B. Douglas. 2009a. Insights into the population structure of blue whales in the eastern North Pacific from recent sightings and photographic identification. *Mar. Mammal Sci.*, 25: 816–832.

Calambokidis, J., G. S. Schorr, G. H. Steiger, J. Francis, M. Bakhtiari, G. Marshall, E. M. Oleson, D. Gendron & K. Robertson. 2009b. Insights into the underwater diving, feeding, and calling behavior of blue whales from a suction-cup-attached video-imaging Tag (CRITTERCAM). *Mar. Technol. Soc. J.*, 41: 19–29.

Calambokidis, J. & G. Steiger. 1997. Blue whales. *Worldlife*. Stillwater, MN. 72 p.

Calambokidis, J., G. H. Steiger, J. C. Cabbage, K. C. Balcomb, C. Ewald, S. Kruse, R. Wells & R. Sears. 1990. Sightings and movements of blue whales off central California 1986-88 from photo-identification of individuals. *Rep. to Int. Whal. Com.*, 343–348.

- Caraveo-Patiño, J., K. A. Hobson & L. A. Soto. 2007. Feeding ecology of gray whales inferred from stable-carbon and nitrogen isotopic analysis of baleen plates. *Hydrobiologia*, 586: 17–25.
- Caraveo-Patiño, J. & L. A. Soto. 2005. Stable carbon isotope ratios for the gray whale (*Eschrichtius robustus*) in the breeding grounds of Baja California Sur, Mexico. *Hydrobiologia*, 539: 99–107.
- Carle, R. 2014. Seasonal and sex-specific diet in rhinoceros auklets. M.Sc. Thesis, The Faculty of Moss Landing Marine Laboratories. 50 p.
- Carretta, J., M. Lowry, C. E. Stinchcomb, M. S. Lynn & R. E. Cosgrove. 2000. Distribution and abundance of marine mammals at San Clemente Island and surrounding offshore waters: results from aerial and ground surveys in 1998 and 1999. Administrative Report LJ-00-02, available from Southwest Fisheries Science Center, P.O. Box 271, La Jolla, CA USA 92038. 44 p.
- Carss, D. N. 1995. Foraging behaviour and feeding ecology of the otter *Lutra lutra*: a selective review. *Hystrix*, 7: 179–194.
- Chelton, D. B., M. G. Schlax & R. M. Samelson. 2007. Summertime coupling between sea surface temperature and wind stress in the California Current System. *J. Phys. Oceanogr.*, 37: 495–517.
- Cherel, Y., K. A. Hobson & C. Guinet. 2015. Milk isotopic values demonstrate that nursing fur seal pups are a full trophic level higher than their mothers. *Rapid Commun. Mass Spectrom.*, 29: 1485–1490.
- Christiansen, F., G. A. Víkingsson, M. H. Rasmussen & D. Lusseau. 2014. Female body condition affects foetal growth in a capital breeding mysticete. *Funct. Ecol.*, 28: 579–588.

- Chuang, Y., S. Mazumdar, T. Park, G. Tang, V. C. Arena & M. J. Nicolich. 2011. Generalized linear mixed models in time series studies of air pollution. *Atmos. Pollut. Res.*, 3: 148.
- Cline, J. D. & I. R. Kaplan. 1975. Isotopic fractionation of dissolved nitrate during denitrification in the eastern tropical North Pacific Ocean. *Mar. Chem.* 3: 271–299.
- Collins, C. A., J. T. Pennington, C. G. Castro, T. A. Rago & F. P. Chavez. 2003. The California Current system off Monterey, California: physical and biological coupling. *Deep-Sea Res. Pt. II*, 50: 2389–2404.
- Collins English Dictionary – Complete and Unabridged, 12th Edition 2014. (1991, 1994, 1998, 2000, 2003, 2006, 2007, 2009, 2011, 2014). Retrieved June 14 2017 from <http://www.thefreedictionary.com/zones+out>
- Corkeron, J. & C. Connor. 1999. Why do baleen whales migrate? *Mar. Mammal Sci.*, 15: 1228–1245.
- Costa-Urrutia, P., S. Sanvito, N. Victoria-Cota, L. Enríquez-Paredes & D. Gendron. 2013. Fine-scale population structure of blue whale wintering aggregations in the Gulf of California. *PLoS One*, 8: e58315.
- Croll, D., B. Marinovic, S. Benson, F. P. Chavez, N. Black, R. Ternullo & B. R. Tershy. 2005. From wind to whales: trophic links in a coastal upwelling system. *Mar. Ecol. Prog. Ser.*, 289: 117–130.
- Deagle, B. E., D. J. Tollit, S. N. Jarman, M. A. Hindell, A. W. Trites & N. J. Gales. 2005. Molecular scatology as a tool to study diet: analysis of prey DNA in scats from captive Steller sea lions. *Mol. Ecol.*, 14(6): 1831–1842.

- Del Angel-Rodríguez, J. A. 1997. Hábitos alimentarios y distribución espacio-temporal de los rorcuales común (*Balaenoptera physalus*) y azul (*Balaenoptera musculus*) en la Bahía de La Paz, B.C.S., México. M.Sc. Thesis, Centro Interdisciplinario de Ciencias Marinas-Instituto Politécnico Nacional. 68 p.
- DeNiro, M. J. & S. Epstein. 1977. Mechanism of carbon isotope fractionation associated with lipid synthesis. *Science*, 197(4300): 261–263.
- DeNiro, M. J. & S. Epstein. 1978. Influence of diet on the distribution of carbon isotopes in animals. *Geochim. Cosmochim. Acta*, 42: 495–506.
- DeNiro, M.J. & S. Epstein. 1981. Influence of diet on the distribution of nitrogen isotopes in animals. *Geochim. Cosmochim. Acta*, 45: 341–351.
- Díaz-Gamboa, R. E. 2003. Diferenciación entre Tursiones *Tursiops truncatus* costeros y oceánicos en el Golfo de California por medio de isótopos estables de carbono y nitrógeno. M.Sc. Thesis, Centro Interdisciplinario de Ciencias Marinas-Instituto Politécnico Nacional. 62 p.
- Donovan, G.P. 1984. Blue whales off Peru, December 1982, with special reference to pygmy blue whales. *Rep. to Int. Whal. Com.*, 34: 473–476.
- Douglas, A., R. Sears, J. Denkinger, E. Dobson, P. Olson, T. Gerrodette & J. Calambokidis. 2015. Movement of a blue whale (*Balaenoptera musculus*) between the Costa Rica Dome and the Galapagos: Management implications of the first documented cross-equatorial movement. In: December 13-18, ed. 21st Biennial Conference of the Society for Marine Mammalogy. San Francisco, California, USA.

- Drago, M., V. Franco-Trecu, L. Cardona, P. Inchausti, W. Tapia & D. Páez-Rosas. 2016. Stable isotopes reveal long-term fidelity to foraging grounds in the Galapagos sea lion (*Zalophus wollebaeki*). *PLoS One*, 11: 1–16.
- Dugdale, 1967. Nutrient limitation in the sea: dynamics, identification and significance. *Limnol. Oceanogr.*, 12: 685–689.
- Durazo, R., G. Gaxiola-Castro, B. Lavaniegos, R. Castro-Valdez, J. Gómez-Valdés & A. D. S. Mascarenhas Jr. 2005. Oceanographic conditions west of the Baja California coast, 2002–2003: A weak El Niño and subarctic water enhancement. *Cienc. Mar.*, 31(3):537-552.
- Durban, J. W. & R. L. Pitman. 2012. Antarctic killer whales make rapid, round-trip movements to subtropical waters: evidence for physiological maintenance migrations? *Biol. Lett.*, 8: 274–7.
- Escalante, F., J. E. Valdez-Holguín, S. Álvarez-Borrego & J. R. Lara-Lara. 2013. Temporal and spatial variation of sea surface temperature, chlorophyll a, and primary productivity in the Gulf of California. *Cienc. Mar.*, 39: 203–215.
- Espino-Pérez, N.M. 2009. Variación temporal en los perfiles de ácidos grasos de ballenas azules *Balaenoptera musculus* que visitan el Golfo de California. M.Sc. Thesis, Centro Interdisciplinario de Ciencias Marinas-Instituto Politécnico Nacional. 51 pp.
- Etnoyer, P., D. Canny, B. R. Mate & L. Morgan. 2004. Persistent pelagic habitats in the Baja California to Bering Sea (B2B) ecoregion. *Oceanography*, 17: 90–101.
- Etnoyer, P., D. Canny, B. R. Mate, L. E. Morgan, J. G. Ortega-Ortiz & W. J. Nichols. 2006. Sea-surface temperature gradients across blue whale and sea turtle

- foraging trajectories off the Baja California Peninsula, Mexico. *Deep Sea Res. Part II Top Stud. Oceanogr.*, 53: 340–358.
- Evans-Ogden, L. J., K. A. Hobson & D. B. Lank. 2004. Blood isotopic ($\delta^{13}\text{C}$ and $\delta^{15}\text{N}$) turnover and diet-tissue fractionation factors in captive dunlin (*Calidris alpina pacifica*). *Auk*, 121: 170–177.
- Farrell, J., T. Pederson, S. Calvert & B. Nielsen. 1995. Glacial-interglacial changes in nutrient utilization in the equatorial Pacific Ocean. *Nature*, 377: 514–517.
- Fiedler, P. C. & M. F. Lavin. 2006. Introduction: A review of eastern tropical Pacific oceanography. *Prog. Oceanogr.*, 69: 94–100.
- Fiedler, P. C., S. B. Reilly, R. P. Hewitt, D. Demer, V. A. Philbrick, S. Smith, W. Armstrong, D. A. Croll, B. R. Tershy & B. R. Mate. 1998. Blue whale habitat and prey in the California Channel Islands. *Deep Sea Res. Part II Top Stud. Oceanogr.*, 45: 1781–1801.
- Fleming, A. H., C. T. Clark, J. Calambokidis & J. Barlow. 2016. Humpback whale diets respond to variance in ocean climate and ecosystem conditions in the California Current. *Glob. Chang. Biol.*, 22: 1214–1224.
- Flores-Cascante, L. & D. Gendron. 2012. Application of McMaster' s technique in live blue whales. *Vet. Rec.*, 179: 220–0.
- Flores-Lozano, N. 2006. Plaguicidas organoclorados y bifenil policlorados como indicadores de la estructura poblacional de la ballena azul (*Balaenoptera musculus*) del Golfo de California. M.Sc. Thesis, Centro Interdisciplinario de Ciencias Marinas-Instituto Politécnico Nacional. 80 p.

- Fontugne, M. R. & J. C. Dupplesey. 1981. Organic carbon isotopic fractionation by marine plankton in the temperature range -1 to 31°C. 4(1): 85–90.
- Foote, A. D., J. Newton, M. C. Ávila-Arcos, M. L. Kampmann, J. A. Samaniego, K. Post, A. Rosing-Asvid, M. H. S. Sinding & T. P. Gilbert. 2013. Tracking niche variation over millennial timescales in sympatric killer whale lineages. *Proc. R. Soc. B.*, 280: 20131481.
- Forney, K. A. & J. Barlow. 1998. Seasonal patterns in the abundance and distribution of California cetaceans, 1991-1992. *Mar. Mammal Sci.*, 14: 460–489.
- Fry, B. 2006. *Stable Isotope Ecology*. Springer New York, Ed. New York, 308 p.
- Fudge, D. S., L. J. Szewciw & A. N. Schwalb. 2009. Morphology and development of blue whale baleen: An annotated translation of Tycho Tullberg's classic 1883 paper. *Aquat. Mamm.*, 35: 226–252.
- Gannes, L. Z., C. Martínez del Río & P. Koch. 1998. Natural abundance variations in stable isotopes and their use in animal physiological ecology. *Comp. Biochem. Physiol.*, 119: 725–737.
- Gendron, D. 1990. Relación entre la abundancia de eufaúsidos y de ballenas azules (*Balaenoptera musculus*) en el Golfo de California. M.Sc. Thesis, Centro Interdisciplinario de Ciencias Marinas-Instituto Politécnico Nacional. 64 p.
- Gendron, D. 2002. Ecología poblacional de la ballena azul, *Balaenoptera musculus*, de la Península de Baja California. Ph.D. Thesis, Centro de Investigación Científica y de Educación Superior de Ensenada. 112 pp.

- Gendron, D., S. Aguñiga & J. D. Carriquiry. 2001. $\delta^{15}\text{N}$ and $\delta^{13}\text{C}$ in skin biopsy samples: a note on their applicability for examining the relative trophic level in three orca species. *J. Cetacean Res. Manag.*, 3: 41–44.
- Gendron, D. & S. L. Mesnick. 2001. Sloughed skin: A method for the systematic collection of tissue samples from Baja California blue whales. *J. Cetacean Res. Manag.*, 3(1)77-79.
- Geraci, J. R., D. J. St. Aubin & B. D. Hicks. 1986. *The epidermis of odontocetes: a view from within*. 3-21, In: Bryden, M. M. & R. Harrison (eds). Research on Dolphins, Part I. Oxford: Clarendon Press.
- Giménez, J., F. Ramírez, J. Almunia, M. G. Forero & R. de Stephanis. 2016. From the pool to the sea: Applicable isotope turnover rates and diet to skin discrimination factors for bottlenose dolphins (*Tursiops truncatus*). *J. Exp. Mar. Bio. Ecol.*, 475: 54–61.
- Goericke, R. & B. Fry. 1994. Variations of marine plankton $\delta^{13}\text{C}$ with latitude, temperature, and dissolved CO_2 in the world ocean. *Global Biogeochem. Cycles*, 8: 85–90.
- Goldbogen, J. A., J. Calambokidis, A. S. Friedlaender, J. Francis, S. L. DeRuiter, A. K. Stimpert, E. Falcone & B. L. Southall. 2013. Underwater acrobatics by the world's largest predator: 360° rolling manoeuvres by lunge-feeding blue whales. *Biol. Lett.*, 9(1): 1–4.
- Goldbogen, J. A., J. Calambokidis, E. Oleson, J. Potvin, N. D. Pyenson & R. E. Shadwick. 2011. Mechanics, hydrodynamics and energetics of blue whale lunge feeding: efficiency dependence on krill density. *J. Exp. Biol.*, 214: 131–46.

- Graham, B. S., P. L. Koch, S. D. Newsome, K. W. McMahon & D. Aurióles-Gamboa. 2010. *Using isoscapes to trace the movements and foraging behavior of top predators in oceanic ecosystems*. 299–318, In: J. B. West, G. J. Bowen, T. E. Dawson & K. P. Tu (eds). *Isoscapes: Understanding movement, pattern, and process on Earth through isotope mapping*. Springer Netherlands: Dordrecht.
- Gunnarson, T. G., J. A. Gill, J. Newton, P. M. Potts & J. Sutherland. 2005. Seasonal matching of habitat quality and fitness in a migratory bird. *Proc. R. Soc. B.*, 271: 2319–2323.
- Harrison, R. & K. W. Thurley. 1974. *Structure of the epidermis in Tursiops, Delphinus, Orcinus and Phocoena*. 45–71, In: R. J. Harrison (eds). *Functional Anatomy of Marine Mammals*, Vol. 2. London: Academic Press.
- Hazen, E. L., D. M. Palacios, K. A. Forney, E. A. Howell, E. Becker, A. L. Hoover, L. Irvine, M. DeAngelis, S. J. Bograd, B. R. Mate & H. Bailey. 2016. WhaleWatch: a dynamic management tool for predicting blue whale density in the California Current. *J. Appl. Ecol.*
- Herberich, E., J. Sikorski & T. Hothorn. 2010. A robust procedure for comparing multiple means under heteroscedasticity in unbalanced designs. *PLoS One*, 5: 1–8.
- Hipfner, J. M., J. Dale & K. J. McGraw. 2010. Yolk carotenoids and stable isotopes reveal links among environment, foraging behavior and seabird breeding success. *Oecologia*, 163: 351–360.
- Hobson, K.A. 1999. Tracing origins and migration of wildlife using stable isotopes: a review. *Oecologia*, 120: 314–326.

- Hobson, K. A. & W. G. Ambrose. 1995. Sources of primary production, benthic-pelagic coupling, and trophic relationships within the Northeast Water Polynya: insights from $\delta^{13}\text{C}$ and $\delta^{15}\text{N}$ analysis. *Mar. Ecol. Prog. Ser.*, 128: 1–10.
- Hobson, K. A., R. Barnett-Johnson & T. Cerling. 2010. *Using isoscapes to track animal migration*. 273–298, In: J. B. West, G. J. Bowen, T. E. Dawson & K. P. Tu (eds). *Isoscapes: understanding movement, pattern, and process on Earth through isotope mapping*. Springer Netherlands: Dordrecht.
- Hobson, K. A., D. M. Schell, D. Renouf & E. Noseworthy. 1996. Stable carbon and nitrogen isotopic fractionation between diet and tissues of captive seals: implications for dietary reconstructions involving marine mammals. *Can J Fish Aquat. Sci.*, 53: 528–533.
- Hoering, T. C. & H. T. Ford. 1960. Isotopic effect in the fixation of nitrogen by *Azotobacter*. *J. Am. Chem. Soc.* 53: 528–533.
- Hoyt, E. 2009. The Blue Whale, *Balaenoptera Musculus*: An Endangered Species Thriving on the Costa Rica Dome. 2009. *Rep. WDC.*, 1–11. Available: www.cbd.int/cms/ui/forums/attachment.aspx?id=73
- Hucke-Gaete, R., L. P. Osman, C. A. Moreno, K. P. Findlay & D. K. Ljungblad. 2004. Discovery of a blue whale feeding and nursing ground in southern Chile. *Proc. R. Soc. B. Biol Sci.*, 271: S170–S173.
- Ingram, T., B. Matthews & C. Harrod. 2007. Lipid extraction has little effect on the $\delta^{15}\text{N}$ of aquatic consumers. *Limnol. Oceanogr. Methods.*, 5: 338–342.
- Irving, L. & J. S. Hart. 1957. The metabolism and insulation of seals as bare-skinned mammals in cold water. *Can. J. Zool.*, 35: 497–511.

- Jackson, A. L., R. Inger, A. C. Parnell & S. Bearhop. 2011. Comparing isotopic niche widths among and within communities: SIBER - Stable Isotope Bayesian Ellipses in R. *J. Anim. Ecol.*, 80: 595–602.
- Jaume-Schinkel, S. M. 2004. Hábitos alimentarios del rorcual común *Balaenoptera physalus* en el Golfo de California mediante el uso de isótopos estables de nitrógeno y carbono. M.Sc. Thesis, Centro Interdisciplinario de Ciencias Marinas-Instituto Politécnico Nacional. 64 p.
- Jenkins, S. G., S. T. Partridge, T. R. Stephenson, S. D. Farley & C. T. Robbins. 2001. Nitrogen and carbon isotope fractionation between mothers, neonates, and nursing offspring. *Oecologia*, 129: 336-341.
- Jiménez-Pinedo, N. C. 2010. Hábitos alimentarios y relación interespecífica entre la ballena azul (*Balaenoptera musculus*) y la ballena de aleta (*B. physalus*) en el suroeste del Golfo de California. M.Sc. Thesis, Centro Interdisciplinario de Ciencias Marinas-Instituto Politécnico Nacional. 78 p.
- Kaehler, S. & E. A. Pakhomov. 2001. Effects of storage and preservation on the $\delta^{13}\text{C}$ and $\delta^{15}\text{N}$ signatures of selected marine organisms. *Mar. Ecol. Prog. Ser.*, 219: 299–304.
- Kelly, J. F. 2000. Stable isotopes of carbon and nitrogen in the study of avian and mammalian trophic ecology. *Can. J. Zool.*, 78: 1–27.
- Kleiber, M. 1975. The Fire of Life: an introduction to animal energetics. 2nd Edition. Robert E. Krieger: New York. 454 p.
- Kline, T. C. 1999. Temporal and spatial variability of $^{13}\text{C}/^{12}\text{C}$ and $^{15}\text{N}/^{14}\text{N}$ in pelagic biota of Prince William Sound, Alaska. *Can. J. Fish Aquat. Sci.*, 56: 94–117.

- Lagerquist, B. A., K. M. Stafford & B. R. Mate. 2000. Satellite-Monitored Blue Whales (*Balaenoptera Musculus*) Off the Central California Coast. *Mar. Mammal Sci.*, 16: 375–391.
- Lavín, M. F., P. C. Fiedler, J. A. Amador, L. T. Ballance, J. Färber-Lorda & A. M. Mestas-Nuñez. 2006. A review of eastern tropical Pacific oceanography: Summary. *Prog. Oceanogr.*, 69: 391–398.
- Lavín, M. F., R. Durazo, E. Palacios, M. L. Argote & L. Carrillo. 1997. Lagrangian observations of the circulation in the northern Gulf of California. *J. Phys. Oceanogr.*, 27: 2298–2305.
- Leduc, R. G., F. I. Archer, A. R. Lang, K. K. Martien, B. Hancock-Hanser, J. P. Torres-Florez, R. Huecke-Gaete, H.C. Rosenbaum, K. Van Waerebeek, Jr. R. L. Brownell & B. L. Taylor. 2017. Genetic variation in blue whales in the eastern pacific: implication for taxonomy and use of common wintering grounds. *Mol. Ecol.*, 26: 740–751.
- Lee, S., D. Schell, T. McDonald & W. Richardson. 2005. Regional and seasonal feeding by bowhead whales *Balaena mysticetus* as indicated by stable isotope ratios. *Mar. Ecol. Prog. Ser.*, 285: 271–287.
- Lesage, V., Y. Morin, È. Rioux, C. Pomerleau, S. Ferguson & É Pelletier. 2010. Stable isotopes and trace elements as indicators of diet and habitat use in cetaceans: predicting errors related to preservation, lipid extraction, and lipid normalization. *Mar. Ecol. Prog. Ser.*, 419: 249–265.
- Liu, K.-K. & I. R. Kaplan. 1989. The eastern Pacific as a source of ¹⁵N-enriched nitrate in seawater off southern California. *Limnol. Oceanogr.* 34(5): 820–830.

- Lluch-Cota, S. E., E. A. Aragón-Noriega, F. Arreguín-Sánchez, D. Aurióles-Gamboa, J. J. Bautista-Romero, R. C. Brusca, R. Cervantes-Duarte, R. Cortés-Altamirano, P. Del-Monte-Luna, A. Esquivel-Herrera, G. Fernández, M. E. Hendrickx, S. Hernández-Vázquez, D. B. Lluch-Cota, J. López-Martínez, S. G. Marinone, M. O. Nevárez-Martínez, S. Ortega-García, M. Ramírez-Rodríguez, C. A. Salinas-Zavala, R. A. Schwartzlose & A. P. Sierra-Beltrán. 2007. The Gulf of California: Review of ecosystem status and sustainability challenges. *Prog. Oceanogr.*, 73: 1–26.
- Logan, J. M., T. D. Jardine, T. J. Miller, S. E. Bunn, R. A. Cunjak & M. E. Lutcavage. 2008. Lipid corrections in carbon and nitrogen stable isotope analyses: comparison of chemical extraction and modelling methods. *J. Anim. Ecol.*, 77: 838–46.
- López-Ibarra, G. A. 2008. Estructura trófica de los copépodos pelágicos en el océano Pacífico oriental tropical. Ph.D. Thesis, Centro Interdisciplinario de Ciencias Marinas-Instituto Politécnico Nacional. 92 p.
- Lynn, R. J. & J. J. Simpson. 1987. The California Current System: The seasonal variability of its physical characteristics. *J. Geophys. Res.*, 92(C12): 12947–12966.
- Lysiak, N. S. 2009. Investigations into the migration and foraging ecology of North Atlantic right whales with stable isotope geochemistry of baleen and zooplankton. Ph.D. Thesis, Boston University Graduate School of Arts and Sciences. 202 p.
- Macko, S. A., W. Y. Lee & P. L. Parker. 1982. Nitrogen and carbon isotope fractionation by two species of marine amphipods: laboratory and field studies. *J. Exp. Mar. Biol. Ecol.*, 63: 145–149.

- Mangiafico, S. S. 2016. *Summary and analysis of extension education program evaluation in R. Rutgers Cooperative Extension, New Brunswick, NJ.*
- Marinone, S. G., A. Parés-Sierra, R. Castro & A. Mascarenhas. 2004. Correction to Temporal and Spatial variation of the surface winds in the Gulf of California. *Geophys. Res. Let.*, 31: L10305.
- Martinez-Levasseur, L. M., M. A. Birch-Machin, A. Bowman, D. Gendron, E. Weatherhead, R. J. Knell & K. Acevedo-Whitehouse. 2013. Whales use distinct strategies to counteract solar ultraviolet radiation. *Sci, Rep.*, 3: 2386.
- Martínez Del Río, C., B. Wolf, S. A. Carleton & L. Z. Gannes. 2009. Isotopic ecology ten years after a call for more laboratory experiments. *Biol. Rev.*, 84: 91–111.
- Mate, B. R., B. A. Lagerquist & J. Calambokidis. 1999. Movements of North Pacific blue whales during the feeding season off southern California and their southern fall migration. *Mar. Mammal Sci.*, 15: 1246–1257.
- Matteson, R. S. 2009. The Costa Rica Dome: A study of physics, zooplankton and blue whales. M.Sc. Thesis, Oregon State University. 36 p.
- Matthews, C.J D. & S. H. Ferguson. 2013. Spatial segregation and similar trophic-level diet among eastern Canadian Arctic/north-west Atlantic killer whales inferred from bulk and compound specific isotopic analysis. *J. Mar. Biol. Assoc. U. K.*, 94: 1343–1355.
- Matthews, C. J. D. & S. H. Ferguson. 2015. Seasonal foraging behaviour of eastern Canada-West Greenland bowhead whales: An assessment of isotopic cycles along baleen. *Mar. Ecol. Prog. Ser.*, 522: 269–286.

- Mauchline, J. 1980. *The biology of mysids and euphausiids. Advances in marine biology*. Academic Press: London and New York. 681 p.
- McClatchie, S, R. Goericke, F. B. Schwing, S. J. Bograd, W. T. Peterson, R. T. Emmett, R. Charter, W. Watson, N. LO, K. Hill, C. Collins, M. Kahru, B. G. Mitchell, J. Gomez-Valdes, B. E. Lavaniegos, G. Gaxiola-Castro, J. Gottschalck, M. L'Heureux, Y. Xue, M. Manzano-Sarabia, E. Bjorkstedt, S. Ralston, J. Field, L. Rogers-Bennet, L. Munger, G. Campbell, K. Merkens, D. Camacho, A. Havron, A. Douglas & J. Hildebrand. 2009. The state of the California Current, spring 2008-2009: Cold conditions drive regional differences in coastal production. *Calif. Coop. Ocean. Fish Investig. Reports.*, 50: 43–68.
- McConnaughey, T. & C. P. McRoy. 1979. Food-Web structure and the fractionation of carbon isotopes in the Bering sea. *Mar. Biol.*, 53: 257–262.
- McDonald, M. A., S. L. Mesnick & J. A. Hildebrand. 2006. Biogeographic characterization of blue whale song worldwide: using song to identify populations. *J. Cetacean Res. Manage.*, 8(1): 55–65.
- McMahon, K. W., L. L. Hamady & S. R. Thorrold. 2013. A review of ecogeochemistry approaches to estimating movements of marine animals. *Limnol. Oceanogr.*, 58: 697–714.
- McMahon, K. W, S. R. Thorrold, T. S. Elsdon & M. D. Mccarthy. 2015. Trophic discrimination of nitrogen stable isotopes in amino acids varies with diet quality in a marine fish. *Limnol. Oceanogr.*, 60: 1076–1087.
- Michener, R. H. & K. Lajtha. 2007. Stable isotopes in ecology and environmental science. Second Edition (Michener, Robert and K Lajtha, eds.). Blackwell publishing, Ed. Malden, MA. 566 p.

- Mikhalev, Y. A. 1997. Additional information about the catches of Soviet whaling fleet Sovetskaya Ukraina. *Rep. to Int. Whal. Com.*, 47: 147–150.
- Miller, T. W. 2006. Trophic Dynamics of Marine Nekton and Zooplankton in the Northern California Current Pelagic Ecosystem. Ph.D. Thesis, Oregon State University. 196 p.
- Miller, T. W., R. D. Brodeur & G. H. Rau. 2008. Carbon stable isotopes reveal relative contribution of shelf-slope production to the Northern California Current pelagic community. *Limnol. Oceanogr.*, 53: 1493–1503.
- Miller, S. A & J. P. Harley. 2009. *Zoology*. 5th Edition. McGraw Hill, Ed. Boston, MA, 608 p.
- Mitani, Y., T. Bando, N. Takai & W. Sakamoto. 2006. Patterns of stable carbon and nitrogen isotopes in the baleen of common minke whale *Balaenoptera acutorostrata* from the western North Pacific. *Fish Sci.*, 72: 69–76.
- Mitchell, D. L., D. Ivanova, R. Rabin, T. J. Brown & K. Redmond. 2002. Gulf of California sea surface temperatures and the North American monsoon: Mechanistic implications from observations. *J. Climate*, 15: 2261–2281.
- Miyake, Y. & E. Wada. 1971. The abundance ratio of $^{15}\text{N}/^{14}\text{N}$ in marine environments. *Rec. Oceanographic Works, Jap.*, 7: 37–57.
- Morales-Guerrero, B., C. Barragán-Vargas, G. R. Silva-Rosales, C. D. Ortega-Ortiz, D. Gendron & L. M. Martínez-Levasseur .2016. Melanin granules melanophages and a fully-melanized epidermis are common traits of odontocete and mysticete cetaceans. *Vet. Dermatol.*, 28(2): 213-e50.

- Moreno-Santillán, D. D., E. A. Lacey, D. Gendron & J. Ortega. 2016. Genetic variation at exon 2 of the MHC class II DQB locus in blue whale (*Balaenoptera musculus*) from the Gulf of California. *PLoS One*, 11: 1–15.
- Morin, P. A., R. G. LeDuc, K. M. Robertson, N. M. Hedrick, W. F. Perrin, M. Etnier, P. Wade & B. L. Taylor. 2006. Genetic analysis of killer whale (*Orcinus orca*) historical bone and tooth samples to identify western U.S. ecotypes. *Mar. Mammal Sci.*, 22: 897–909.
- Morin, P. A., A. Nestler, N. T. Rubio-Cisneros, K. M. Robertson & S. L. Mesnick. 2005. Interfamilial characterization of a region of the ZFX and ZFY genes facilitates sex determination in cetaceans and other mammals. *Mol. Ecol.*, 14: 3275–3286.
- Nelson, D. L. & C. M. Michael .2005. *Lehninger principles of biochemistry*. 6th Edition. W H Freeman & Co (Sd), Ed. New York, 1340 p.
- Nemoto, T. 1959. Food of baleen whales with references to whale movements. *Sci. Reports Whales. Res. Inst.*, 14: 149–290.
- Nemoto, T. & A. Kawamura.1977. Characteristics of food habits and distribution of baleen whales with special reference to the abundance of North Pacific sei and Bryde's whales. *Rep. Int. Whal. Com. Spec. Issue.*, 80–87.
- Newsome, S. D., M. T. Clementz & P. L. Koch. 2010. Using stable isotope biogeochemistry to study marine mammal ecology. *Mar. Mammal Sci.*, 26: 509–572.
- Newsome, S. D., P. L. Koch, M. A. Etnier & D. Auriolles-Gamboa. 2006. Using carbon and nitrogen isotope values to investigate maternal strategies in northeast pacific otariids. *Mar. Mammal Sci.*, 22: 556–572.

- Newsome, S. D., C. Martínez del Río, S. Bearhop & D. L. Phillips. 2007. A niche for isotopic ecology. *Front. Ecol. Environ.*, 5: 429–436.
- Ocean Exploration Trust & National Oceanic and Atmospheric Administration Office of Ocean Exploration and Research. 2014. Workshop: Telepresence-enabled exploration of the eastern Pacific Ocean. December 11–13. Exploratorium, San Francisco. Website: <http://www.oceanexplorationtrust.org/2014pacificworkshop>
- Odum, E. P. & G. W. Barrett. 2004. *Fundamentals of Ecology*. 5th Edition. Thomson Brooks/Cole: Belmont, CA. 624 p.
- Oleson, E. M., J. Calambokidis, J. Barlow & J. A. Hildebrand. 2007a. Blue whale visual and acoustic encounter rates in the southern California bight. *Mar. Mammal Sci.*, 23: 574–597.
- Oleson, E. M., J. Calambokidis, W. C. Burgess, M. A. McDonald, C. A. LeDuc & J. A. Hildebrand. 2007b. Behavioral context of call production by eastern North Pacific blue whales. *Mar. Ecol. Prog. Ser.*, 330: 269–284.
- Oleson, E. M., S. M. Wiggins & J. A. Hildebrand. 2007c. Temporal separation of blue whale call types on a southern California feeding ground. *Anim. Behav.*, 74: 881–894.
- Oliver, J. S., P. N. Slattery, M. A. Silberstein & E. F. O'Connor. 1983. A comparison of gray whale, *Eschrichtius robustus*, feeding in the Bering Sea and Baja California. *Fish. Bull.*, 81: 513–522.
- Páez-Rosas, D., D. Aurióles-Gamboa, J. J. Alava & D. M. Palacios. 2012. Stable isotopes indicate differing foraging strategies in two sympatric otariids of the Galapagos Islands. *J. Exp. Mar. Bio. Ecol.*, 424–425: 44–52.

- Palacios, D. M. 1999. Blue whale (*Balaenoptera musculus*) occurrence off the Galapagos Islands, 1978-1995. *J. Cetacean Res. Manag.*, 1: 41–51.
- Pancost, R. D., K. H. Freeman, S. G. Wakeham, C. Y. Robertson. 1997. Controls on carbon isotope fractionation by diatoms in the Peru upwelling region. *Geochim Cosmochim Acta*, 61: 4983–4991.
- Paniagua-Mendoza, A., D. Gendron, E. Romero-Vivas & J. A. Hildebrand. 2017. Seasonal acoustic behavior of blue whales (*Balaenoptera musculus*) in the Gulf of California, Mexico. *Mar. Mammal. Sci.*, 33: 206–218.
- Pardo, M. A., T. Gerrodette, E. Beier, D. Gendron, K. A. Forney, S. J. Chivers, J. Barlow & D. M. Palacios. 2015. Inferring cetacean population densities from the absolute dynamic topography of the ocean in a hierarchical bayesian framework. *PLoS One*, 10: 1–23.
- Pardo, M. A., N. Silverberg, D. Gendron, E. Beier & D. M. Palacios. 2013. Role of environmental seasonality in the turnover of a cetacean community in the southwestern Gulf of California. *Mar. Ecol. Prog. Ser.*, 487: 245–260.
- Parnell, A. C., R. Inger, S. Bearhop & A. L. Jackson. 2010. Source partitioning using stable isotopes: coping with too much variation. *PLoS One*, 5: e9672.
- Peng, R. D., F. Dominici & T. A. Louis. 2006. Model choice in time series studies of air pollution and mortality. *J. R. Stat. Soc. Ser. A.*, 169: 179–203.
- Penzias, A. A. 1979. The origin of the elements. *Science*, 205:549–554.
- Perrin, W. F., B. Würsig & J. G. M. Thewissen. 2002. Encyclopedia of marine mammals. Academic Press: San Diego, CA. 1414 p.

- Perry, R. I., P. A. Thompson, D. L. Mackas, P. J. Harrison & D. R. Yelland. 1999. Stable carbon isotopes as pelagic food web tracers in adjacent shelf and slope regions off British Columbia, Canada. *Can. J. Fish. Aquat. Sci.*, 56: 2477–2486.
- Podlesak, D. W., S. R. McWilliams & K. A. Hatch. 2005. Stable isotopes in breath, blood, feces and feathers can indicate intra-individual changes in the diet of migratory songbirds. *Oecologia*, 142: 501–510.
- Popp, B., E. A. Laws, R. R. Bidigare, J. E. Dore, K. L. Hanson & S. G. Wakeham. 1998. Effect of phytoplankton cell geometry on carbon isotopic fractionation. *Geochim. Cosmochim. Acta*, 62: 69–77.
- Popp, B. N., B. S. Graham, R. J. Olson, C. C. S. Hannides, M. J. Lott, G. A. López-Ibarra, F. Galván-Magaña & B. Fry. 2007. Insight into the trophic ecology of yellowfin tuna, *Thunnus albacares*, from compound-specific nitrogen isotope analysis of proteinaceous amino acids. *Isot as Indic Ecol Chang.*, 1:173–190.
- Post, D. M. 2002. Using stable isotopes to estimate trophic position: models, methods, and assumptions. *Ecology*, 83: 703–718.
- Potvin, J., J. A. Goldbogen & R. E. Shadwick. 2012. Metabolic expenditures of lunge feeding rorquals across scale: implications for the evolution of filter feeding and the limits to maximum body size. *PLoS One*, 7: e44854.
- Poulsen, T. 2010. *Introduction to Chemistry*. CK-112 Foundations, Ed. U.S.A., 250 p.
- R Development Core T. 2017. R: A language and environment for statistical computing. R Foundation for Statistical Computing: Vienna, Austria.

- Rau, G. 1982. *The relationship between trophic level and stable isotopes of carbon and nitrogen*. 143–148, In: W. Bascom (ed). Coastal water research project biennial report for the years 1981-1982. Southern California coastal water research project annual report. Ed. W. Bascom. California, Long Beach.
- Rau, G. H. & N. H. Anderson. 1981. Use of $^{13}\text{C}/^{12}\text{C}$ to trace dissolved and particulate organic matter utilization by populations of an aquatic invertebrate. *Oecologia*, 48: 19–21.
- Rau, G. H., F. P. Chavez & G. E. Friederich. 2001. Plankton $^{13}\text{C}/^{12}\text{C}$ variations in Monterey Bay, California: Evidence of non-diffusive inorganic carbon uptake by phytoplankton in an upwelling environment. *Deep Res. Part I Oceanogr. Res. Pap.*, 48: 79–94.
- Rau, G. H., A. J. Mearns, D. R. Young, R. J. Olson, H. A. Schafer & I. R. Kaplan. 1983. Animal $^{13}\text{C}/^{12}\text{C}$ correlates with trophic level in pelagic food webs. *Ecology*, 64: 1314–1318.
- Rau, G. H., M. D. Ohman & A. Pierrot-Bults. 2003. Linking nitrogen dynamics to climate variability off central California: a 51year record based on $^{15}\text{N}/^{14}\text{N}$ in CalCOFI zooplankton. *Deep Sea Res. Part II Top Stud. Oceanogr.*, 50: 2431–2447.
- Rau, G. H., R. E. Sweeney & I. R. Kaplan. 1982. Plankton $^{13}\text{C}:^{12}\text{C}$ ratio changes with latitude: differences between northern and southern oceans. *Deep Sea Res. Part A, Oceanogr. Res. Pap.*, 29: 1035–1039.
- Reilly, S. B., J. L. Bannister, P. B. Best, M. Brown, Jr. R. L. Brownell, D. S. Butterworth, P. J. Clapham, J. Cooke, G. P. Donovan, J. Urbán & A. N. Zerbini. 2008a. *Balaenoptera musculus*. IUCN Red List Threat Species, e.T2477A9447146.

- Reilly, S. B., J. L. Bannister, P. B. Best, M. Brown, Jr. R. L. Brownell, D. S. Butterworth, P. J. Clapham, J. Cooke, G. P. Donovan, J. Urbán & A. N. Zerbini. 2008b. *Megaptera novaeangliae*. IUCN Red List Threat Species, e.T13006A3405371.
- Reilly, S. B. & V. G. Thayer .1990. Blue whale (*Balaenoptera musculus*) distribution in the eastern tropical Pacific. *Mar. Mammal Sci.*, 6: 265–277.
- Rice, D. W. 1974. *Whales and whale research in the eastern North Pacific*. 170–195, In: W. E. Schevill (ed.). *The whale problem: a status report*. Harvard University Press: Cambridge, MA.
- Ripa, P. 1997. Towards a physical explanation of the seasonal dynamics and thermodynamics of the Gulf of California. *J. Phys. Oceanogr.*, 27: 597–614.
- Roberts, K., E. Granum, R. C. Leegood & J. A. Raven. 2007. C₃ and C₄ pathways of photosynthetic carbon assimilation in marine diatoms are under genetic, not environmental, control. *Plant Physiol.*, 145: 230–235.
- Rowntree, V. J., L. O. Valenzuela, P. F. Fraguas & J. Seger. 2008. Foraging behaviour of southern right whales (*Eubalaena australis*) inferred from variation of carbon stable isotope ratios in their baleen. *Rep. to Int. Whal. Com.*, 19: 256–263.
- Rueda-Flores, M. 2007. Variabilidad de perfiles de ácidos grasos de ballena azul, *Balaenoptera musculus*, en el Golfo de California. M.Sc. Thesis, Centro Interdisciplinario de Ciencias Marinas-Instituto Politécnico Nacional. 67 p.
- Ryan, C., B. McHugh, C. N. Trueman, C. Harrod, S. D. Berro & I. O'Connor. 2012. Accounting for the effects of lipids in stable isotope ($\delta^{13}\text{C}$ and $\delta^{15}\text{N}$ values)

- analysis of skin and blubber of balaenopterid whales. *Rapid Commun. Mass Spectrom.*, 26: 2745–2754.
- Sachs, J. P. & S. N. Ladd. 2010. Climate and oceanography of the Galapagos in the 21st century: expected changes and research needs. *Galapagos Res.*, 67: 50–54.
- Sackett, W. M., W. R. Eckelmann, M. L. Bender & A. W. H. Be. 1965. Temperature dependence of carbon isotopic composition in marine plankton and sediments. *Science*, 148: 235–237.
- Sampson, L., F. Galván–Magaña, R. De Silva-Dávila, S. Aguiniga-Garcia & J. B. O’Sullivan. 2010. Diet and trophic position of the devil rays *Mobula thurstoni* and *Mobula japonica* as inferred from stable isotope analysis. *Mar. Biol. Assoc. United Kingdom.*, 90: 969–976.
- Sarakinos, H. C. H., M. L. Johnson & M. Vander Zanden. 2002. A synthesis of tissue-preservation effects on carbon and nitrogen stable isotope signatures. *Can. J. Zool.*, 80: 381–387.
- Schell, D. M., S. M. Saupe & N. Haubenstock. 1989a. *Natural isotope abundances in bowhead whale (Balaena mysticetus) baleen: markers of aging and habitat usage*. 260–269, In: P. W. Rundel, J. R. Ehleringer & K. A. Nagy (eds.). *Stable isotopes in ecological research*. Springer-Verlag, New York.
- Schell, D. M., S. M. Saupe & N. Haubenstock. 1989b. Bowhead whale (*Balaena mysticetus*) growth and feeding as estimated by $\delta^{13}\text{C}$ techniques. *Mar. Biol.*, 103: 433–443.
- Schneider, N., E. Di Lorenzo & P. P. Niiler. 2005. Salinity Variations in the Southern California Current. *J. Phys. Oceanogr.*, 35: 1421–1436.

- Schoeller, D. A. 1999. Isotope fractionation: Why aren't we what we eat? *J. Archaeol. Sci.*, 26: 667–673.
- Schoenherr, J. R. 1991. Blue whales feeding on high concentrations of euphausiids around Monterey Submarine Canyon. *Can. J. Zool.*, 69: 583–594.
- Sears, R. 1987. The photographic identification of individual blue whales (*Balaenoptera musculus*) in the Sea of Cortez. *Cetus*. 7:14-17.
- Sears, R., C. Ramp, A. B. Douglas & J. Calambodikis. 2013. Reproductive parameters of eastern North Pacific blue whales *Balaenoptera musculus*. *Endanger. Species Res.*, 22: 23–31.
- Semmens, B. X., E. J. Ward, J. W. Moore & C. T. Darimont. 2009. Quantifying inter- and intra-population niche variability using hierarchical bayesian stable isotope mixing models. *PLoS One*, 4: e6187.
- Sheehan, D. & B. B. Hrapchak. 1980. *Theory and practice of histotechnology*. 2nd Edition. St. Louis, MO: C.V, Ed. Mosby Co. 481p.
- Silva, R. G. 2004. Assessment of body surface temperature in cetaceans: an iterative approach. *Braz. J. Biol.*, 64: 719–24.
- St Aubin, D. J., T. G. Smith & J. R. Geraci. 1990. Seasonal epidermal molt in beluga whales, *Delphinapterus leucas*. *Can. J. Zool.*, 68: 359–364.
- Stafford, K. M., D. R. Bohnenstiehl, M. Tolstoy, E. Chapp, D. K. Mellinger & S. E. Moore. 2004. Antarctic-type blue whale calls recorded at low latitudes in the Indian and eastern Pacific Oceans. *Deep Sea Res. Part I Oceanogr. Res. Pap.*, 51: 1337–1346.

- Stafford, K. M., S. L. Nieukirk & C. G. Fox. 2001. Geographic and seasonal variation of blue whale calls in the North Pacific. *J. Cetacean Res. Manag.*, 3: 65–76.
- Stock, B. & B. X. Semmens. 2016. MixSIAR GUI User Manual. Version 3.1.
- Sydeman, W. J., K. A. Hobson, P. Pyle & E. B. McLaren. 1997. Trophic relationships among seabirds in central California: Combined stable isotope and conventional dietary approach. *Condor*, 99: 327–336.
- Tershy, B. R., D. Breese & C. S. Strong. 1990. Abundance, seasonal distribution and population composition of baleenopterid whales in the Canal de Ballenas, Gulf of California, Mexico. *Reports Int. Whal. Comm.*, 369–375.
- Thomas, S. M. & T. W. Crowther. 2015. Predicting rates of isotopic turnover across the animal kingdom: A synthesis of existing data. *J. Anim. Ecol.*, 84: 861–870.
- Thunell, R. C. 1998. Seasonal and annual variability in particle fluxes in the Gulf of California. *Deep Sea Res. Part I Oceanogr. Res. Pap.*, 45(12): 2059–2083.
- Tieszen, L. L., T. W. Boutton, K. G. Tesdahl & N. A. Slade. 1983. Fractionation and turnover of stable carbon isotopes in animal tissues: Implications for $\delta^{13}\text{C}$ analysis of diet. *Oecologia*, 57: 32–37.
- Todd, S., P. Ostrom, J. Lien & J. Abrajano. 1997. Use of biopsy samples of humpback whale (*Megaptera novaeangliae*) skin for stable isotope ($\delta^{13}\text{C}$) determination. *J. Northw. Atl. Fish. Sci.*, 22: 71–76.
- Tomczak., M. & J. S. Godfrey. 2003. *Regional oceanography: An introduction*. 2nd ed. Daya Publishing House, Ed. Delhi. 390 p.

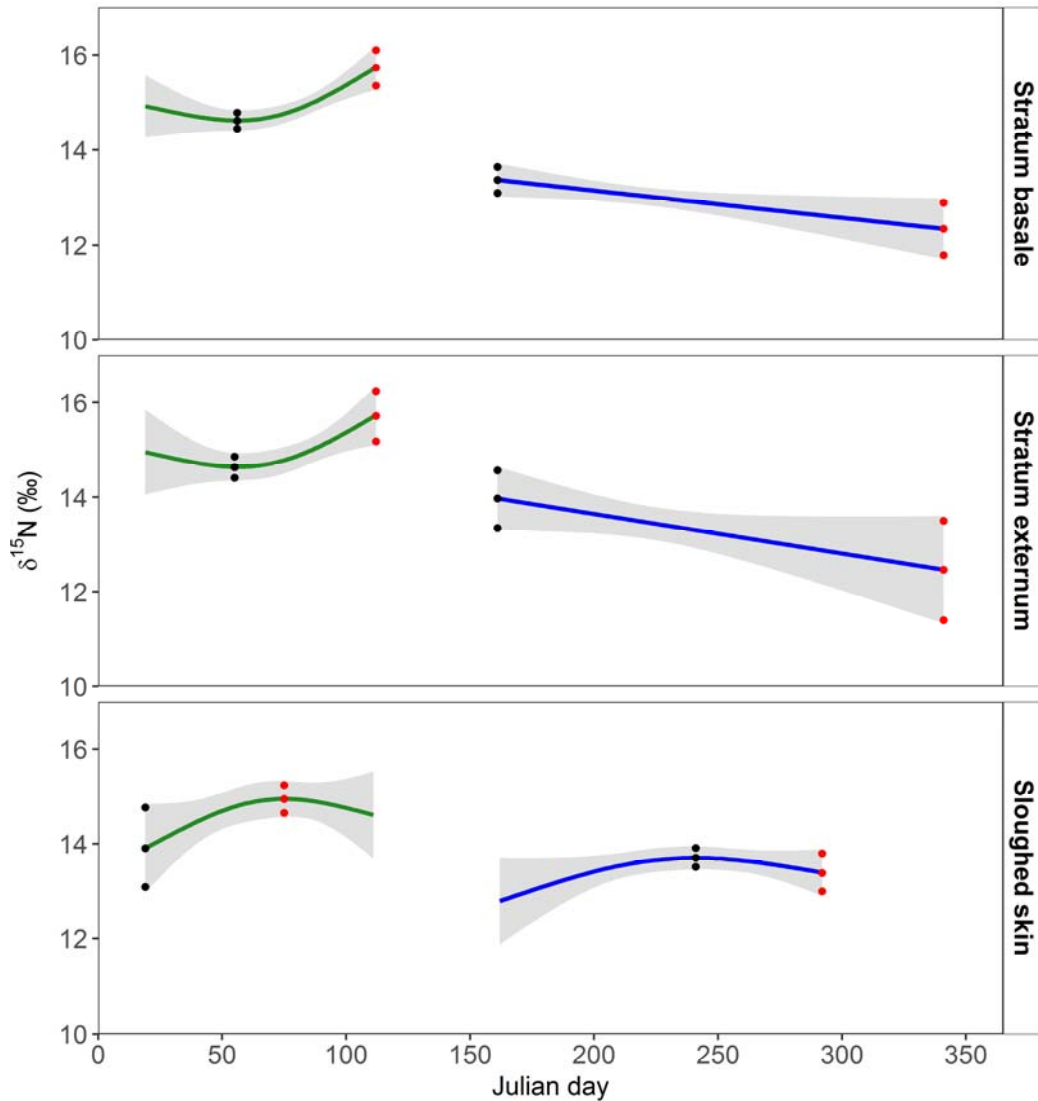
- Torres-Florez, J. P., P. A. Olson, L. Bedriñana-Romano, H. C. Rosenbaum, J. Ruiz, R. LeDuc & R. Hucke-Gaete. 2015. First documented migratory destination for eastern South Pacific blue whales. *Mar. Mammal Sci.*, 31: 1580–1586.
- Torres-Florez, J., R. Hucke-Gaete, R. LeDuc, A. Lang, B. Taylor, L. E. Pimper, L. Bedriñana-Romano & H. C. Rosenbaum & C. C. Figueroa. 2014. Blue whale population structure along the eastern South Pacific Ocean: evidence of more than one population. *Mol. Ecol.*, 23: 5998–6010.
- Torres-Orozco, E. 1993. Análisis volumétrico de las masas de agua del Golfo de California. M.Sc. Thesis, CICESE. Ensenada, B.C., México. 79 p.
- Ugalde de la Cruz, A. 2008. Abundancia y tasas de supervivencia de ballenas azules en el Golfo de California. M.Sc. Thesis, Centro Interdisciplinario de Ciencias Marinas-Instituto Politécnico Nacional. 54 p.
- Ugalde de la Cruz, A. 2015. Movimientos migratorios, estructura poblacional y tasa de supervivencia de las ballenas azules del Pacífico noroeste con base en datos de foto-identificación. Ph.D. Thesis, Centro Interdisciplinario de Ciencias Marinas-Instituto Politécnico Nacional. 75 p.
- Ulloa, O., J. J. Wright, L. Belmar & S. J. Hallam. 2013. 7.- *Pelagic oxygen minimum zone microbial communities*. 113–122, In: E. F. Rosenberg, S. Lory E. Stackebrandt & F. Thompson (eds). *The prokaryotes: Prokaryotic communities and ecophysiology*. Springer-Verlag, Ed. Berlin, Heidelberg.
- Unkovich, M., J. Pate, A. McNeill & D. J. Gibbs. 2001. *Stable isotope techniques in the study of biological processes and functioning of ecosystems*. Springer Netherlands, Ed. Dordrecht, 289 p.

- Vikingsson, G. A. 1990. Energetic studies on fin and sei whales caught off Iceland. *Rep. Int. Whal. Comm.* 40:365–373.
- Voigt, C. C. 2003. Low turnover rates of carbon isotopes in tissues of two nectar-feeding bat species. *J. Exp. Biol.*, 206: 1419–1427.
- Voss, M., J. W. Dippner & J. P. Montoya. 2001. Nitrogen isotope patterns in the oxygen-deficient waters of the Eastern Tropical North Pacific Ocean. *Deep Sea Res. Part I Oceanogr. Res. Pap.*, 48: 1905–1921.
- Walton, M. J., M. A. Silva, S. M. Magalhães, R. Prieto & R. S. Santos. 2008. Fatty acid characterization of lipid fractions from blubber biopsies of sperm whales *Physeter macrocephalus* located around the Azores. *J. Mar. Biol. Assoc. U.K.*, 88(6): 1109–1115.
- Williams, R. 2013. Trophic ecology of oxygen minimum zone zooplankton revealed by Carbon and Nitrogen Stable Isotopes. Ph.D. Thesis, University of Rhode Island. 150 p.
- Williams, R. L., S. Wakeham, R. McKinney & K. F. Wishner. 2014. Trophic ecology and vertical patterns of carbon and nitrogen stable isotopes in zooplankton from oxygen minimum zone regions. *Deep Res. Part I Oceanogr. Res. Pap.*, 90: 36–47.
- Wisner, R. L. 1974. *The taxonomy and distribution of lanternfishes (family Myctophidae) of the eastern Pacific Ocean*. Navy Ocean Research and Development Activity; Bay St. Louis, Miss.
- Witteveen, B. H., J. M. Straley, E. Chenoweth, C. S. Baker, J. Barlow, C. Matkin, C. M. Gabriele, J. Neilson, D. Steel, O. v. Ziegesar, A. G. Andrews & A. Hirons. 2011. Using movements, genetics and trophic ecology to differentiate inshore

- from offshore aggregations of humpback whales in the Gulf of Alaska. *Endanger Species Res.*, 14: 217–225.
- Witteveen, B. H., G. A. J. Worthy, R. J. Foy & K. M. Wynne. 2012. Modeling the diet of humpback whales: An approach using stable carbon and nitrogen isotopes in a Bayesian mixing model. *Mar. Mammal Sci.*, 28: 1–18.
- Wood, S.N. 2006. *Generalized additive models: an introduction with R*. 384 p.
- Würsig, B. & C. Clark. 1993. *Behavior*. 157–199, In: J. J. Burns, J. J. Montague & C. J. Cowles (eds). The bowhead whale. Alien Press, Lawrence, K.S.
- Xiang, D. 2001. Fitting generalized additive models with the GAM procedure. *SAS Institute, Cary, NC.*, Paper 256-26 p.
- Yee, T. W. & N. D. Mitchell. 1991. Generalized additive models in plant ecology (DW Pond, Ed.). *J. Veg. Sci.*, 2: 587–602.
- Vander Zanden, M. J., M. K. Clayton, E. K. Moody, C. T. Solomon & B. C. Weidel. 2015. Stable isotope turnover and half-life in animal tissues: A literature synthesis. *PLoS One*, 10: 1–16.
- Vander Zanden, M. J. & J. B. Rasmussen. 2001. Variation in $\delta^{15}\text{N}$ and $\delta^{13}\text{C}$ trophic fractionation: Implications for aquatic food web studies. *Limnol. Oceanogr.*, 46: 2061–2066.

12. APPENDIX

APPENDIX I. Sections used from the GAM model predictions to infer $\delta^{15}\text{N}$ isotopic incorporation rates of blue whale skin strata in each foraging zone. The lines represent the GAM model fit (predictions) in the Gulf of California (green) and the California Current System (blue). The fringe around the lines show the 95% confidence intervals. The black dot represents the initial point (*i.e.* diet switch) and the red dot the final point of the sections from the predictions that were used from the fit and the lower and upper confidence intervals. Per mil (‰) differences and days passed between points were estimated and then used to extrapolated to a 1.6‰ increase in the Gulf of California, or decrease in California Current System, for skin to reach steady-state isotopic equilibrium with the local prey isotopic signal.

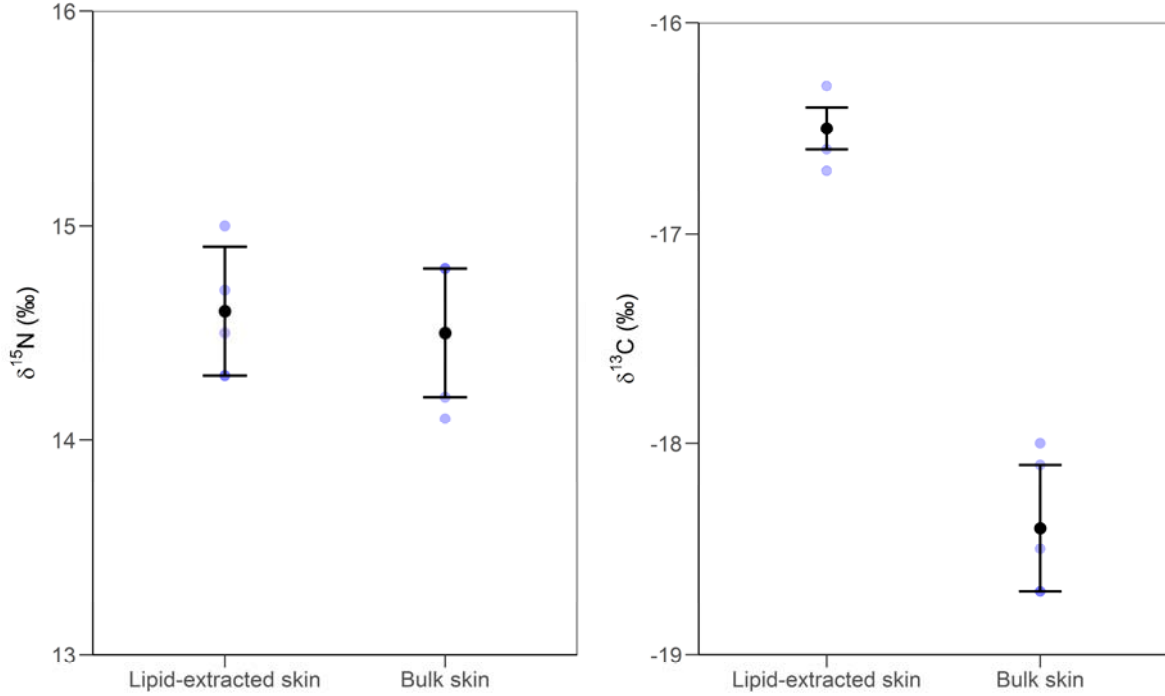


APPENDIX II. Results from the GAM model sections used to infer $\delta^{15}\text{N}$ isotopic incorporation rates of blue whale skin strata in Gulf of California (GC) and California Current System (CCS). CI, confidence interval limit.

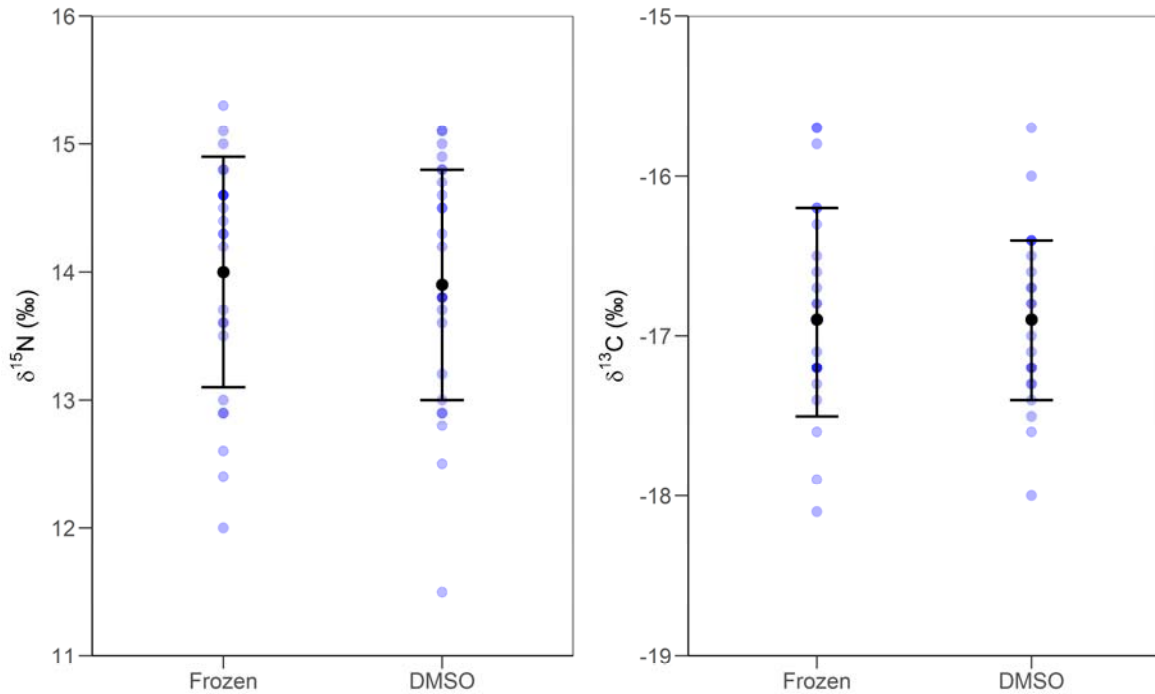
Zone	Strata	Model section	Initial $\delta^{15}\text{N}$ (diet switch)	Final $\delta^{15}\text{N}$	Per mil differences (‰)	Days passed between initial and final $\delta^{15}\text{N}$	Extrapolate to a 1.6‰ change
GC	Basale	Fit	14.6	15.7	1.1	56	81
	Basale	Upper 95% CI	14.8	16.1	1.3	56	69
	Basale	Lower 95% CI	14.4	15.4	1.0	56	90
	Externum	Fit	14.6	15.7	1.1	56	81
	Externum	Upper 95% CI	14.9	16.2	1.3	56	69
	Externum	Lower 95% CI	14.4	15.2	0.8	56	112
	Sloughed skin	Fit	13.9	14.9	1.0	56	90
	Sloughed skin	Upper 95% CI	14.6	15.2	0.6	56	149
	Sloughed skin	Lower 95% CI	13.2	14.7	1.5	56	60
CCS	Basale	Fit	13.4	12.3	-1.1	180	262
	Basale	Upper 95% CI	13.6	12.8	-0.8	180	360
	Basale	Lower 95% CI	13.1	11.8	-1.3	180	222
	Externum	Fit	14.0	12.5	-1.5	180	192
	Externum	Upper 95% CI	14.5	13.3	-1.2	180	240
	Externum	Lower 95% CI	13.4	11.6	-1.8	180	160
	Sloughed skin	Fit	13.7	13.4	-0.3	51	272
	Sloughed skin	Upper 95% CI	13.9	13.8	-0.1	51	816
	Sloughed skin	Lower 95% CI	13.5	13.0	-0.5	51	163

APPENDIX III. $\delta^{15}\text{N}$ and $\delta^{13}\text{C}$ in blue whale skin processed using different processing methods. Graphs show all the blue whale skin isotopic data (blue dots), and the mean \pm SD (black dot and whiskers) for each treatment.

A) Treatment: Lipid-extracted vs bulk skin

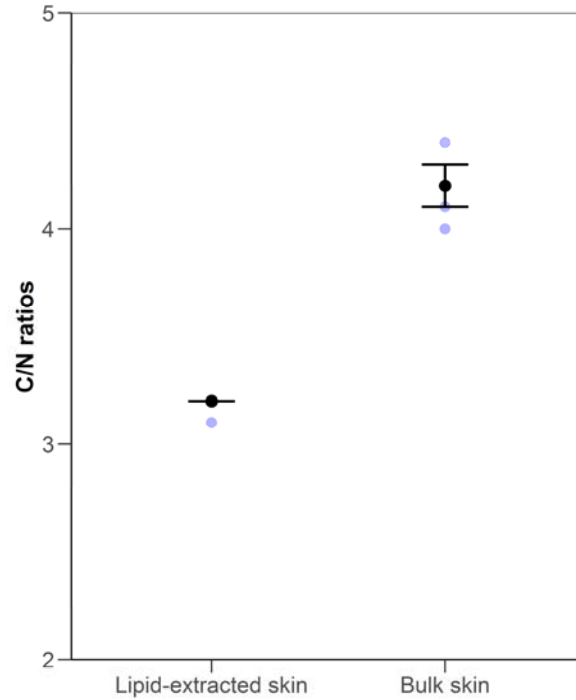


B) Preservation method: Skin preserved frozen (control) vs DMSO

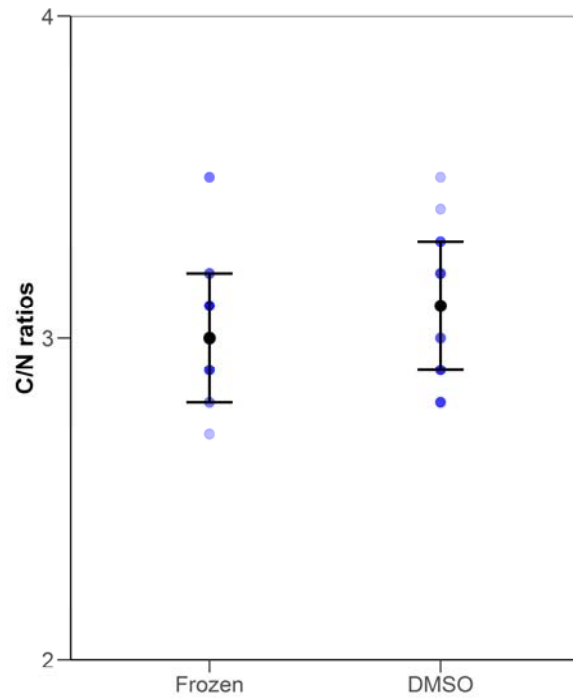


APPENDIX IV. Weight percent C/N ratios in blue whale skin processed using different treatments. Graphs show all the blue whale C/N ratios (blue dots), and the mean \pm SD (black dot and whiskers) for each treatment.

A) Treatment: Lipid-extracted vs bulk skin

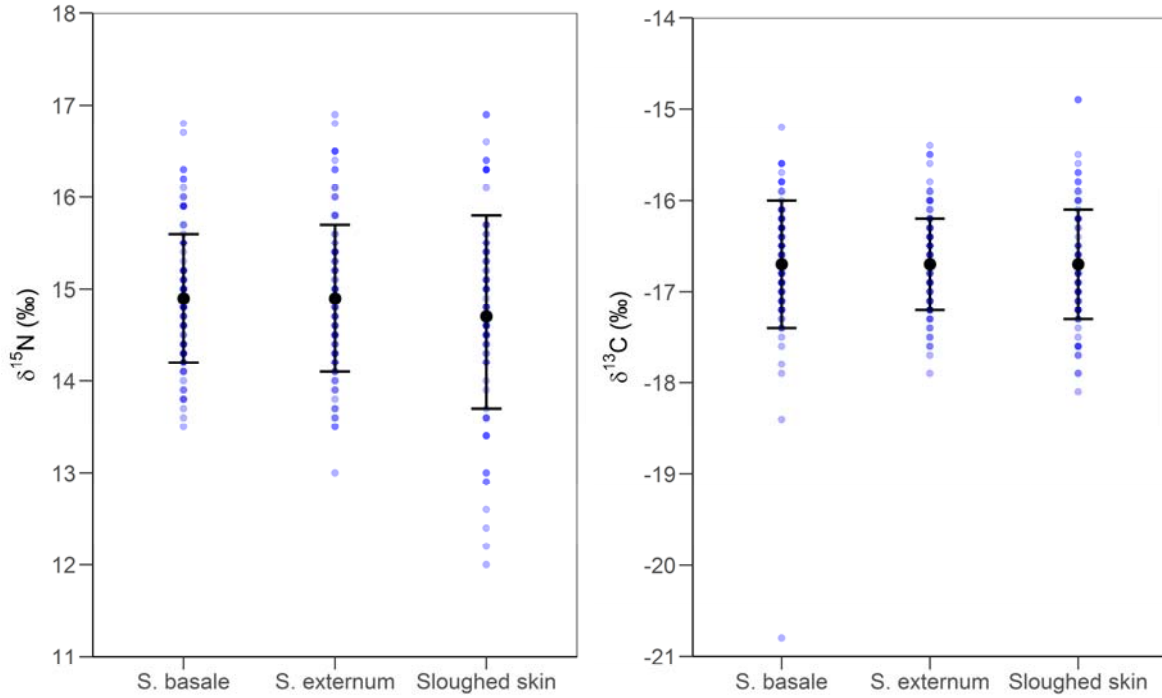


B) Preservation method: Skin preserved frozen (control) vs DMSO skin

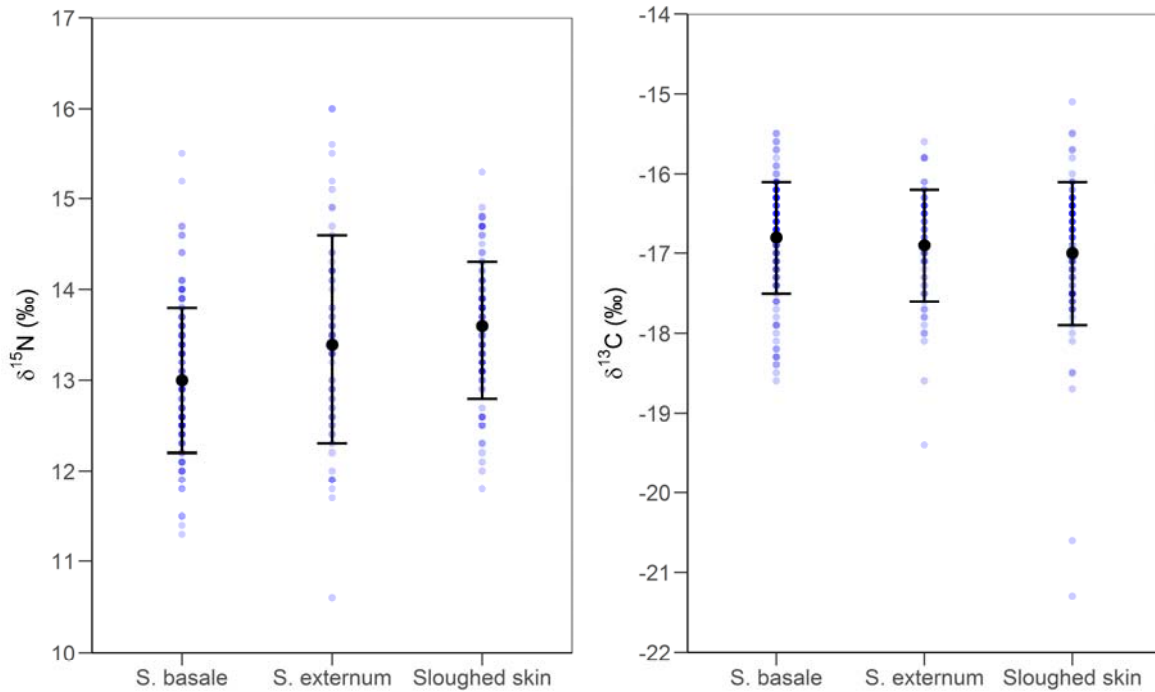


APPENDIX V. $\delta^{15}\text{N}$ and $\delta^{13}\text{C}$ in blue whale skin strata. Graphs show all the blue whale skin isotopic data (blue dots), and the mean \pm SD (black dot and whiskers) of each skin strata.

A) Gulf of California



B) California Current System



APPENDIX VI. Monthly blue whale $\delta^{13}\text{C}$, $\delta^{15}\text{N}$ and weight percent C/N ratios (Mean \pm SD) in skin strata of whales sampled in the different foraging zones in the eastern Pacific Ocean.

Zone/Years	Month	Julian day	Skin stratum	n	Mean \pm SD		
					$\delta^{13}\text{C}$	$\delta^{15}\text{N}$	C/N
Gulf of California/ 2002-2009, 2011- 2013, 2015	January	19-30	Basale	4	-16.7 \pm 0.6	14.7 \pm 0.4	3 \pm 0.2
			Externum	3	-16.6 \pm 0.6	14.6 \pm 0.6	2.9 \pm 0.2
			Sloughed skin	7	-16.8 \pm 0.7	14 \pm 0.6	3 \pm 0.1
	February	31-57	Basale	20	-16.8 \pm 0.5	14.8 \pm 0.6	2.9 \pm 0.2
			Externum	21	-16.7 \pm 0.5	14.8 \pm 0.8	3 \pm 0.2
			Sloughed skin	24	-16.8 \pm 0.6	14.7 \pm 1	3.1 \pm 0.2
	March	59-88	Basale	59	-16.7 \pm 0.8	14.7 \pm 0.6	2.9 \pm 0.2
			Externum	46	-16.6 \pm 0.6	14.7 \pm 0.8	3 \pm 0.2
			Sloughed skin	38	-16.7 \pm 0.6	14.9 \pm 1.2	3 \pm 0.2
	April	93-112	Basale	18	-16.7 \pm 0.4	15.6 \pm 0.8	2.8 \pm 0.2
			Externum	15	-16.8 \pm 0.4	15.6 \pm 0.8	2.9 \pm 0.2
			Sloughed skin	12	-16.6 \pm 0.9	14.7 \pm 0.8	3.1 \pm 0.3
California Current System/ 1996, 1998, 2000- 2006, 2008-2011	June	161-180	Basale	23	-16.6 \pm 0.5	13.1 \pm 0.7	3 \pm 0.1
			Externum	5	-16.7 \pm 0.3	12.9 \pm 0.4	3.2 \pm 0.2
			Sloughed skin	3	-16.8 \pm 0.3	12.1 \pm 0.1	3.2 \pm 0.1
	July	186-211	Basale	29	-16.8 \pm 0.6	13.4 \pm 0.8	3.1 \pm 0.1
			Externum	19	-16.8 \pm 0.6	14.2 \pm 1	3.1 \pm 0.1
			Sloughed skin	13	-16.9 \pm 0.5	13.8 \pm 0.8	3.2 \pm 0.1
	August	212-242	Basale	40	-17 \pm 0.7	13 \pm 0.7	3.1 \pm 0.1
			Externum	25	-17.1 \pm 0.6	13.2 \pm 1.1	3.2 \pm 0.1
			Sloughed skin	32	-17 \pm 0.7	13.7 \pm 0.7	3.2 \pm 0.1
	September	243-272	Basale	21	-17 \pm 0.9	12.5 \pm 0.8	3.2 \pm 0.1
			Externum	9	-16.9 \pm 1.1	13 \pm 1	3.2 \pm 0.1
			Sloughed skin	34	-17.1 \pm 1.3	13.5 \pm 0.6	3.3 \pm 0.2
October	274-304	Basale	3	-16.6 \pm 0.4	13.4 \pm 1	3 \pm 0	
		Externum	2	-16.5 \pm 0	13.8 \pm 1.2	3.2 \pm 0.1	
		Sloughed skin	11	-16.8 \pm 0.7	13.6 \pm 0.8	3.3 \pm 0.2	
November	321	Basale	2	-15.9 \pm 0.4	11.8 \pm 0.4	3.1 \pm 0.2	
		Externum	1	-16.4	11.8	3.3	
		Sloughed skin	0	-	-	-	
December	337-341	Basale	2	-16.9 \pm 1.3	13.2 \pm 0.3	3.1 \pm 0	
		Externum	2	-16.9 \pm 1.6	13 \pm 0.8	3.2 \pm 0.2	
		Sloughed skin	0	-	-	-	
Costa Rica Dome/ 1999, 2000, 2003	October	285-304	Basale	2	-17.6 \pm 0.3	11.9 \pm 0.1	3.2 \pm 0.1
			Externum	2	-17.3 \pm 0.3	11.5 \pm 0.2	3.4 \pm 0.1
			Sloughed skin	0	-	-	-
	November	305-330	Basale	7	-16.9 \pm 0.3	12.1 \pm 0.7	3 \pm 0
			Externum	6	-17.3 \pm 0.4	11.9 \pm 1.4	3.2 \pm 0.2
			Sloughed skin	0	-	-	-
Galapagos/Peru 1999, 2003	October	285-304	Basale	6	-17.5 \pm 0.3	7.4 \pm 0.7	3.0 \pm 0.1
			Externum	5	-17.8 \pm 0.4	6.8 \pm 0.2	3.2 \pm 0.1
			Sloughed skin	0	-	-	-
	November	305-330	Basale	16	-17.7 \pm 1.3	7.9 \pm 1.0	3.1 \pm 0.1
			Externum	13	-18.5 \pm 1.0	7.1 \pm 1.0	3.2 \pm 0.1
			Sloughed skin	0	-	-	-

APPENDIX VII. SIBER code to estimate SEA_B , SEA_C , and the overlap between ellipses. Code obtained from: <https://github.com/AndrewLJackson/SIBER>

```
#####  
##### SIBER introduction and guide: Estimating  $SEA_B$  and  $SEA_C$  #####  
#####
```

```
knitr::opts_chunk$set(collapse = TRUE, comment = "#>",  
  fig.width = 6, fig.height = 5)
```

```
# Load the viridis package and create a new palette with 3 colours, one for  
# each of the 3 groups we have in this dataset.
```

```
library(viridis)  
palette(viridis(4))
```

```
# This user manual introduces the basic functionality of this standalone version  
# of SIBER, which was previously part of the siar package. SIBER contains two  
# types of analysis, although both are founded on the same principle of fitting  
# ellipses to groups of data. The questions are very different though and it is  
# important that you satisfy yourself with which one you want for the questions  
# you have of your own data. There are additional learning resources available at  
# SIAR-examples-and-queries. N.B. these examples currently still use the SIBER  
# functions embedded within the SIAR package, which I will update shortly, but  
# the concepts are exactly the same.
```

```
# Setting up our R session for this demonstration
```

```
# In this example, we are going to work with a bundled example dataset that  
# I created previously using the function generateSiberData(). This dataset  
# is loaded using data("demo.siber.data") but it is also provided as a raw *.csv  
# file which is more usually the format you would work with when organising  
# your own dataset for analysis using SIBER. We then use createSiberObject()  
# to convert this raw data form into an object that contains information summary  
# statistics that are useful for plotting, and a z-score transformed version of  
# the data which is used in the model fitting process before being back-transformed  
# using the summary statistic information.
```

```
# remove previously loaded items from the current environment and remove previous  
# graphics.
```

```
rm(list=ls())  
graphics.off()
```

APPENDIX VII. SIBER code to estimate SEA_B , SEA_C , and the overlap between ellipses. Code obtained from: <https://github.com/AndrewLJackson/SIBER> (CONTINUES)

```
# Here, I set the seed each time so that the results are comparable.
# This is useful as it means that anyone that runs your code, *should*
# get the same results as you, although random number generators change
# from time to time.

set.seed(1)

library(SIBER)

# load in the included demonstration dataset
data <- read.csv("~/3_TRABAJO_INVESTIGACION/My_R/Tesis_PHD/SIBER_ZONES.csv",header=T)

#
# create the siber object
siber.example <- createSiberObject(data)

# Or if working with your own data read in from a *.csv file, you would use
# This *.csv file is included with this package. To find its location
# type fname <- system.file("extdata", "demo.siber.data.csv", package = "SIBER")
# in your command window. You could load it directly by using the
# returned path, or perhaps better, you could navigate to this folder
# and copy this file to a folder of your own choice, and create a
# script from this vignette to analyse it. This *.csv file provides
# a template for how your own files should be formatted.

# mydata <- read.csv(fname, header=T)
# siber.example <- createSiberObject(mydata)

# Plotting the raw data
#
# With the siber object created, we can now use various functions
# to create isotope biplots of the data, and also calculate some
# summary statistics on each group and/or community in the dataset.
# Community 1 comprises 3 groups and drawn as black, red and green
# circles community 2 comprises 3 groups and drawn as black, red and
# green triangles Various plotting options are collated into lists
# and then passed to the high-level SIBER plotting function
# plotSiberObject which is a wrapper function for easy plotting.
# We will access the more specific plotting functions directly a
```

APPENDIX VII. SIBER code to estimate SEA_B , SEA_C , and the overlap between ellipses. Code obtained from: <https://github.com/AndrewLJackson/SIBER> (CONTINUES)

```
# little later on to create more customised graphics.
# ax.pad determines the padding applied around the extremes of
# the data.
# iso.order is a vector of length 2 specifying which isotope
# should be plotted on the x and y axes.N.B. there is currently a
# problem with the addition of the group ellipses using if you
# deviate from the default of iso.order = c(1,2). This argument
# will be deprecated in a future release, and plotting order will
# be achieved at point of data-entry. I recommond you set up your
# original data with the chemical element you want plotted on the
# x-axis being the first column, and the y-axis in the second.
# Convex hulls are drawn between the centres of each group within a
# community with hulls = T.
# Ellipses are drawn for each group independently with ellipses = T.
# These ellipses can be made to be maximum likelihood standard
# ellipses by setting p = NULL, or can be made to be prediction
# ellipses that contain approximately p proportion of data.
# For example, p = 0.95 will draw an ellipse that encompasses
# approximately 95% of the data. The parameter n determines how
# many points are used to make each ellipse and hence how smooth the
# curves are. Convex hulls are draw around each group
# independently with group.hulls = T. Create lists of plotting
# arguments to be passed onwards to each of the three plotting functions.
```

```
community.hulls.args <- list(col = 1, lty = 1, lwd = 1)
group.ellipses.args <- list(n = 100, p.interval = 0.40, lty = 1, lwd = 2)
group.hull.args <- list(lty = 2, col = "grey20")
```

```
par(mfrow=c(1,1))
plotSiberObject(siber.example,
  ax.pad = 2,
  hulls = F, community.hulls.args,
  ellipses = T, group.ellipses.args,
  group.hulls = T, group.hull.args,
  bty = "L",
  iso.order = c(1,2),
  xlab = expression({delta}^13*C~'\u2030'),
  ylab = expression({delta}^15*N~'\u2030')
)
```

APPENDIX VII. SIBER code to estimate SEA_B , SEA_C , and the overlap between ellipses. Code obtained from: <https://github.com/AndrewLJackson/SIBER> (CONTINUES)

```
# Summary statistics and custom graphic additions

# Although the intention of SIBER is to use Bayesian methods to allow
# us to make statistical comparisons of what are otherwise typically
# point estimates of dispersion within and among communities and
# groups, the basic summary statistics are informative and useful
# for checking that our Bayesian analysis is working as intended. One
# feature of the Standard Ellipse is that it contains approximately
# 40% of the data. SIBER now includes code to scale this ellipse so
# that it contains approximately any % of the data you wish.
# Additionally, the ellipse can be scaled so that it represents
# a % confidence ellipse of the bivariate means
# (rather than of the data). We create the bi-plot again here
# and this time add the additional ellipses overlayed on the basic
# plot that this time omits group hulls and group standard ellipses.

community.hulls.args <- list(col = 1, lty = 1, lwd = 1)
group.ellipses.args <- list(n = 100, p.interval = 0.95, lty = 1, lwd = 2)
group.hull.args <- list(lty = 2, col = "grey20")

# this time we will make the points a bit smaller by
# cex = 0.5

par(mfrow=c(1,1))
plotSiberObject(siber.example,
  ax.pad = 2,
  hulls = F, community.hulls.args,
  ellipses = F, group.ellipses.args,
  group.hulls = F, group.hull.args,
  bty = "L",
  iso.order = c(1,2),
  xlab=expression({delta}^13*C~'\u2030'),
  ylab=expression({delta}^15*N~'\u2030'),
  cex = 0.5
)
```

APPENDIX VII. SIBER code to estimate SEA_B , SEA_C , and the overlap between ellipses. Code obtained from: <https://github.com/AndrewLJackson/SIBER> (CONTINUES)

```
# Calculate summary statistics for each group: TA, SEA and SEAc
group.ML <- groupMetricsML(siber.example)
print(group.ML)
# You can add more ellipses by directly calling plot.group.ellipses()

# Add an additional p.interval % prediction ellipse

plotGroupEllipses(siber.example, n = 100, p.interval = 0.40,
                  lty = 1, lwd = 2)

# or you can add the XX% confidence interval around the bivariate means
# by specifying ci.mean = T along with whatever p.interval you want.

plotGroupEllipses(siber.example, n = 100, p.interval = 0.95, ci.mean = T,
                  lty = 1, lwd = 2)

# Alternatively, we may wish to focus on comparing the two
# communities represented in these plots by the open circles
# and the open triangles. To illustrate these groupings, we might
# draw the convex hull between the means of each of the three groups
# comprising each community. Additionally, I have highlighted the
# location of each group by adding the 95% confidence interval of
# their bivariate mean. A second plot provides information more suitable
# to comparing the two communities based on the community-level
# Layman metrics this time we will make the points a bit smaller by
# cex = 0.5

plotSiberObject(siber.example,
                ax.pad = 2,
                hulls = T, community.hulls.args,
                ellipses = F, group.ellipses.args,
                group.hulls = F, group.hull.args,
                bty = "L",
                iso.order = c(1,2),
                xlab=expression({delta}^13*C~'\u2030'),
                ylab=expression({delta}^15*N~'\u2030'),
                cex = 0.5
                )
```

APPENDIX VII. SIBER code to estimate SEA_B , SEA_C , and the overlap between ellipses. Code obtained from: <https://github.com/AndrewLJackson/SIBER> (CONTINUES)

```
# or you can add the XX% confidence interval around the bivariate  
# means by specifying ci.mean = T along with whatever p.interval you  
# want.
```

```
plotGroupEllipses(siber.example, n = 100, p.interval = 0.95,  
                  ci.mean = T, lty = 1, lwd = 2)
```

```
# Calculate the various Layman metrics on each of the communities.
```

```
community.ML <- communityMetricsML(siber.example)  
print(community.ML)
```

```
# Fitting the Bayesian models to the data  
# Whether your intended analysis is to compare isotopic niche width  
# among groups, or among communities, the initial step is to fit  
# Bayesian multivariate normal distributions to each group in the  
# dataset. The decision as to whether you then want to compare the  
# area of the ellipses among groups, or any / all of the 6 Layman  
# metrics comes later. These multivariate normal distributions are  
# fitted using the jags software run via the package rjags. This  
# method relies on an iterated Gibbs Sampling technique and some  
# information on the length, number and iterations of sampling chains  
# is required. Additionally, the prior distributions for the  
# parameters need to be specified. In SIBER, these are bundled into  
# two list objects: parms which holds the parameters defining how  
# the sampling algorithm is to run; and priors which holds  
# information on the prior distributions of the parameters to be  
# estimated. Typically, the priors are left vague and you should  
# use these same values in your own analysis. Since the data are  
# z-scored internally before the models are fitted to the data, the  
# expected means are inherently close to zero, and the marginal  
# variances close to one. This greatly aids the jags fitting process.
```

```
# After calling siberMVN() you will see output in the command window  
# indicating that the jags models are being fitted, one block of  
# output for each group in your dataset. A subset of these blocks  
# are shown below.
```

APPENDIX VII. SIBER code to estimate SEA_B , SEA_C , and the overlap between ellipses. Code obtained from: <https://github.com/AndrewLJackson/SIBER> (CONTINUES)

```
# options for running jags
parms <- list()
parms$n.iter <- 2 * 10^4 # number of iterations to run the model for
parms$n.burnin <- 1 * 10^3 # discard the first set of values
parms$n.thin <- 10 # thin the posterior by this many
parms$n.chains <- 2 # run this many chains

# define the priors
priors <- list()
priors$R <- 1 * diag(2)
priors$k <- 2
priors$tau.mu <- 1.0E-3

# fit the ellipses which uses an Inverse Wishart prior
# on the covariance matrix Sigma, and a vague normal prior on the
# means. Fitting is via the JAGS method.

ellipses.posterior <- siberMVN(siber.example, parms, priors)

# Comparing among groups using the Standard Ellipse Area
# When comparing individual groups with each other, be it within a
# single community, or groups among communities, the Standard
# Ellipse Area (SEA) is the recommended method. Since the
# multivariate normal distributions have already been fitted to
# each group, it only remains to calculate the SEA on the posterior
# distribution of covariance matrices for each group, thereby
# yielding the Bayesian SEA or SEA-B. We can also use the summary
# statistics we calculated earlier to add the maximum likelihood
# estimates of SEA-c to the Bayesian estimates.

# Plotting is via the function siberDensityPlot() which is
# essentially the same as siardensityplot() from the older
# version of SIAR. Credible intervals can be extracted by calling
# the function hdr from the hrcde package.
```

APPENDIX VII. SIBER code to estimate SEA_B , SEA_C , and the overlap between ellipses. Code obtained from: <https://github.com/AndrewLJackson/SIBER> (CONTINUES)

```
# The posterior estimates of the ellipses for each group can be used
# to calculate the SEA.B for each group.
```

```
SEA.B <- siberEllipses(ellipses.posterior)
```

```
siberDensityPlot(SEA.B, xticklabels = colnames(group.ML),
  xlab = c("Community | Group"),
  ylab = expression("Standard Ellipse Area " ("\"u2030\" ^2) ),
  bty = "L",
  las = 1,
  main = "SIBER ellipses on each group"
)
```

```
OUT <- data.frame(SEA.B)
write.csv(OUT, file = "SEAB.csv")
```

```
# Add red x's for the ML estimated SEA-c
```

```
points(1:ncol(SEA.B), group.ML[3,], col="red", pch = "x", lwd = 2)
```

APPENDIX VIII. MixSIAR model in R, deviance information criteria, summary statistics and model diagnosis.

```
#####
##### SIBER introduction and guide: Overlap #####
#####
```

```
# Fix spatstat bug
```

```
# # install.packages("devtools") # install if necessary
```

```
# devtools::install_github("andrewljackson/SIBER",
```

```
#           build_vingettes = TRUE)
```

```
library(SIBER)
```

```
## ---- echo = FALSE-----
```

```
knitr::opts_chunk$set(collapse = TRUE, comment = "#>",
```

```
  fig.width = 6, fig.height = 5)
```

APPENDIX VII. SIBER code to estimate SEA_B , SEA_C , and the overlap between ellipses. Code obtained from: <https://github.com/AndrewLJackson/SIBER> (CONTINUES)

```
## -----  
# remove previously loaded items from the current environment and remove previous graphics.  
rm(list=ls())  
graphics.off()  
  
# Here, I set the seed each time so that the results are comparable.  
# This is useful as it means that anyone that runs your code, *should*  
# get the same results as you, although random number generators change  
# from time to time.  
set.seed(1)  
  
# load SIBER  
library(SIBER)  
library(viridis)  
  
# set a new three-colour palette from the viridis package  
palette(viridis::viridis(4))  
  
# load in the included demonstration dataset  
data <-  
read.csv("~/3_TRABAJO_INVESTIGACION/My_R/Tesis_PHD/SIBER_Thesis/ZONES/SIBER_ZONES  
.csv",header=T)  
  
#  
# create the siber object  
siber.example <- createSiberObject(data)  
  
# Or if working with your own data read in from a *.csv file, you would use  
# This *.csv file is included with this package. To find its location  
# type  
# fname <- system.file("extdata", "demo.siber.data.csv", package = "SIBER")
```

APPENDIX VII. SIBER code to estimate SEA_B , SEA_C , and the overlap between ellipses. Code obtained from: <https://github.com/AndrewLJackson/SIBER> (CONTINUES)

```
# in your command window. You could load it directly by using the
# returned path, or perhaps better, you could navigate to this folder
# and copy this file to a folder of your own choice, and create a
# script from this vignette to analyse it. This *.csv file provides
# a template for how your own files should be formatted.

# mydata <- read.csv(fname, header=T)
# siber.example <- createSiberObject(mydata)

# Create lists of plotting arguments to be passed onwards to the
# plotting functions. With p.interval = NULL, these are SEA. NB not SEAc though
# which is what we will base our overlap calculations on. This implementation
# needs to be added in a future update. For now, the best way to plot SEAc is to
# add the ellipses manually following the vignette on this topic.
group.ellipses.args <- list(n = 100, p.interval = 0.40, lty = 1, lwd = 2)

par(mfrow=c(1,1))
plotSiberObject(siber.example,
  ax.pad = 2,
  hulls = F, community.hulls.args,
  ellipses = T, group.ellipses.args,
  group.hulls = F, group.hull.args,
  bty = "L",
  iso.order = c(1,2),
  xlab = expression({delta}^13*C~'\u2030'),
  ylab = expression({delta}^15*N~'\u2030')
)
```

APPENDIX VII. SIBER code to estimate SEA_B , SEA_C , and the overlap between ellipses. Code obtained from: <https://github.com/AndrewLJackson/SIBER> (CONTINUES)

```
## ---- MLOverlap-----  
# In this example, I will calculate the overlap between ellipses for groups 2  
# and 3 in community 1 (i.e. the green and yellow open circles of data).  
  
# The first ellipse is referenced using a character string representation where  
# in "x.y", "x" is the community, and "y" is the group within that community.  
# So in this example: community 1, group 2  
ellipse1 <- "1.1"  
  
# Ellipse two is similarly defined: community 1, group3  
ellipse2 <- "1.2"  
  
# The overlap of the maximum likelihood fitted standard ellipses are  
# estimated using  
sea.overlap <- maxLikOverlap(ellipse1, ellipse2, siber.example,  
                             p.interval = 0.40, n = 1000)  
  
# the overlap between the corresponding 95% prediction ellipses is given by:  
ellipse95.overlap <- maxLikOverlap(ellipse1, ellipse2, siber.example,  
                                   p.interval = 0.40, n = 1000)  
  
# so in this case, the overlap as a proportion of the non-overlapping area of  
# the two ellipses, would be  
prop.95.over <- ellipse95.overlap[3] / (ellipse95.overlap[2] +  
                                       ellipse95.overlap[1] -  
                                       ellipse95.overlap[3])
```

APPENDIX VII. SIBER code to estimate SEA_B , SEA_C , and the overlap between ellipses. Code obtained from: <https://github.com/AndrewLJackson/SIBER> (CONTINUES)

```
## ---- bayesOverlap-----
# options for running jags
parms <- list()
parms$n.iter <- 2 * 10^4 # number of iterations to run the model for
parms$n.burnin <- 1 * 10^3 # discard the first set of values
parms$n.thin <- 10 # thin the posterior by this many
parms$n.chains <- 2 # run this many chains

# define the priors
priors <- list()
priors$R <- 1 * diag(2)
priors$k <- 2
priors$tau.mu <- 1.0E-3

# fit the ellipses which uses an Inverse Wishart prior
# on the covariance matrix Sigma, and a vague normal prior on the
# means. Fitting is via the JAGS method.
ellipses.posterior <- siberMVN(siber.example, parms, priors)

# and teh corresponding Bayesian estimates for the overlap between the
# 95% ellipses is given by:
bayes95.overlap <- bayesianOverlap(ellipse1, ellipse2, ellipses.posterior,
                                  draws = 500, p.interval = 0.40, n = 500)

OUT <- data.frame(bayes95.overlap)
write.csv(OUT, file = "ZONES_95.csv")
```

APPENDIX VII. SIBER code to estimate SEA_B , SEA_C , and the overlap between ellipses. Code obtained from: <https://github.com/AndrewLJackson/SIBER> (CONTINUES)

```
# a histogram of the overlap
hist(bayes95.overlap[,3], 10)

# and as above, you can express this a proportion of the non-overlapping area of
# the two ellipses, would be
bayes.prop.95.over <- (bayes95.overlap[,3] / (bayes95.overlap[,2] +
                                     bayes95.overlap[,1] -
                                     bayes95.overlap[,3])
)

hist(bayes.prop.95.over, 10)

OUT <- data.frame(bayes.prop.95.over)
write.csv(OUT, file = "ZONES_95.csv")
```

APPENDIX VIII. MixSIAR model in R, deviance information criteria, summary statistics and model diagnosis.

A) Model in R

```
# source$data_type: means
# source$by_factor: NA
# random effects: 0
# fixed effects: 0
# nested factors:
# factors:
# continuous effects: 0
# error structure: Residual * Process
# source$conc_dep: FALSE

model{
  for(src in 1:n.sources){
    for(iso in 1:n.iso){
      src_mu[src,iso] ~ dnorm(MU_array[src,iso], n_array[src]/SIG2_array[src,iso]); # Eqn 3.8 but with
precision instead of variance
      tmp.X[src,iso] ~ dchisqr(n_array[src]);
      src_tau[src,iso] <- tmp.X[src,iso]/(SIG2_array[src,iso]*(n_array[src] - 1)); # Eqn 3.9, following the
simulation on p.580
    }
  }

# Draw p.global (global proportion means) from an uninformative Dirichlet,
# Then ilr.global is the ILR-transform of p.global
p.global[1:n.sources] ~ ddirch(alpha[1:n.sources]);
for(src in 1:(n.sources-1)){
  gmean[src] <- prod(p.global[1:src])^(1/src);
  ilr.global[src] <- sqrt(src/(src+1))*log(gmean[src]/p.global[src+1]); # page 296, Egozcue 2003
}
```

APPENDIX VIII. MixSIAR model in R, deviance information criteria, summary statistics and model diagnosis. (CONTINUES)

```
# DON'T generate individual deviates from the global/region/pack mean (but keep same model
structure)
for(i in 1:N) {
  for(src in 1:(n.sources-1)) {
    ilr.ind[i,src] <- 0;
    ilr.tot[i,src] <- ilr.global[src] + ilr.ind[i,src]; # add all effects together for each individual (in ilr-
space)
  }
}

# Inverse ILR math (equation 24, page 294, Egozcue 2003)
for(i in 1:N){
  for(j in 1:(n.sources-1)){
    cross[i,,j] <- (e[,j]^ilr.tot[i,j])/sum(e[,j]^ilr.tot[i,j]);
  }
  for(src in 1:n.sources){
    tmp.p[i,src] <- prod(cross[i,src,]);
  }
  for(src in 1:n.sources){
    p.ind[i,src] <- tmp.p[i,src]/sum(tmp.p[i,]);
  }
}

for(src in 1:n.sources) {
  for(i in 1:N){
    # these are weights for variances
    p2[i,src] <- p.ind[i,src]*p.ind[i,src];
  }
}
```

APPENDIX VIII. MixSIAR model in R, deviance information criteria, summary statistics and model diagnosis. (CONTINUES)

```
# For each isotope and population, calculate the predicted mixtures
for(iso in 1:n.iso) {
  for(i in 1:N) {

    mix.mu[iso,i] <- inprod(src_mu[,iso],p.ind[i,]) + inprod(frac_mu[,iso],p.ind[i,]);
  }
}

# Multiplicative residual error
for(iso in 1:n.iso){
  resid.prop[iso] ~ dunif(0,20);
}

# Calculate process variance for each isotope and population
for(iso in 1:n.iso) {
  for(i in 1:N) {

    process.var[iso,i] <- inprod(1/src_tau[,iso],p2[i,]) + inprod(frac_sig2[,iso],p2[i,]);
  }
}

# Construct Sigma, the mixture precision matrix
for(ind in 1:N){
  for(i in 1:n.iso){
    for(j in 1:n.iso){
      Sigma.ind[ind,i,j] <- equals(i,j)/(process.var[i,ind]*resid.prop[i]);
    }
  }
}

# Likelihood
for(i in 1:N) {
  X_iso[i,] ~ dnorm(mix.mu[,i], Sigma.ind[i,,]);
}
}# end model
```

APPENDIX VIII. MixSIAR model in R, deviance information criteria, summary statistics and model diagnosis. (CONTINUES)

b) Deviance information criteria (DIC) and summary statistics

```
#####
```

```
# Summary Statistics
```

```
#####
```

Deviance Information Criteria = 1925.242

	Mean	SD	2.5%	5%	25%	50%	75%	95%	97.5%
p.global.CCS	0.300	0.152	0.018	0.037	0.180	0.317	0.430	0.517	0.529
p.global.CRD	0.165	0.105	0.008	0.016	0.075	0.153	0.246	0.348	0.364
p.global.GC	0.535	0.051	0.451	0.459	0.494	0.530	0.574	0.623	0.633

c) Model diagnosis

```
#####
```

```
# Gelman-Rubin Diagnostic
```

```
#####
```

Generally, the Gelman diagnostic should be < 1.05

Out of 5 variables: 0 > 1.01

0 > 1.05

0 > 1.1

The worst variables are:

	Point est.	Upper C.I.
p.global[2]	1.0009415	1.0046040
p.global[1]	1.0008949	1.0044371
p.global[3]	1.0007618	1.0036784
resid.prop	1.0003020	1.0022550
deviance	0.9996427	0.9997924

APPENDIX VIII. MixSIAR model in R, deviance information criteria, summary statistics and model diagnosis. (CONTINUES)

And here are the Gelman diagnostics for all variables:

	Point est.	Upper C.I.
deviance	0.9996427	0.9997924
p.global[1]	1.0008949	1.0044371
p.global[2]	1.0009415	1.0046040
p.global[3]	1.0007618	1.0036784
resid.prop	1.0003020	1.0022550

```
#####  
# Geweke Diagnostic  
#####
```

The Geweke diagnostic is a standard z-score, so we'd expect 5% to be outside +/-1.96
Number of variables outside +/-1.96 in each chain (out of 5):

	Chain 1	Chain 2	Chain 3
Geweke	4	4	1

And here are the Geweke diagnostics for all variables:

	chain1	chain2	chain3
deviance	-0.251	0.992	0.362
p.global[1]	-3.539	2.078	1.116
p.global[2]	3.586	-1.987	-1.214
p.global[3]	3.311	-2.260	-0.916
resid.prop	-2.481	2.426	2.007

APPENDIX IX. MixSIAR model assuming a $\Delta^{15}\text{N}:1.9\pm0.3\text{‰}$, deviance information criteria, summary statistics and model diagnosis.

```
#####
# Summary Statistics
#####
```

Deviance information criteria = 1925.123

	Mean	SD	2.5%	5%	25%	50%	75%	95%	97.5%
p.global.CCS	0.344	0.173	0.024	0.044	0.205	0.358	0.497	0.590	0.604
p.global.CRD	0.184	0.121	0.007	0.014	0.080	0.174	0.283	0.393	0.415
p.global.GC	0.471	0.056	0.380	0.389	0.425	0.466	0.514	0.570	0.580

```
#####
# Gelman-Rubin Diagnostic
#####
```

Generally the Gelman diagnostic should be < 1.05

Out of 5 variables: 0 > 1.01; 0 > 1.05; 0 > 1.1

The worst variables are:

	Point est.	Upper C.I.
p.global[3]	1.001764	1.005531
p.global[1]	1.001652	1.005015
p.global[2]	1.001439	1.004537
deviance	1.000796	1.004160
resid.prop	1.000155	1.001373

And here are the Gelman diagnostics for all variables:

	Point est.	Upper C.I.
deviance	1.000796	1.004160
p.global[1]	1.001652	1.005015
p.global[2]	1.001439	1.004537
p.global[3]	1.001764	1.005531
resid.prop	1.000155	1.001373

```
#####  
# Geweke Diagnostic  
#####
```

The Geweke diagnostic is a standard z-score, so we'd expect 5% to be outside +/-1.96
Number of variables outside +/-1.96 in each chain (out of 5):

	Chain 1	Chain 2	Chain 3
Geweke	0	0	0

And here are the Geweke diagnostics for all variables:

	chain1	chain2	chain3
deviance	0.820	0.587	-0.610
p.global[1]	0.637	-0.542	1.632
p.global[2]	-0.649	0.586	-1.557
p.global[3]	-0.628	0.471	-1.789
resid.prop	0.918	-0.070	1.853

APPENDIX X. Thesis achievements:

RESEARCH ARTICLE

Estimating blue whale skin isotopic incorporation rates and baleen growth rates: Implications for assessing diet and movement patterns in mysticetes

Geraldine Busquets-Vass¹, Seth D. Newsome², John Calambokidis³, Gabriela Serra-Valente⁴, Jeff K. Jacobsen⁵, Sergio Aguíñiga-García¹, Diane Gendron^{1*}

1 Instituto Politécnico Nacional, Centro Interdisciplinario de Ciencias Marinas, La Paz, Baja California Sur, Mexico, **2** Biology Department, University of New Mexico, Albuquerque, New Mexico, United States of America, **3** Cascadia Research Collective, Olympia, Washington, United States of America, **4** Marine Mammal and Turtle Division, Southwest Fisheries Science Center, National Marine Fisheries Service, National Oceanic and Atmospheric Administration, La Jolla, California, United States of America, **5** Vertebrate Museum, Department of Biological Sciences, Humboldt State University, Arcata, California, United States of America

* dianegendroncicimar@gmail.com



OPEN ACCESS

Citation: Busquets-Vass G, Newsome SD, Calambokidis J, Serra-Valente G, Jacobsen JK, Aguíñiga-García S, et al. (2017) Estimating blue whale skin isotopic incorporation rates and baleen growth rates: Implications for assessing diet and movement patterns in mysticetes. PLoS ONE 12 (5): e0177880. <https://doi.org/10.1371/journal.pone.0177880>

Editor: Mark S. Boyce, University of Alberta, CANADA

Received: January 16, 2017

Accepted: May 4, 2017

Published: May 31, 2017

Copyright: This is an open access article, free of all copyright, and may be freely reproduced, distributed, transmitted, modified, built upon, or otherwise used by anyone for any lawful purpose. The work is made available under the [Creative Commons CC0](https://creativecommons.org/licenses/by/4.0/) public domain dedication.

Data Availability Statement: All relevant data are within the paper and its Supporting Information files.

Funding: The authors received financial support from Instituto Politécnico Nacional: SIP: 20130223; 20140495; 20150115; 20160496 (<http://www.ipn.mx/Paginas/inicio.aspx>) and the University of New Mexico Center for Stable Isotopes (Albuquerque, NM; <http://csi.unm.edu/>). GBV received a PhD

Abstract

Stable isotope analysis in mysticete skin and baleen plates has been repeatedly used to assess diet and movement patterns. Accurate interpretation of isotope data depends on understanding isotopic incorporation rates for metabolically active tissues and growth rates for metabolically inert tissues. The aim of this research was to estimate isotopic incorporation rates in blue whale skin and baleen growth rates by using natural gradients in baseline isotope values between oceanic regions. Nitrogen ($\delta^{15}\text{N}$) and carbon ($\delta^{13}\text{C}$) isotope values of blue whale skin and potential prey were analyzed from three foraging zones (Gulf of California, California Current System, and Costa Rica Dome) in the northeast Pacific from 1996–2015. We also measured $\delta^{15}\text{N}$ and $\delta^{13}\text{C}$ values along the lengths of baleen plates collected from six blue whales stranded in the 1980s and 2000s. Skin was separated into three strata: basale, externum, and sloughed skin. A mean (\pm SD) skin isotopic incorporation rate of 163 ± 91 days was estimated by fitting a generalized additive model of the seasonal trend in $\delta^{15}\text{N}$ values of skin strata collected in the Gulf of California and the California Current System. A mean (\pm SD) baleen growth rate of 15.5 ± 2.2 cm y^{-1} was estimated by using seasonal oscillations in $\delta^{15}\text{N}$ values from three whales. These oscillations also showed that individual whales have a high fidelity to distinct foraging zones in the northeast Pacific across years. The absence of oscillations in $\delta^{15}\text{N}$ values of baleen sub-samples from three male whales suggests these individuals remained within a specific zone for several years prior to death. $\delta^{13}\text{C}$ values of both whale tissues (skin and baleen) and potential prey were not distinct among foraging zones. Our results highlight the importance of considering tissue isotopic incorporation and growth rates when studying migratory mysticetes and provide new insights into the individual movement strategies of blue whales.

grant from the Consejo Nacional de Ciencia y Tecnología (CONACYT; <http://www.conacyt.mx/>), a research grant from Cetacean Society International (<http://www.csiwhalesalive.org/index.php>) specifically for processing the baleen plates, and a grant from American Cetacean Society - Monterey Bay (<http://acsonline.org/>) to process skin samples. The funders had no role in study design, data collection and analysis, decision to publish, or preparation of the manuscript.

Competing interests: The authors have declared that no competing interests exist.

Introduction

The blue whale (*Balenoptera musculus*) in the northeast Pacific is an endangered migratory mysticete [1]. In summer and fall, blue whales are distributed as far north as the Gulf of Alaska [2,3], but the highest aggregations have been observed off southern California [4]. By mid-fall (~October), they usually migrate south to the west coast of the Baja California Peninsula [2,4–8] and then continue migrating to one of two regions that are recognized as overwintering zones: a calving ground in the Gulf of California [2,9–12], or the Costa Rica Dome in the eastern tropical Pacific [2,7,8]. Calves have also been observed in the Costa Rica Dome, but little is known about the population dynamics in this zone [13].

Blue whales forage throughout their annual migratory cycle mainly on aggregations of krill (Order: Euphausiacea) [14–18] and occasionally on other crustaceans (*i.e.* copepods, *Calanus spp.*) [16,19] or small fish (*i.e.* lanternfish: Family Myctophidae) [20]. The observation that blue whales forage year-round suggests this species has high energetic demands relative to other migratory mysticetes like the humpback whale (*Megaptera novaeangliae*) and the gray whale (*Eschrichtius robustus*), that typically fast for months during their breeding season in low latitudes [21,22]. The general migratory patterns of blue whales in the northeast Pacific have been described [2,3,5,7,10,11,23], specifically for the California feeding population [3]; however, there are still many gaps in our understanding of their feeding ecology and plasticity in individual movement patterns across multi-year timescales.

Stable isotope analysis (SIA) is a proven tool for studying the diet and movement patterns of marine mammals [24]. The isotopic composition of animal tissues are influenced by diet [25–27] and the isotopic composition of the base of the food web, which can vary in time and space within and among oceanic ecosystems [24,28–31]. Physiological processes produce predictable offsets in isotope values between consumers and their diet, which is often called trophic discrimination [24,32]. In general, consumer tissues have carbon ($\delta^{13}\text{C}$) and nitrogen ($\delta^{15}\text{N}$) isotope values that are 0.5–3.0‰ and 2–5‰ higher than that of their prey respectively, depending on the species, diet quality, and type of tissue analyzed [24–26,33,34].

Tissues assimilate dietary inputs at different temporal scales. Most metabolically active tissues reflect recent dietary inputs, consumed within days to months (*e.g.* plasma, muscle), depending on their isotopic incorporation rates that typically scale with body mass such that larger animals have slower incorporation rates [35]. In contrast, metabolically inert tissues (*e.g.* whiskers, nails) deposit at distinct intervals, and each deposition of tissue retains the isotopic composition of dietary sources incorporated when anabolized, thus reflecting dietary input over several years depending on tissue growth rate [24,36]. Consequently, to make accurate inferences on ecological aspects of free ranging animals by using SIA it is essential to have information on the isotopic incorporation rate of metabolically active tissues and the growth rates of metabolically inert tissues; otherwise, the interpretation of the data can be highly misleading.

SIA of mysticete skin and baleen plates has frequently been used to infer diet and seasonal movements of this difficult to study group of cetaceans [37–44]. Cetacean skin (epidermis) is a metabolically active tissue, subdivided into cellular strata: the stratum basale, the stratum spinosum, and the stratum externum [45,46]. Skin growth begins in the stratum basale a single row of cells that replicate actively. Newly formed cells constantly displace the older cells upward, first to the stratum spinosum, and subsequently to the stratum externum, the outermost layer of skin. Finally, the stratum externum is sloughed off to the environment as sloughed skin [45]. Variation in the isotopic composition among these strata has never been described for any cetacean species. The isotopic incorporation rates of cetacean skin have only been measured in controlled “diet switch” feeding experiments on captive odontocetes [47,48]. These studies used exponential fit models because theoretically, after diet switch, changes in the

isotopic composition of tissues will follow an exponential curve over time [49–52]. Estimates of the isotopic incorporation for carbon ($\delta^{13}\text{C}$) and nitrogen ($\delta^{15}\text{N}$) in odontocete skin slightly differ; incorporation for $\delta^{13}\text{C}$ is 2 to 3 months, while that for $\delta^{15}\text{N}$ is longer and more variable at 2 to 6 months [47,48]. The increasing use of SIA in mysticetes to characterize diet and movement patterns requires the development of a method to estimate skin isotopic incorporation rates for free-ranging populations.

Baleen consists of a series of keratin plates inserted in the upper gum of mysticetes that functions as a filter-feeding apparatus [53]. In contrast to skin, baleen is a metabolically inert tissue that grows continuously from the gums and abrades at the terminal end [54]. The oscillations in isotope values along the length of baleen plates can be used to estimate growth rates and generate multi-year records of individual movement strategies, habitat use, and diet [38,42–44,55–57]. Baleen growth rates have been estimated in several species of mysticetes [37,42–44,55,57], but currently there are no published estimates for blue whale baleen.

Potential prey of blue whales in their distinct summer–fall (California Current System: west coast of U.S. and Baja California Peninsula; Fig 1) and winter–spring (Gulf of California and Costa Rica Dome; Fig 1) foraging zones have contrasting isotope values [58–64] due to differences in oceanographic and biogeochemical processes that influence baseline isotope values in these zones [31,58,62,65]. Specifically, $\delta^{15}\text{N}$ values of prey (*e.g.* krill) are higher in the Gulf of California, intermediate in the California Current System, and lowest in the Costa Rica Dome [58–64]. We assumed that blue whale skin strata (stratum basale, stratum externum, and sloughed skin) and baleen plates record these isotopic differences. Then, we evaluated if the seasonal patterns of tissue isotope values could be used to estimate the isotopic incorporation rates and baleen growth rates of blue whale skin and baleen, respectively. We also assessed if carbon isotopes were useful for examining blue whale diet and movement patterns in the northeast Pacific, however, we expected little variation in $\delta^{13}\text{C}$ values of prey among foraging zones based on previous studies [58–64]. Overall, our results highlight the importance of carefully considering the temporal window represented by metabolically active and inert tissues when studying migratory mysticetes.

Materials and methods

Ethic statement

All whale tissues used in this study were collected and processed under special permits issued by the Secretaría de Medio Ambiente y Recursos Naturales (SEMARNAT) in México (codes: 180796-213-03, 071197-213-03, DOO 750-00444/99, DOO.0-0095, DOO 02.-8318, SGPA/DGVS-7000, 00624, 01641, 00560, 12057, 08021, 00506, 08796, 09760, 10646, 00251, 00807, 05036, 01110; 00987; CITES export permit: MX 71395), and the National Oceanic and Atmospheric Administration–National Marine Fisheries Service (NOAA/NMFS) (NMFS MMPA/Research permits codes: NMFS-873; 1026; 774-1427; 774-1714; 14097; 16111; CITES import permit: 14US774223/9) in the United States of America. All tissues were collected using non-lethal sampling techniques.

Sample collection

Blue whale skin biopsies ($n = 255$) and sloughed skin ($n = 174$) were selected from tissue banks at NOAA Southwest Fisheries Science Center (NOAA-SWFSC), Cascadia Research Collective (CRC), and Centro Interdisciplinario de Ciencias Marinas-Instituto Politecnico Nacional (CICIMAR-IPN). These samples were collected from 1996–2015 in the Gulf of California (GC) (Jan–Apr; $n = 115$ biopsies, $n = 81$ sloughed skin; Fig 1), California Current System (CCS) (Jun–Dec; $n = 129$ biopsies, $n = 93$ sloughed skin; Fig 1) and the Costa Rica Dome

(CRD) (Oct–Nov; $n = 11$ biopsies; Fig 1). Skin samples were collected during marine mammal surveys conducted by NOAA-SWFSC, CRC, and CICIMAR-IPN. Skin biopsies were collected via dart sampling methods [66], and sloughed skin was directly collected from the water with a net [67] or from suction cups of satellite-tagged whales.

Krill ($n = 34$) and lanternfish ($n = 7$) samples were opportunistically collected during marine mammal surveys conducted by CICIMAR-IPN within the GC (2005–2015). Krill samples were collected by towing a conical net (diameter 50 cm., mesh size 200 μm) when blue

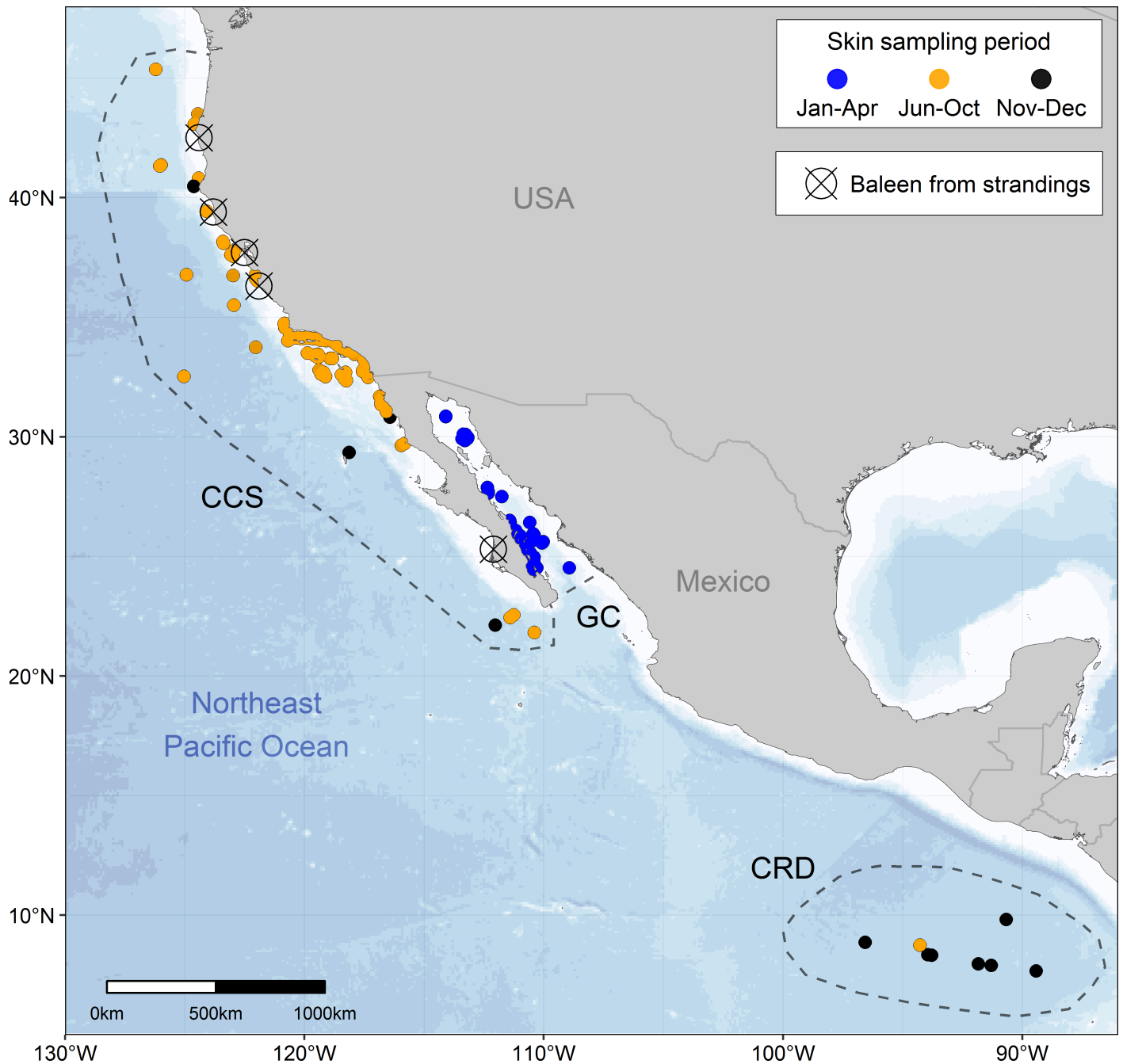


Fig 1. Northeast Pacific sampling zones. Dots represent blue whale skin samples collected in the California Current System (CCS), Gulf of California (GC) and Costa Rica Dome (CRD). Dots with a cross represent blue whale baleen plates collected from dead stranded whales.

<https://doi.org/10.1371/journal.pone.0177880.g001>

whales were observed feeding near the surface. Lanternfish samples were collected with a fishing net (mesh size 5 mm), when aggregations were found near the surface. Prey samples were preserved frozen in liquid nitrogen (-195°C). The assignment of lanternfish to the Family Myctophidae and classification of krill species was made using identification guides [68,69]; *Nyctiphanes simplex* was the only krill species present in all samples.

To assess the isotope variability between blue whale skin strata it was necessary to identify tissue structure. Histological preparations of five skin biopsies were stained with hematoxylin & eosin following the protocol of Sheehan and Hrapchak [70]. Based on these preparations the skin biopsy was divided into two strata: (1) stratum basale, closest to the blubber, and (2) stratum externum, the outermost layer that easily separated from the stratum spinosum (Fig 2A). We did not include stratum spinosum in our analysis because we assumed it would exhibit intermediate isotope values between the stratum basale and the stratum externum. Some skin biopsy samples were incomplete as they had been used for previous studies, and only one of the two strata were available. Sloughed skin samples were also included in the analysis, but were only available for some years (S1 Dataset).

Baleen plates collected from six dead stranded blue whales were obtained from Humboldt State University Vertebrate Museum (HSU-VM), CICIMAR-IPN, the California Department of Parks and Recreation-Prairie Creek Redwoods State Park (CDPR-PCRSP), and the Oregon Marine Mammal Stranding Network (OMMSN) (S1 Table). Stranding reports including sex identification were available for all but one individual, which was determined at NOAA-SWFSC using genetic methods [71,72].

Standardizing blue whale skin sample preparation

Numerous studies show that two factors that are unrelated to ecology can alter isotope values of metabolically active tissues. The first factor is tissue lipid content. Lipids have lower $\delta^{13}\text{C}$ values than associated carbohydrates and proteins [24,73,74]. Thus, the potential influence of lipid content on bulk tissue $\delta^{13}\text{C}$ values must be considered when using SIA to make ecological inferences [24,75,76]. Chemical lipid-extraction removes the influence of lipids on bulk tissues, but a side effect of this procedure is that it may affect $\delta^{15}\text{N}$ values of tissues [75,76]. To evaluate the effect of lipid-extraction on the isotope values of blue whale skin, five skin samples were divided into two subsamples, one subsample was lipid-extracted with three ~24 hour soaks in a 2:1 chloroform:methanol solvent solution, rinsed with ionized water and lyophilized. The second subsample was simply lyophilized, and analyzed as bulk tissue.

The second factor that can alter tissue isotopic composition is how samples are preserved prior to isotopic analysis. Ideally, all tissues would be stored frozen since freezing does not alter isotope values [24,77–79]. Most of the skin samples selected for this study were stored frozen prior to isotope analysis, but some ($n = 100$) were stored in a 20% salt saturated solution of dimethyl sulfoxide (DMSO). Previous studies have shown that the effect of DMSO on the isotope values of tissues can be removed via lipid-extraction [76,80,81]. To determine if this strategy would work for blue whale skin samples preserved in DMSO, we selected 25 sloughed skin samples from the GC (2005–2007). During field collection, each of these skin samples were divided into two sections and preserved one of two ways for one year before they were prepared for isotope analysis: the first set was preserved in DMSO and the second (control) set was frozen in liquid nitrogen (-195°C).

Stable isotope analysis

All skin and prey samples were lipid-extracted, lyophilized, and homogenized by grinding them into a fine powder; as noted above the small set of subsamples that were analyzed to test

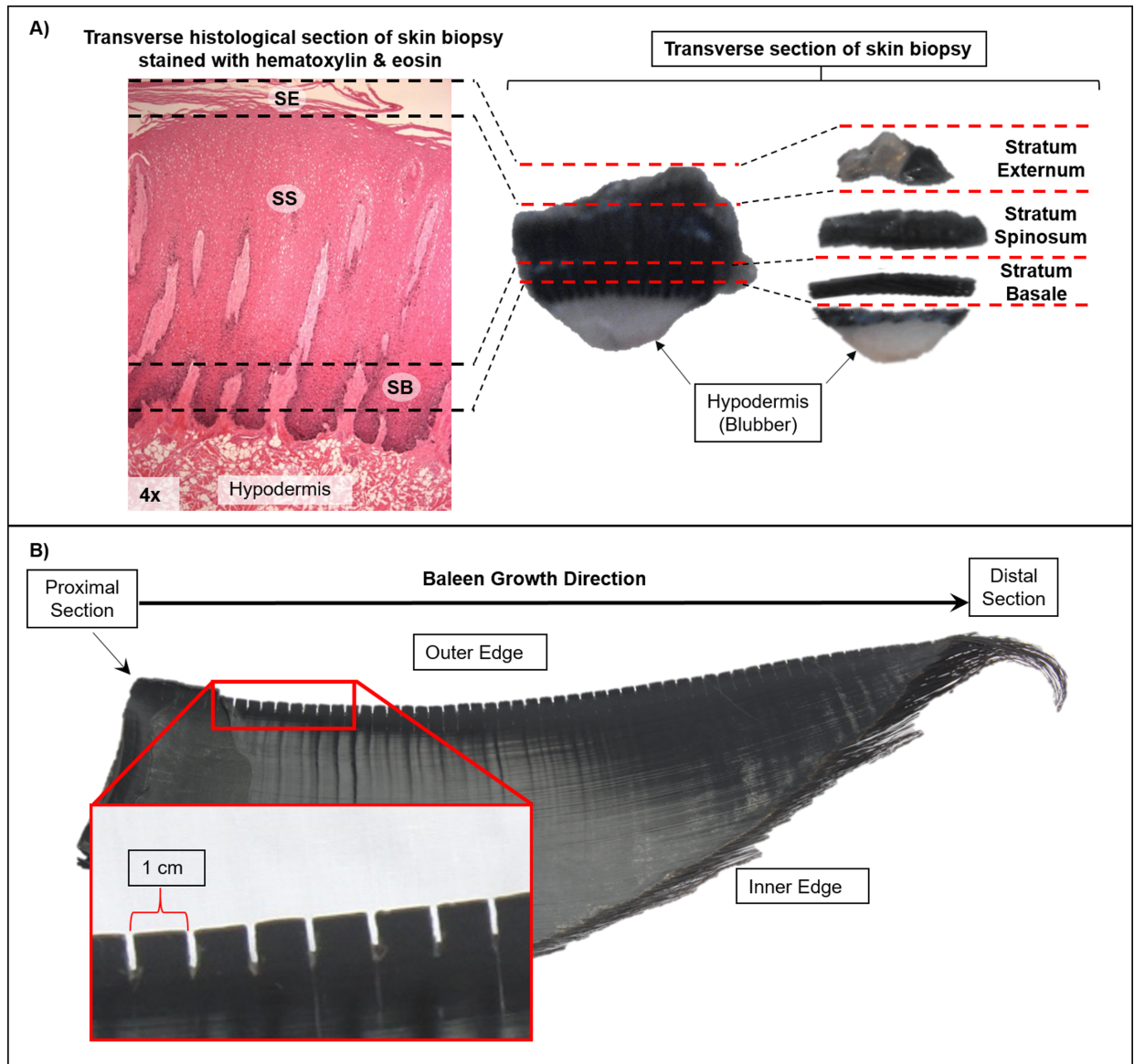


Fig 2. Methods for blue whale skin and baleen plate preparation. (A) Biopsy skin separation into strata: Stratum Basale (SB), Stratum Spinosum (SS) Stratum Externum (SE). The dermal papillae (DP) can be observed embedded in the skin. Dashed lines show where the cuts were made to separate the skin into strata. (B) Blue whale baleen plate sampling: baleen powder was sub-sampled in 1 cm intervals along the outer edge of the plate starting from the proximal section of the plate nearest the gum.

<https://doi.org/10.1371/journal.pone.0177880.g002>

the effects of lipid-extraction were not lipid-extracted (bulk tissue). Baleen plates were cleaned with a solution of 2:1 chloroform:methanol to remove surface contaminants. Sub-samples of keratin powder were collected with a Dremel rotatory drill fitted to a flexible engraving shaft at 1 cm intervals along the outer edge of each baleen, starting at the proximal section inserted in the gum (which represents the newest tissue) (Fig 2B). Baleen grows uniformly on the transverse perspective at a constant (but unknown) rate; thus our sampling strategy would yield equal time intervals between adjacent sub-samples [37,42–44,55,57,82]. Previous studies have confirmed the consistency of isotope values along the length of two adjacent baleen plates of a gray whale (*Eschrichtius robustus*) [82] and two plates from opposing sides of the mouth of a

bowhead whale (*Balaena mysticetus*) [43]. Consequently, we assumed that each baleen provides a consistent record of the past foraging history for each blue whale. Lastly, we compiled $\delta^{13}\text{C}$ and $\delta^{15}\text{N}$ data from the literature of blue whale prey from foraging zones in the northeast Pacific (S2 Table).

Approximately 0.5–0.6 mg of each tissue sample (dried skin, baleen, and prey) was weighed into a tin capsule. Carbon ($\delta^{13}\text{C}$) and nitrogen ($\delta^{15}\text{N}$) isotope values were measured with a Costech 4010 elemental analyzer coupled to Thermo Scientific Delta V isotope ratio mass spectrometer at the Center for Stable Isotopes at the University of New Mexico (Albuquerque, NM). Isotope data are reported as delta δ values, $\delta^{13}\text{C}$ or $\delta^{15}\text{N} = 1000 [(R_{\text{sample}} / R_{\text{standard}}) - 1]$, where $R = {}^{13}\text{C}/{}^{12}\text{C}$ or ${}^{15}\text{N}/{}^{14}\text{N}$ ratio of sample and standard [83]. Values are in units of parts per thousand or per mil (‰) and the internationally accepted standards are atmospheric N_2 for $\delta^{15}\text{N}$ and Vienna-Pee Dee Belemnite limestone (V-PDB) for $\delta^{13}\text{C}$ [83]. Within-run analytical precision was estimated via analysis of two proteinaceous internal reference materials, which was $\pm 0.2\text{‰}$ for both $\delta^{13}\text{C}$ and $\delta^{15}\text{N}$ values. We also measured the weight percent carbon and nitrogen concentration of each sample and used the C/N ratio as a proxy of lipid content [84].

Statistical analysis

All statistical analyses were performed using R [85]. The effects of preservation (DMSO-lipid extracted vs frozen-lipid extracted) and the different treatments (lipid-removal vs bulk tissue) on skin $\delta^{13}\text{C}$, $\delta^{15}\text{N}$ and C/N ratios were evaluated with a max- t test for multiple comparisons of means. This procedure was chosen because it is designed to work in scenarios of unbalanced group sizes, non-normality and heteroscedasticity [86]. The isotopic variability between skin strata (basale, externum, sloughed skin) was also evaluated by using the max- t test, which has a higher power to detect differences between group means compared to other methods [86]. These analyses were performed separately for each zone (GC and CCS) and isotope ($\delta^{13}\text{C}$ or $\delta^{15}\text{N}$). The CRD skin isotope values were excluded from this analysis as sloughed skin samples were not available for this zone.

The prey data were used to establish the reference mean ($\pm\text{SD}$) baseline isotope values within each zone, hereafter called the prey zone mean, which was estimated by pooling the means and variances of all the data. The pooled prey zone mean for the GC included lanternfish and the krill species *Nyctiphanes simplex*, because molecular analysis of fecal samples has shown that blue whales forage only on combined aggregations of both taxonomic groups in this zone [14,20]. Lanternfish was the only teleost fish present in blue whale fecal samples [20]. In the CCS, we included isotope values of its main prey, the krill species *Thysanoessa spinifera* and *Euphausia pacifica* [15,18]. In the CRD, diving behavior and the presence of whale fecal samples confirmed that blue whales forage on patches of krill [17], however, the species of krill was not identified, so we used previously reported data for krill in this zone [62].

Our approach to estimate the blue whale skin isotopic incorporation rate was to mimic a diet switch in controlled feeding experiments, but at population level (sampling the same individual whale across its annual migratory cycle is logistically impossible). Blue whales in the northeast Pacific are ideal for this approach because they feed year-round and seasonally migrate between zones that have distinct baseline isotope values [28,31,58,62,64,87]. To achieve this, first we evaluated if blue whale skin $\delta^{13}\text{C}$ and $\delta^{15}\text{N}$ values exhibited seasonal trends in the GC (Jan-Apr) and the CCS (Jun-Dec). Sampling effort within each zone was not homogeneous for all years, thus blue whale skin samples collected in different years were integrated into a single analysis. We assessed the seasonal trend by fitting a generalized additive model (GAM) of the skin $\delta^{15}\text{N}$ and $\delta^{13}\text{C}$ values as functions of time (Julian day, which ranges from 1 to 365). This was done separately for each skin stratum (basale, externum, and sloughed

skin) in both foraging zones (GC and CCS). We used GAMs because they are especially useful when the functional form of the relationship between the response (e.g. $\delta^{15}\text{N}$ and $\delta^{13}\text{C}$ values) and explanatory variables (e.g. time) is unknown [88]. GAMs were fitted using the “mgcv” package in R [85,89]. To model the main trend of the data, the smoothing parameters (degrees of freedom) were set to three. This conservative approach can be applied when sample size is low [90]. Blue whale skin strata $\delta^{13}\text{C}$ did not show seasonal trends (see Results and S1 Fig), therefore, the isotopic incorporation rate was only estimated for skin $\delta^{15}\text{N}$.

To compare the $\delta^{15}\text{N}$ values of the three skin strata to potential prey, we assumed a trophic discrimination factor ($\Delta^{15}\text{N}$) of 1.6‰, based on controlled feeding experiments on captive bottlenose dolphins (*Tursiops truncatus*) [47,48], and calculated the trophic-corrected mean blue whale skin values for each zone by adding this trophic discrimination factor to the prey zone mean values. These trophic-corrected skin values would represent the expected mean $\delta^{15}\text{N}$ values if blue whale skin had fully equilibrated with that of local prey (or reached steady-state isotopic equilibrium), and we assumed that this method would allow us to assign any given blue whale skin isotope value to a specific foraging zone.

Based on the gradient in the prey mean isotope values for each foraging zone (GC>CCS>CRD; S2 Table), and the trophic-corrected blue whale skin values (see Results), our hypothesis was that blue whales would arrive to the GC with lower skin $\delta^{15}\text{N}$ values due to consumption of prey in the CCS and CRD. Skin isotope values would then increase throughout the winter season as they equilibrate with local prey (see Results). In contrast, most whales would arrive in the CCS with higher skin isotope values, except for individuals that migrated from the CRD. Thus, we predicted that skin isotope values would decrease throughout the summer season as skin isotopically equilibrated with the local prey in the CCS. Therefore, we used the GAMs seasonal predictions to estimate the isotopic incorporation rate for each skin stratum, as the days that it would take for the skin $\delta^{15}\text{N}$ to increase (GC) or decrease (CCS) by the assumed trophic discrimination factor ($\Delta^{15}\text{N} = 1.6\text{‰}$) to reach isotopic equilibrium with the local diet. This period was derived by extrapolating from the distance between the predicted extremes in $\delta^{15}\text{N}$ for each stratum, from the lowest to the highest in the GC and vice versa for the CCS (S3 Table, S2 Fig). In this case, we assumed that the equivalent to the diet switch stage would be the lowest initial $\delta^{15}\text{N}$ value within the GC and the highest initial $\delta^{15}\text{N}$ value in the CCS (S2 Fig). We used the same method with the 95% upper and lower confidence intervals to assess uncertainty (S3 Table, S2 Fig). Unfortunately, the uncertainty associated to individual variability in isotopic incorporation rates given the potential variation in individual arrival and departure times to/from the GC and CCS, could not be considered in the model.

Due to sample size limitations, we had to integrate all the skin data collected in different years into a single seasonal model to estimate blue whale $\delta^{15}\text{N}$ isotopic incorporation rate. This assumes that the relative difference in prey $\delta^{15}\text{N}$ values between foraging zones is consistent across years, which has been suggested in previous studies [58,91]. We evaluated this assumption by fitting a generalized linear model (GLM) of skin $\delta^{15}\text{N}$ values as a function of time (Julian Date, or date of sample collection). Julian Dates are a continuous count of days based on a standard starting point, which we chose as January 1, 1970 (Universal Time, Coordinated). This analysis was made separately for each foraging zone (GC, CCS and CRD) by using all skin strata, which allowed us to evaluate the trends in skin $\delta^{15}\text{N}$ across years in each zone. The GLMs were fitted by using the “glm” function in R [92].

Oscillations in $\delta^{13}\text{C}$ and $\delta^{15}\text{N}$ values of baleen plates were also evaluated with a GAM model and smoothing parameters were selected by standard data-driven methods for time series using Akaike Information Criteria [93,94]. Similar to skin, baleen $\delta^{13}\text{C}$ values were not distinct among foraging zones (see Results and S3 Fig), consequently growth rates were estimated using $\delta^{15}\text{N}$ values. Blue whale baleen growth rate was determined by assuming that the

oscillation in $\delta^{15}\text{N}$ values along the total length of the outer edge of the baleen plates represent the annual movement between winter/spring and summer/fall foraging grounds. Thus, the distance between two sequential $\delta^{15}\text{N}$ minimums represents the growth of the baleen plate during a single year [37,42–44,55]. Additionally, to characterize the movement of whales among isotopically distinct foraging zones, we compared baleen $\delta^{15}\text{N}$ values with the trophic-corrected $\delta^{15}\text{N}$ values for each foraging zone based on the same $\Delta^{15}\text{N}$ used in the skin analysis [47,48].

Results

Blue whale skin isotope values are available in [S1 Dataset](#). The max-*t* test results comparing the effect of different treatments (bulk tissue vs lipid-extracted; frozen vs DMSO) on skin $\delta^{15}\text{N}$, $\delta^{13}\text{C}$ and C/N ratios are presented in [S4 Table](#). Lipid-extracted skin (-16.5 ± 0.1) had mean $\delta^{13}\text{C}$ values that were significantly higher (1.9‰) than bulk skin samples (-18.4 ± 0.4 ; $t = -10.4$, $p < 0.001$), and the weight percent C/N ratios of bulk skin were significantly higher (4.2 ± 0.1) than lipid extracted samples (3.2 ± 0.0 ; $t = 12.9$, $p < 0.001$). In contrast, skin $\delta^{15}\text{N}$ values did not differ significantly between lipid-extracted (14.6 ± 0.3) and bulk skin (14.5 ± 0.3 ; $t = -0.4$, $p = 0.7$). Lastly, $\delta^{15}\text{N}$, $\delta^{13}\text{C}$, and C/N ratios of skin samples stored in DMSO ($\delta^{15}\text{N}$: 13.9 ± 0.9 ; $\delta^{13}\text{C}$: -16.9 ± 0.5 ; C/N: 3.0 ± 0.2) did not differ significantly from skin stored frozen ($\delta^{15}\text{N}$: 14.0 ± 0.9 ; $\delta^{13}\text{C}$: -16.9 ± 0.6 ; C/N: 3.0 ± 0.2); $\delta^{15}\text{N}$: $t = 0.2$, $p = 0.8$; $\delta^{13}\text{C}$: $t = 0.2$, $p = 0.8$; C/N: $t = -0.4$, $p = 0.7$.

The max-*t* test results comparing the $\delta^{15}\text{N}$ and $\delta^{13}\text{C}$ values among skin strata (basale, externum and sloughed skin) in each zone (GC and CCS) are shown in [S5 Table](#). Skin $\delta^{15}\text{N}$ and $\delta^{13}\text{C}$ did not differ significantly between different skin strata within the GC ([S5 Table](#)). In the CCS, mean $\delta^{15}\text{N}$ values of sloughed skin ($13.6\pm 0.7\text{‰}$) and stratum externum ($13.4\pm 1.1\text{‰}$) did not differ significantly ($t = -0.4$, $p = 0.7$), and both of these strata had slightly but significantly higher $\delta^{15}\text{N}$ (stratum externum: $t = 2.6$, $p < 0.001$; sloughed skin: $t = -4.9$, $p < 0.001$) than the stratum basale ($13.0\pm 0.8\text{‰}$). $\delta^{13}\text{C}$ values did not differ significantly among strata in the CCS ([S5 Table](#)).

The GLM model of blue whale skin $\delta^{15}\text{N}$ values as a function of time (Julian Date) was not significant in the CRD (1999–2003; [S6 Table](#), [S4 Fig](#)). Conversely, the relationship between these variables was significant and positive in the GC and the CCS ([S6 Table](#), [S4 Fig](#)). The GLM model predicts an overall increase of 1.2‰ over 15 years (1996–2011) in the CCS, and an increase of 0.8‰ over 13 years (2002–2015) in the GC ([S6 Table](#), [S4 Fig](#)); overall, these shifts result in a 0.1‰ increase per year in each zone. Thus, skin $\delta^{15}\text{N}$ values showed a slight and consistent trend in both zones, therefore the gradient in $\delta^{15}\text{N}$ values between zones would also remain constant. This result would validate the integration of blue whale skin $\delta^{15}\text{N}$ values in a single seasonal GAM model to infer skin $\delta^{15}\text{N}$ isotopic incorporation rate for each zone.

Skin isotopic incorporation and baleen growth rates

Prey from the three zones had distinct $\delta^{15}\text{N}$ values ([S2 Table](#)), with values decreasing from the GC to the CCS and CRD. The trophic-corrected blue whale skin $\delta^{15}\text{N}$ values for each foraging zone are presented in [Table 1](#). The magnitude of differences in prey between these zones ranged from 1.9‰ to 6.1‰ ([S2 Table](#)), which allowed us to assign the origin of measured $\delta^{15}\text{N}$ values of the different blue whale skin strata, independently of the zone where whales were sampled ([Table 1](#), [Fig 3](#)).

The GAM results of the relationship between blue whale skin $\delta^{15}\text{N}$ values and time (seasonal trend) are shown in [Table 2](#). The GAM that used $\delta^{15}\text{N}$ values in blue whale skin stratum basale and externum in relation to time indicated a weak, but slightly significant positive

Table 1. Trophic-corrected blue whale skin $\delta^{15}\text{N}$ values for each foraging zone.

Zone	Prey zone mean (\pm SD) $\delta^{15}\text{N}$	$\Delta^{15}\text{N}$	Trophic-corrected blue whale skin $\delta^{15}\text{N}$
Gulf of California	14.6 \pm 1.0	1.6	16.2 \pm 1.0
California Current System	10.4 \pm 0.3	1.6	12.0 \pm 0.3
Costa Rica Dome	8.5 \pm 1.1	1.6	10.1 \pm 1.1

Values were estimated by using the prey zone mean \pm SD (S2 Table) and assuming $\Delta^{15}\text{N}$ of 1.6‰.

<https://doi.org/10.1371/journal.pone.0177880.t001>

relationship in the GC, and a weak, but slightly significant negative relationship for the CCS (Table 2, Fig 3). These relationships were anticipated based on the observed pattern in prey $\delta^{15}\text{N}$ values among zones and the trophic-corrected blue whale skin values for each foraging zone (Table 1, S2 Table). For samples collected in the GC, $\delta^{15}\text{N}$ values increased to ~17‰ by April (Fig 3), which likely reflected isotopic equilibration with the $\delta^{15}\text{N}$ of local prey (Table 1). The opposite pattern was observed in the CCS, where the $\delta^{15}\text{N}$ values decreased with time to a low of ~13‰ by December (Fig 3), which also suggests gradual equilibration of the tissue to the local prey. In contrast, the relation between sloughed skin $\delta^{15}\text{N}$ values and time was not significant in the GC or CCS (Table 2). The GAM model for sloughed skin showed a parabolic relationship with time, with a slight tendency of the $\delta^{15}\text{N}$ values to increase and subsequently decrease with time in both zones (Fig 3). Therefore, we used the same method than that for the stratum basale and externum within each zone to estimate the isotopic incorporation rate of sloughed skin (S2 Fig).

The CRD skin $\delta^{15}\text{N}$ values were used as a reference to determine if the isotopic signal of this foraging zone was present in the skin sampled in the GC and the CCS. Some of the observed $\delta^{15}\text{N}$ values in the stratum basale and stratum externum from skin sampled in the CCS could represent transitional values between the CRD isotopic signal and the CCS signal. One of the values observed in the stratum externum sampled in August was assigned to the CRD (Fig 3).

The deviance explained in the relationship between skin $\delta^{15}\text{N}$ values and time for all six GAM models was low (6.7 to 21.1%; Table 2) due to the high degree of dispersion observed in skin data. This degree of variation was expected since the duration of time individual whales had spent in the zone where skin was collected was unknown at the time of sampling. As such, this variation is likely driven by a combination of recently arrived whales that had isotope values reflective of other foraging zones, individuals in the equilibration period with intermediate isotope values that represent a mixture of prey consumed in two foraging zones, or individuals that had reached skin steady-state isotopic equilibrium with the isotopic composition of local prey (Fig 3).

Estimates of $\delta^{15}\text{N}$ isotopic incorporation rate of blue whale skin strata in each foraging zone are shown in Table 3 and S3 Table. In the GC, the stratum basale (81 d), stratum externum (81 d), and sloughed skin (90 d) had similar incorporation rates (Table 3). In the CCS, the stratum basale had longer incorporation rates (262 d) than the stratum externum (192 d). Sloughed skin (272 d) had the lowest isotopic incorporation rate in CCS, although the later estimate had a high degree of uncertainty (Table 3). The average skin strata isotopic incorporation rate in the CCS (242 d) was 158 days lower than the GC (84 d) (Table 3). The overall mean of the $\delta^{15}\text{N}$ isotopic incorporation rate of blue whale skin was estimated, integrating all strata in both zones (163 d, Table 3).

Blue whale baleen isotope values are available in S1 Dataset and S7 Table. Stranding information of baleen plates collected from six blue whales (A to F), is presented in S1 Table and

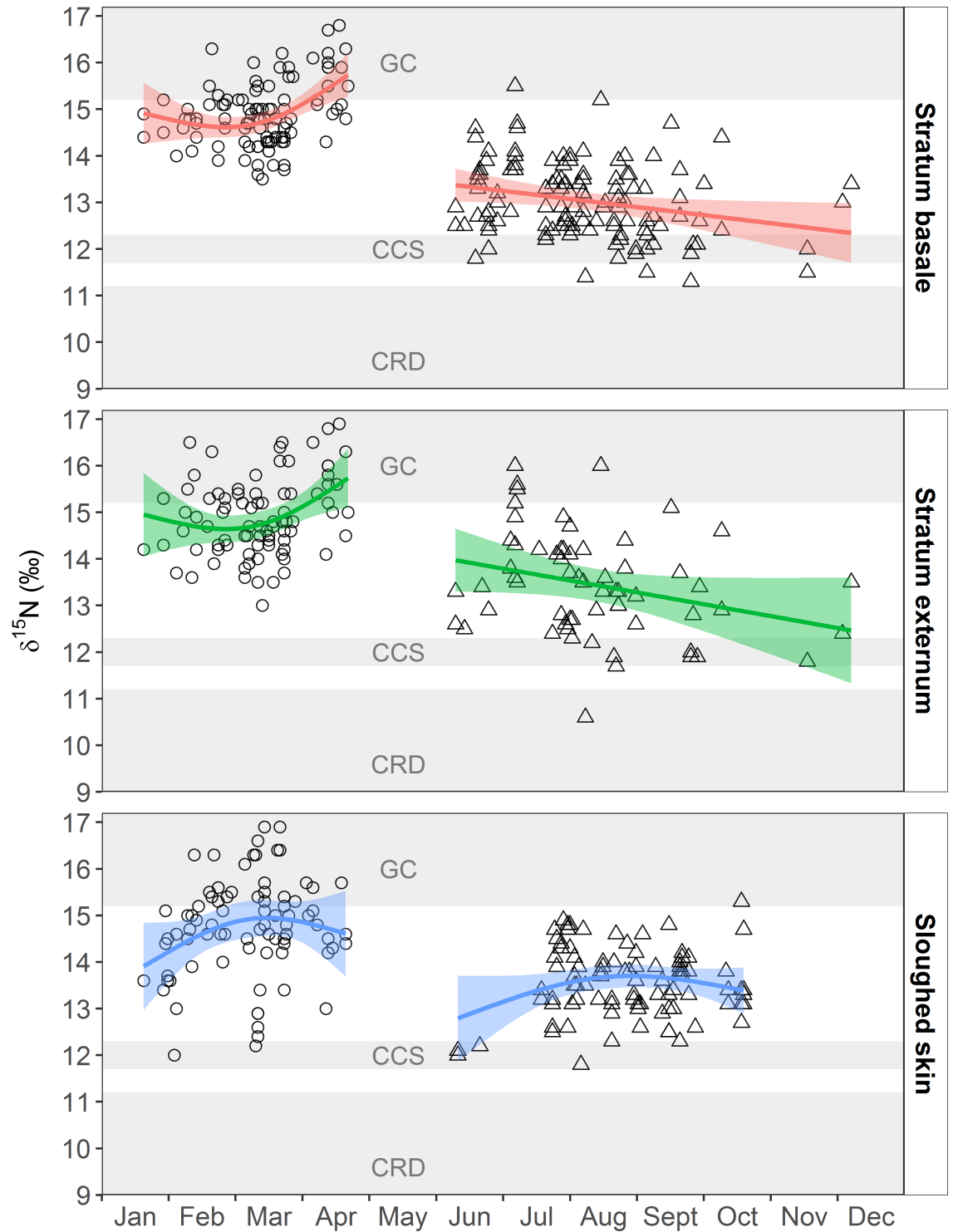


Fig 3. GAM analysis of the seasonal trend of skin strata $\delta^{15}\text{N}$ values in two foraging zones. The points represent the actual $\delta^{15}\text{N}$ values of skin collected from whales within the Gulf of California (open circles) and the California Current System (open triangles). The colored lines represent the GAM model fit (predictions) and the fringe around the lines show the 95% confidence intervals. The gray shaded area represents the mean \pm SD of the trophic-corrected blue whale skin values for each foraging zone: Gulf of California (GC), the California Current System (CCS) and the Costa Rica Dome (CRS).

<https://doi.org/10.1371/journal.pone.0177880.g003>

Table 2. GAM results for the seasonal trends of $\delta^{15}\text{N}$ and $\delta^{13}\text{C}$ values in different skin strata sampled in the Gulf of California (GC) and California Current System (CCS).

Isotope	Skin stratum	Zone	n	<i>E.df.</i>	F	Adjusted R ²	<i>P</i>	Deviance explained (%)
$\delta^{15}\text{N}$	Basale	GC	101	1.9	13.4	0.2	< 0.001	21.1
	Basale	CCS	120	1.0	8.4	0.6	< 0.01	6.7
	Externum	GC	85	1.9	7.4	0.1	< 0.01	14.7
	Externum	CCS	63	1.0	5.5	0.1	< 0.1	8.3
	Sloughed skin	GC	81	1.8	3.3	0.1	0.7	7.7
	Sloughed skin	CCS	93	1.8	2.6	0.0	0.7	6.7
$\delta^{13}\text{C}$	Basale	GC	101	1.0	0.2	-0.0	0.7	0.2
	Basale	CCS	120	1.9	3.6	0.1	< 0.1	6.2
	Externum	GC	85	1.5	1.3	0.1	0.4	2.8
	Externum	CCS	63	1.5	0.6	0.0	0.6	2.8
	Sloughed skin	GC	81	1.0	1.3	0.0	0.3	1.6
	Sloughed skin	CCS	93	1.0	0.1	-0.0	0.8	0.1

E.df., Estimated degrees of freedom; F, test of whether the smoothed function significantly reduces model deviance; *P*, p-values in bold were considered statistically significant (<0.05).

<https://doi.org/10.1371/journal.pone.0177880.t002>

Fig 1. The results of the GAM models to assess the fluctuations in $\delta^{15}\text{N}$ values along baleen plates, and of baleen growth rates estimations are shown in Tables 4 and 5, respectively. The GAM fit showed that the amplitude of the oscillations differed among individuals (Tables 4 and 5, Fig 4). Three baleen plates (A–C, one male and two females; S1 Table) exhibited the expected fluctuations in $\delta^{15}\text{N}$ ranging from 10.6‰ to 14.9‰ (Fig 4A–4C), and the length of baleen between these fluctuations ranged between 13 and 19 cm (Table 5). The other three baleen plates (D–F, all males; S1 Table) maintained relatively constant $\delta^{15}\text{N}$ values, ranging between 11.7‰ and 13.1‰ along the plate (Fig 4D–4F). Inter-individual differences in the amplitude of the oscillations are likely related to the individual migratory strategies and residency time within each foraging zone [37,38,43,55]. By using the trophic-corrected skin $\delta^{15}\text{N}$ values based on that of prey (Table 1), it was possible to associate these oscillations with the potential foraging zone that each individual whale visited. From these data, it could be inferred that whale B moved between all three zones, showing relatively regular cycles (Fig 4B), whereas whale C did not enter the GC, but moved constantly between the CCS and the CRD, in less

Table 3. $\delta^{15}\text{N}$ isotopic incorporation rates of blue whale skin strata in the Gulf of California and California Current System. The number of days were estimated by extrapolating from the GAM predictions (model fit and the upper and lower 95% confidence limits) for skin $\delta^{15}\text{N}$ values to change by 1.6‰ to isotopically equilibrate with local prey in each zone.

Zone	Skin Stratum	$\delta^{15}\text{N}$ isotopic incorporation rate of blue whale skin		
		Model fit	Lower limit	Upper limit
Gulf of California	Basale	81	90	69
	Externum	81	112	69
	Sloughed Skin	90	60	149
	Mean±SD	84±15		
California Current System	Basale	262	222	360
	Externum	192	160	240
	Sloughed Skin	272	163	816
	Mean±SD	242±44		
	Overall Mean±SD	163±91		

<https://doi.org/10.1371/journal.pone.0177880.t003>

Table 4. GAM results to assess the fluctuations of $\delta^{15}\text{N}$ and $\delta^{13}\text{C}$ in baleen plates.

Isotope	Baleen code	n	<i>E.df.</i>	F	Adjusted R ²	<i>P</i>	Deviance explained (%)
$\delta^{15}\text{N}$	A	41	23.8	61.4	1	< 0.001	99.0
	B	68	27.2	108.0	1	< 0.001	98.7
	C	67	27.3	95.9	1	< 0.001	98.6
	D	55	23.3	25.2	0.9	< 0.001	95.7
	E	71	26.5	27.2	0.9	< 0.001	94.8
	F	58	23.8	31.3	0.9	< 0.001	96.3
$\delta^{13}\text{C}$	A	41	21.9	55.8	1	< 0.001	98.8
	B	68	20.3	15.6	0.9	< 0.001	89.3
	C	67	27.7	64.9	1	< 0.001	98.0
	D	55	24.9	68.4	1	< 0.001	98.5
	E	71	27.5	65.1	1	< 0.001	97.8
	F	58	25.0	25.1	0.9	< 0.001	95.7

E.df., Estimated degrees of freedom; F, test of whether the smoothed function significantly reduces model deviance; *P*, p-values in bold were considered statistically significant (<0.05).

<https://doi.org/10.1371/journal.pone.0177880.t004>

regular cycles (Fig 4C). Whale A remained mainly within the CCS, potentially only migrating twice to the CRD (Fig 4A). In the case of whales D, E and F, the data suggests that these individuals remained within the CCS, throughout several years (Fig 4D–4F). Only whales A, B, and C were used to estimate the baleen growth rates (Fig 4A–4C). The mean (\pm SD) growth per year of baleen plates was estimated for each whale (A = 13.5 \pm 2.2; B = 14.8 \pm 1.7; C = 17.5 \pm 1.5 cm y⁻¹; Table 5), and also integrated in an overall mean (\pm SD) (15.5 \pm 2.2 cm y⁻¹; Table 5).

$\delta^{13}\text{C}$ values of skin and baleen plates

The mean $\delta^{13}\text{C}$ value of the prey in the GC was 0.7‰ and 2.9‰ higher than the CCS and the CRD, respectively (S2 Table). However, the standard deviation of the CRD overlapped with all the zones and it was not possible to accurately assign the origin of measured $\delta^{13}\text{C}$ from skin nor baleen plates.

Table 5. Blue whale baleen growth rate: Estimated by using the distance between sequential $\delta^{15}\text{N}$ minimums along the baleen plates from whales A to C.

Baleen code	Sex	Intervals between $\delta^{15}\text{N}$ minimums (cm)	Growth rate (cm y ⁻¹)
A	Male	10–24	14.0
		24–37	13.0
Mean\pmSD			13.5\pm0.7
B	Female	4–17	13.0
		17–31	14.0
		31–48	17.0
		48–63	15.0
Mean\pmSD			14.8\pm1.7
C	Female	9–27	18.0
		27–46	19.0
		46–62	16.0
Mean\pmSD			17.5\pm1.5
Overall Mean\pmSD			15.5\pm2.2

<https://doi.org/10.1371/journal.pone.0177880.t005>

The GAM model revealed a very weak though significant positive relationship between the $\delta^{13}\text{C}$ and time for the stratum basale sampled within the CCS. The GAMs applied to the other skin strata, from the other two foraging zones, did not show any relationship between the $\delta^{13}\text{C}$ values and time (Table 2, S1 Fig), and thus the isotopic incorporation rate of $\delta^{13}\text{C}$ in blue whale skin could not be estimated.

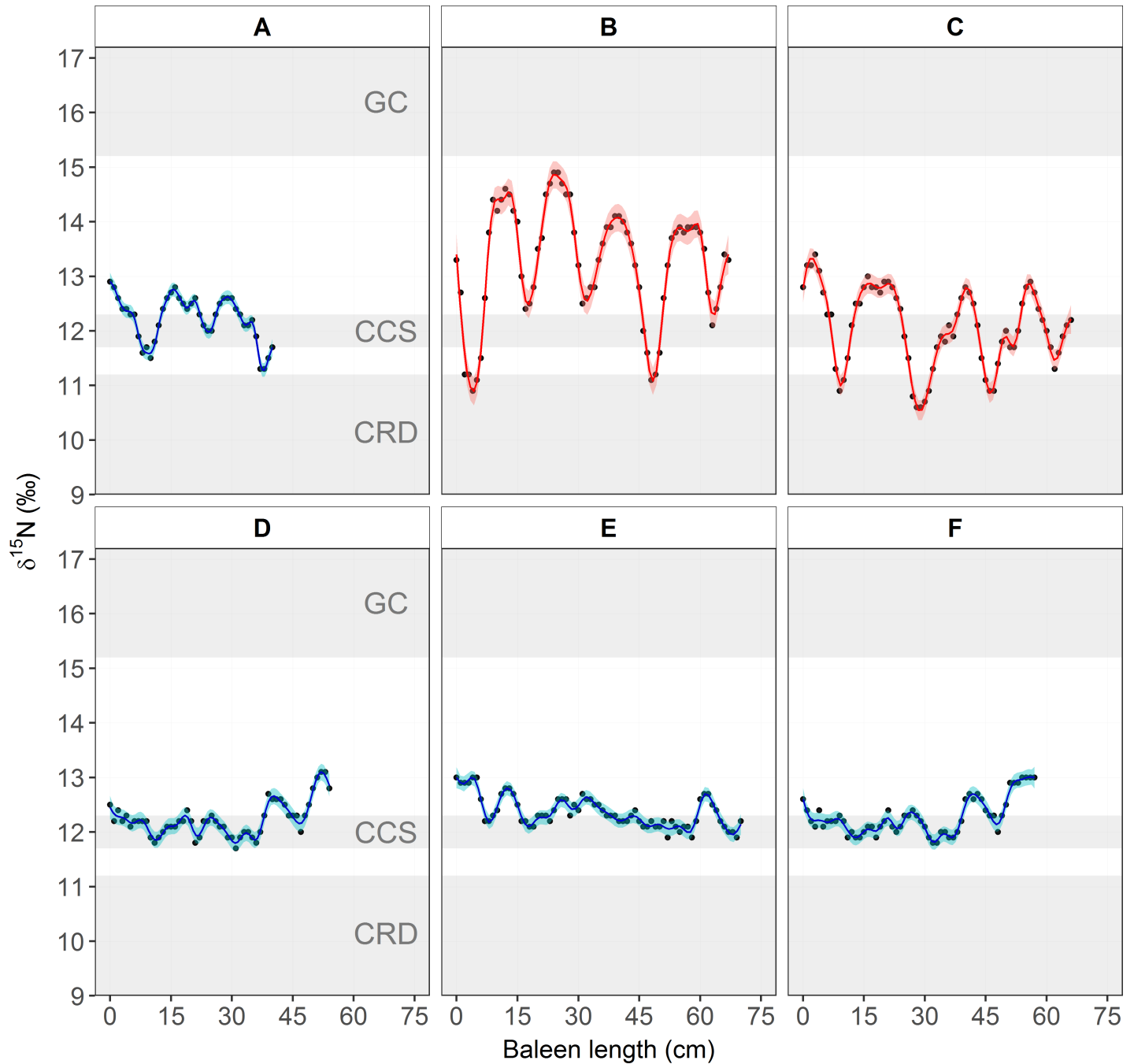


Fig 4. $\delta^{15}\text{N}$ values along the baleen plates from six whales, identified as A–F. Points represent actual values. The continuous line (blue: males; red: females) represents the GAM model fit and the narrow fringe around the lines represent the 95% confidence intervals. The gray shaded area represents the mean \pm SD of the trophic-corrected blue whale skin values for each foraging zone: Gulf of California (GC), the California Current System (CCS) and the Costa Rica Dome (CRS).

<https://doi.org/10.1371/journal.pone.0177880.g004>

Mean (\pm SD) $\delta^{13}\text{C}$ values of six baleen plates (A–F) are presented in [S7 Table](#). The GAM fits ([Table 4](#), [S3 Fig](#)) showed that all individuals presented small oscillations in the $\delta^{13}\text{C}$ values along the baleen that ranged between -18.3 to -16.1. These oscillations could not be linked to the foraging zones because of the overlap in prey $\delta^{13}\text{C}$ among zones ([S2 Table](#)). Therefore, baleen growth rates were inferred only using baleen $\delta^{15}\text{N}$ values.

Discussion

Influence of lipid-extraction and DMSO preservation on skin $\delta^{13}\text{C}$ and $\delta^{15}\text{N}$ values

Our results suggest that lipid-extraction is necessary to remove biases in skin $\delta^{13}\text{C}$ values associated with lipid content ([S4 Table](#)), which agrees with previous studies on mysticetes [[75,76](#)]. In regard to the effects of lipid-extraction on $\delta^{15}\text{N}$ values of cetacean skin, some authors [[48,75,76](#)] recommend analyzing bulk tissues because lipid-extraction can influence $\delta^{15}\text{N}$ values, although this effect varied between species [[75,76](#)] and tissues [[75](#)]. In our study, we only compared the $\delta^{15}\text{N}$ of five biopsy samples from which we analyzed paired bulk and lipid-extracted subsamples; however, $\delta^{15}\text{N}$ values between these treatments did not differ significantly, which would be in accordance with the results reported for other marine organisms [[95](#)]. With regard to preservation in DMSO ([S4 Table](#)), after lipid-extraction, blue whale skin $\delta^{13}\text{C}$, $\delta^{15}\text{N}$ and C/N ratios of samples preserved in DMSO were similar to those of samples preserved frozen. Our results concur with previous studies that show lipid-extraction via a 2:1 chloroform:methanol solvent solution was a sound method for removing the combined effect that DMSO and tissue lipid content have on skin $\delta^{13}\text{C}$ values [[76,81](#)].

Skin $\delta^{15}\text{N}$ isotopic incorporation rates

Only two studies have estimated isotopic incorporation rates of cetacean skin, and both utilized controlled feeding experiments on captive bottlenose dolphins [[47,48](#)]. Our approach was to use gradients in baseline $\delta^{15}\text{N}$ values between the GC and CCS as a natural diet switch experiment ([Fig 3](#)). Our mean estimate of $\delta^{15}\text{N}$ isotopic incorporation rates (163 ± 91 d; [Table 3](#)) for blue whale skin is similar to that observed in the longest experiment on captive bottlenose dolphins (180 ± 71 d) [[48](#)]. The similarity in incorporation rate estimates for these two distantly related cetacean species that differ in weight by over two orders of magnitude is striking, but suggests that these estimates can be applied to other odontocetes and mysticetes.

We found that isotopic incorporation rates varied among skin strata and foraging zones ([Table 3](#)); however, all of these estimates fell within the range of those observed for bottlenose dolphins in previous studies (106–275 d and ~60–90 d) [[47,48](#)]. It is possible that the observed variation in skin incorporation rates among zones could be influenced by water temperature [[10,96–100](#)], with higher rates in the warmer waters of GC in comparison to the CCS ([Table 3](#)). In cold waters, marine mammals reduce peripheral blood flow to maintain a constant internal body temperature, which results in a decrease of epidermal metabolism [[101–103](#)]. In contrast, incursion into warmer waters accelerates the turnover of superficial skin cells and increase the proliferation rate of cells by intensifying blood flow to the skin stratum basale [[104](#)]. Observations suggest that odontocetes, such as belugas (*Delphinapterus leucas*) [[104](#)] and killer whales (*Orcinus orca*) [[105](#)], move from colder to warmer waters to molt or promote skin regeneration. A study on blue whales in the GC and CCS found that at sites with lower water temperatures, sloughed skin was observed less often in comparison to warmer sites [[67](#)].

A novel approach in this study was to analyze different skin strata: basale, externum, and sloughed skin ([Figs 2A and 3](#)). We hypothesised that the different skin strata could provide

information about temporal shifts in diet. The stratum basale, where cells are constantly produced, would most likely reflect the most recent dietary information, while the isotopic composition of stratum externum and sloughed skin would record information of the diet consumed in the past, perhaps when individuals were in a different foraging zone than the one where skin samples were collected. The isotopic comparison of strata in the CCS supports this hypothesis since the stratum basale had significantly lower $\delta^{15}\text{N}$ values than the stratum externum and sloughed skin (S5 Table), suggesting that the stratum basale was equilibrating with local prey, characterized by lower $\delta^{15}\text{N}$ values than those which occur in the GC (Table 1, S2 Table). In the GC, skin strata did not have significantly different $\delta^{15}\text{N}$ values; however, sloughed skin had $\delta^{15}\text{N}$ values that were similar to those expected if the skin was grown in the CCS (Table 1, Fig 3), suggesting that sloughed skin samples have a higher probability of providing information about past diets. Thus, skin samples collected from migratory mysticetes can reflect information about past diets independent of where sampling occurs, demonstrating that skin is a valuable tissue to estimate relative contributions of food consumed in different foraging zones utilized during the annual life cycle. Since collecting skin from free ranging cetaceans is cost- and time-intensive, we recommend dividing skin biopsies into strata and collecting sloughed skin when available to increase the amount of information that can be gleaned from isotope analysis of this tissue.

Baleen growth rates

Our estimate of baleen growth rates for blue whales ($\sim 15.5 \pm 2.2 \text{ cm y}^{-1}$; Table 5) are consistent with previous estimates for other balaenopterids, such as the fin whale (*Balaenoptera physalus*, $20 \pm 2.6 \text{ cm y}^{-1}$) [37,55], and minke whale (*Balenoptera acutorostrata*, 12.9 cm y^{-1}) [57], as well as for other mysticetes such as bowhead whales ($16\text{--}25 \text{ cm y}^{-1}$ in adults) [42,43]. In contrast, baleen growth rate estimates were lower than those for southern right whales (*Eubalaena australis*, $\sim 27 \text{ cm y}^{-1}$) [44]. Variation in baleen growth rates among blue whales sampled in this study (Table 4) could be influenced by differences in individual movement strategies (Fig 4A–4C), a hypothesis proposed in previous studies of other mysticete species [37,38,43,55]. For example, variation in the period of time spent within a specific foraging zone or in migration between zones would produce wider or narrower oscillations in baleen $\delta^{15}\text{N}$, which would influence growth rate estimates (Table 5, Fig 4).

Three of the six baleen plates we analyzed did not show marked oscillations in the $\delta^{15}\text{N}$ values (Fig 4D–4F). These individuals were males: two adults, and one of unknown age class (S1 Table). A potential explanation for a lack of inter-annual variation in $\delta^{15}\text{N}$ is that these whales remained close or within the CCS foraging zone for several years prior to their death. By applying the mean annual growth rate of $\sim 15.5 \text{ cm y}^{-1}$ to the baleen records of these three males, they remained within the CCS ecosystems for ~ 3.5 (Fig 4D), ~ 4.5 (Fig 4E) and ~ 3.7 (Fig 4F) years. In contrast, the other three baleen plates, collected from one male and two females, exhibited oscillations in the $\delta^{15}\text{N}$ values along their outer edge that indicate cyclical migrations between foraging zones during ~ 2.5 (Fig 4A), ~ 4.3 (Fig 4B) and ~ 4.2 (Fig 4C) years.

The observed differences in movement strategies of blue whale individuals may be influenced by a combination of the following factors. One general explanation is related to changes in the availability of prey in different foraging zones because it is known that blue whale distribution is influenced by variations in the abundance of their primary prey [2,3]. A more specific explanation is that females are more likely to migrate to warmer waters in winter/spring to nurse their calves, a hypothesis that has been proposed for other mysticetes, although other mysticetes generally do not feed while on their winter/spring breeding grounds [106]. Moreover, the patterns in the baleen of whale C (Fig 4C) suggest a high fidelity of females to

returning to specific winter/spring foraging grounds year after year. This would be in accordance with the high site fidelity observed in GC of some well-identified females obtained via photo-identification and genetic analysis [9,11,107]. In the case of males, our data indicate three males remained in the CCS and one migrated twice to the CRD (Fig 4). The female:male sex ratio (1.4:1) in the GC is biased towards females [9,107], suggesting that only a portion of the males in the northeast Pacific are using this zone in winter/spring. Photo-identification data has also shown that some males have a high site fidelity to the GC [9] or possibly other winter/spring foraging grounds. Baleen isotope data from one male in our study also indicates that it had a high fidelity to the CRD, since it migrated only to this zone (Fig 4A). Blue whales are not frequently sighted in the CCS during winter and spring [108,109], although this could be attributed to low search effort during this season. However, vocalizations specific to male blue whales have been recorded year round in the CCS [110–113]. The baleen data of males D, E, F (Fig 4D–4F) is in agreement with this observation. Therefore, we hypothesize that there are two migratory strategies for blue whale males in the northeast Pacific. Some individuals migrate to winter/breeding grounds in the GC or CRD, while others remain within the CCS. How these two migratory strategies influence mating success for males is not known.

$\delta^{15}\text{N}$ trophic discrimination factors

$\delta^{15}\text{N}$ trophic discrimination factors have not been estimated for blue whale tissues, therefore our approach was to assume a 1.6‰ (Table 1) discrimination factor between whales and their prey based on the controlled feeding experiments on bottlenose dolphins [47,48]. Borrell *et al.* [114] suggested using a trophic discrimination factor of 2.8‰ for balaenopterid skin and baleen plates. However, the mean (\pm SD) baleen $\delta^{15}\text{N}$ value of the three male blue whales (D: 12.2 ± 0.3 ; E: 12.4 ± 0.3 ; F: 12.3 ± 0.4 ; S7 Table, Fig 4D–4F) that presumably remained within the CCS for ~2–3 years prior to death, and by extension were isotopically equilibrated with local food sources, were enriched by only 1.7–1.9‰ relative to local prey sources (10.5 ± 0.2 ; S2 Table), and is similar to estimates for skin of captive bottlenose dolphins ($1.6\pm 0.5\%$) [47,48].

Temporal consistency of baseline $\delta^{15}\text{N}$ values among foraging zones

The observed seasonal trend in skin $\delta^{15}\text{N}$ values within each zone and the oscillations along baleen plates support our hypothesis that these tissues record baseline shifts in nitrogen isotope values across the northeast Pacific. Our approach assumes that such baseline gradients are temporarily consistent at a decadal scale. To test this assumption, it would be ideal to have prey $\delta^{15}\text{N}$ data from each foraging zone for each year blue whales were sampled; however, such sampling resolution is logistically impossible. Our approach was to use a GLM to evaluate inter-annual trends in skin $\delta^{15}\text{N}$ values, which showed that they slightly increased in the GC and CCS (see Results); no evident trend was observed in the CRD (S6 Table, S4 Fig).

Published datasets show that isotope values of blue whale prey and zooplankton collected from the CCS were consistent over decadal timescales (1994, 2000–2001, 2013) and between sites (Monterey Bay and British Columbia) [60,61,63,64,115]. Moreover, the $\delta^{15}\text{N}$ values in blue whale baleen plates that were assigned to the CCS show a remarkably consistent pattern regardless of when the baleen was collected (1980s vs. 2000s; S1 Table, Fig 4). These patterns suggest that a relatively stable $\delta^{15}\text{N}$ baseline existed in the CCS for nearly three decades. Furthermore, these data suggest that the slight inter-annual increase in skin $\delta^{15}\text{N}$ values of blue whales in the CCS is likely the result of uneven seasonal sampling rather than a shift in the baseline.

$\delta^{15}\text{N}$ values of the dominant krill species (*Nyctiphanes simplex*) in the GC are variable, likely due to their omnivorous feeding behavior [116], but are consistently higher than krill in the

CCS and the CRD (S2 Table) [58–62,64,117,118]. Isotope data for potential blue whale prey from the CRD were only available from one study (S2 Table) [62], but zooplankton data also suggest that this zone has lower $\delta^{15}\text{N}$ values in comparison to the CCS and GC [65]. Additionally, baleen $\delta^{15}\text{N}$ patterns from whales that likely visited the CRD (Fig 4A–4C) indicate that baseline $\delta^{15}\text{N}$ values may be consistently lower than those of the other zones. Another factor that may contribute to the observed differences in $\delta^{15}\text{N}$ values among foraging zones is that blue whales in the GC forage on combined aggregations of krill and higher trophic level lanternfish [20]. Thus, blue whale tissues synthesized in the GC will have higher $\delta^{15}\text{N}$ values that result from a combination of baseline and diet factors relative to tissues grown in other foraging zones in the northeast Pacific (Table 1, S3 Table, Figs 3 and 4).

$\delta^{13}\text{C}$ values in blue whale skin and baleen plates

$\delta^{13}\text{C}$ incorporation rates for skin could not be estimated because of the similarity in $\delta^{13}\text{C}$ values among prey from different foraging zones (S2 Table), and by extension $\delta^{13}\text{C}$ values were not useful to estimate baleen growth rates. Another variable that could contribute to the lack of spatial signal in $\delta^{13}\text{C}$ is movement of blue whales between coastal ^{13}C -enriched and ^{13}C -depleted oceanic ecosystems [24] within a specific foraging zone [2]. Thus, any latitudinal variation in blue whale skin and baleen $\delta^{13}\text{C}$ values between the CCS, GC, and CRD may be obscured by longitudinal movement between coastal and offshore areas within foraging zones.

Conclusions

Blue whale skin isotopic incorporation rates and baleen growth rates are similar to other odontocetes and mysticetes, respectively. We recommend collecting skin samples throughout the seasonal residency of migratory mysticetes within specific foraging zones, and dividing skin biopsies into strata. This approach allows for an assessment of seasonal variation in isotope values that could provide insights into movement and/or shifts in seasonal foraging strategies. Furthermore, analyzing both skin and baleen can provide information on the inter-annual variation in prey isotope values within and among foraging zones, as well as provide information about the migratory strategies of individual whales over several years of life, that currently cannot be obtained from satellite telemetry tags that (at best) collect a single year of movement information [2].

Supporting information

S1 Fig. GAM analysis relating skin $\delta^{13}\text{C}$ values to Julian day (presented in months). The points represent the actual $\delta^{13}\text{C}$ values of skin collected from whales within the Gulf of California (open circles) and the California Current System (open triangles). Lines represent the fit (projections) of the GAM model and the fringe around the lines show the 95% confidence intervals.
(TIF)

S2 Fig. Sections used from the GAM model predictions to infer $\delta^{15}\text{N}$ isotopic incorporation rates of blue whale skin strata in each foraging zone. The lines represent the GAM model fit (predictions) in the Gulf of California (green) and the California Current System (blue). The fringe around the lines show the 95% confidence intervals. The black dot represents the initial point (*i.e.* diet switch) and the red dot the final point of the sections from the predictions that were used from the fit and the lower and upper confidence intervals. Per mil (‰) differences and days passed between points were estimated and then used to extrapolated to a 1.6‰ increase in the Gulf of California, or decrease in California Current System, for skin to reach steady-state isotopic equilibrium with the local prey isotopic signal.
(TIF)

S3 Fig. $\delta^{13}\text{C}$ values along the baleen plates from six whales, identified as A-F. Points represent actual values, the continuous line (blue: males; red: females) represents the GAM model fit and the fringe around the lines show the narrow 95% confidence intervals.

(TIF)

S4 Fig. GLM analysis relating skin $\delta^{15}\text{N}$ values to time (Julian date, presented in years).

Points represent the actual $\delta^{15}\text{N}$ values of blue whale skin collected in different zones of the northeast Pacific. Lines represent the fit of the GLM model and the fringe around the lines show the 95% confidence intervals. The gray shaded area represents the mean \pm SD of the trophic-corrected blue whale skin values for each foraging zone; Gulf of California (GC), California Current System (CCS), and Costa Rica Dome (CRD).

(TIF)

S1 Table. Information of baleen plates collected from six blue whales.

(DOCX)

S2 Table. Mean (\pm SD) $\delta^{13}\text{C}$, $\delta^{15}\text{N}$, and weight percent C/N ratios of potential blue whale prey from each of the three foraging zones in the northeast Pacific.

(DOCX)

S3 Table. Results from the GAM model sections used to infer $\delta^{15}\text{N}$ isotopic incorporation rates of blue whale skin strata in Gulf of California (GC) and California Current System (CCS).

(DOCX)

S4 Table. Max-*t* test results comparing the effect of different treatments on skin $\delta^{15}\text{N}$, $\delta^{13}\text{C}$ and weight percent C/N ratios.

(DOCX)

S5 Table. Max-*t* test results for the comparison of $\delta^{13}\text{C}$ and $\delta^{15}\text{N}$ values among different skin strata in the Gulf of California (GC) and California Current System (CCS).

(DOCX)

S6 Table. GLM results relating blue whale skin $\delta^{15}\text{N}$ values to time (Julian date) in the Gulf of California (GC), California Current System (CCS) and Costa Rica Dome (CRD).

(DOCX)

S7 Table. Mean (\pm SD) $\delta^{13}\text{C}$, $\delta^{15}\text{N}$ and weight percent C/N ratios of blue whale baleen plates collected from stranded whales.

(DOCX)

S1 Dataset. $\delta^{13}\text{C}$, $\delta^{15}\text{N}$ and weight percent C/N ratios of blue whale skin and baleen plates used in this study.

(XLSX)

Acknowledgments

We would like to thank the institutions that facilitated the use of tissues samples and issued the permits to collect and process these samples: NOAA-SWFSC, CRC, CICIMAR-IPN, HSU-Vertebrate Museum, Museo de la Ballena y Ciencias del Mar (La Paz, BCS), the California Department of Parks and Recreation-Prairie Creek Redwoods State Park, NOAA/NMFS and SEMARNAT. We are also very grateful to all the personnel from the former institutions, the Stranding Network of California, and the Center for Stable Isotopes of the University of New Mexico who participated in the collection and processing of the tissue samples. We would also

like to thank the John H. Prescott Marine Mammal Rescue Assistance Grant Program that has provided grants to the stranding networks. J. Rice, J. Loomis, T. Holmes, and F.J. Gómez-Díaz collaborated during the process of locating potential baleen plates for this study and we are very beholden for their support. We would also like to give special recognition to K. Robertson who helped with the logistics of sample selection and the sex identification of an important baleen sample at the genetics lab in SWFSC. M.A. Pardo, H. Villalobos-Ortiz, C. Arnold, and two anonymous reviewers made some valuable comments to improve the manuscript.

Author Contributions

Conceptualization: GBV SDN DG.

Formal analysis: GBV.

Funding acquisition: GBV SDN DG SAG.

Investigation: GBV SDN GSV JKJ.

Methodology: GBV DG.

Project administration: GBV.

Resources: GBV SDN JC GSV JKJ SAG DG.

Visualization: GBV SDN.

Writing – original draft: GBV SDN DG.

Writing – review & editing: GBV SDN JC GSV JKJ SAG DG.

References

1. Reilly SB, Bannister JL, Best PB, Brown M, Brownell RL Jr., Butterworth DS, et al. *Balaenoptera musculus*. IUCN Red List Threat Species. 2008; e.T2477A9447146.
2. Bailey H, Mate BR, Palacios DM, Irvine L, Bograd SJ, Costa DP. Behavioural estimation of blue whale movements in the Northeast Pacific from state-space model analysis of satellite tracks. *Endanger Species Res*. 2009; 10: 93–106.
3. Calambokidis J, Barlow J, Ford JKB, Chandler TE, Douglas AB. Insights into the population structure of blue whales in the Eastern North Pacific from recent sightings and photographic identification. *Mar Mammal Sci*. 2009; 25: 816–832.
4. Calambokidis J, Barlow J. Abundance of blue and humpback whales in the eastern North Pacific estimated by capture-recapture and line-transect methods. *Mar Mammal Sci*. 2004; 20: 63–85.
5. Etnoyer P, Canny D, Mate BR, Morgan LE, Ortega-Ortiz JG, Nichols WJ. Sea-surface temperature gradients across blue whale and sea turtle foraging trajectories off the Baja California Peninsula, Mexico. *Deep Sea Res Part II Top Stud Oceanogr*. 2006; 53: 340–358.
6. Etnoyer P, Canny D, Mate BR, Morgan L. Persistent pelagic habitats in the Baja California to Bering Sea (B2B) Ecoregion. *Oceanography*. 2004; 17: 90–101.
7. Mate BR, Lagerquist BA, Calambokidis J. Movements of North Pacific blue whales during the feeding season off southern California and their southern fall migration. *Mar Mammal Sci*. 1999; 15: 1246–1257.
8. Reilly SB, Thayer VG. Blue whale (*Balaenoptera musculus*) distribution in the eastern tropical Pacific. *Mar Mammal Sci*. 1990; 6: 265–277.
9. Gendron D. Ecología poblacional de la ballena azul, *Balaenoptera musculus*, de la Peninsula de Baja California. Ph.D. Thesis, Centro de Investigación Científica y de Educación Superior de Ensenada. 2002.
10. Pardo MA, Silverberg N, Gendron D, Beier E, Palacios DM. Role of environmental seasonality in the turnover of a cetacean community in the southwestern Gulf of California. *Mar Ecol Prog Ser*. 2013; 487: 245–260.

11. Sears R, Ramp C, Douglas AB, Calambokidis J. Reproductive parameters of eastern North Pacific blue whales *Balaenoptera musculus*. *Endanger Species Res.* 2013; 22: 23–31.
12. Tershy BR, Breese D, Strong CS. Abundance, seasonal distribution and population composition of baleen whales in the Canal de Ballenas, Gulf of California, Mexico. *Reports Int Whal Comm.* 1990; 369–375.
13. Hoyt E. The blue whale, *Balaenoptera Musculus*: An endangered species thriving on the Costa Rica Dome. Rep WDC. 2009; 1–11. Available: www.cbd.int/cms/ui/forums/attachment.aspx?id=73
14. Del Angel-Rodríguez JA. Hábitos alimentarios y distribución espacio-temporal de los rorcuales común (*Balaenoptera physalus*) y azul (*Balaenoptera musculus*) en la Bahía de La Paz, B.C.S., México. M. Sc. Thesis, Centro Interdisciplinario de Ciencias Marinas-Instituto Politécnico Nacional. 1997. Available: <http://tesis.ipn.mx/handle/123456789/3026>
15. Croll DA, Marinovic B, Benson S, Chavez FP, Black N, Ternullo R, et al. From wind to whales: trophic links in a coastal upwelling system. *Mar Ecol Prog Ser.* 2005; 289: 117–130.
16. Nemoto T, Kawamura A. Characteristics of food habits and distribution of baleen whales with special reference to the abundance of North Pacific sei and bryde's whales. *Rep Int Whal Com Spec Issue.* 1977; 80–87.
17. Matteson RS. The Costa Rica Dome: A study of physics, zooplankton and blue whales. M.Sc. Thesis, Oregon State University. 2009. Available: <http://scholar.google.com/scholar?hl=en&btnG=Search&q=intitle:No+Title#0>
18. Fiedler PC, Reilly SB, Hewitt RP, Demer D, Philbrick VA, Smith S, et al. Blue whale habitat and prey in the California Channel Islands. *Deep Sea Res Part II Top Stud Oceanogr.* 1998; 45: 1781–1801.
19. Calambokidis J, Steiger G. Blue whales. Stillwater, Minnesota: Worldlife Series Library, Voyager Press; 1997.
20. Jiménez-Pinedo NC. Hábitos alimentarios y relación interespecífica entre la ballena azul (*Balaenoptera musculus*) y la ballena de aleta (*B. physalus*) en el suroeste del Golfo de California. M.Sc. Thesis, Centro Interdisciplinario de Ciencias Marinas-Instituto Politécnico Nacional. 2010. Available: <http://www.repositoriodigital.ipn.mx/bitstream/handle/123456789/13508/jimenezp1.pdf?sequence=1>
21. Oliver JS, Slattery PN, Silberstein MA, O'Connor EF. A comparison of gray whale, *Eschrichtius robustus*, feeding in the Bering Sea and Baja California. *Fish Bull.* 1983; 81: 513–522.
22. Baraff LS, Clapham PJ, Mattila DK. Feeding behavior of a humpback whale in low-latitude waters. *Mar Mammal Sci.* 1991; 7: 197–202.
23. Hazen EL, Palacios DM, Forney KA, Howell EA, Becker E, Hoover AL, et al. WhaleWatch: a dynamic management tool for predicting blue whale density in the California Current. *J Appl Ecol.* 2016;
24. Newsome SD, Clementz MT, Koch PL. Using stable isotope biogeochemistry to study marine mammal ecology. *Mar Mammal Sci.* 2010; 26: 509–572.
25. DeNiro MJ, Epstein S. Influence of diet on the distribution of nitrogen isotopes in animals. *Geochim Cosmochim Acta.* 1981; 45: 341–351.
26. DeNiro MJ, Epstein S. Influence of diet on the distribution of carbon isotopes in animals. *Geochim Cosmochim Acta.* 1978; 42: 495–506.
27. Gannes LZ, Martínez del Rio C, Koch P. Natural abundance variations in stable isotopes and their use in animal physiological ecology. *Comp Biochem Physiol.* 1998; 119: 725–737.
28. Altabet MA., Pilskaln C, Thunell R, Pride C, Sigman D, Chavez F, et al. The nitrogen isotope biogeochemistry of sinking particles from the margin of the Eastern North Pacific. *Deep Sea Res Part I Oceanogr Res Pap.* 1999; 46: 655–679.
29. Graham BS, Koch PL, Newsome SD, McMahon KW, Auriolos D. Using isoscapes to trace the movements and foraging behavior of top predators in oceanic ecosystems. 2010; 299–318.
30. McMahon KW, Hamady LL, Thorrold SR. A review of ecogeochemistry approaches to estimating movements of marine animals. *Limnol Oceanogr.* 2013; 58: 697–714.
31. Williams RL, Wakeham S, McKinney R, Wishner KF. Trophic ecology and vertical patterns of carbon and nitrogen stable isotopes in zooplankton from oxygen minimum zone regions. *Deep Res Part I Oceanogr Res Pap.* Elsevier; 2014; 90: 36–47.
32. McMahon KW, Thorrold SR, Elsdon TS, McCarthy MD. Trophic discrimination of nitrogen stable isotopes in amino acids varies with diet quality in a marine fish. *Limnol Oceanogr.* 2015; 60: 1076–1087.
33. Vander Zanden MJ, Rasmussen JB. Variation in $\delta^{15}\text{N}$ and $\delta^{13}\text{C}$ trophic fractionation: Implications for aquatic food web studies. *Limnol Oceanogr.* 2001; 46: 2061–2066.
34. McCutchan JH, Lewis WM, Kendall C, McGrath CC. Variation in trophic shift for stable isotope ratios of carbon, nitrogen, and sulfur. *Oikos.* 2003; 102: 378–390.

35. Thomas SM, Crowther TW. Predicting rates of isotopic turnover across the animal kingdom: A synthesis of existing data. *J Anim Ecol*. 2015; 84: 861–870. <https://doi.org/10.1111/1365-2656.12326> PMID: 25482029
36. Martínez Del Rio C, Wolf N, Carleton SA, Gannes LZ. Isotopic ecology ten years after a call for more laboratory experiments. *Biological Reviews*. 2009. pp. 91–111. <https://doi.org/10.1111/j.1469-185X.2008.00064.x> PMID: 19046398
37. Aguilar A, Giménez J, Gómez-Campos E, Cardona L, Borrell A. $\delta^{15}\text{N}$ value does not reflect fasting in mysticetes. *PLoS One*. 2014; 9: e92288. <https://doi.org/10.1371/journal.pone.0092288> PMID: 24651388
38. Matthews CJD, Ferguson SH. Seasonal foraging behaviour of eastern Canada-West Greenland bowhead whales: An assessment of isotopic cycles along baleen. *Mar Ecol Prog Ser*. 2015; 522: 269–286.
39. Matthews CJD, Ferguson SH. Spatial segregation and similar trophic-level diet among eastern Canadian Arctic/north-west Atlantic killer whales inferred from bulk and compound specific isotopic analysis. *J Mar Biol Assoc United Kingdom*. 2013; 94: 1343–1355.
40. Gendron D, Aguíñiga S, Carriquiry JD. $\delta^{15}\text{N}$ and $\delta^{13}\text{C}$ in skin biopsy samples: a note on their applicability for examining the relative trophic level in three rorqual species. *J Cetacean Res Manag*. 2001; 3: 41–44.
41. Witteveen BH, Worthy GAJ, Foy RJ, Wynne KM. Modeling the diet of humpback whales: An approach using stable carbon and nitrogen isotopes in a Bayesian mixing model. *Mar Mammal Sci*. 2012; 28: 1–18.
42. Schell DM, Saupé SM, Haubenstock N. Natural isotope abundances in bowhead whale (*Balaena mysticetus*) baleen: markers of aging and habitat usage. In: Rundel PW, Ehleringer JR, Nagy KA, editors. *Stable isotopes in ecological research*. Springer-Verlag, New York; 1989. pp. 260–269.
43. Schell DM, Saupé SM, Haubenstock N. Bowhead whale (*Balaena mysticetus*) growth and feeding as estimated by $\delta^{13}\text{C}$ techniques. *Mar Biol*. 1989; 103: 433–443.
44. Best PB, Schell DM. Stable isotopes in southern right whale (*Eubalaena australis*) baleen as indicators of seasonal movements, feeding and growth. *Mar Biol*. 1996; 124: 483–494.
45. Geraci J, St. Aubin DJ, Hicks B. The epidermis of odontocetes: a view from within. In: Bryden MM, Harrison R, editors. *Research on Dolphins, Part I*. Oxford: Clarendon Press; 1986. pp. 3–21.
46. Harrison R, Thurley KW. Structure of the epidermis in *Tursiops*, *Delphinus*, *Orcinus* and *Phocoena*. In: Harrison RJ, editor. *Functional Anatomy of Marine Mammals, Vol. 2*. London: Academic Press; 1974. pp. 45–71.
47. Browning NE, Dold C, I-Fan J, Worthy GAJ. Isotope turnover rates and diet-tissue discrimination in skin of ex situ bottlenose dolphins (*Tursiops truncatus*). *Clin Cancer Res*. 2014; 217: 214–221.
48. Giménez J, Ramírez F, Almunia J, Forero MG, de Stephanis R. From the pool to the sea: Applicable isotope turnover rates and diet to skin discrimination factors for bottlenose dolphins (*Tursiops truncatus*). *J Exp Mar Bio Ecol*. 2016; 475: 54–61.
49. Podlesak DW, McWilliams SR, Hatch KA. Stable isotopes in breath, blood, feces and feathers can indicate intra-individual changes in the diet of migratory songbirds. *Oecologia*. 2005; 142: 501–510. <https://doi.org/10.1007/s00442-004-1737-6> PMID: 15586297
50. Tieszen LL, Boutton TW, Tesdahl KG, Slade NA. Fractionation and turnover of stable carbon isotopes in animal tissues: Implications for $\delta^{13}\text{C}$ analysis of diet. *Oecologia*. 1983; 57: 32–37. <https://doi.org/10.1007/BF00379558> PMID: 28310153
51. Evans Ogden LJ, Hobson KA, Lank DB. Blood isotopic ($\delta^{13}\text{C}$ and $\delta^{15}\text{N}$) turnover and diet-tissue fractionation factors in captive dunlin (*Calidris alpina pacifica*). *Auk*. 2004; 121: 170–177.
52. Voigt CC. Low turnover rates of carbon isotopes in tissues of two nectar-feeding bat species. *J Exp Biol*. 2003; 206: 1419–1427. PMID: 12624176
53. Berta A, Sumich J, Kovacs K. *Marine mammals: Evolutionary biology*. 2nd ed. San Diego, California: Academic Press; 2006.
54. Fudge DS, Szewciw LJ, Schwalb AN. Morphology and development of blue whale baleen: An annotated translation of Tycho Tullberg's classic 1883 paper. *Aquat Mamm*. 2009; 35: 226–252.
55. Bentaleb I, Martin C, Vrac M, Mate B, Mayzaud P, Siret D, et al. Foraging ecology of mediterranean fin whales in a changing environment elucidated by satellitetracking and baleen plate stable isotopes. *Mar Ecol Prog Ser*. 2011; 438: 285–302.
56. Lee SH, Schell DM, McDonald TL, Richardson WJ. Regional and seasonal feeding by bowhead whales *Balaena mysticetus* as indicated by stable isotope ratios. *Mar Ecol Prog Ser*. 2005; 285: 271–287.

57. Mitani Y, Bando T, Takai N, Sakamoto W. Patterns of stable carbon and nitrogen isotopes in the baleen of common minke whale *Balaenoptera acutorostrata* from the western North Pacific. *Fish Sci.* 2006; 72: 69–76.
58. Auriolles-Gamboa D, Rodríguez-Pérez M, Sánchez-Velasco L, Lavín M. Habitat, trophic level, and residence of marine mammals in the Gulf of California assessed by stable isotope analysis. *Mar Ecol Prog Ser.* 2013; 488: 275–290.
59. Becker BH, Peery MZ, Beissinger SR. Ocean climate and prey availability the trophic level and reproductive success of the marbled murrelet, an endangered seabird. *Mar Ecol Prog Ser.* 2007; 329: 267–279.
60. Hipfner JM, Dale J, McGraw KJ. Yolk carotenoids and stable isotopes reveal links among environment, foraging behavior and seabird breeding success. *Oecologia.* 2010; 163: 351–360. <https://doi.org/10.1007/s00442-010-1618-0> PMID: 20397031
61. Carle RD. Seasonal and sex-specific diet in rhinoceros auklets. M.Sc. Thesis, The Faculty of Moss Landing Marine Laboratories. 2014. Available: http://scholarworks.sjsu.edu/etd_theses/4454/
62. Williams R. Trophic ecology of Oxygen Minimum Zone zooplankton revealed by carbon and nitrogen stable isotopes. Ph.D. Thesis, University of Rhode Island. 2013. Available: http://digitalcommons.uri.edu/cgi/viewcontent.cgi?article=1148&context=oa_diss
63. Sydeman WJ, Hobson KA, Pyle P, McLaren EB. Trophic relationships among seabirds in central California: Combined stable isotope and conventional dietary approach. *Condor.* 1997; 99: 327–336.
64. Miller TW. Trophic dynamics of marine nekton and zooplankton in the northern California Current pelagic ecosystem. Ph.D. Thesis, Oregon State University. 2006. Available: http://ir.library.oregonstate.edu/xmlui/bitstream/handle/1957/2589/TMiller_Dissertation_FINAL.pdf?sequence=1
65. Popp BN, Graham BS, Olson RJ, Hannides CCS, Lott MJ, Lopez-Ibarra G a, et al. Insight into the trophic ecology of yellowfin tuna, *Thunnus albacares*, from compound-specific nitrogen isotope analysis of proteinaceous amino acids. In: Dawson T, Siegwolf R, editors. *Stable isotopes as indicators of ecological changes.* Amsterdam, Netherlands: Elsevier Academic Press; 2007; pp 173–190.
66. Barrett-Lennard LG, Smith TG, Ellis GM. A cetacean biopsy system using lightweight pneumatic darts, and its effect on the behavior of killer whales. *Mar Mammal Sci.* 1996; 12: 14–27.
67. Gendron D, Mesnick SL. Sloughed skin: A method for the systematic collection of tissue samples from Baja California blue whales. *J Cetacean Res Manag.* 2001; 3: 77–79.
68. Brinton E, Ohman MD, Townsend AW, Knight MD, Bridgeman AL. *Euphausiids of the World Ocean (cd-room Expert System).* Springer-Verlag, Heidelberg; 2000.
69. Wisner RL. *The taxonomy and distribution of lanternfishes (family Myctophidae) of the eastern Pacific Ocean.* Bay St. Louis, Miss.: Navy Ocean Research and Development Activity; 1974.
70. Sheehan D, Hrapchak BB. *Theory and Practice of Histotechnology.* 2nd Edition. St. Louis, MO: C.V. Mosby Co.; 1980.
71. Morin PA, LeDuc RG, Robertson KM, Hedrick NM, Perrin WF, Etnier M, et al. Genetic analysis of killer whale (*Orcinus orca*) historical bone and tooth samples to identify western U.S. ecotypes. *Mar Mammal Sci.* 2006; 22: 897–909.
72. Morin PA, Nestler A, Rubio-Cisneros NT, Robertson KM, Mesnick SL. Interfamilial characterization of a region of the ZFX and ZFY genes facilitates sex determination in cetaceans and other mammals. *Mol Ecol.* 2005; 14: 3275–3286. <https://doi.org/10.1111/j.1365-294X.2005.02651.x> PMID: 16101791
73. DeNiro M, Epstein S. Mechanism of carbon isotope fractionation associated with lipid synthesis. *Science.* 1977; 197: 261–263. PMID: 327543
74. McConnaughey T, McRoy CP. Food-web structure and the fractionation of carbon isotopes in the Bering sea. *Mar Biol.* 1979; 53: 257–262.
75. Ryan C, McHugh B, Trueman CN, Harrod C, Berrow SD, O'Connor I. Accounting for the effects of lipids in stable isotope ($\delta^{13}\text{C}$ and $\delta^{15}\text{N}$ values) analysis of skin and blubber of balaenopterid whales. *Rapid Commun Mass Spectrom.* 2012; 26: 2745–2754. <https://doi.org/10.1002/rcm.6394> PMID: 23124665
76. Lesage V, Morin Y, Rioux È, Pomerleau C, Ferguson S, Pelletier É. Stable isotopes and trace elements as indicators of diet and habitat use in cetaceans: predicting errors related to preservation, lipid extraction, and lipid normalization. *Mar Ecol Prog Ser.* 2010; 419: 249–265.
77. Kaehler S, Pakhomov EA. Effects of storage and preservation on the $\delta^{13}\text{C}$ and $\delta^{15}\text{N}$ signatures of selected marine organisms. *Mar Ecol Prog Ser.* 2001; 219: 299–304.
78. Sarakinos HCH, Johnson ML, Vander Zanden M. A synthesis of tissue-preservation effects on carbon and nitrogen stable isotope signatures. *Can J Zool.* 2002; 80: 381–387.

79. Barrow LM, Bjorndal KA, Reich KJ. Effects of preservation method on stable carbon and nitrogen isotope values. *Physiol Biochem Zool.* 2008; 81: 688–693. <https://doi.org/10.1086/588172> PMID: 18752417
80. Todd S, Ostrom P, Lien J, Abrajano J. Use of biopsy samples of humpback whale (*Megaptera novaeangliae*) skin for stable isotope ($\delta^{13}\text{C}$) determination. *J Northwest Atl Fish Sci.* 1997; 22: 71–76.
81. Burrows DG, Reichert WL, Bradley Hanson M. Effects of decomposition and storage conditions on the $\delta^{13}\text{C}$ and $\delta^{15}\text{N}$ isotope values of killer whale (*Orcinus orca*) skin and blubber tissues. *Mar Mammal Sci.* 2014; 30: 747–762.
82. Caraveo-Patiño J, Soto LA. Stable carbon isotope ratios for the gray whale (*Eschrichtius robustus*) in the breeding grounds of Baja California Sur, Mexico. *Hydrobiologia.* 2005; 539: 99–107.
83. Fry B. *Stable Isotope Ecology.* New York, NY: Springer New York; 2006.
84. Logan JM, Jardine TD, Miller TJ, Bunn SE, Cunjak RA, Lutcavage ME. Lipid corrections in carbon and nitrogen stable isotope analyses: comparison of chemical extraction and modelling methods. *J Anim Ecol.* 2008; 77: 838–46. <https://doi.org/10.1111/j.1365-2656.2008.01394.x> PMID: 18489570
85. R Development Core T. R: A language and environment for statistical computing. Vienna, Austria: R Foundation for Statistical Computing; 2011. Available: <http://www.r-project.org/>
86. Herberich E, Sikorski J, Hothorn T. A robust procedure for comparing multiple means under heteroscedasticity in unbalanced designs. *PLoS One.* 2010; 5: 1–8.
87. Miller TW, Brodeur RD, Rau GH. Carbon stable isotopes reveal relative contribution of shelf-slope production to the Northern California Current pelagic community. *Limnol Oceanogr.* 2008; 53: 1493–1503.
88. Yee TW, Mitchell ND. Generalized additive models in plant ecology. Pond DW, editor. *J Veg Sci.* 1991; 2: 587–602.
89. Wood SN. *Generalized additive models: an introduction with R.* Wiley Interdisciplinary Reviews. 2006.
90. Xiang D. *Fitting generalized additive models with the GAM procedure.* SAS Institute, Cary, NC. 2001; 256–26. Available: <http://www2.sas.com/proceedings/sugi26/p256-26.pdf>
91. Fleming AH, Clark CT, Calambokidis J, Barlow J. Humpback whale diets respond to variance in ocean climate and ecosystem conditions in the California Current. *Glob Chang Biol.* 2016; 22: 1214–1224. <https://doi.org/10.1111/gcb.13171> PMID: 26599719
92. Mangiafico SS. *Summary and analysis of extension education program evaluation in R.* Rutgers Cooperative Extension, New Brunswick, NJ; 2016. Available: <http://rcompanion.org/documents/RHandbookProgramEvaluation.pdf>
93. Peng RD, Dominici F, Louis TA. Model choice in time series studies of air pollution and mortality. *J R Stat Soc Ser A.* 2006; 169: 179–203.
94. Chuang Y, Mazumdar S, Park T, Tang G, Arena VC, Nicolich MJ. Generalized linear mixed models in time series studies of air pollution. *Atmos Pollut Res.* Elsevier; 2011; 3: 148.
95. Ingram T, Matthews B, Harrod C, Stephens T, Grey J, Markel R, et al. Lipid extraction has little effect on the $\delta^{15}\text{N}$ of aquatic consumers. *Limnol Oceanogr Methods.* 2007; 5: 338–342.
96. Chelton DB, Schlax MG, Samelson RM. Summertime coupling between sea surface temperature and wind stress in the California Current System. *J Phys Oceanogr.* 2007; 37: 495–517.
97. Escalante F, Valdez-Holguín JE, Álvarez-Borrego S, Lara-Lara JR. Temporal and spatial variation of sea surface temperature, chlorophyll a, and primary productivity in the Gulf of California. *Cienc Mar.* 2013; 39: 203–215.
98. Lluch-Cota SE, Aragón-Noriega EA, Arreguín-Sánchez F, Aurióles-Gamboa D, Jesús Bautista-Romero J, Brusca RC, et al. The Gulf of California: Review of ecosystem status and sustainability challenges. *Prog Oceanogr.* 2007; 73: 1–26.
99. McClatchie S, Goericke R, Schwing FB, Bograd SJ, Peterson WT, Emmett R, et al. The state of the California Current, spring 2008–2009: Cold conditions drive regional differences in coastal production. *Calif Coop Ocean Fish Investig Reports.* 2009; 50: 43–68.
100. Schneider N, Di Lorenzo E, Niiler PP. Salinity variations in the Southern California Current. *J Phys Oceanogr.* 2005; 35: 1421–1436.
101. Irving L, Hart JS. The metabolism and insulation of seals as bare-skinned mammals in cold water. *Can J Zool.* 1957; 35: 497–511.
102. Silva RG. Assessment of body surface temperature in cetaceans: an iterative approach. *Braz J Biol.* 2004; 64: 719–24. Available: <http://www.ncbi.nlm.nih.gov/pubmed/15620012> PMID: 15620012
103. Boily P. Theoretical heat flux in water and habitat selection of phocid seals and beluga whales during the annual molt. *J Theor Biol.* 1995; 172: 235–244.

104. St Aubin DJ, Smith TG, Geraci JR. Seasonal epidermal molt in beluga whales, *Delphinapterus leucas*. *Can J Zool*. 1990; 68: 359–364.
105. Durban JW, Pitman RL. Antarctic killer whales make rapid, round-trip movements to subtropical waters: evidence for physiological maintenance migrations? *Biol Lett*. 2012; 8: 274–7. <https://doi.org/10.1098/rsbl.2011.0875> PMID: 22031725
106. Corkeron J, Connor C. Why do baleen whales migrate? *Mar Mammal Sci*. 1999; 15: 1228–1245.
107. Costa-Urrutia P, Sanvito S, Victoria-Cota N, Enríquez-Paredes L, Gendron D. Fine-scale population structure of blue whale wintering aggregations in the Gulf of California. *PLoS One*. 2013; 8: e58315. <https://doi.org/10.1371/journal.pone.0058315> PMID: 23505485
108. Forney KA, Barlow J. Seasonal patterns in the abundance and distribution of California cetaceans, 1991–1992. *Mar Mammal Sci*. 1998; 14: 460–489.
109. Carretta JV, Lowry MS, Stinchcomb CE, Lynn MS, Cosgrove RE. Distribution and abundance of marine mammals at San Clemente Island and surrounding offshore waters: results from aerial and ground surveys in 1998 and 1999. La Jolla, California: Southwest Fisheries Science Center Report. 2000.
110. Oleson EM, Wiggins SM, Hildebrand JA. Temporal separation of blue whale call types on a southern California feeding ground. *Anim Behav*. 2007; 74: 881–894.
111. Oleson EM, Calambokidis J, Burgess WC, McDonald MA, LeDuc CA, Hildebrand JA. Behavioral context of call production by eastern North Pacific blue whales. *Mar Ecol Prog Ser*. 2007; 330: 269–284.
112. Oleson EM, Calambokidis J, Barlow J, Hildebrand JA. Blue whale visual and acoustic encounter rates in the southern California bight. *Mar Mammal Sci*. 2007; 23: 574–597.
113. Stafford KM, Nieukirk SL, Fox CG. Geographic and seasonal variation of blue whale calls in the North Pacific. *J Cetacean Res Manag*. 2001; 3: 65–76.
114. Borrell A, Giménez J, Aguilar A. Discrimination of stable isotopes in fin whale tissues and application to diet assessment in cetaceans. 2012; 1596–1602. <https://doi.org/10.1002/rcm.6267> PMID: 22693115
115. Rau GH, Ohman MD, Pierrot-Bults A. Linking nitrogen dynamics to climate variability off central California: a 51 year record based on $^{15}\text{N}/^{14}\text{N}$ in CalCOFI zooplankton. 2003; 50: 2431–2447.
116. Mauchline J. The biology of mysids and euphausiids. *Advances in marine biology*. London and New York: Academic Press; 1980.
117. Jaume-Schinkel SM. Hábitos alimentarios del rorcual común *Balaenoptera physalus* en el Golfo de California mediante el uso de isótopos estables de nitrógeno y carbono. M.Sc. Thesis, Centro Interdisciplinario de Ciencias Marinas-Instituto Politécnico Nacional. 2004. Available: <http://www.repositoriodigital.ipn.mx/bitstream/handle/123456789/14439/jaume1.pdf?sequence=1>
118. Sampson L, Galván-Magaña F, De Silva-Dávila R, Aguiniga-García S, O'Sullivan JB. Diet and trophic position of the devil rays *Mobula thurstoni* and *Mobula japanica* as inferred from stable isotope analysis. *Mar Biol Assoc United Kingdom*. 2010; 90: 969–976.



La Sociedad Mexicana de Mastozoología Marina, A.C. otorga la presente

CONSTANCIA

De que el trabajo

TRASLAPE TRÓFICO ENTRE REGIONES DE ALIMENTACIÓN DE LA BALLENA AZUL EN EL PACÍFICO ORIENTAL.

Busquets-Vass G, Newsome S, Calambokidis J, Aguñiga-García S, Serra-Valente G, Jacobsen J, Gendron D

**Obtuvo el PRIMER LUGAR en la modalidad
presentación oral: nivel Doctorado**

Durante la XXXV Reunión Internacional para el Estudio de los Mamíferos Marinos, celebrada en las instalaciones de la Universidad Autónoma de B.C.S. en la Ciudad de La Paz, B.C.S. MÉXICO, del 1 al 5 de mayo de 2016

Dr. Jorge Urbán Ramírez
Presidente del Comité Organizador

Dr. Armando Jaramillo Legorreta
Presidente de la SOMEMMA A.C.

Society for Marine Mammalogy
Biennial Conference San Francisco December 13-18 2015
<http://www.marinemammalogy.org>

This is to certify that the person named below attended this conference:

Name: Geraldine Rosalie Busquets Vass

Affiliation: CICIMAR-IPN



President
Nick Gales

A handwritten signature in black ink, appearing to read "Nick Gales".

Australian Antarctic Division
Channel Highway
Kingston Tasmania 7050, Australia
nick.gales@aad.gov.au



AMERICAN CETACEAN SOCIETY MONTEREY BAY

P.O. Box HE

Pacific Grove, CA 93950

May 9, 2014

Geraldine R. Busquets Vass, MC
Estudiante del Doctorado en Ciencias Marinas
Centro Interdisciplinario de Ciencias Marinas – Instituto Politecnico Nacional
Departamento de Pesquerias y Biologia Marina
Laboratorio de Ecologia de Cetaceos y Quelonios
La Paz, Baja California Sur, Mexico
<http://www.cicimar.ipn.mx>

Dear Geraldine R. Busquets Vass,

Congratulations! We are pleased to inform you that our Board has approved an award of \$1,500.00 (US) to support your research:

Foraging Ecology of the Blue Whale in the Northeast Pacific Inferred by Stable Isotopes of Nitrogen and Carbon

We wish you success in your work and ask that the American Cetacean Society/Monterey Bay be acknowledged in any publications which may result from this research.

Sincerely,

Chair, Grant Awards Committee

CETACEAN SOCIETY INTERNACIONAL -CSI

September 04, 2014

Dear Geraldine,

Thank you for your very clear answers. Your US\$1000 CSI grant was sent to you, "Geraldine Rosalie Busquets Vass". It is very important that you tell both of us immediately when you receive the money, or if there are problems.

We wish you great success,

Executive Director, Advocacy, Science & Grants
Cetacean Society International
65 Redding Road-0953
Georgetown, CT 06829-0953 USA
t/c: 203.770.8615
www.csiwhalesalive.org

Ceremonia de Posgrado

Ciclo Escolar 2015-2016

Se otorga el presente

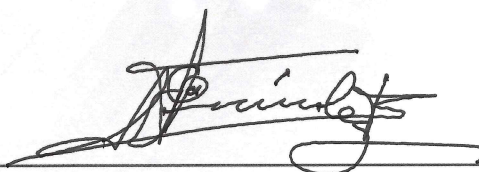
DIPLOMA

a

Geraldine Rosalie Busquets Vass

del Centro Interdisciplinario de Ciencias Marinas

Por haber obtenido el Mejor Desempeño Académico durante
el ciclo escolar 2015-2016



Dr. Enrique Fernández Fassnacht
Director General

México, D. F., a 11 de noviembre de 2016